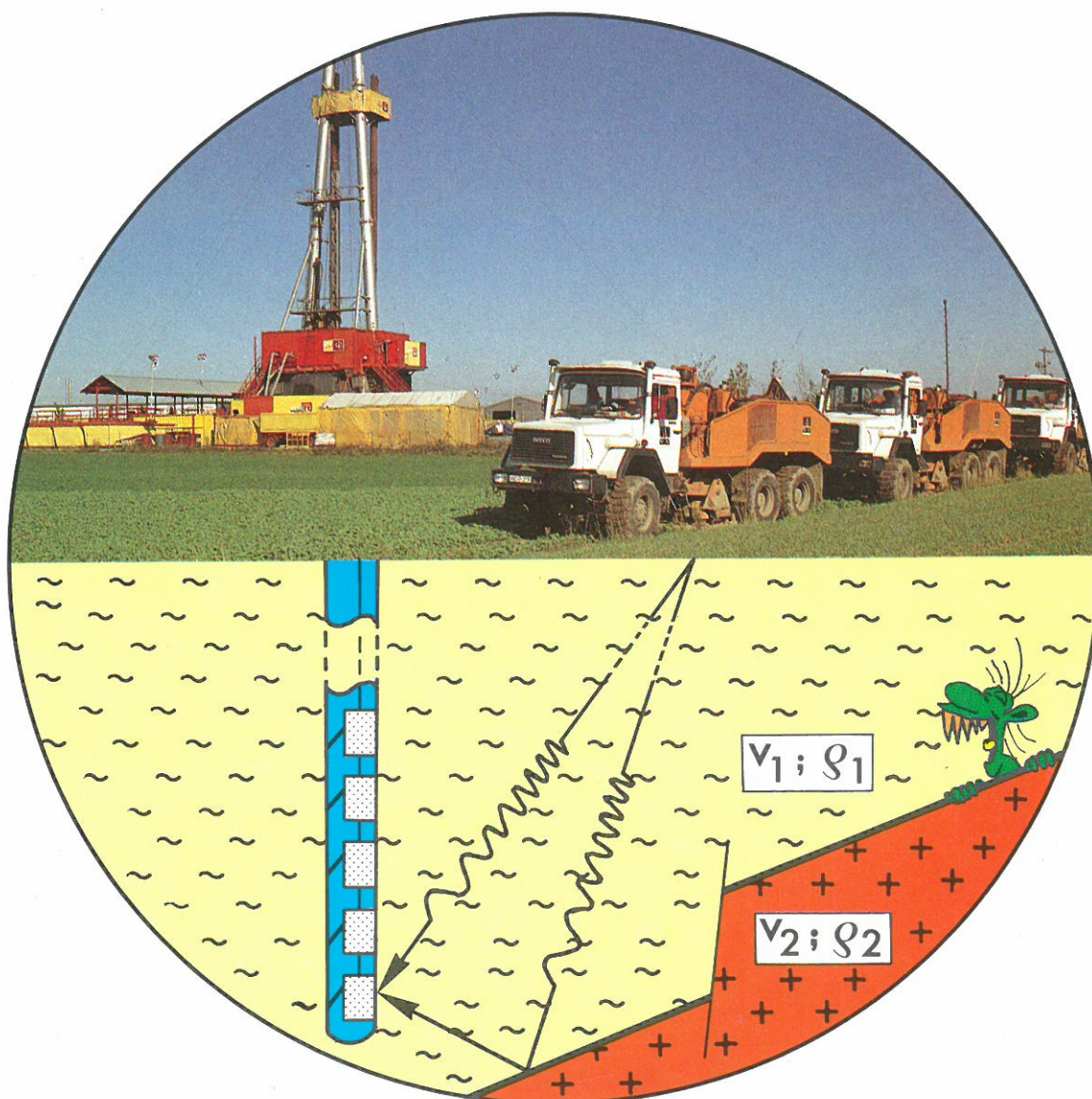


KTB REPORT 90-6b

DEKORP REPORT

Integrated Seismics Oberpfalz 1989

Longterm Logging and Testing Programme
of the KTB-Oberpfalz VB



Edited by
Projektleitung Deutsches Kontinentales Reflexionsseismisches Programm
and
Projektleitung Kontinentales Tiefbohrprogramm der Bundesrepublik Deutschland
im Niedersächsischen Landesamt für Bodenforschung

H.-J. Dürbaum, Ch. Reichert, K. Bram

Editors: Dr. H.-J. Dürbaum, Dipl. Geophys. Ch. Reichert,
Dr. K. Bram

Printed by: Wittmann & Wäsch, D-3007 Gehrden

Front cover: Vibrator trucks in operation close to the KTB pilot hole. The emitted compressional and shear wave energy is detected by a chain of borehole geophones. Partly the seismic energy travels directly to the receivers, partly it is reflected from geological structures in the surroundings.

All projects reported hereafter are entirely funded by the Bundesministerium für Forschung und Technologie. The Editors cannot be held responsible for the opinions given and statements made in the articles published, the responsibility resting with the authors.

© Niedersächsisches Landesamt für Bodenforschung
Hannover 1990.

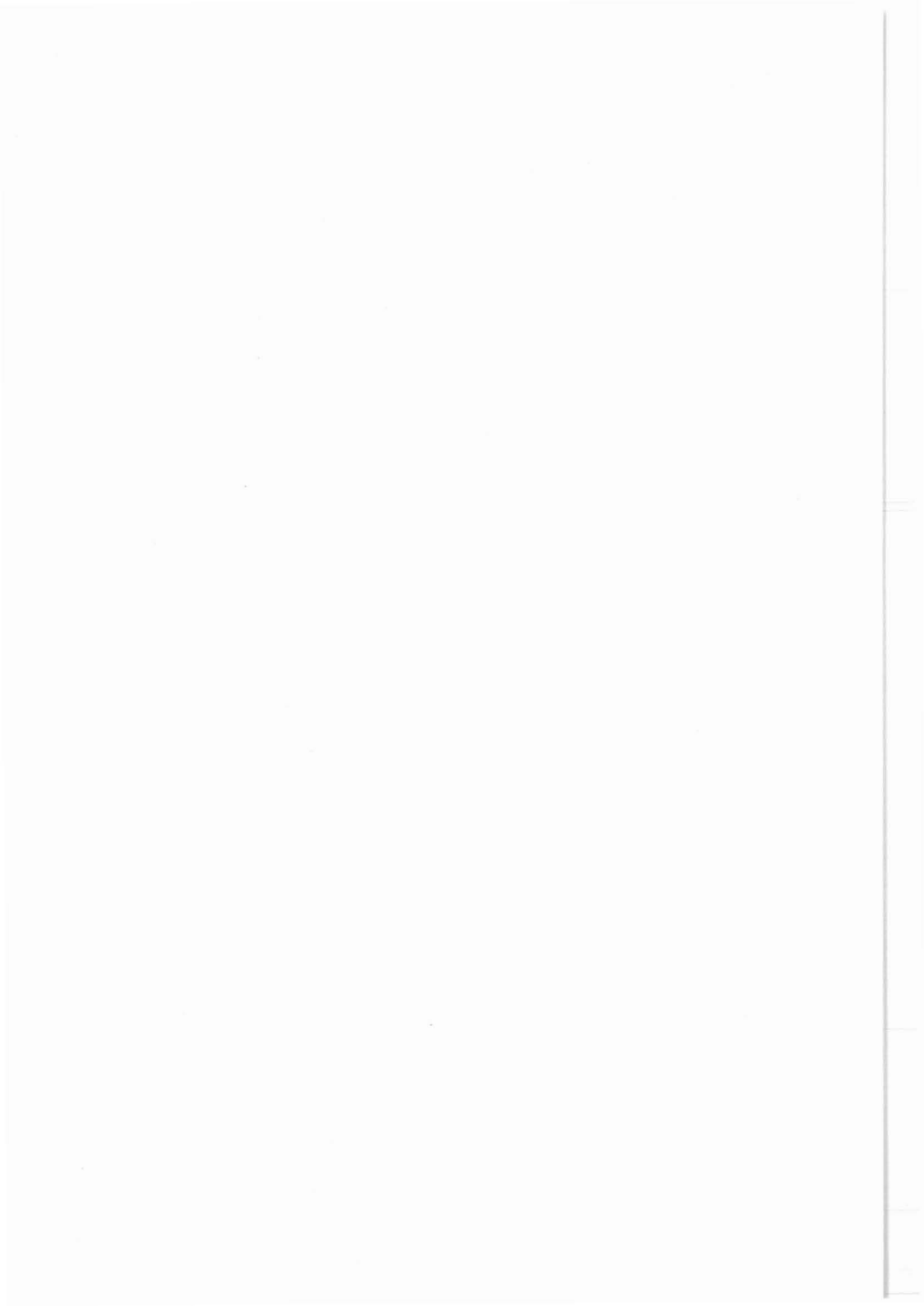
Reprinting, copying and translations, broadcasting, reproduction by photomechanical or in other ways as well as storage in data banks - even in parts - are subject to prior permission.

All rights are reserved.

Editors' address: Niedersächsisches Landesamt für Bodenforschung, POB 51 01 53, D-3000 Hannover 51.
Phone: 0511/643-3495 or 0511/643-2667.

CONTENTS

	Page
H.-J. Dürbaum: Introduction to ISO 89	3
Rehling, J.G. and Stiller, M.: 3-D Reflection Seismic Survey of the Area around the KTB Drilling Site	9
Albrecht, J. and Teichert, D.: Experiment "Durchschallung" - Calculation of Static Corrections from Seismic Borehole Records Using the Vibrator Signals of the 3-D Seismic Reflection Survey within ISO89	57
Wiederhold, H.: 3-D ESP - Experiment of the Integrated Seismics Ober- pfalz 1989	67
Lüschen, E., Söllner, W., Hohrath, A. and Rabbel, W.: Integrated P- and S-Wave Borehole Experiments at the KTB-Deep Drilling Site	85
Harjes, H.-P., Janik, M. and Kemper, M.: Moving Source Profiling - A Link between KTB-Borehole Data and Seismic Surface Measurements	137
Mylius, J., Nolte, E. and Scharf, U.: Use of the Seismic Receiver Chain SEKAN 5 within the Framework of Integrated Seismics in the Oberpfalz	159
Gebrande, H., Bopp, M., Meichelböck, M. and Neurieder, P.: 3-D Wide-Angle Investigations in the KTB Surroundings as part of the "Integrated Seismics Oberpfalz 1989 (ISO89)"	183



Introduction to ISO 89

H.-J. Dürbaum

INTRODUCTION TO ISO 89

Hans-Jürgen Dürbaum

Only at the end of January 89 the decision was finally made by the Federal Ministry of Research and Technology (BMFT) to support the complete programme of the so-called Integrated Seismic Experiment Oberpfalz (ISO) 89. This ended a long discussion on the priorities of the various experiments which had been proposed, and - at least for some time - on the value of a 3-D reflection seismic survey of an area around the KTB pilot hole. Fig. 1 lists in the form of a matrix the various seismic experiments on one side and the objectives on the other side indicating where contributions are hopefully expected. Details of the technical realisation are described in the following contributions by authors from the various groups of scientists involved, together with first results as they have been obtained so far. The timetable of the experiments as actually performed is given in fig. 2. One of the important instruments needed for the ISO 89 was a chain of five 3-components-geophones called SEKAN 5, supplied by PRAKLA-SEISMOS the performance of which has been described in an additional paper of this report. As such a long-time use of a chain of geophones is quite unusual in the exploration industry much experience has been obtained during ISO 89, and during the second half of the experiment its performance has been quite satisfactory.

Smoothly carrying through such a complex combination of observations together with the 3-D seismic survey in an area of difficult topography and widely covered with forests- and this practically in time with only few days of delay - is mainly due to the efficient work of Horst SCHWANITZ and his crew of PRAKLA-SEISMOS and his good cooperation with all the other groups involved, but also to the untiring assistance of Christian REICHERT and Johannes SCHMOLL of the DEKORP Project Management. This is gratefully acknowledged. I also thank all the others involved in ISO 89 for their excellent work and cooperation hoping that the results will be worth the joint efforts.

Authors' Address: DEKORP Project Management, Niedersächsisches Landesamt für Bodenforschung, Stilleweg 2, D-3000 Hannover 51

EXPERIMENTS OBJECTIVES	3-D	"Durchschallung"	3-D Expanding Spread	Shear wave Common Midpoint Profiling	Vertical Seismic Profile	Moving Source Profile	Multiple Azimuth Shear wave Experiment	Wide-Angle experiment
Exploring complex 3-D structures	X							
Mapping of steeply dipping elements	X				X	X		
High resolution mapping of structures in space					X	X		
Identification of reflecting elements in KTB boreholes	X				X	X		
Extension of the "Erbendorf-Body" in space	X							X
Dip of fault planes of the Franconian Line	X							X
Azimuth of joint systems, stress components							X	
3-D velocity structure		X	X				X	
Anisotropy of elastic properties		X	X				X	
Conclusion on lithological properties				X	X			X

Abb. 1: Objectives of ISO 89 and related experiments.

INTEGRATED SEISMICS OBERPFALZ 1989

Time table of the actual performance

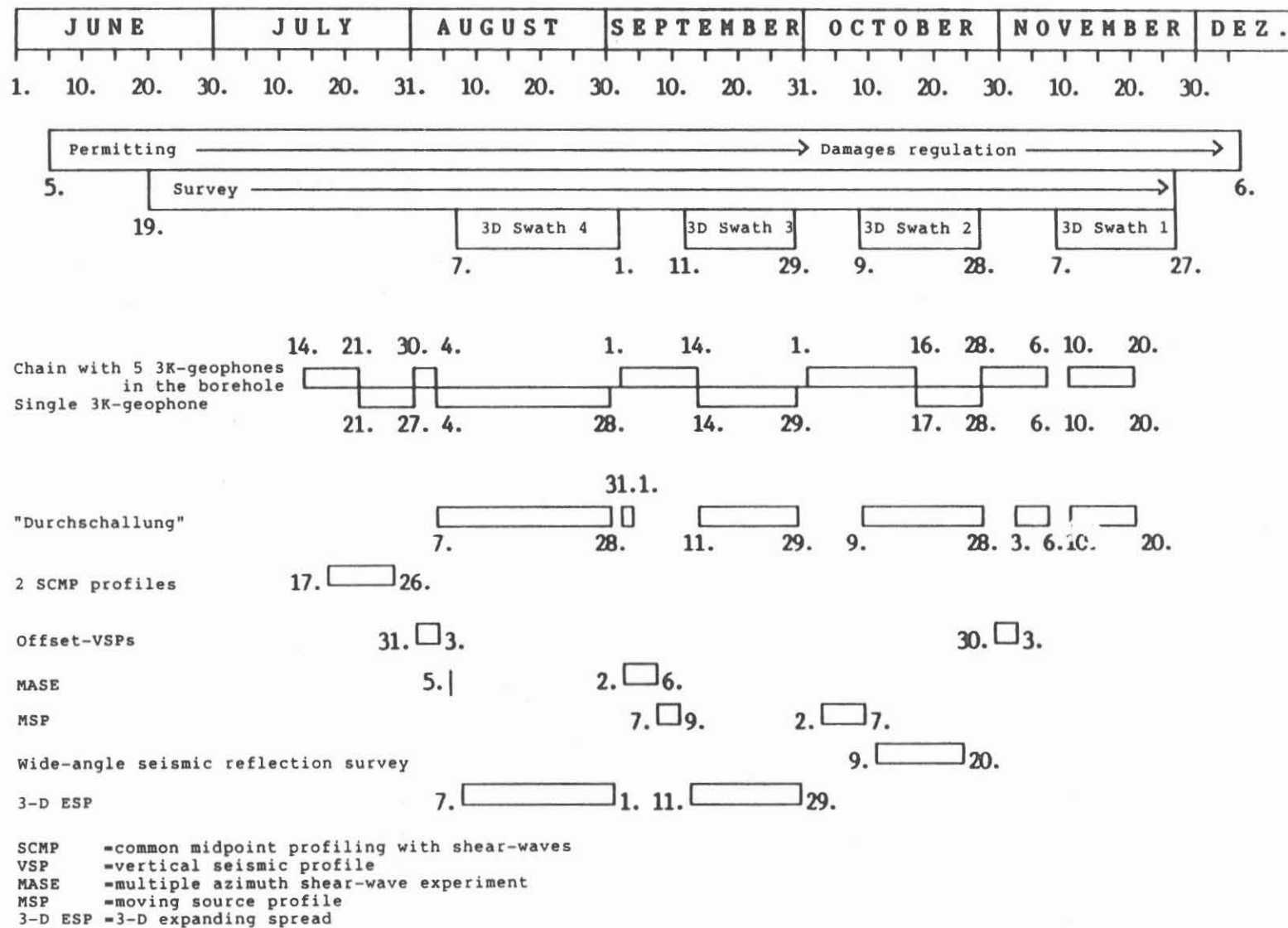
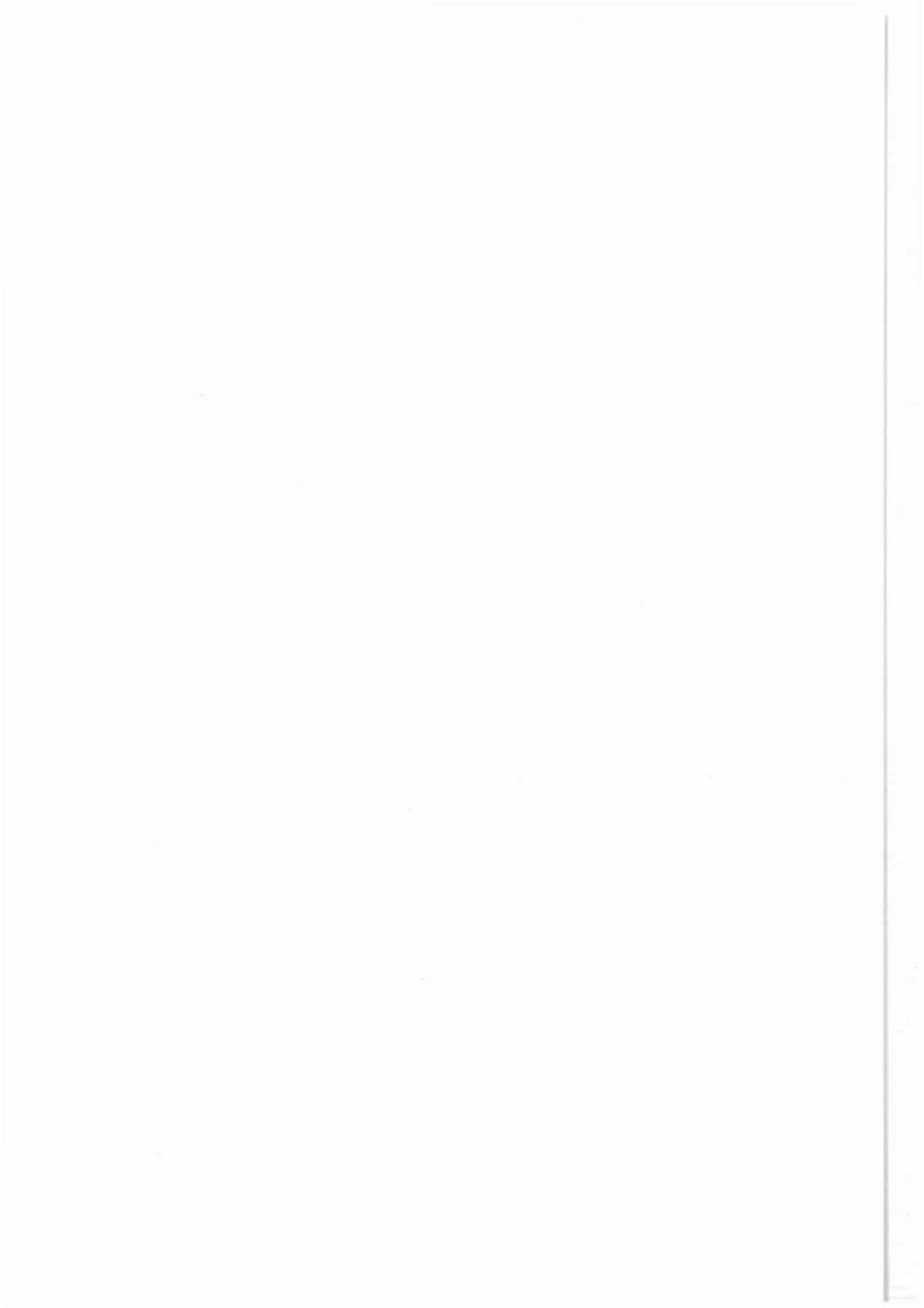


Fig. 2: Time table of ISO 89.



3-D Reflection Seismic Survey
of the Area around the KTB Drilling Site

M. Stiller
J. G. Rehling



3-D Reflection Seismic Survey
of the Area around the KTB Drilling Site

J.G. Rehling & M. Stiller

Abstract:

A brief description is given of the field geometry of the 3-D reflection seismic survey of the area around the KTB (Continental Deep Drilling Project) borehole site and the initial processing results of the DEKORP Processing Center (DPC) in Clausthal. This survey was the main part of the experiment ISO '89 (Integrated Seismics Oberpfalz). The objectives and the resulting array set-up are discussed, as well as the planned course of the survey. The problems of the actual survey and their solutions are then described.

The parameters needed for processing the survey data are discussed: geophone groups, shot points, seismic traces, data and bins, CDP distribution, offset and angle distributions. The geology, topography, and the technical data for the survey are presented.

The SSL software system for 3-D processing is briefly introduced. The processing steps for handling the geometry and the checking of the data are discussed as well as the planned processing sequence. An example of the raw data is given in which the reflections from the Erbendorf structure can be distinctly recognized.

Authors' address: DEKORP Processing Center,
Institut für Geophysik der Technischen Universität Clausthal,
Arnold-Sommerfeld-Str. 1, D-3392 Clausthal-Zellerfeld

1. The Survey Area and Planning of the Field Work

The objective of the 3-D seismic survey of the area around the KTB borehole site is to extend the results of the KTB pilot borehole to the surrounding area and clarify the relationships between the geological structures. This seismic survey connects the previously surveyed profiles DEKORP 4 and KTB 8502 with the pilot borehole, making it possible to directly determine the physical and lithological properties of the reflectors in the crystalline basement, permitting predictions for the main KTB borehole, which is to be begun in September 1990. ISO '89 as a whole was conducted within the framework of DEKORP (Deutsches Kontinentales Reflexionsseismisches Programm) and financed by the BMFT (Federal Ministry for Research and Technology).

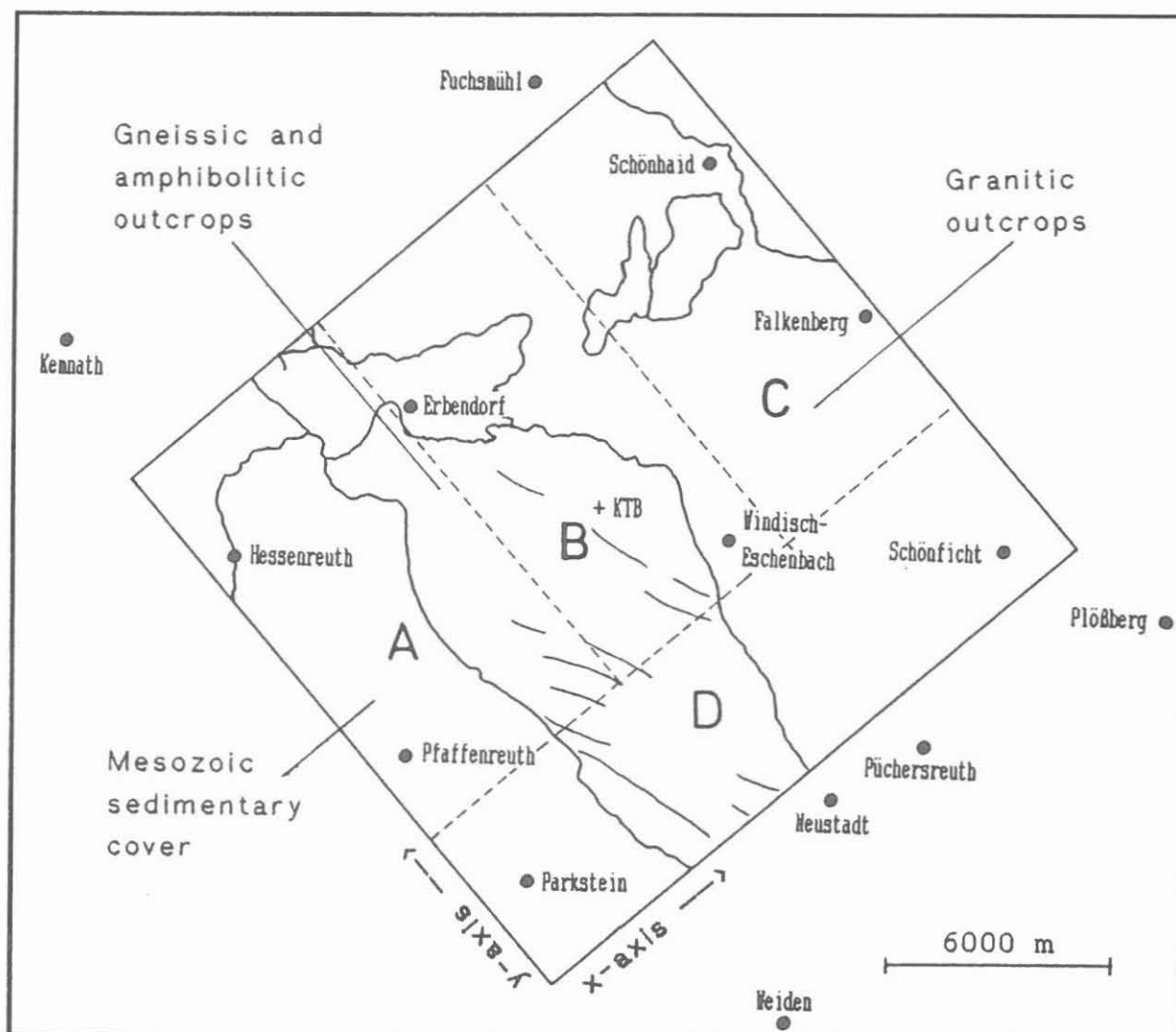


Fig. 1: Location map; A, B, C, & D = subareas for processing

The approximate center of the survey area of about 20x20 km was the KTB drilling site near Windischeschenbach (Fig. 1). The area can be divided geologically into two subareas. In the northeast the basement has a high seismic velocity and extends up to ground level. In the southwest, mesozoic and paleozoic sediments with mainly low velocities extend to a depth of up to more than 3 km. These two areas are separated by the Franconian Line, which passes through the area from NW to SE. For processing, the survey area had to be divided into four subareas of about equal size because disk capacity was not sufficient to process the area as a whole.

The array set-up was designed by H. Horstmeyer and M. Stiller, together with Professors Bortfeld and Krey, at the DPC Clausthal. Required was a 12 - 15-fold coverage for a minimum volume of about 10x10x10 km after migration. Two types of single array set-ups (type A and B) were used, differing only in the sequence of shot point separations (Fig. 2). The two types were alternated so that the shot points of the one set-up were opposite the gaps between shot points of the other (please note that in seismic processing the denotation 'shot' is commonly used even when it was a 'vibration' in reality). Each set-up consisted of 10 geophone lines each with 48 geophones groups. The distance between geophone lines was 400 m, the geophone group centers were placed 100 m apart. The shot point lines were laid out perpendicular to the geophone lines, an arrangement called a cross array.

The shot point lines were 8 km long (defined as parallel to the y-axis) with 40 shot points each. The shot locations were spaced in a recurring pattern of 200 m, 300 m, 200 m, 100 m. For each swath of 10 geophone lines across the entire survey area (parallel to the x-axis) there were 21 shot point lines 800 m apart, giving a total of 840 shot points. Four swaths of 10 geophone lines were needed to cover the survey area, giving 3360 shot points. Because the shot point lines overlap by 20 shot points, each line contains 100 shot points. Thus, 60 % of the shot points were in two groups of geophone lines and only 2100 different shot locations were necessary. The theoretical source-receiver offsets were between 72 and 6212 m.

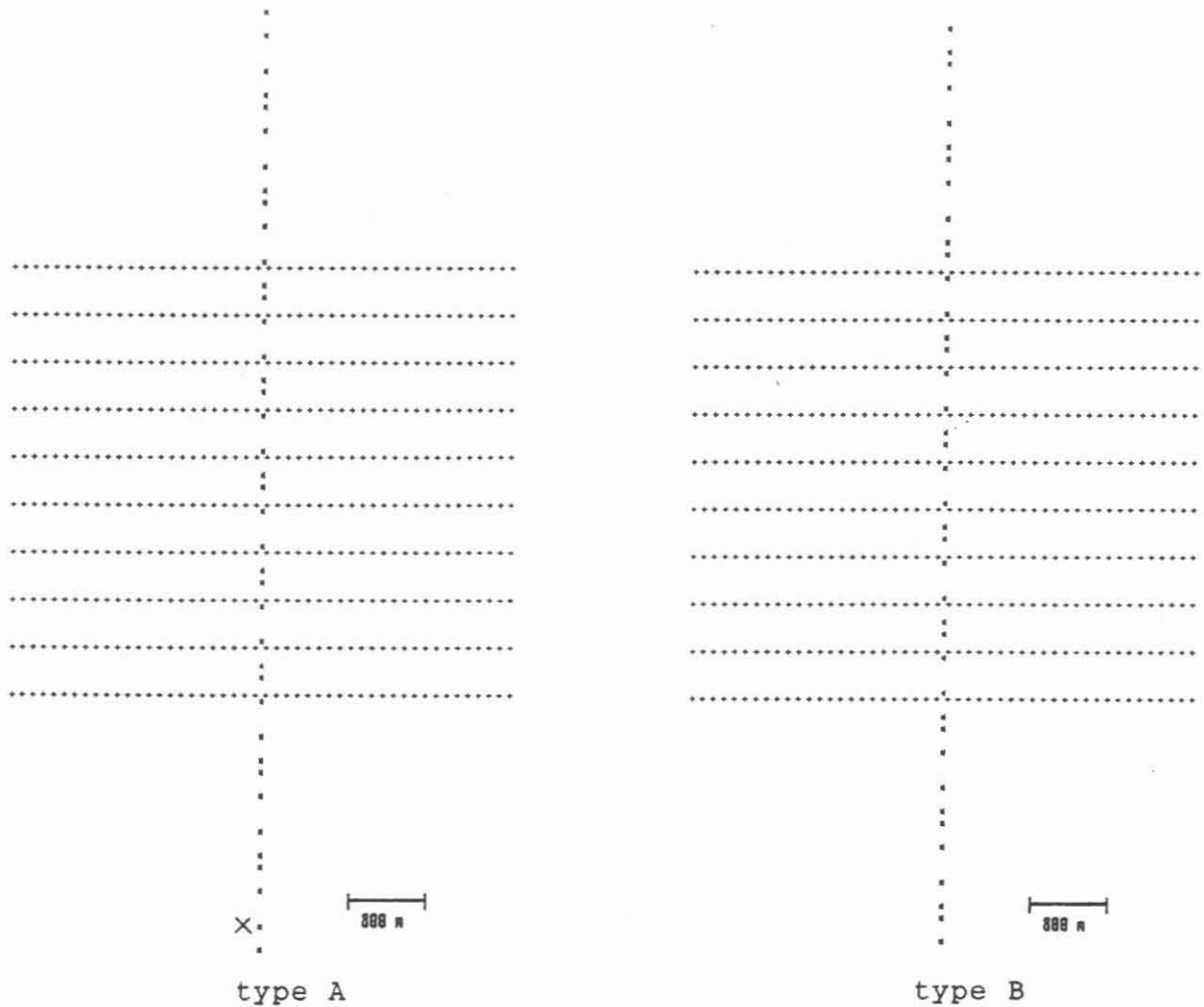


Fig. 2: Array set-ups
vertical : shot point lines
horizontal: geophone lines
X : see chapter 5.

The Franconian Line separates a crystalline basement area in the northeast from a sediment area in the southwest. The large difference in velocities between these two areas presented a problem for the orientation of the array.

Generally, the largest offsets should be in the direction of strike so that minimum offset-dependent travelttime errors are obtained during processing. These errors are difficult to correct for and would lead to inexact values for the stacking velocities or even make it impossible to determine them. However, the strike was not uniform throughout the area; it could be distinctly observed only locally and changed with depth.

In order to minimize traveltimes problems, it was agreed to choose the direction of the Franconian Line for the orientation of the array. Because the maximum offsets in the array set-up used for this survey are in the direction of the shot point lines, these lines had to be arranged parallel to the Franconian Line. Thus, the shot point lines were laid out NW-SE (323.2°), the geophone lines aligned NE-SW (53.2°).

With this survey scheme, an area of 17.8×18.4 km was covered with one-fold coverage or more and an area of 14.4×15.2 km was covered 15-fold. The variation of the coverage is shown in Figure 3. The theoretical shot and geophone locations are shown in Figure 4. An advantage of this array set-up is that already the seismic traces in the offset range of 0 - 850 m provide one-fold coverage of nearly the entire area (Fig. 5). Taking initial trace muting into consideration, there will be full coverage after about one second of traveltimes.

To calculate the subsurface coverage, the area was subdivided into 50×50 m squares (the so-called bins). The reason for this bin size is that the best resolution is 50×50 m, resulting from the geophone group spacing of 100 m. Thus, the 17.8×18.4 km area contains a total of 131,008 bins (356×368) and the 14.4×15.2 km area with 15-fold coverage contains 87,552 bins (288×304), which corresponds to 66.8 % of the total area.

An area of 2.4×5.8 km is covered by a type A array. Owing to its different shot point sequence, the type B array covers an area of 2.4×5.7 km. A single array set-up provides a maximum of 5-fold coverage. Thus, three set-ups, shifted 800 m along the geophone line (i.e. along the x-axis), are needed to obtain the desired 15-fold coverage.

A group of ten geophone lines was surveyed for 21 shot point lines (i.e. one swath). The equipment was then moved 4 km along the y-axis and the process repeated (Fig. 6). In this way the required 15-fold coverage was obtained at the overlapping edges of adjacent swaths. Neighboring shot point lines alternated between type A and B in order to guarantee a homogenous distribution of small offsets.

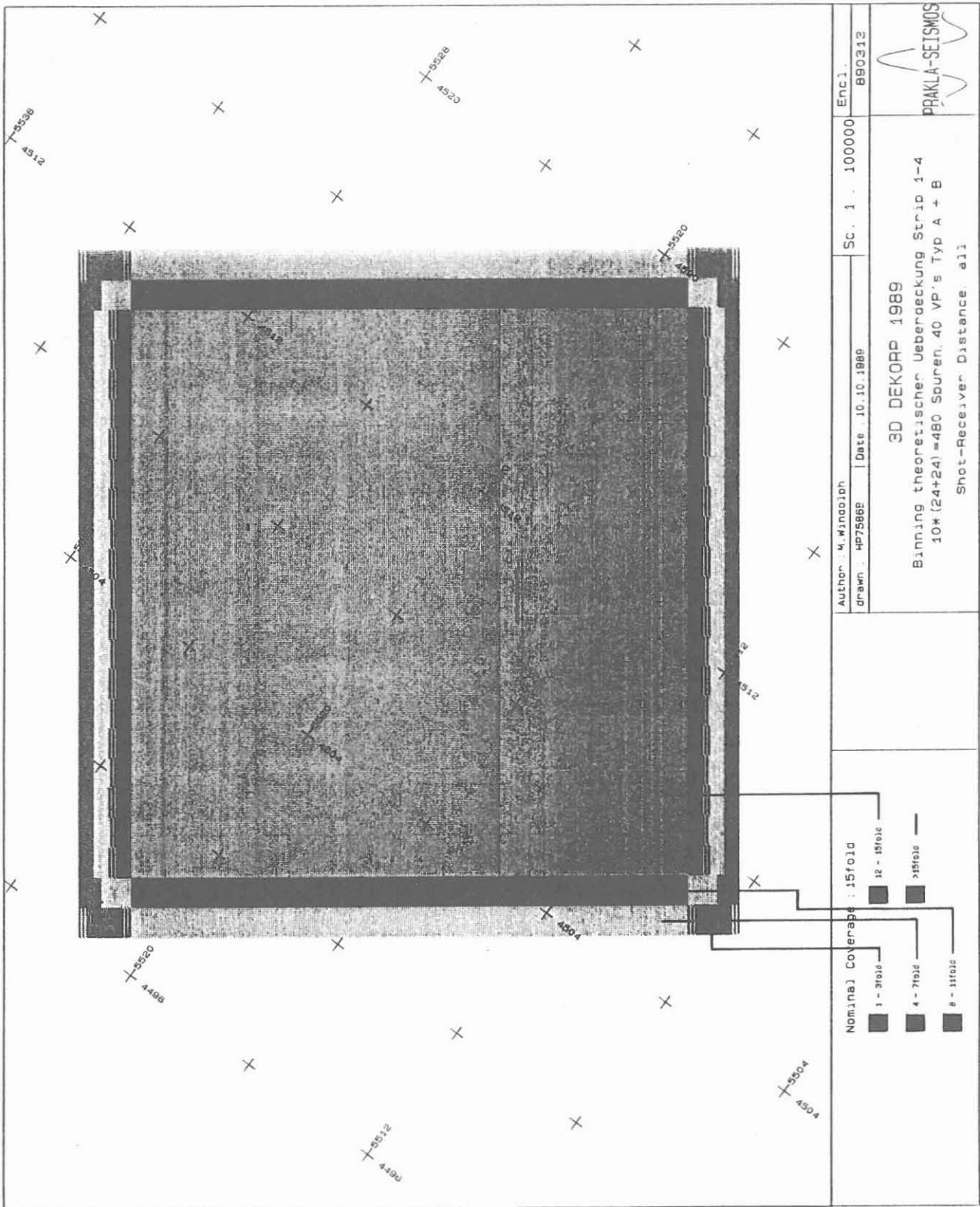
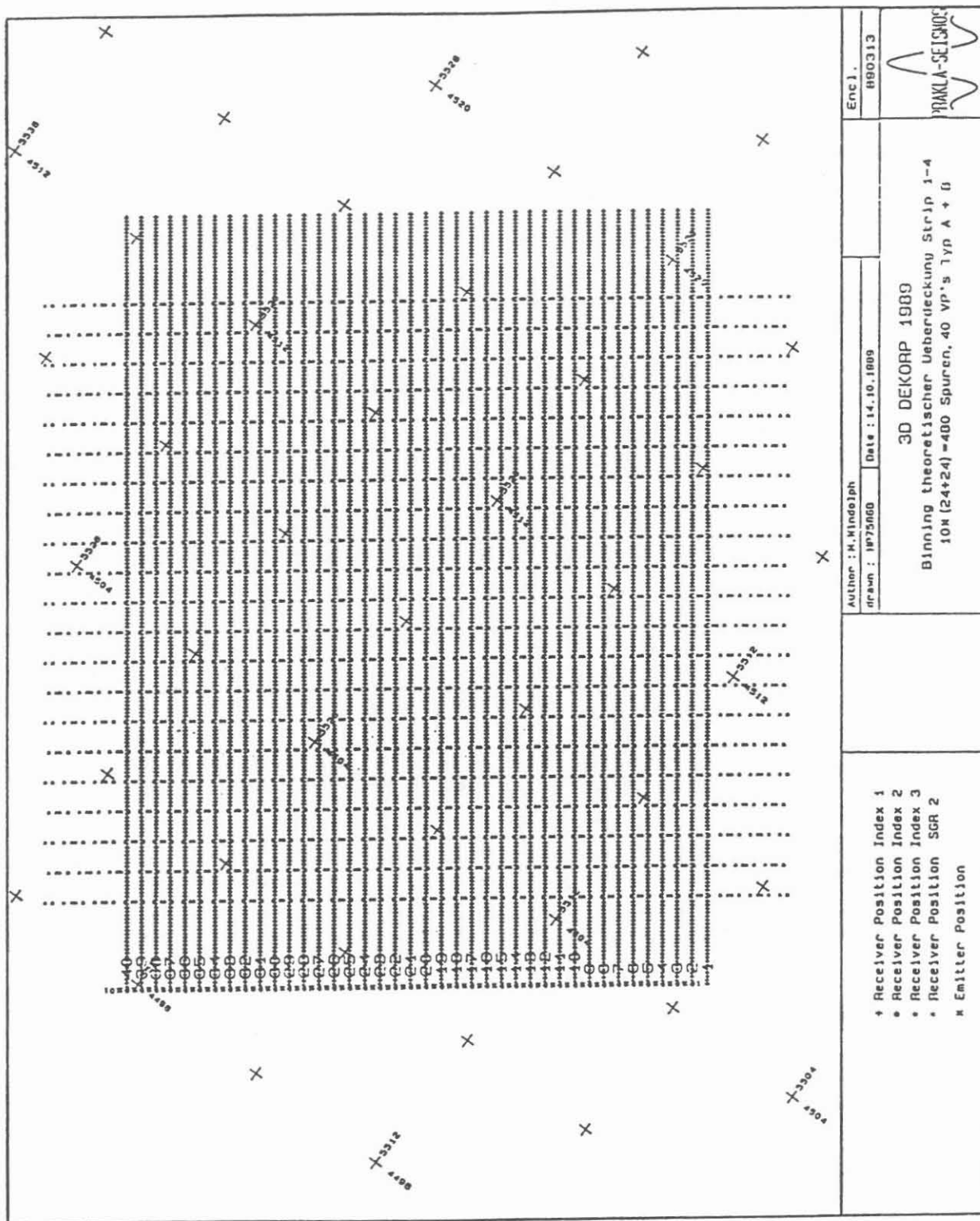


Fig. 3: Theoretical coverage, all source-receiver offsets
 (prepared by Prakla-Seismos AG)



Author : K. WIndelph (drawn : 1975/60)		Date : 14.10.1989	
3D DEKORP 1989 Binning theoretischer Ueberdeckung Strip 1-4 10x (24+24) = 480 Spuren, 40 VP's Typ A + U		Enc 1. 890313	
+ Receiver Position Index 1 • Receiver Position Index 2 • Receiver Position Index 3 • Receiver Position SGR 2 x Emitter Position		PRAKLA-SEISMOS	

Fig. 4: Theoretical shot and geophone locations
 (prepared by Prakla-Seismos AG)

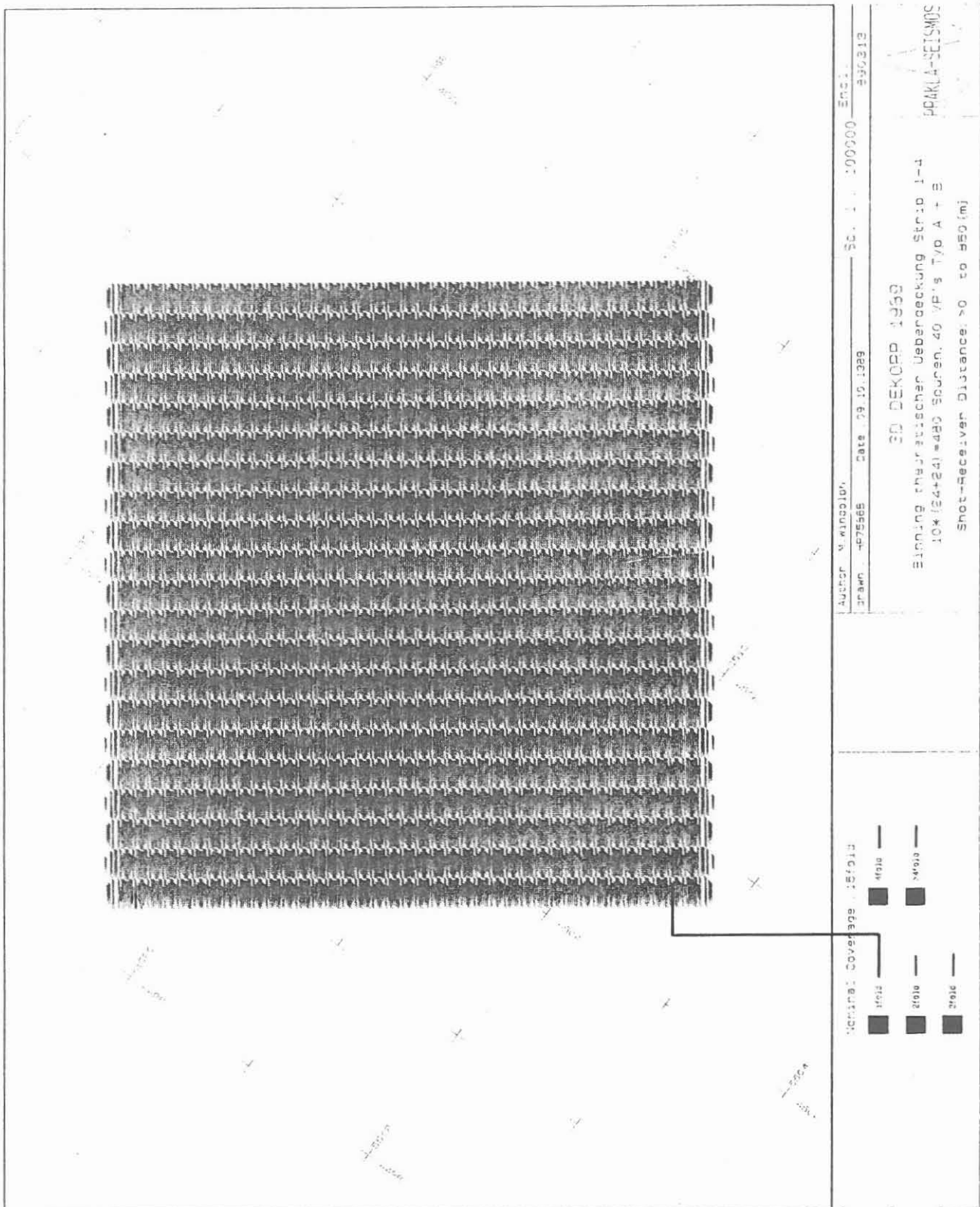


Fig. 5: Theoretical coverage, shot-receiver offsets 0 - 850 m
(prepared by Prakla-Seismos AG)

21 shot point lines

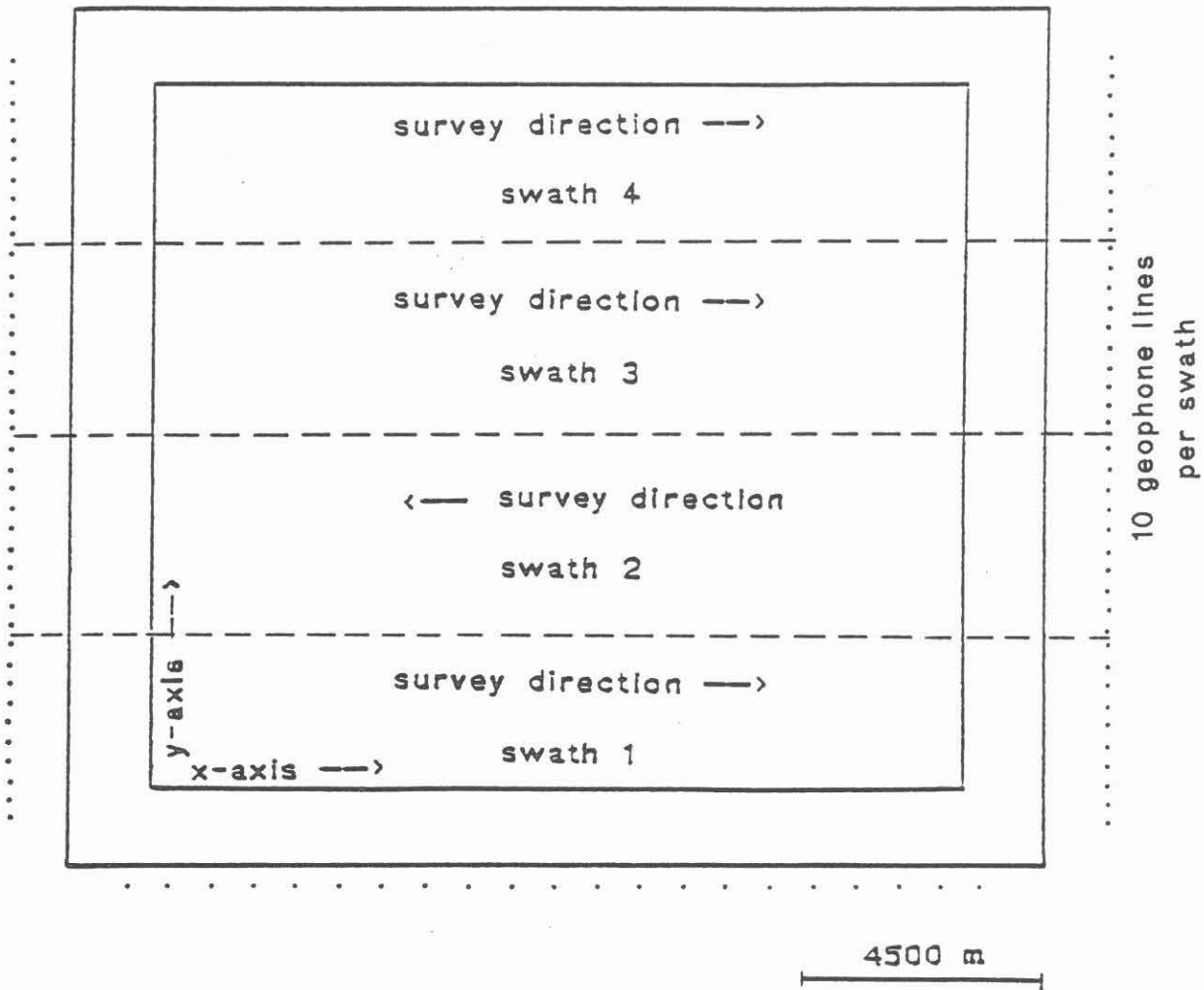


Fig. 6: Scheme for carrying out the survey

With a theoretical number of 3360 shots with 480 channels each, 1,612,800 seismic traces are possible. It is known from experiences in 2-D vibroseismics that not any shot point is realizable in this kind of area. Owing to the used frequency range of the sweep, it is not possible to vibrate within villages, and a lot of forest-roads and field-paths is not practicable with vibrators. With an estimated loss of 20 %, at least 1,290,240 traces could be expected. The survey was planned to be completed within 70 work days in late summer and fall of 1989 (Aug. 7 - Nov. 15).

2. The Survey

The field work was carried out by Prakla-Seismos AG. The seismic work was done from August 7 to November 21, topographical surveying was started one month before. A reflection time of 12 s with a sampling rate of 4 ms was recorded on a 480 channel SERCEL SN 368 via telemetry. The seismic vibrations (up-sweep 12 - 48 Hz, length 20 s) were produced by five vibrators. The vertical stacking varied between five- and eight-fold.

To carry out the scheme shown in Figure 6, detailed knowledge of the survey area was necessary. Because only a few of the theoretical shot locations could be reached with the vibrator trucks, the main problem was to find the most appropriate substitute sites. The area was visited for several weeks in early 1989 to locate (and mark on a 1:25 000 topographic map) all tracks that could be driven with vibrators.

In Clausthal these maps were then placed on a digitizing table so that an interactive program prepared by DPC staff members could be used to determine the suitability of all reachable sites as substitute shot locations. These substitute sites were then plotted on topographic maps.

Thus, it was possible to specify all 2100 shot locations before the field work was started and to guarantee by performing a full pre-binning that the desired coverage could be obtained in all bins. These topographic maps were also the base maps for the surveyors in the field. There were two requirements for all surveyed sites:

- (a) The difference between the planned and actual shot locations was not to exceed 35 m in order to achieve placement of the reflection points within the proper bin.
- (b) The survey results had to be influenced as little as possible by unavoidable last-minute shifts in shot point sites.

These two aspects were not critical for the geophone positions, which are not dependent on the road net. But despite thorough preparatory field work, a number of shot points had to be shifted on the spot, e.g. due to road construction work, forestry work, harvesting, danger of damage to fields, presence of pipelines or nearby houses.

Thus, it was necessary for two staff members of the DPC to accompany the field work to optimize any last-minute shifts in shot points. One of their tasks was to check that the coordinates of all sites marked in the field by the surveyors corresponded to the planned positions. If the deviation was more than 35 m, the point had to be resurveyed and rechecked until all seismic traces were within the proper bin. The geophone locations were handled just as carefully, ensuring that all of the source and receiver positions were properly sited before the seismic records were made.

A further task of the two Clausthal staff members was to check whether the set-up of the geophone groups was done properly. A geophone group contained 18 geophones arranged in the shape of a 3-vane fan (Fig. 7). This arrangement allows the suppression of surface waves from all directions.

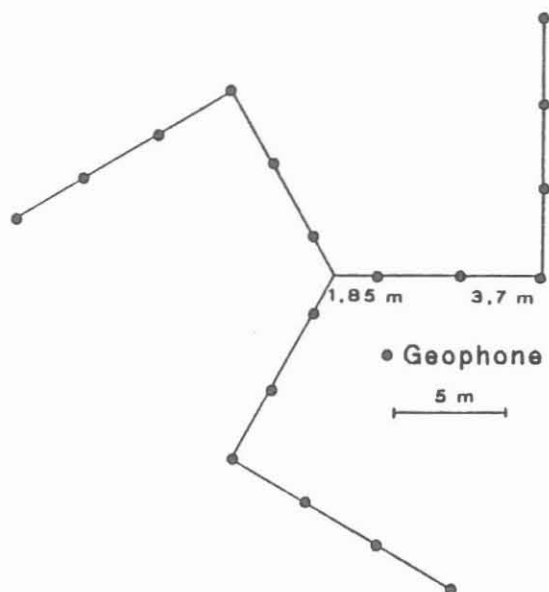


Fig. 7: Geophone group, arranged in a 3-vane fan

Wherever possible, shot points were shifted only laterally and changes in the in-line coordinates were avoided. The necessity for this is clear if the effect of shifting a shot position on the results is understood:

(a) Lateral shift (Fig. 8):

Shifting a shot point 100 m perpendicular to the shot point line will result in loss of a trace in each of 10 bins on one side (black) and addition of an undesired trace in each of 10 bins on the other side (hatched) of the area covered by a single array set-up. Thus, for a single use of this shot position there is a change in 20 bins, for a double use there is a change in 40 bins. The number of affected bins changes proportionally to the distance of the shift.

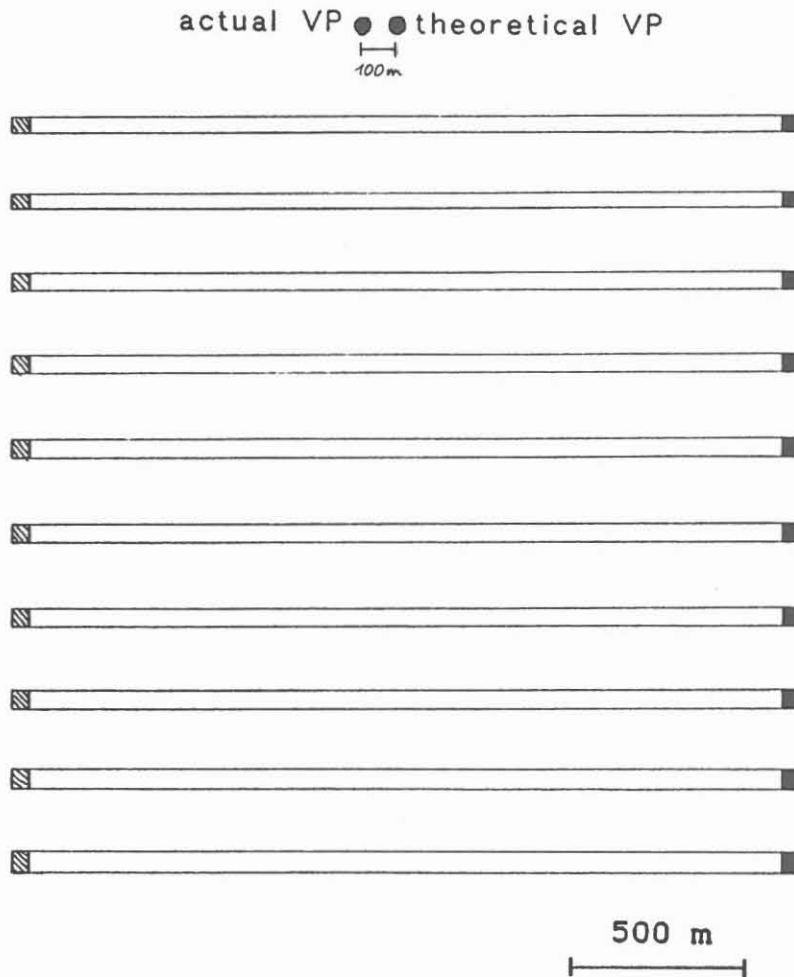


Fig. 8: Effect of a lateral shot point shift

(b) In-line shift of 50 - 350 m (Fig. 9):

If the shot point is shifted along the shot point line 100 m, for example, 48 bins per geophone line will lack a trace (black) and 48 bins per geophone line will have an additional trace (hatched), i.e. a total of 960 affected bins for a single use of this shifted position or 1920 bins for a double use, which is nearly 50 times more than for a lateral shift of 100 m.

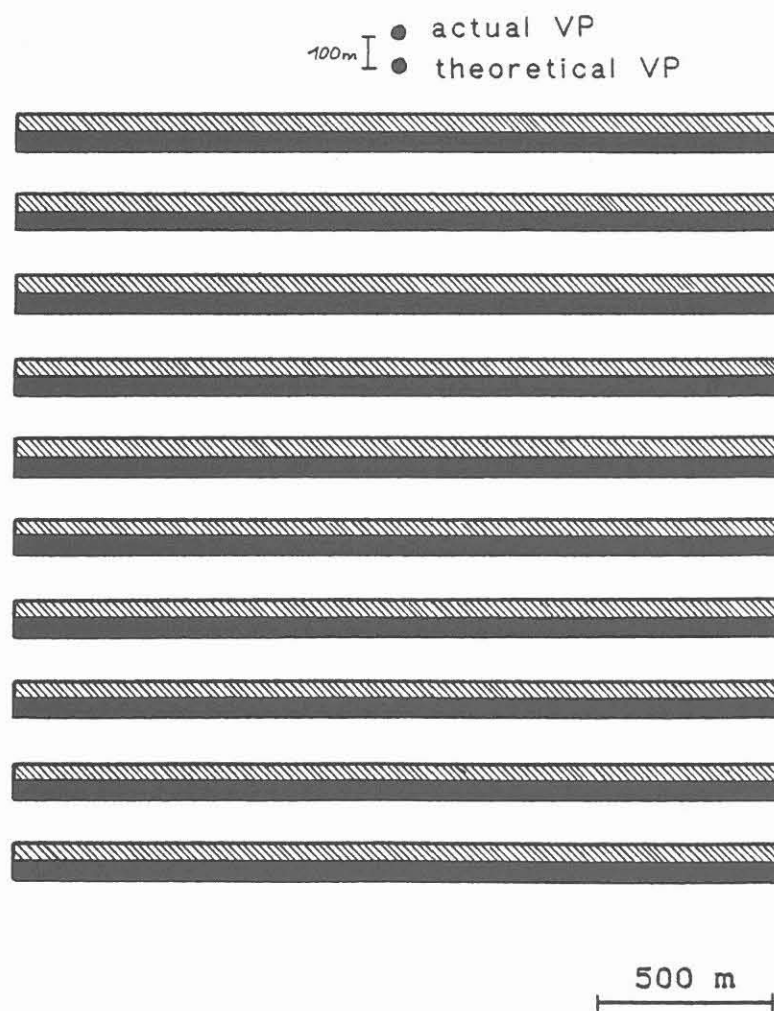


Fig. 9: Effect of an in-line shift of 50 - 350 m

(c) In-line shift of 350 - 450 m (Fig. 10):

For an in-line shift of 400 m, for example, the number of affected bins is reduced to 96, because most of the reflection points are again in the proper bin. On one side of the covered area there will be 48 bins in which a trace is lacking (black) and on the other side 48 bins will have one trace too many (hatched). All the other bins will have the proper number of traces. For double use of this shifted shot point, 192 bins will be affected, which is about 5 times more than for a lateral shift of 100 m.

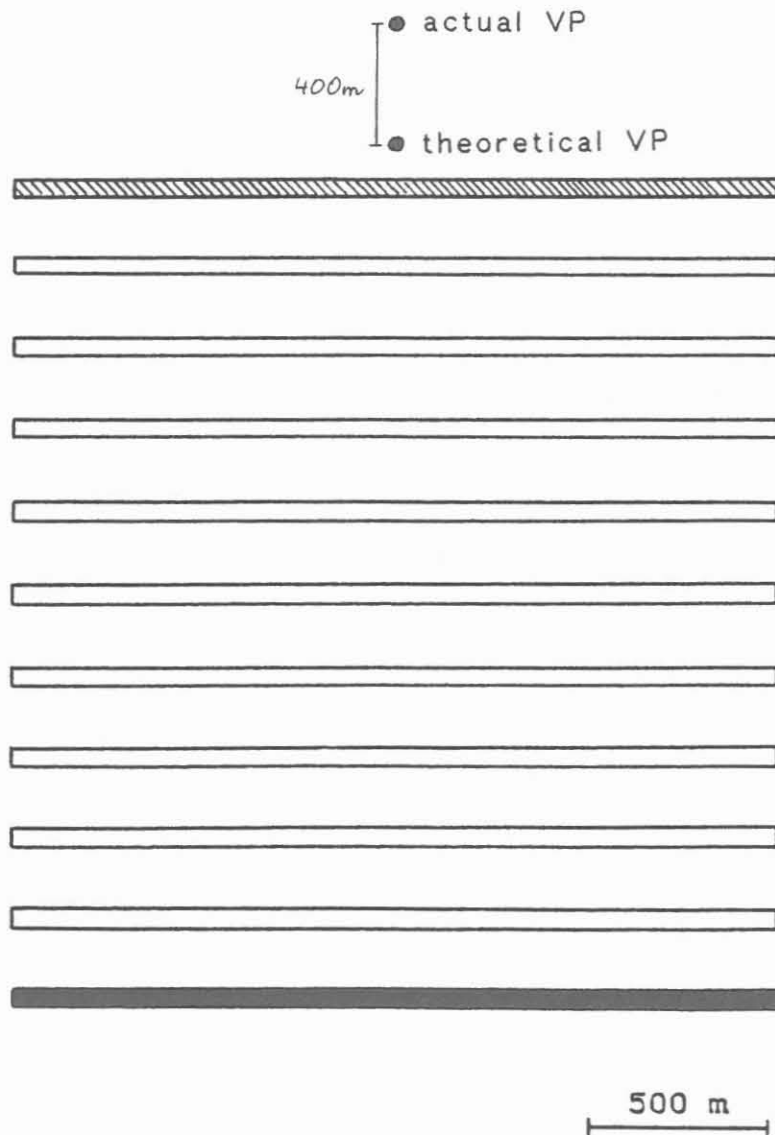


Fig. 10: Effect of an in-line shift of 350 - 450 m

Thus, in order to hold the number of changed bins to a minimum, it was necessary to permit only lateral shot point shifts as far as possible. It was better to allow a relatively large lateral shift than a rather small in-line shift.

A further consideration was that a clear bin assignment should be possible after the shift. This is illustrated in Figure 11. Let us assume that shot point A is to be shifted. For the theoretical shot position, the reflection points are in the middle of each of the marked bins. For a shift of less than 35 m, i.e. within the gray square, the reflection points fall within the white squares of the marked bins and are thus clearly within the bins. For a larger shift, the reflection points would be too close to the edge of the marked bins.

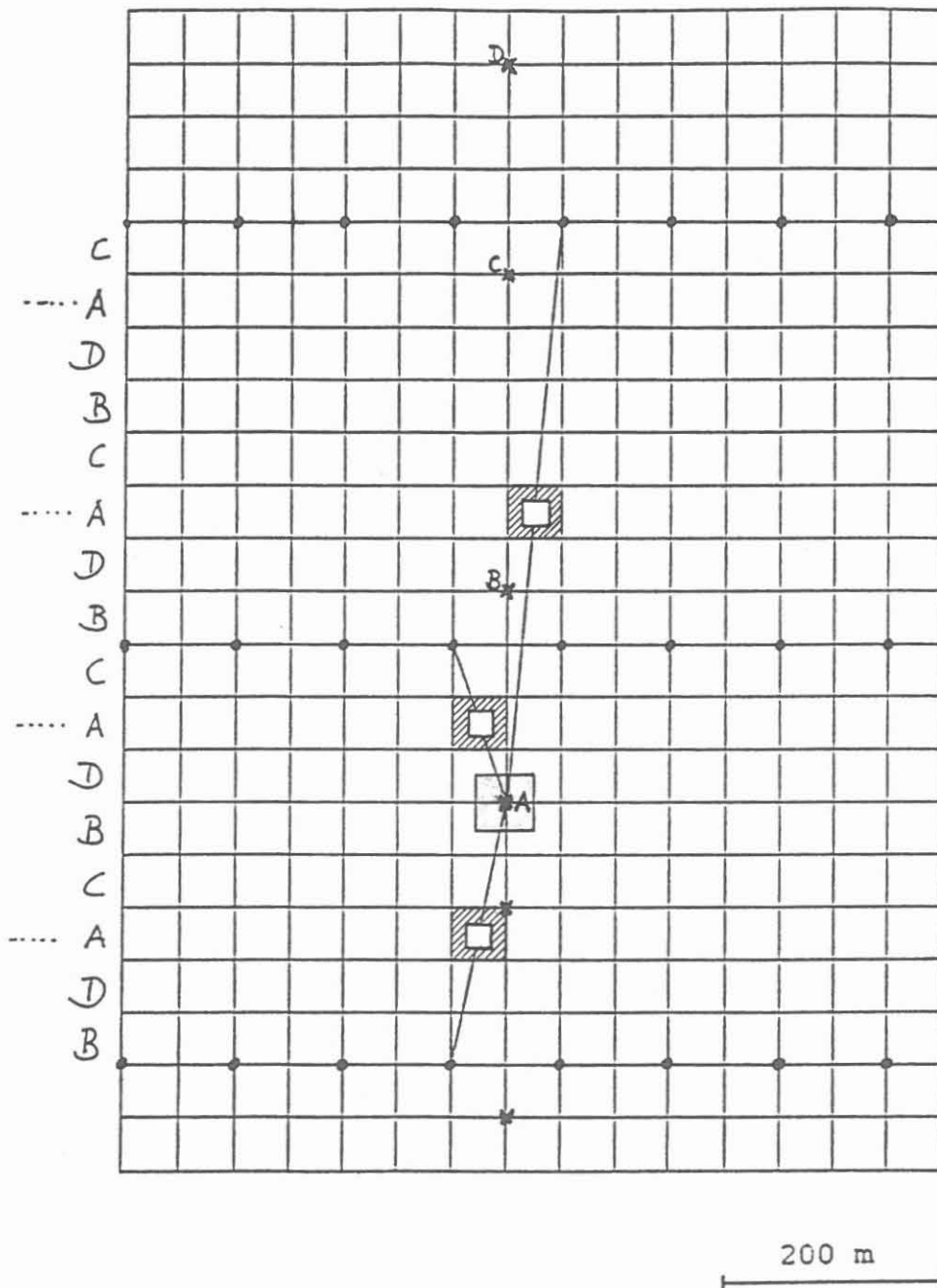


Fig. 11: Bin assignment for a shift of less than 35 m

To make sure the shifts are unambiguously within the proper range, a forbidden zone ($n+25$ to $n+75$ m) and an allowed zone ($n+75$ to $n+125$ m) were introduced, where $n = 0, 100, 200$ m, ... These zones can be recognized by the irregular shape of the histogram of the lateral offsets of all 3327 shots. Of the 3309 necessary lateral shifts, 1431 positions were in forbidden zones and 1878 in allowed zones (Fig. 12). Of the 3319 in-line shifts, only 17 were greater than 50 m, 3229 were less than 35 m, i.e. within the range for which bin assignment is unambiguous. Thus, only 90 in-line shifts, 2.79 % of all shot point shifts, were in a problematic range (Fig. 13).

In the field, a transparent sheet was used to recognize allowed and forbidden zones on the map. This was useful when it was necessary to make shot point shifts on the spot. By working closely with the surveying team and the field supervisor, nearly all of the 2100 shot locations were positioned so that the desired 12 - 15-fold coverage was obtained in almost all of the bins. In a small number of bins up to a 19-fold coverage was attained (Fig. 14). This happened when the shifts caused neighboring shot point lines to be rather close together. On the other hand, increased shot point line separations resulted in bins in which the 12 - 15-fold coverage was not obtained.

A good approximation of the desired at least one-fold coverage for source-receiver offsets of 0 - 850 m was also obtained (Fig. 15). This is even more surprising when it is considered that the actual shot and geophone locations (Fig. 16) are seldom close to the theoretical ones shown in Figure 4.

Instead of the planned 480 channels per shot, only 478 were recorded because the field correlator had a storage capacity for only this number of traces. Thus, always the first two geophone groups of each single array set-up were disconnected. Instead of the planned overall 8-fold vertical stacking, only 5-fold stacking was done for some of the shot points between the geophone lines. In a few cases at particularly vulnerable sites (gas lines, dikes, etc.) only three vibrators with lower energy output were used instead of the planned five vibrators.

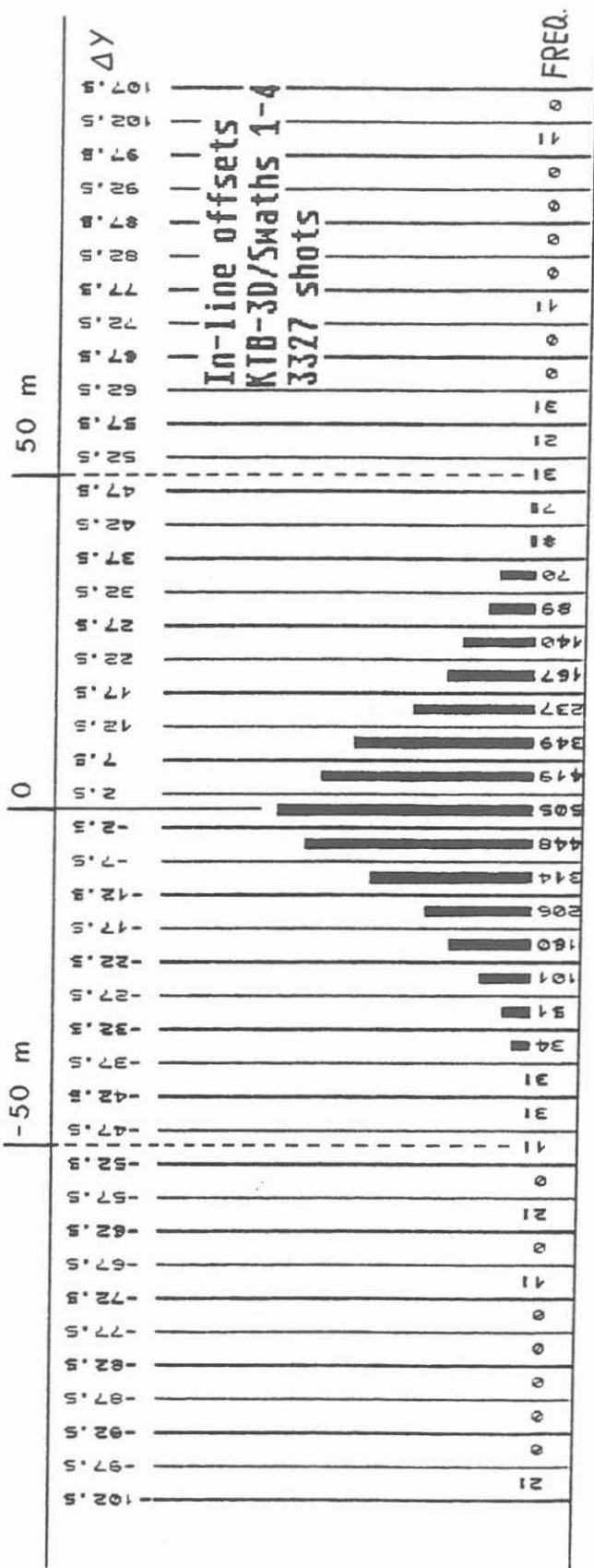
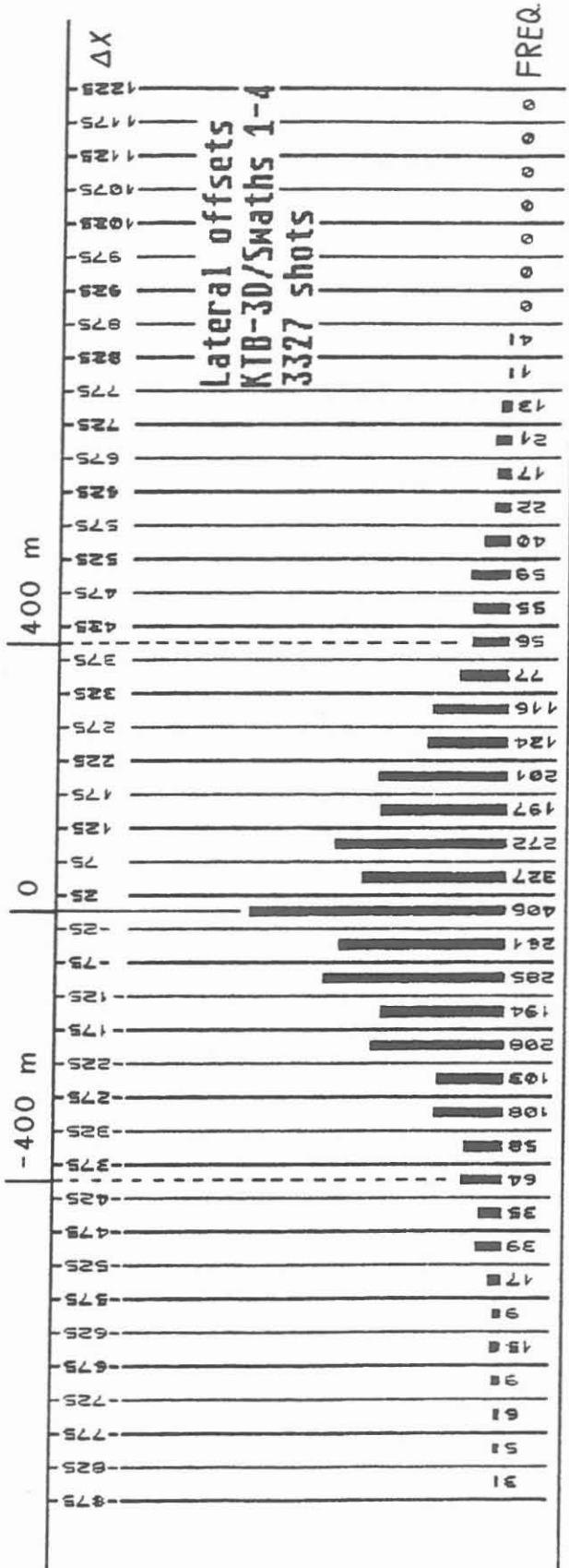


Fig. 12: Lateral offsets

Fig. 13: In-line offsets

Histograms of the lateral and in-line offsets for the KTB 3-D seismic survey, swaths 1 - 4 (3327 records)

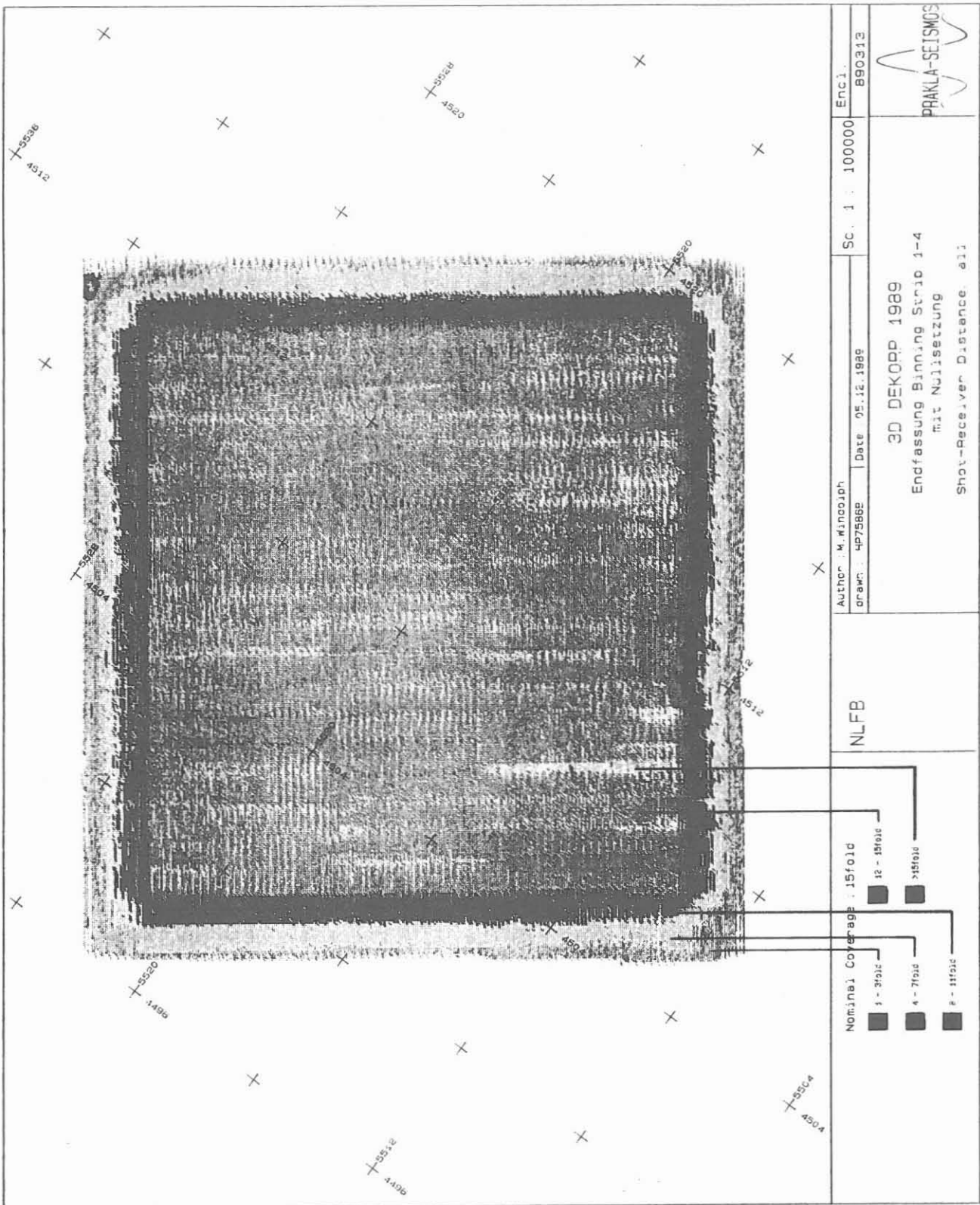


Fig. 14: Actual coverage, all source-receiver offsets
 (prepared by Prakla-Seismos AG)

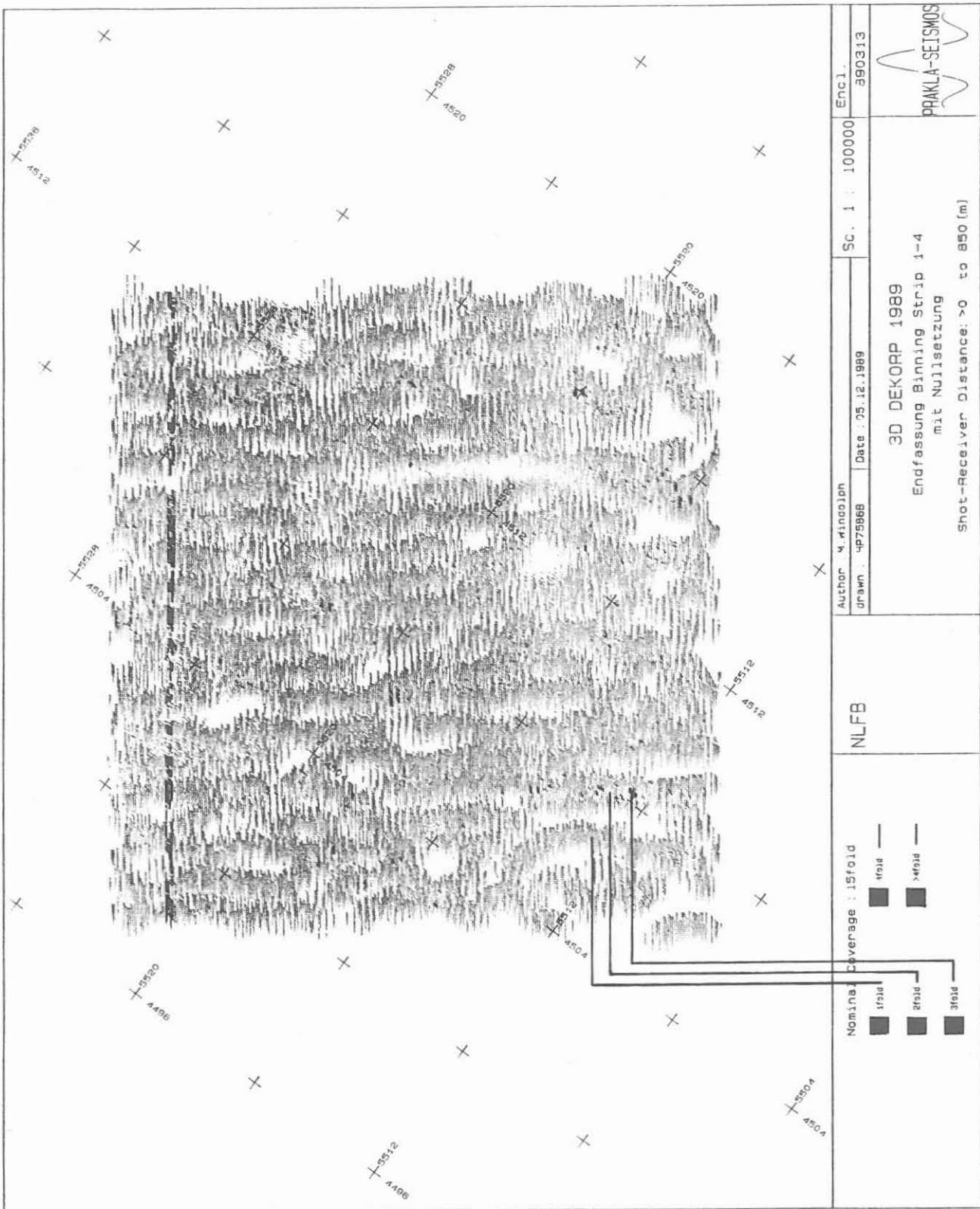
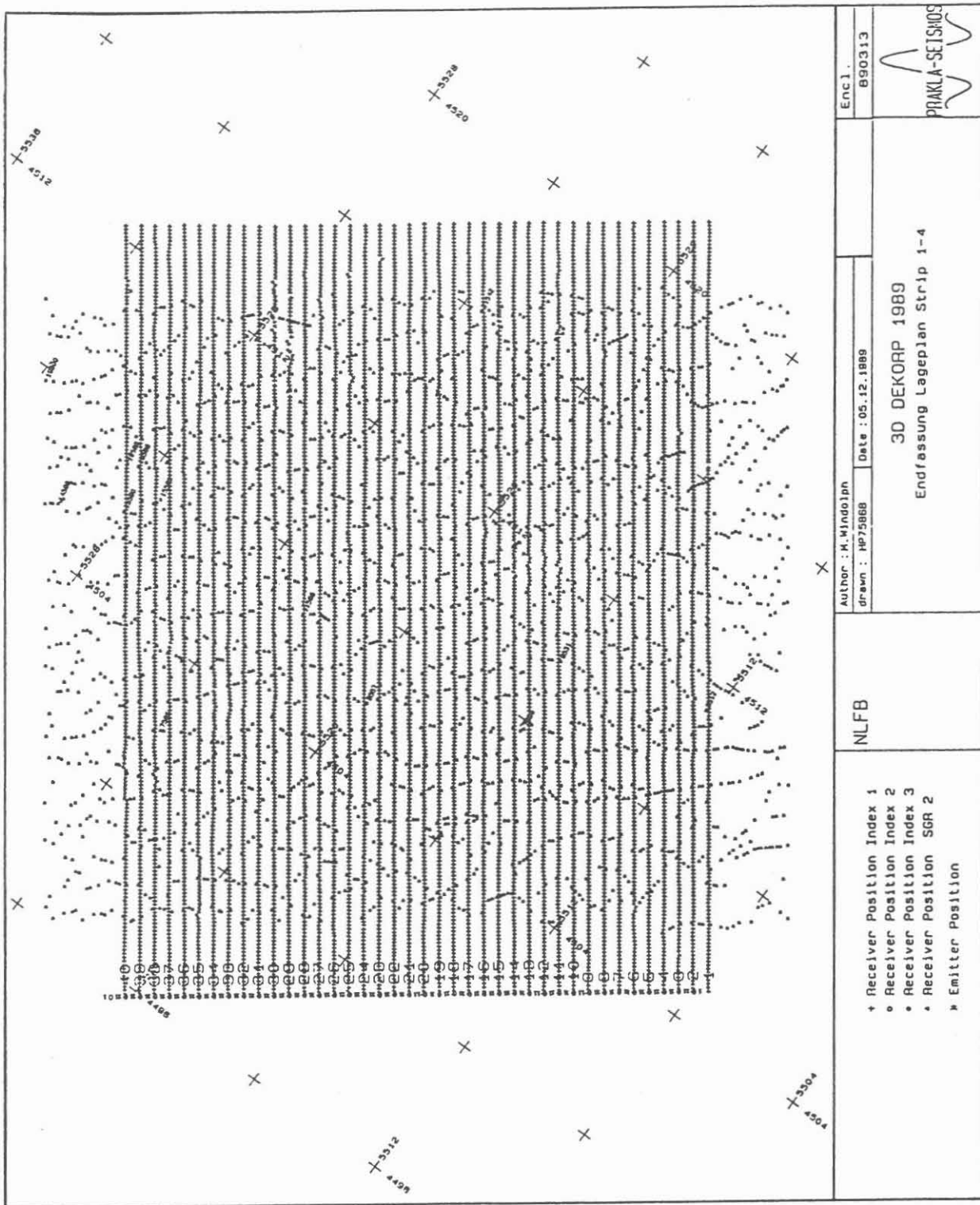


Fig. 15: Actual coverage, source-receiver offsets 0 - 850 m
(prepared by Prakla-Seismos AG)



NLFB	Author : H. WINDOLF	Date : 05.12.1989	ENC 1
	drawn : HP75868		B90313
3D DEKORP 1989 Endfassung Lageplan Strip 1-4			PRAKLA-SEISMOS
† Receiver Position Index 1 ○ Receiver Position Index 2 ● Receiver Position Index 3 * Receiver Position SGR 2 ✱ Emitter Position			

Fig. 16: Actual shot and geophone locations
(prepared by Prakla-Seismos AG)

Because special situations had to be taken into consideration (e.g. harvest time and the beginning of winter, which would have made many tracks impassable) the work was not done in a uniform manner, e.g. work was begun in swath 4 from SW to NE, as was also done in swath 3. Swath 2 was worked in the opposite direction, i.e. from NE to SW, and swath 1 was worked from SW to NE (Fig. 6). The survey took one week longer than planned.

3. Statistics

3.1 Geophone Groups, Shots, Seismic Traces, Data, and Bins

Because numerous geophone positions were the same for different array set-ups, only 8320 geophone positions needed to be surveyed. Owing to the reduction of channels per shot from 480 to 478 the theoretical number of seismic traces was also reduced from 1,612,800 to 1,606,080.

A total of 3327 shots were made. The difference between the actual and theoretical number of shots was only 33, or only 0.98 %. Trace loss owing to temporarily dead geophone locations amounted to 27,628 traces or 1.7 %. Total trace loss amounted to 50,122, or only 3.1 %, and thus was much less than the allowed maximum of 20 %. The total amount of data was more than 18 Gigabytes (1,562,678 traces) for a reflection time of 12 s. More than 250 magnetic tapes were necessary to record this data. By editing and arranging selected traces in an appropriate way 20 cross and 20 in-line single-fold sections were produced already during the seismic survey to allow an initial interpretation.

After the survey was finished the processing of the entire data immediately started including the first 7 s of reflection time, which amounts to 11.1 Gbytes. The covered area was divided into 50x50 m bins as planned. Owing to the lateral shifts of shot points at the edges of the survey area, the actual size of the at least one-fold covered area was 136,374 bins (357x382) instead of 131,008 bins (356x368) in the theoretical scheme.

3.2 CDP Distribution

In the theoretical scheme, the reflection points (called CDPs) are all in the bin centers. However, the lateral and in-line shifts in the field also shift the reflection points, so that in the real case they are distributed throughout each bin.

The first step after carrying out the 3-D binning (e.g. subdividing the area by a grid into bins) was the construction of a CDP bin and CMP scatter plot showing the distribution of the reflection points within each bin. A section of this plot is shown in Figure 17.

The CDP fold plot corresponding to this section is shown in Figure 18. The number in each square gives the number of the seismic traces within the respective bin, i.e. the subsurface coverage. The presence of a homogenous distribution of the desired 12 - 15-fold coverage can be clearly seen over this area.

To check the position of each reflection point within the bins, each bin was divided into 10-cm squares and a computer program counted the reflection points within each of these squares. The result is shown in Figure 19 in the form of frequency distribution curves for the distance of the reflection points from the bin edges (one for the left edge and one for the bottom edge). It can be seen that most of the points are near the bin center, as they should be (maxima at 25 m on x-axis and 25 m on y-axis). Thus, there was an optimum selection of origin and orientation of the defined grid of 50x50 m bins.

The ratio of maximum to minimum frequency is about 10 times greater for the y-axis than for the x-axis. The reason for this is that the in-line shifts in shot positions (allowed max. 35 m) were considerably less than those in the lateral direction (allowed max. 800 m).

The 25 bins within the marked square in Fig. 17 represent the area around the KTB borehole site. In this area the scatter of the points is close to the mean or smaller.

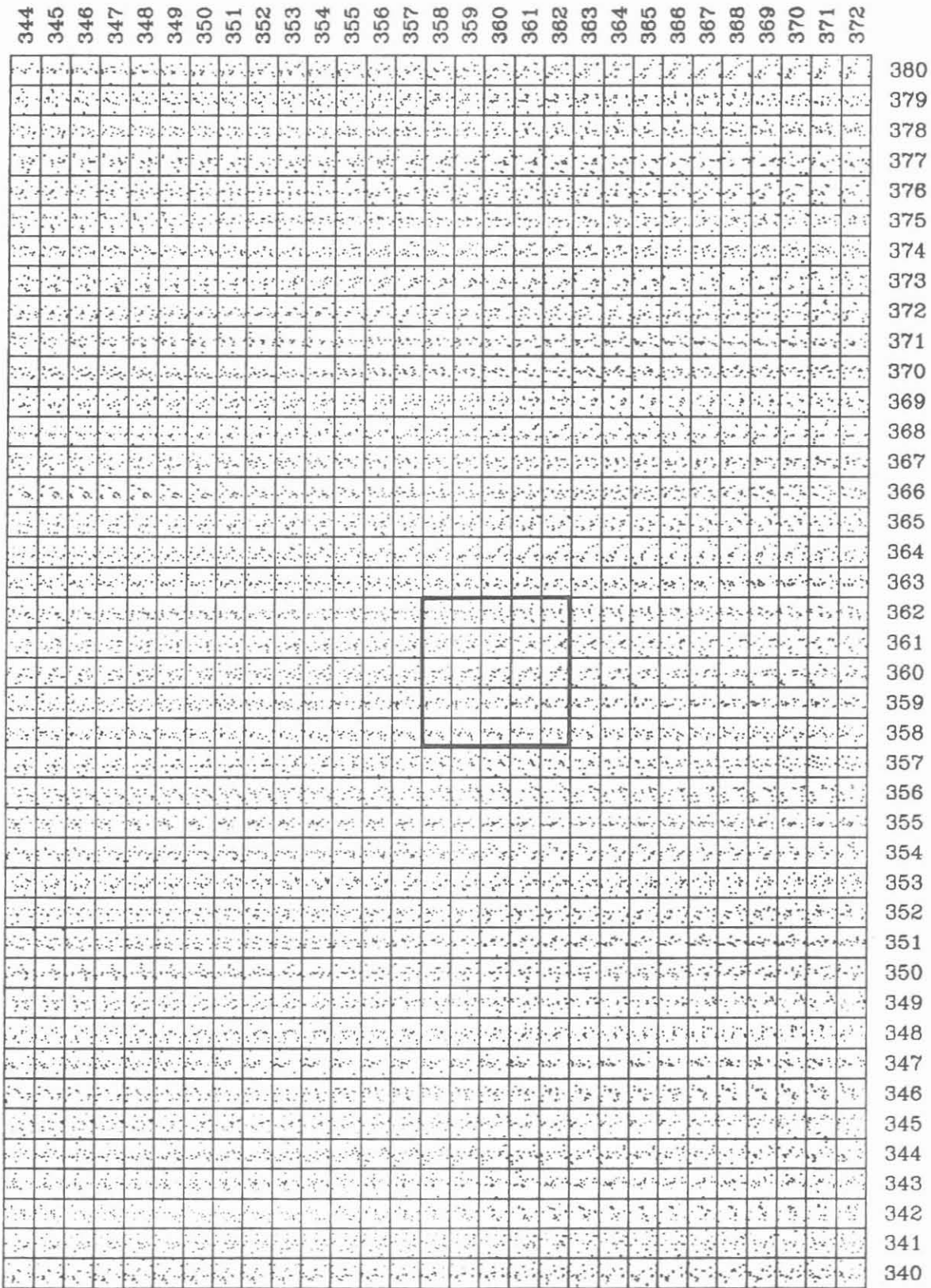


Fig. 17: CDP bin and CMP scatter plot

344	13	14	15	15	14	15	15	15	14	18	15	15	18	15	16	16	16	14	16	15	18	13	15	14	15	17	16	16	14	380	
345	15	15	15	15	15	14	15	14	14	15	14	15	15	16	16	15	18	15	15	15	15	15	15	15	15	16	15	15	14	15	379
346	15	18	14	15	15	14	15	14	13	12	13	16	15	16	15	14	14	15	15	15	13	16	15	16	18	15	15	14	378		
347	15	14	15	16	15	14	15	14	13	15	14	15	16	14	15	16	16	16	16	15	15	14	14	13	13	16	16	15	377		
348	15	13	15	16	15	14	15	14	15	16	16	14	15	15	16	16	17	15	16	15	15	14	14	15	14	15	15	15	376		
349	15	15	15	15	15	14	15	16	16	16	14	15	16	15	15	16	16	15	15	18	14	15	15	17	15	15	15	14	375		
350	14	15	15	15	15	14	15	13	13	14	15	15	15	14	15	14	15	14	15	15	14	14	14	15	14	16	16	15	374		
351	15	15	15	15	16	14	15	15	14	16	15	15	16	15	16	14	13	15	15	14	14	14	15	15	13	13	12	16	15	373	
352	15	15	15	15	15	15	15	15	15	18	15	16	15	15	16	15	16	17	17	16	18	16	16	14	15	15	14	16	14	372	
353	15	14	15	15	15	15	14	16	16	16	13	14	15	16	17	16	15	15	15	15	15	15	15	15	16	15	17	17	15	371	
354	15	15	15	15	15	14	15	15	13	13	14	16	15	15	15	14	15	15	15	15	15	15	15	14	15	15	14	15	16	370	
355	15	14	15	15	15	15	13	14	13	15	14	14	14	13	15	14	15	16	15	15	15	15	15	15	15	13	16	14	17	17	369
356	15	16	14	16	16	15	15	15	17	17	16	17	16	17	17	17	16	17	14	15	15	15	13	15	16	16	16	15	368		
357	14	15	15	15	14	15	15	16	16	16	14	15	16	16	16	16	16	15	14	15	15	15	15	15	16	15	16	16	15	367	
358	15	15	15	15	15	15	15	13	13	14	15	14	15	16	14	15	15	14	15	15	15	15	14	15	15	15	15	15	15	366	
359	15	15	15	15	16	14	15	15	14	16	15	15	16	15	16	16	16	16	15	14	14	14	14	14	13	14	16	16	13	365	
360	15	15	16	14	15	15	15	15	15	16	16	15	15	16	16	17	15	16	16	16	16	16	16	15	16	17	16	16	15	364	
361	16	15	14	15	15	14	15	15	16	16	16	14	15	15	15	16	16	16	15	14	15	15	14	16	17	16	16	16	15	363	
362	15	16	15	15	15	14	15	15	13	13	14	16	15	15	15	15	14	15	15	15	15	15	15	13	15	15	15	17	15	362	
363	15	15	15	14	15	15	15	14	16	15	14	15	15	16	15	15	14	15	15	15	15	15	15	16	14	16	15	15	16	361	
364	15	16	15	15	15	15	15	15	16	16	16	14	15	16	17	17	16	17	15	15	15	15	14	14	15	16	16	15	360		
365	15	15	15	14	15	15	15	14	17	18	14	15	15	16	16	16	16	15	15	15	15	14	15	17	16	16	16	15	359		
366	16	15	15	16	15	14	15	16	13	12	14	16	15	14	15	15	14	15	15	14	15	15	15	14	15	15	15	15	358		
367	14	15	15	15	13	14	14	14	14	14	14	14	15	14	15	17	16	16	16	14	14	15	15	17	13	14	15	17	16	357	
368	14	15	15	15	15	16	16	15	16	16	17	15	17	16	16	18	14	16	15	15	16	14	14	15	16	16	16	14	356		
369	15	15	15	15	15	15	15	16	16	16	14	14	15	16	16	16	16	16	15	14	15	15	15	15	16	16	17	15	16	355	
370	15	16	15	15	15	15	15	13	13	13	16	15	15	14	15	15	15	15	15	15	15	15	13	15	15	15	15	14	354		
371	15	15	15	15	15	15	15	14	16	15	15	16	15	15	16	16	15	16	15	16	15	18	15	15	14	14	16	15	17	16	353
372	15	15	15	14	16	15	15	15	16	16	16	15	15	15	15	16	16	16	16	15	15	15	14	15	15	16	16	15	352		
	15	15	15	15	14	15	16	15	15	16	16	14	15	15	16	16	16	16	15	15	15	14	15	16	16	16	16	16	351		
	16	15	15	15	15	15	15	13	13	13	15	15	16	15	15	15	15	15	14	15	15	15	17	13	16	15	15	15	350		
	14	14	15	15	15	14	15	14	16	14	15	16	16	16	16	16	16	16	16	15	15	14	14	15	12	15	15	15	14	349	
	16	15	15	14	15	15	15	15	16	16	16	15	14	16	17	16	17	15	16	14	14	16	14	15	16	18	16	15	348		
	14	15	15	15	15	14	14	15	16	16	14	14	16	16	16	16	16	14	15	14	14	14	14	15	15	17	16	16	347		
	15	15	13	14	15	15	15	12	13	14	16	15	15	15	15	15	15	15	15	15	15	16	14	13	14	15	15	15	346		
	14	13	15	14	14	14	14	13	14	12	14	16	14	15	16	16	14	17	12	13	13	14	15	13	15	16	17	17	345		
	14	15	15	16	16	16	15	16	16	16	15	17	16	16	16	16	16	16	16	15	15	16	16	13	14	15	16	16	344		
	15	15	14	15	15	15	15	16	15	15	14	15	16	16	15	16	15	14	14	15	14	14	15	17	14	16	15	15	343		
	15	15	15	15	15	14	15	14	14	13	14	15	14	16	15	15	15	15	16	15	14	14	15	14	14	13	15	14	15	342	
	12	14	14	14	14	14	14	12	15	15	15	16	16	16	16	16	15	15	15	15	14	15	15	15	15	13	14	17	17	341	
	15	14	14	16	16	17	16	16	16	15	16	14	16	14	16	16	17	16	17	15	15	16	13	14	14	15	16	17	15	340	

Fig. 18: CDP fold plot

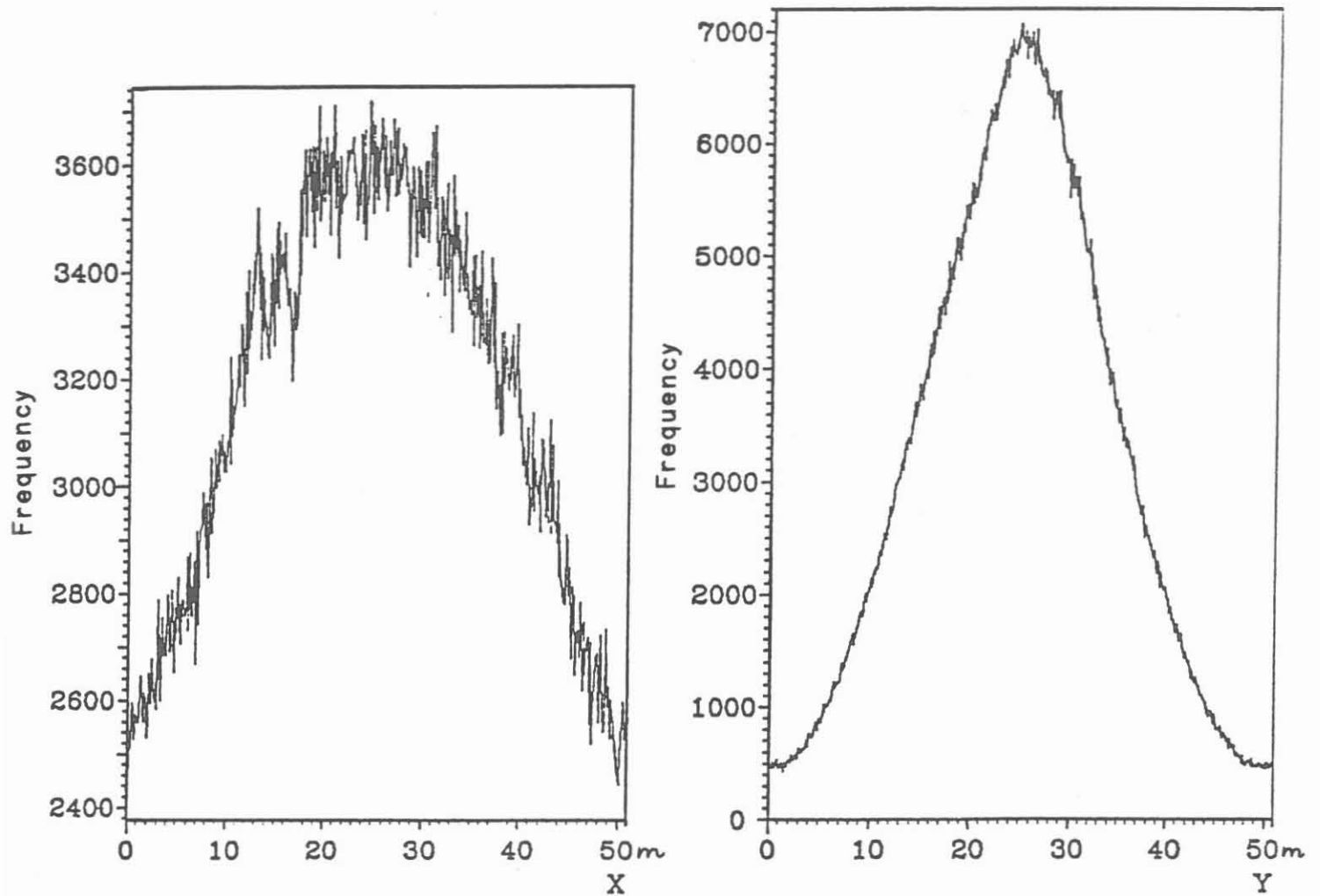


Fig. 19: Frequency distribution curves for the distance of the
CMPs from the edges of the bins
left : distance from the left edge
right: distance from the bottom edge

3.3 Offset and Angle Distributions

Owing to the unavoidable in-line and lateral shifts of shot points, the actual source-receiver offset range (2 - 6580 m) was somewhat larger than the theoretical one (72 - 6212 m). The frequency distribution of the offsets for the 3360 theoretical shot points is shown in Figure 20. It can be seen that the frequencies for some offset ranges (e.g. 2300 - 2400 m and 2700 - 2800 m) deviate considerably from a smooth distribution curve, whereas the histogram for the 3327 actual shot points (Fig. 21) is significantly smoother, because of statistical equalization.

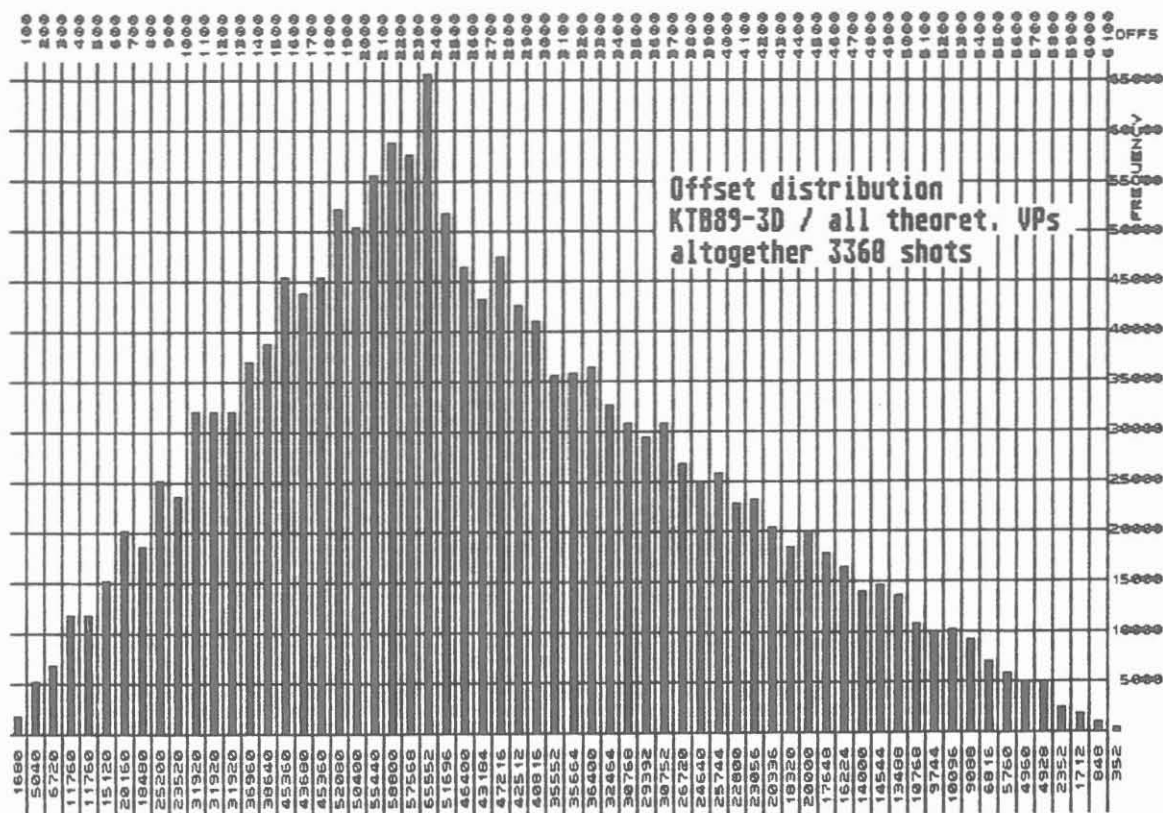


Fig. 20: Frequency distribution of the source-receiver offsets for the theoretical shot points

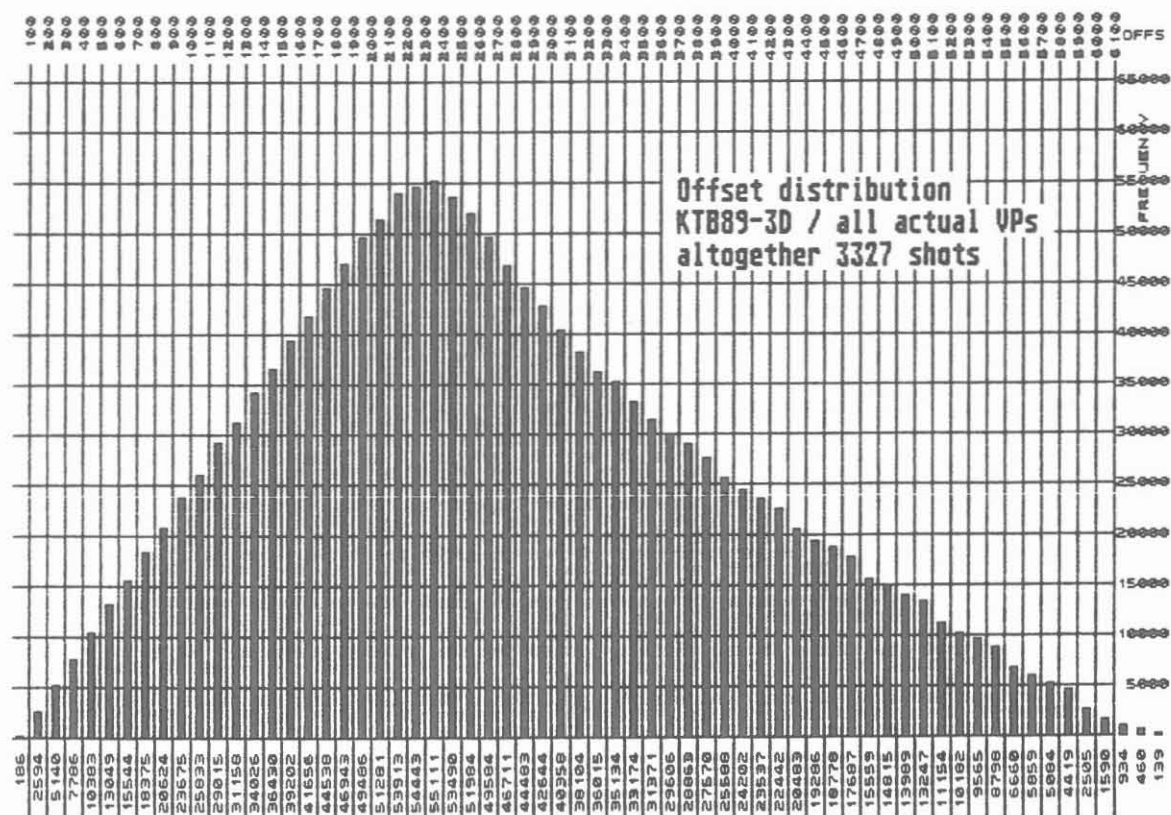


Fig. 21: Frequency distribution of the source-receiver offsets for the actual shot points

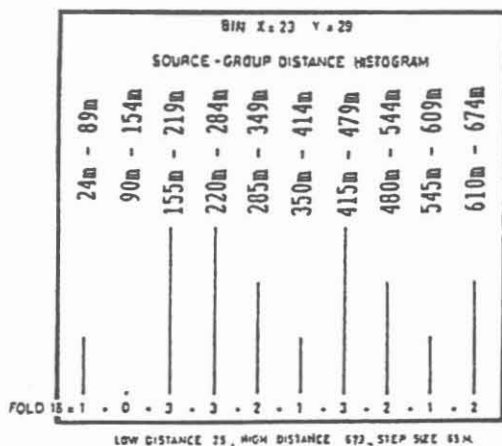


Fig. 22:

Histogram of the source-receiver offsets for one bin

The distribution of source-receiver offsets for a selected bin is shown by the histogram in Figure 22. The offset distributions in the area around the KTB drilling site are shown in Figure 23. In the marked 25 bins immediately around the KTB borehole the distribution is close to the mean or somewhat poorer.

The most frequent offsets are in the 2300 - 2400 m range. The connection lines between sources and receivers for a single array set-up are shown for this offset range in Figure 24. It can be seen that nearly every source-receiver azimuth is present.

A relatively large number of angles occur also for very small offsets, as can be seen in Figure 25 for the source-receiver offset range of 300 - 400 m. Only the azimuths close to the direction of the geophone lines are underrepresented.

A different situation is seen for the range of very large source-receiver offsets (e.g. the range from 5600 - 5700 m shown in Fig. 26). The azimuths here are all in the range of 10 - 23° from the direction of the shot point lines.

For 3-D seismics, it is very important that the azimuth distribution is homogeneous, in contrast to 2-D seismics, for which all connection lines between sources and receivers have nearly the same direction (i.e. the profile direction).

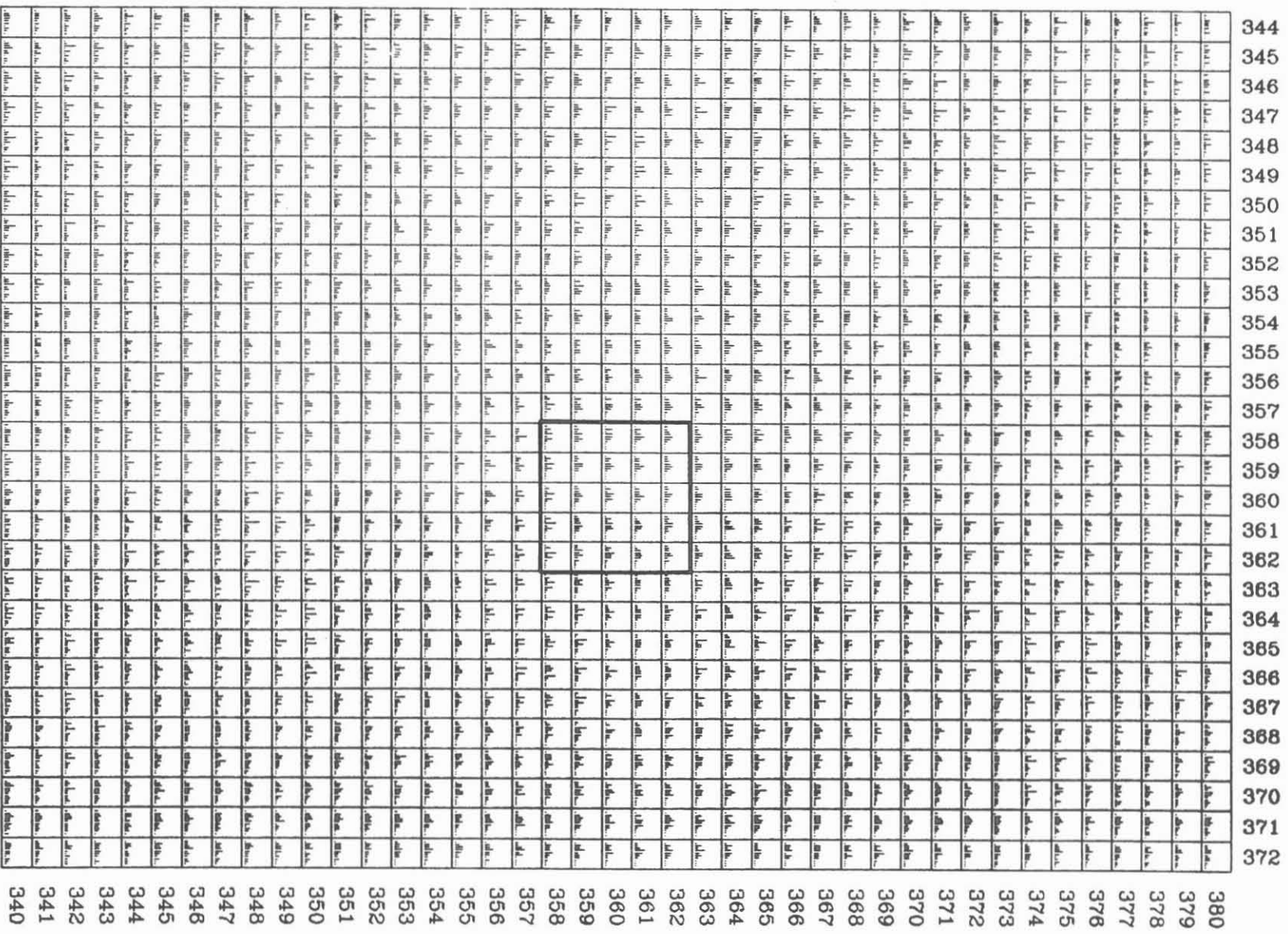


Fig. 23: Distribution of the source-receiver offsets in the area around the KTB borehole site

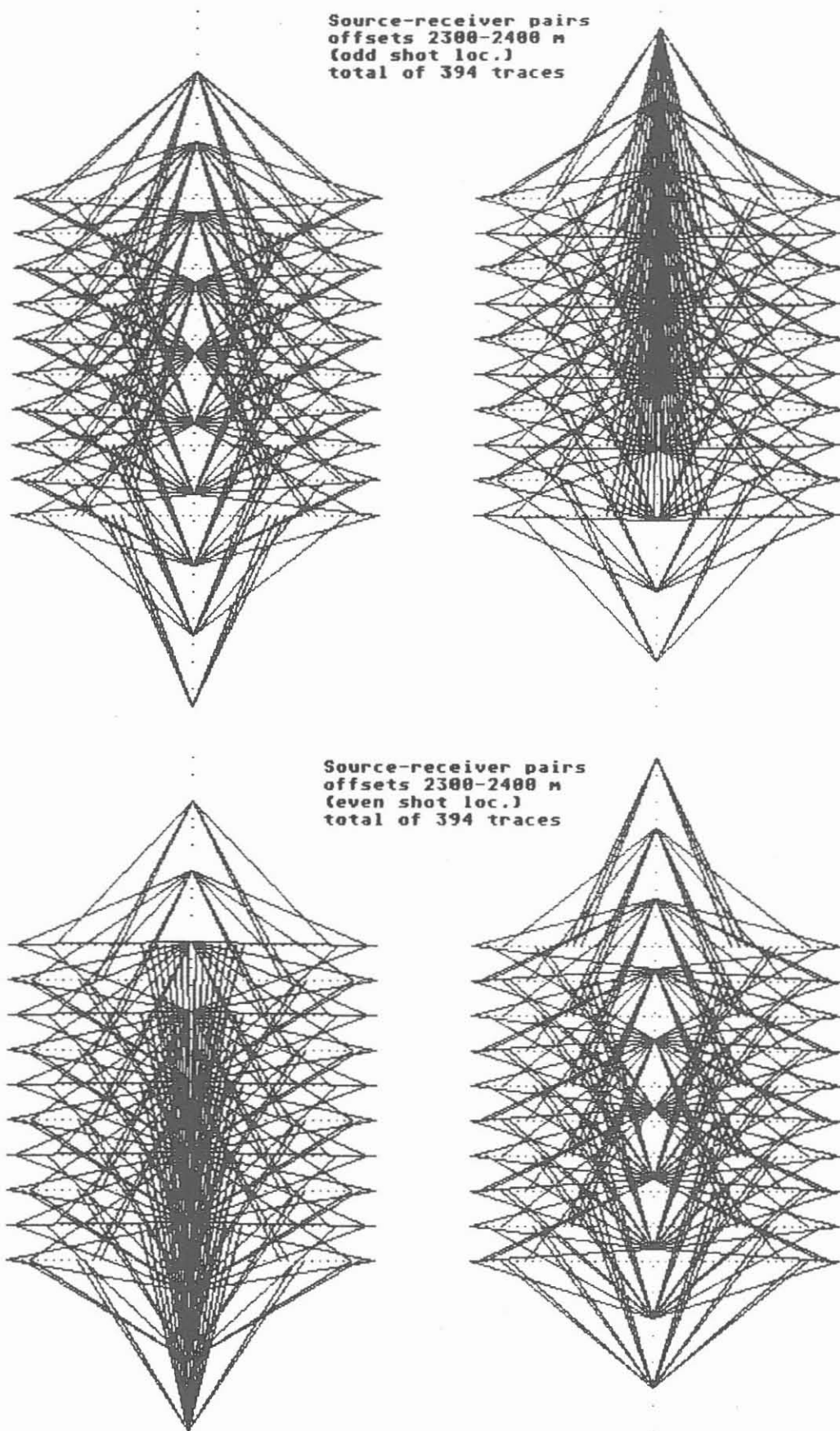


Fig. 24: Connection lines between sources and receivers for the offset range from 2300 - 2400 m

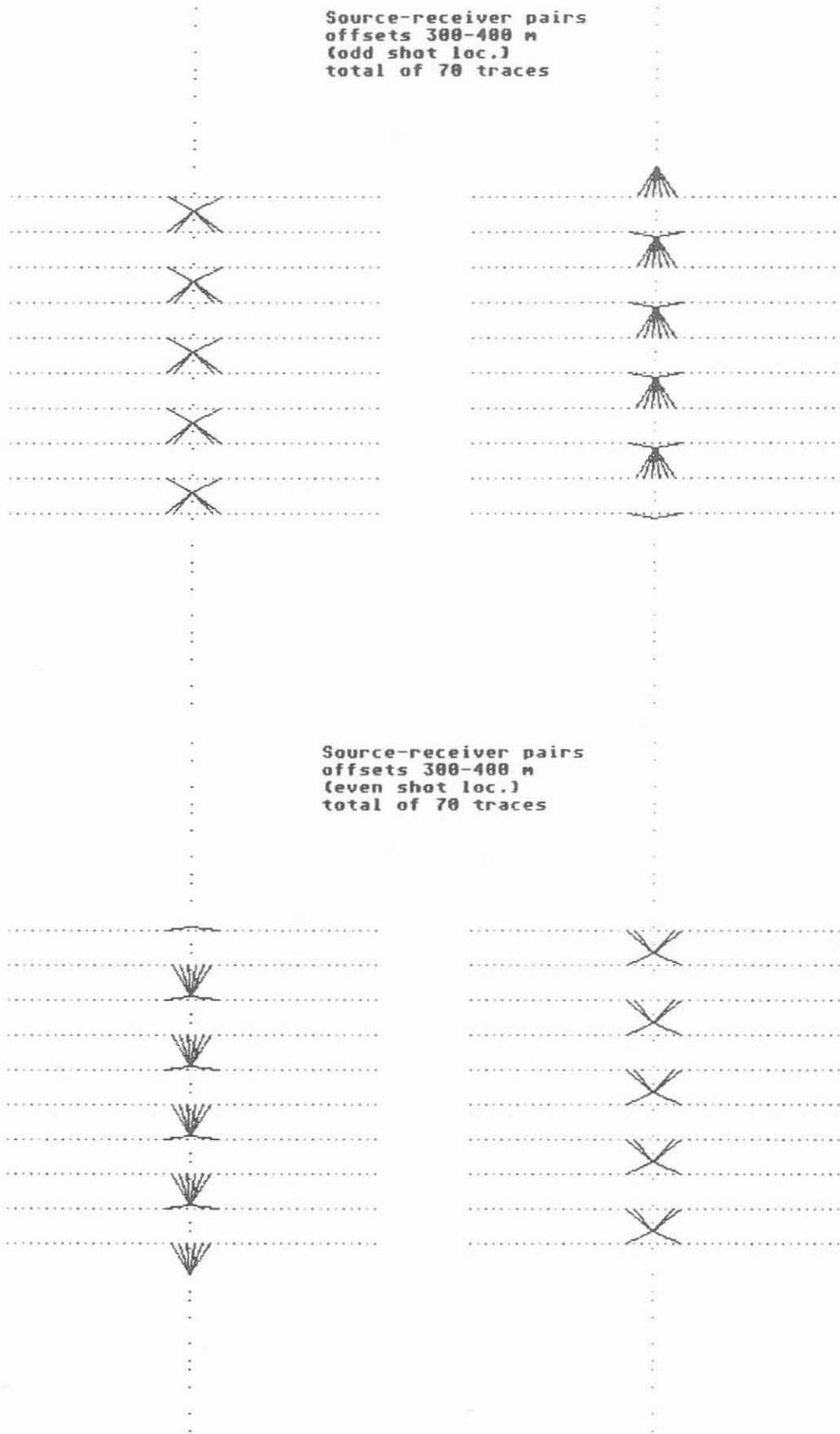


Fig. 25: Connection lines between sources and receivers for the offset range from 300 - 400 m

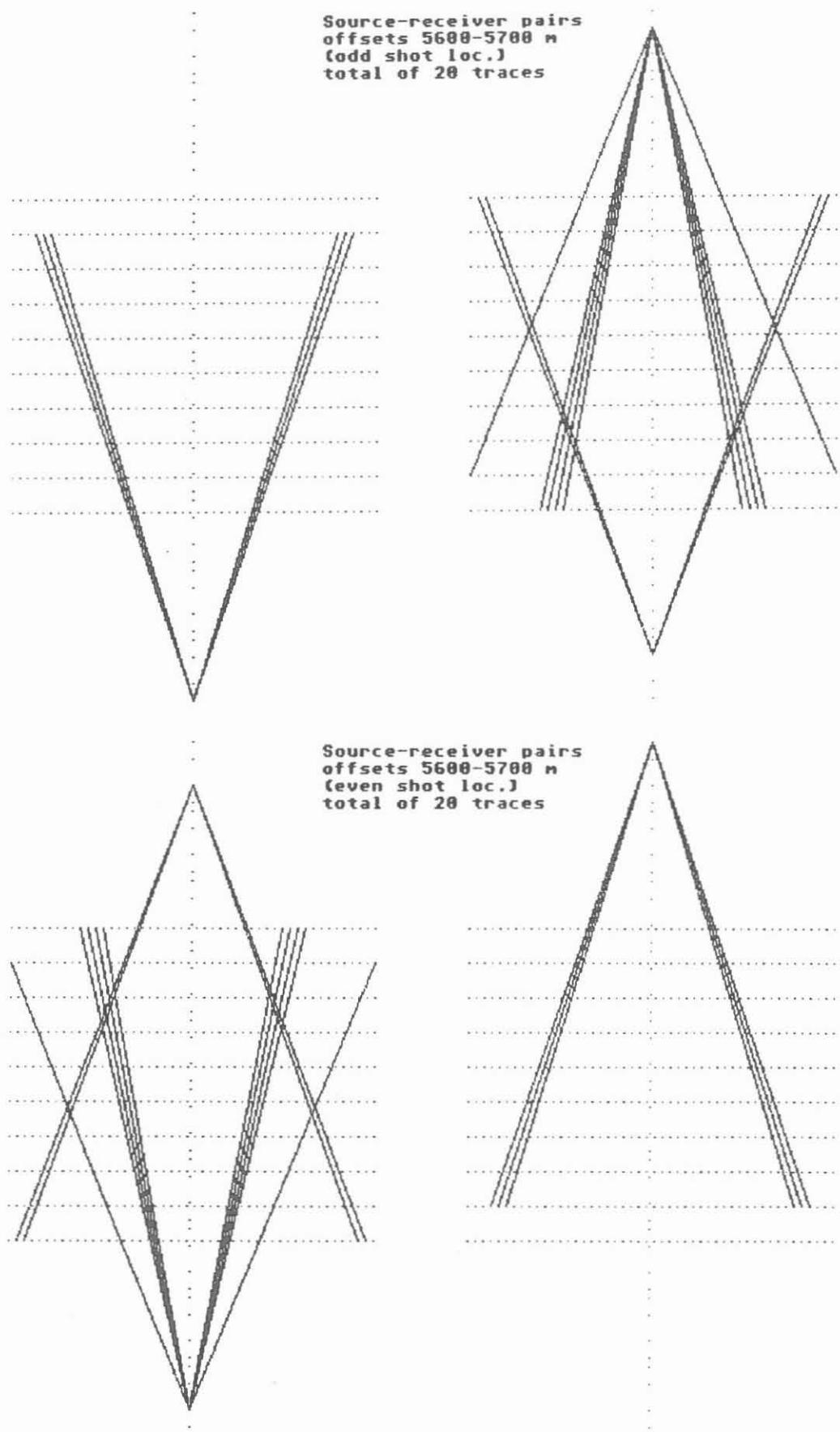


Fig. 26: Connection lines between sources and receivers for the offset range from 5600 - 5700 m

Whereas in 2-D seismics only a single stacking velocity can be used for a specific horizon (due to uniform source-receiver azimuths), in 3-D seismics the stacking velocity for the same horizon changes with the source-receiver azimuth. The largest stacking velocity is for an azimuth parallel to the dip direction, the smallest one is for an azimuth parallel to the direction of strike. Thus, for an event produced by a dipping horizon on different traces of a bin the dynamic corrections are a function of the source-receiver azimuth, even when the source-receiver offsets are the same.

When the stacking velocities for all azimuths of a dipping horizon are plotted, an ellipse is obtained (Fig. 27). The short axis represents the stacking velocity parallel to strike, the long axis represents the stacking velocity parallel to the dip. The angle β represents the angle between the direction of dip and the connection line between shot point and geophone group.

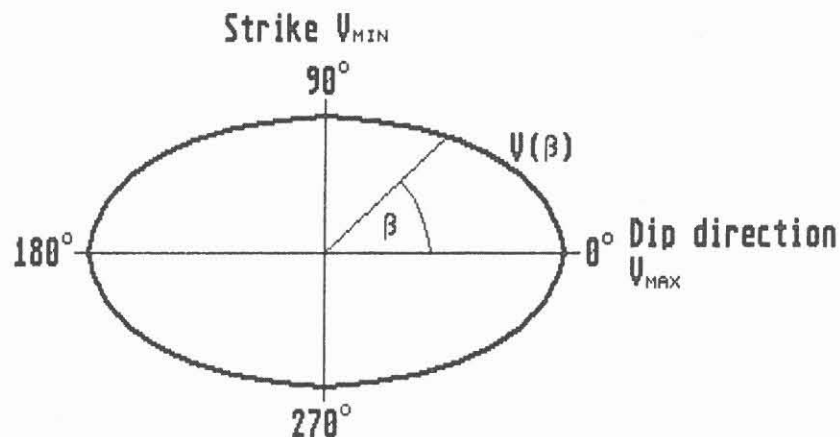


Fig. 27: Ellipse of stacking velocities for a dipping layer

When 3-D data is processed, the stacking velocity is determined for four direction ranges separated by 45° (Fig. 28). For this purpose, a half circle is divided into four 45° ranges, yielding the angles α_i ($i=1,2,3,4$) in the middle of each range. The ranges $180^\circ+\alpha_i$ are treated in the same way as the ranges α_i , since they represent only the exchange of source and receiver. The optimum stacking velocities for the four azimuth ranges α_i are used to construct a velocity ellipse (least squares method). This ellipse is then used to calculate the dynamic correction for each individual source-receiver azimuth.

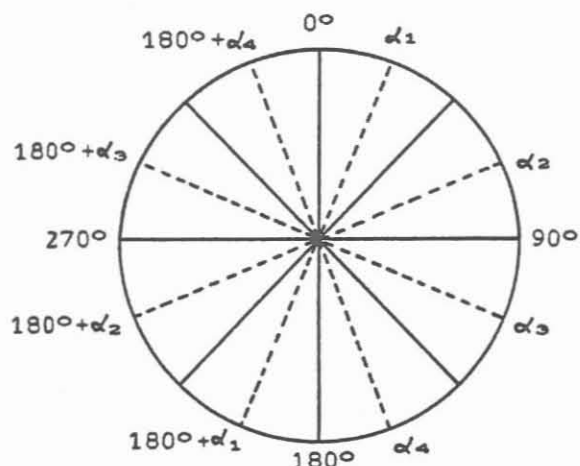


Fig. 28:

Division of a circle into 45° azimuth ranges

The length of each line in an angular distribution plot for one bin (Fig. 29) represents the number of traces in that azimuth range. A poor distribution of angles is indicated by the presence of lines considerably longer than the others. Lines of uniform length indicate a good distribution of source-receiver azimuths and nearly the same number of traces in all directions.

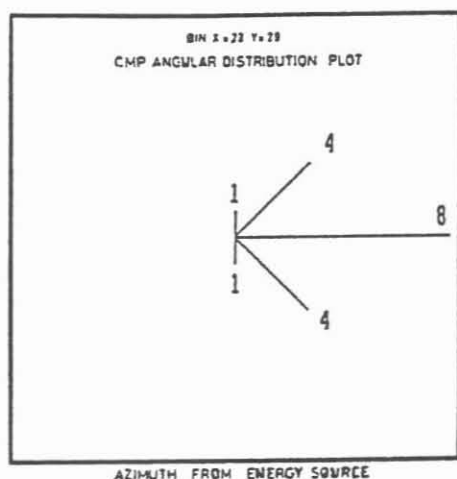


Fig. 29:

CMP angular distribution for one bin

There is a uniform distribution of angles in the 25 bins marked in Figure 30, representing the area immediately around the KTB borehole site. The frequency distribution of the source-receiver azimuths of the 3360 theoretical shot points is shown in Figure 31. The azimuths in geophone line direction are somewhat less frequent than those in the direction of the shot point lines. The histogram for the 3327 actual shot points (Fig. 32) is again smoother because of statistical equalization.

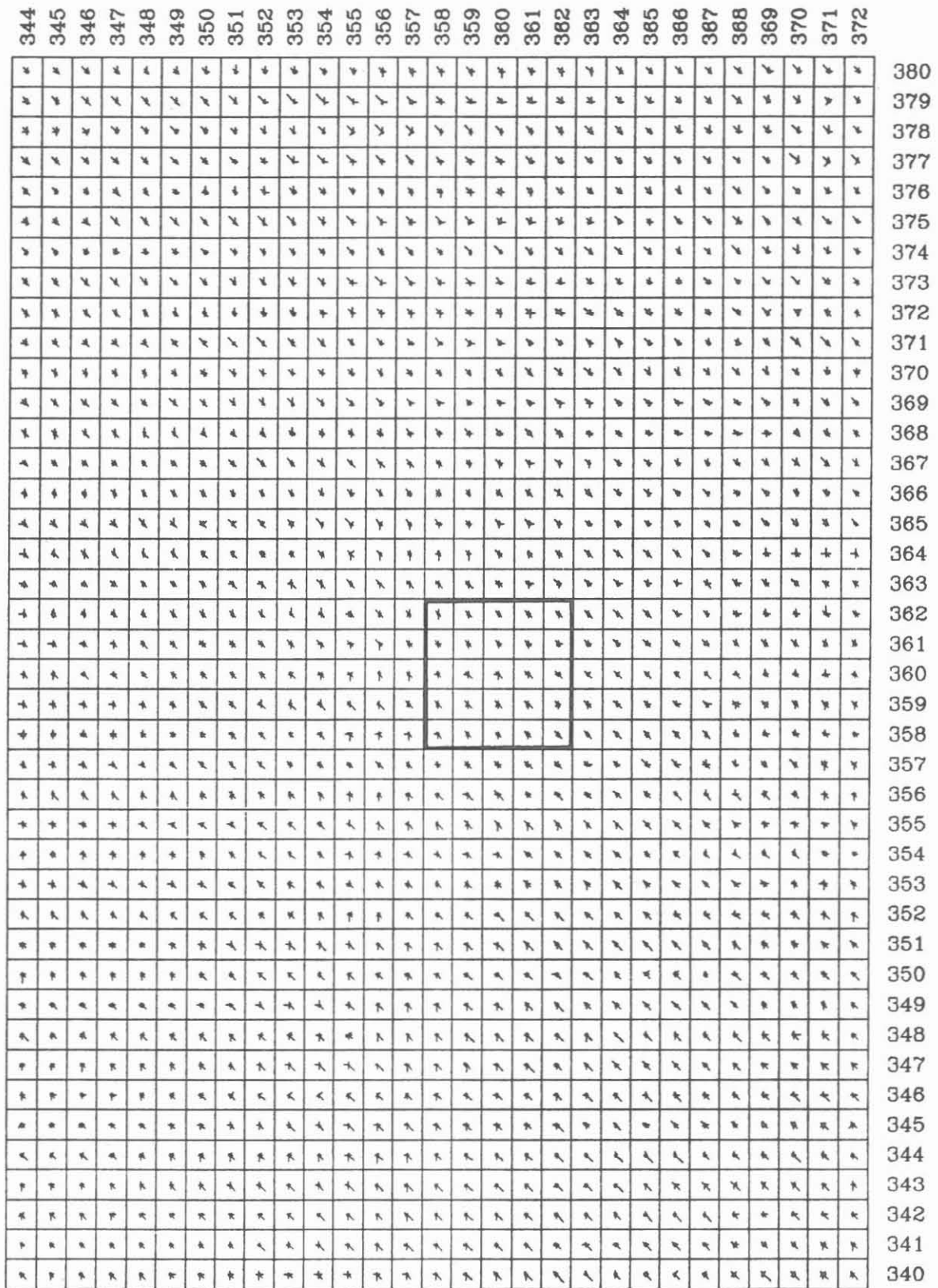


Fig. 30: Distribution of source-receiver azimuths in the area around the KTB borehole site

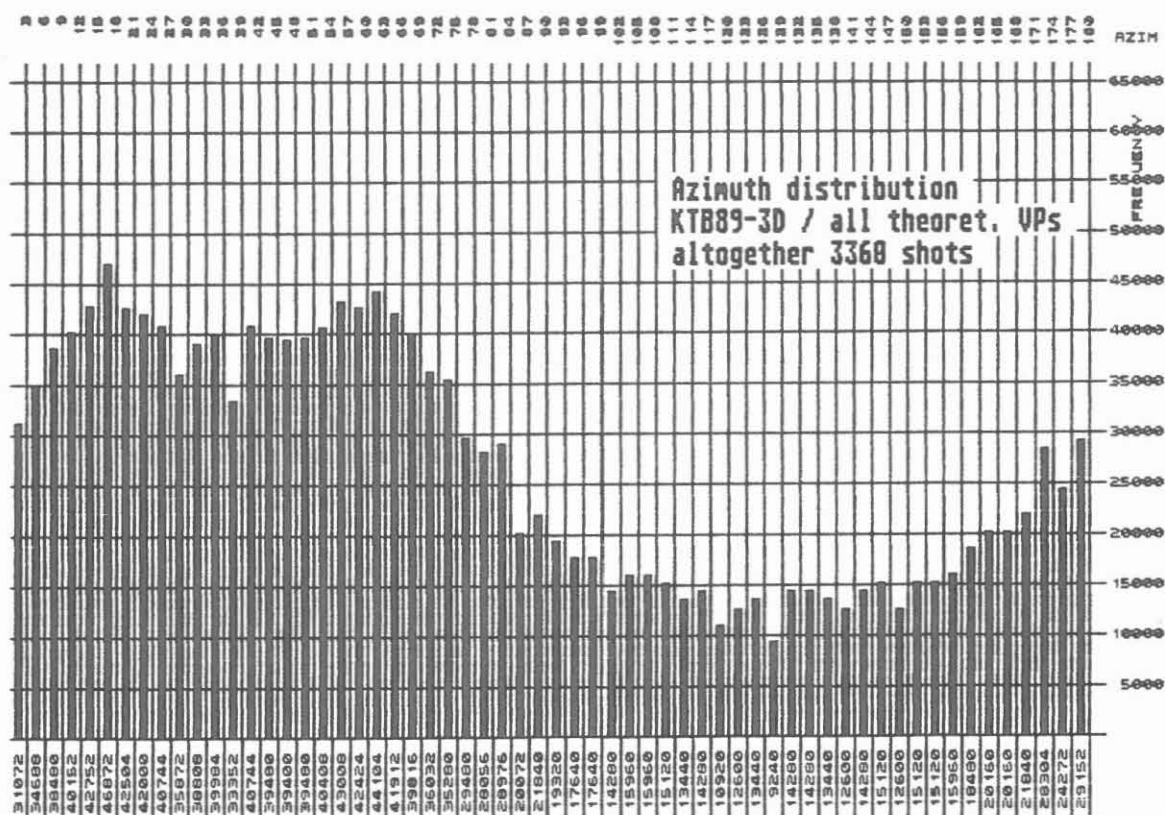


Fig. 31: Frequency distribution of the source-receiver azimuths for the theoretical shot points

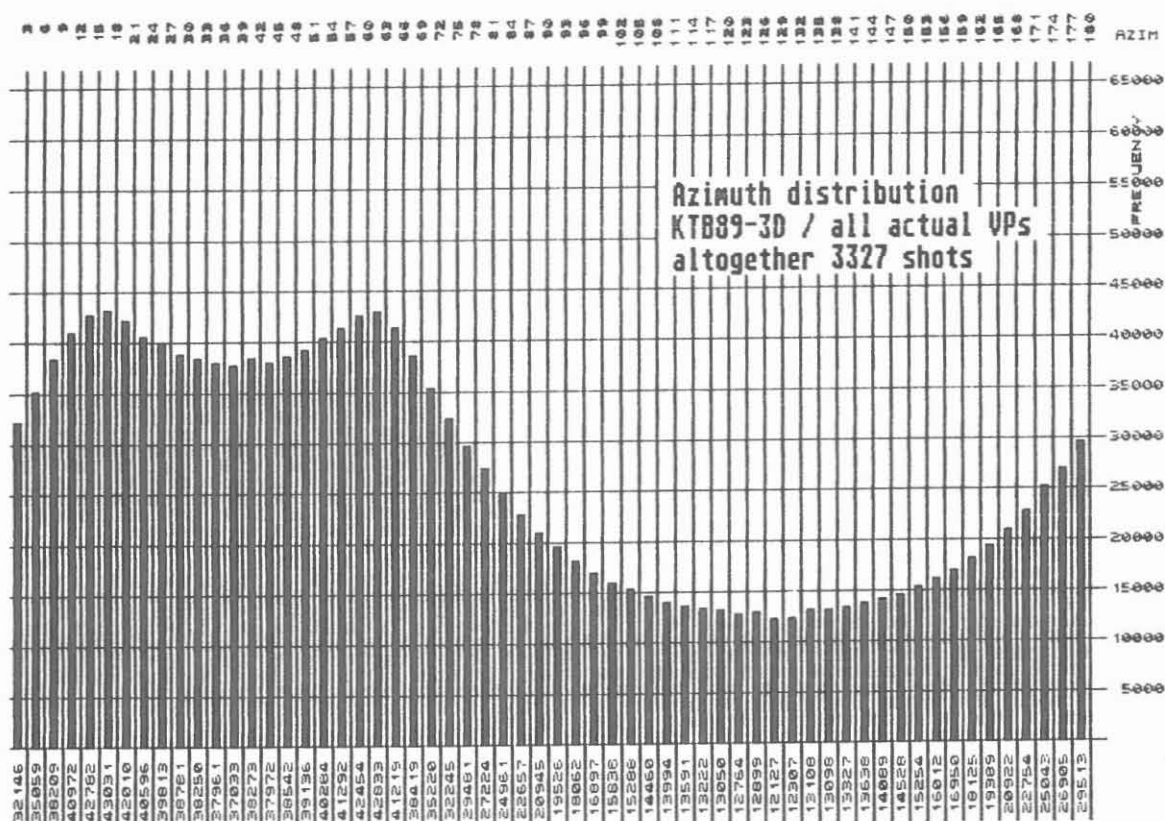


Fig. 32: Frequency distribution of the source-receiver azimuths for the actual shot points

The following table summarizes all important survey parameters:

method:	Vibroseis
equipment:	SERCEL SN 368 (telemetric)
sampling rate:	4 ms
instrument filter:	8Hz 18db/o. 88.8Hz 72db/o.
source:	5 vibrators VVEA
vertical stacking rate:	5 - 8 fold
sweep frequency:	12 - 48 Hz (up-sweep)
sweep length:	20 s
reflection time:	12 s (after correlation)
recording configuration:	cross array
datum level:	500 m above msl
number of swaths:	4
separation between swath centers:	4 km
geophone lines per swath:	10
total number of geophon lines:	40
separation between geophone lines:	400 m
geophone groups per geophon line and swath:	208
geophone groups per shot:	478 (theor. 480)
geophone groups per geophon line and shot:	48 (first line 46)
separation between geophone groups:	100 m
geophones per geophone group:	18 (3-vane fan)
total number of geophone locations:	8320
shot point lines per swath:	21
separation between shot point lines:	800 m
shot points per shot point line and swath:	40
total number of shot points per shot line:	100
separation between shot points:	100 - 300 m
total number of shots:	3327 (theor. 3360)
total number of shot locations:	2084 (theor. 2100)
bin size:	50x50 m
area covered by a single array set-up:	2.4x5.8 km
one-fold covered area:	17.9x19.1 km (theor. 17.8x18.4 km)
15-fold covered area:	15.2x14.4 km
total number of bins:	357x382=136.374 (theor. 356x368=131.008)
total number of traces:	1.562.678 (theor. 1.612.800)
source-receiver offset:	2-6580 m (theor. 72-6212 m)
maximum fold:	19 (theor. 15)
average fold:	11.5 (theor. 12.3)

3.4 Elevations

The elevations surveyed during this seismic survey have been processed into a relief model of the survey area, shown for subarea B (see location map in Fig. 1) in Figure 33.

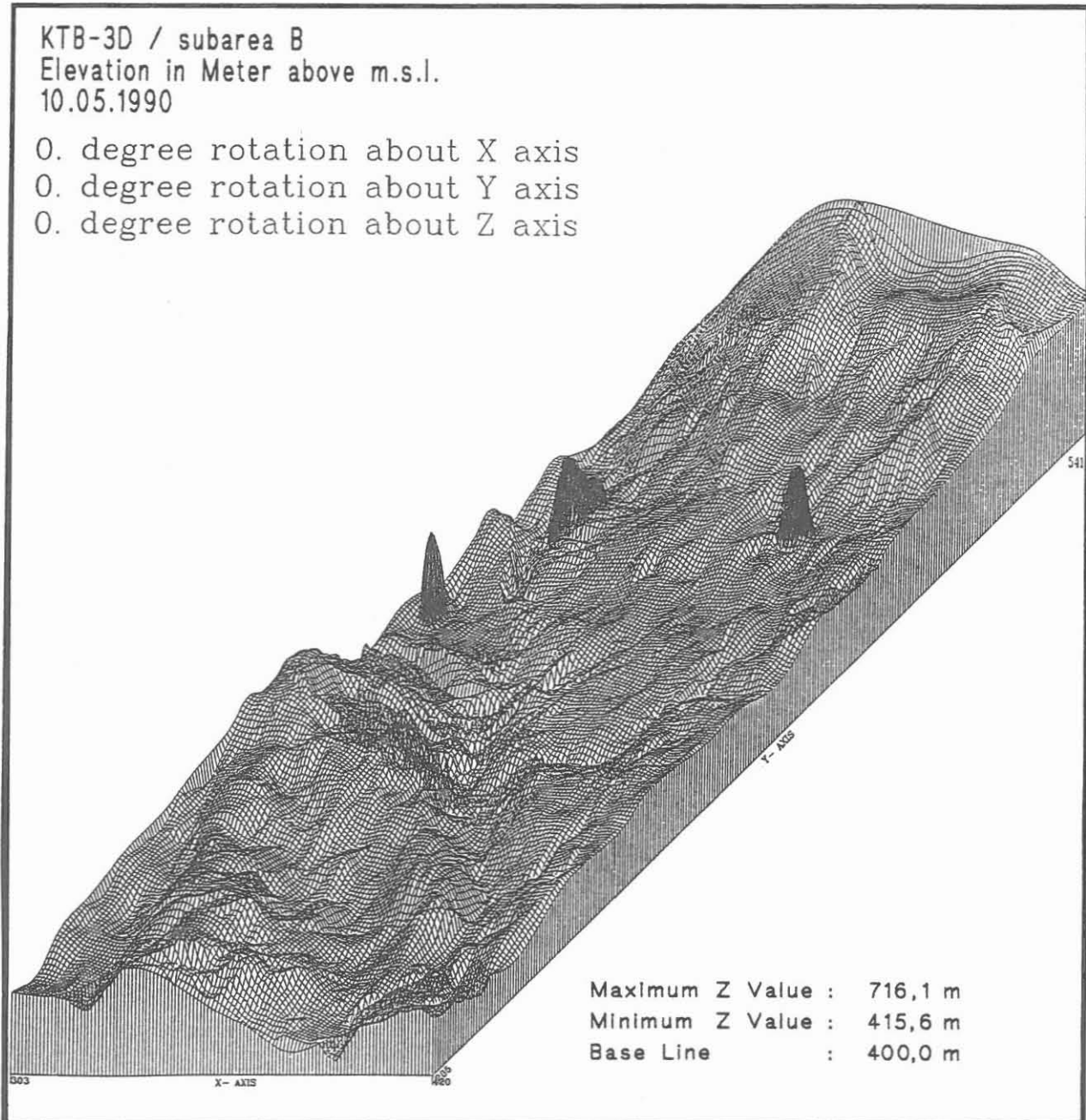


Fig. 33: Relief model of surveyed elevations of subarea B

In the northeast part of the survey area, the hilly Bohemian Massif is represented by metamorphic and plutonic outcrops with elevations of 600 - 800 m. The sediments in the southwest part of the area present a hilly landscape with elevations of 400 - 600 m. There is good overall agreement between this computer model and the topographic map of the area.

The course of the Fichtelnaab River, which flows from north to south through the area, can be clearly seen on the relief plot. It enters the area at an elevation of about 470 m and leaves the area at an elevation of about 410 m. Hills rise to the left and right of the river to elevations of 460 to 550 m. The Steinwald area adjoins to the northeast with elevations of 600 - 700 m. This area can also be clearly recognized on the model of subarea B, although at the edges of the area the relief is unnaturally smooth because there were not enough points for correct interpolation.

There are four areas within the model that show extremely high gradients (as much as 100 m between two neighboring points). These few incorrectly surveyed points have been corrected so that they will not influence the final static corrections.

3.5 Equipment

The following items provide an indication of the amount of work necessary for this seismic survey:

The following equipment was in daily use:

800	electrical cables (totalling 90 km)
18,000	geophones
800	telemetry boxes
about 150	repeater boxes
40 - 45	vehicles (in October an additional 35 mobile drilling rigs were needed for the wide-angle seismic measurements)
50	2-way radios in the vehicles and
30	2-way portable radios
2 - 4	relay stations.

The field work was carried out by:

80 personnel (plus an additional 40 in October for
the wide-angle seismic measurements)
50 students.

In addition, the following items were used during the survey:

4,900 kg explosives (for the wide-angle seismics)
500 ignition fuses (for the wide-angle seismics)
300 electrical cables were replaced due to damage
150 boreholes, each 30 m deep for a total of 4500 m
(for the wide-angle seismic measurements)
500,000 km were driven, more than 100,000 l fuel consumed.

4. Processing

4.1 Seismic Software from Seismograph Service Limited

The land 3-D software from SSL is a disk-oriented program package with two database structures: one for the pre-stack parameters and one for the post-stack parameters. The parameters of the individual traces, mainly the geometry data, are handled in the former; the parameters of the individual bins, mainly stacking velocities, are handled in the latter. The databases can be divided into subsets. For this survey they had to be divided into four subsets, corresponding to the four subareas shown in Figure 1. A description of the relations between the seismic traces and the controlling databases will be given in Chapter 4.4.

4.2 Field Geometry and Pre-stack Database

Very exact geometry data is needed for processing 3-D seismic surveys. In addition to the coordinates of the geophones and shot points, as well as the elevations and static corrections, a file must contain the actual array set-up for each shot. This makes it possible to arrange the seismic data in CSP order (common shot point) as well as in CMP order (common midpoint).

First, the geometry data is entered in the pre-stack database. A grid of bins over the entire area is defined. Each trace is then assigned to the bin midway between source and receiver location on the assumption that this bin represents the location of the reflection points.

Each bin is assigned a number, analogous to the CDP numbers in 2-D processing. So that each bin can be easily located within the grid, it is also assigned x and y bin numbers.

4.3 Checking the Data and First Arrival Times

The seismic data and nonseismic data must be in complete agreement if the 3-D processing is to produce valid results. Thus, the data must be checked for a one-to-one match between the input traces and the related databases.

The first arrival times are also checked: The program takes from the geometry file the source-receiver offset for each trace and calculates the corresponding first arrival time from an estimated velocity and depth for the weathering layer. The trace is then followed in a time window and tested for changes in amplitude. If there is no significant change within the expected time range, the trace is marked as faulty.

An example of checking first arrivals is shown in Figure 34. The curve above the first arrivals represents the calculated first arrival times minus a user-given constant (40 ms in the example). This constant is applied to separate the calculated from the actual first arrival to allow a visual comparison.

If all traces for a shot are labeled as "bad traces", either a "misfiring" occurred or there is an error in the field geometry (e.g. incorrect coordinates and thus incorrect source-receiver offsets). After the exact one-to one match and the quality of all seismic traces contained on the field tapes have been checked, the data of one subarea are written to disk and the controlling databases can take the handling for all further processing steps via disk pointers.

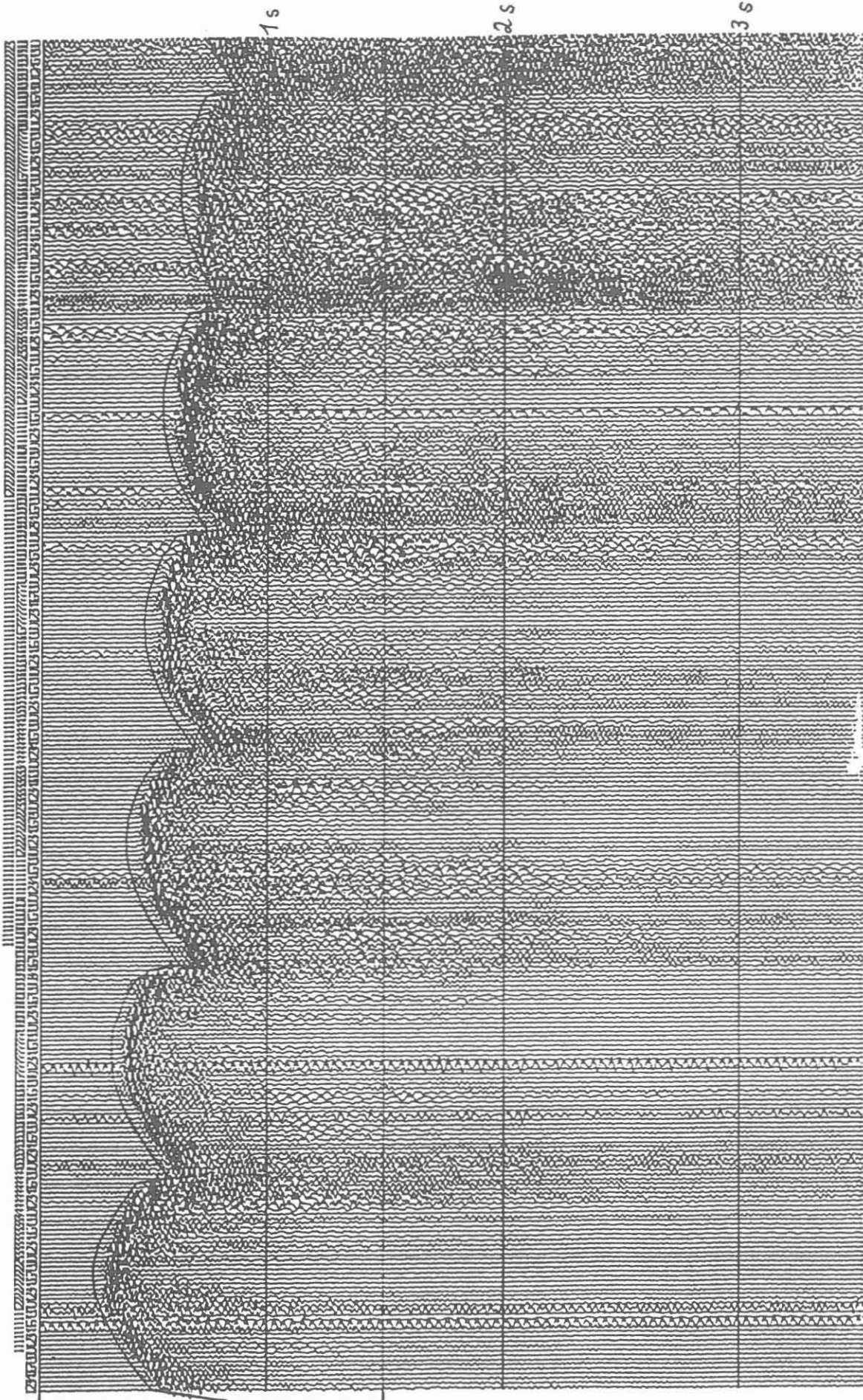


Fig. 34: An example of checking first arrivals

5. Example of the Data and Processing Plan

The ten geophone lines of a single array set-up were lined up one after the other to produce the seismic section shown in Figure 35 as an example of the data quality. This section is for the raw traces from shot position 17542, located about 4.5 km ENE of the KTB borehole and about 2 km below the respective geophone lines (marked with an x in Fig. 2). For this location relative to the geophone lines, the increase in the first arrival times from geophone line 1 (left) to geophone line 10 (right) can be distinctly seen.

The reflections from the Erbendorf structure can be easily recognized for the eight inner geophone lines. They are shown in gray in the figure and are about 3.6 s below the first arrivals, which have traveltimes of 0.4 - 1.1 s. Only for geophone lines 1 and 10 are the events not distinct. The reflections from the Erbendorf structure, one of the objectives of the main KTB borehole, are present in almost the entire survey area. In many other records there are indications of steeply inclined structures (60° true dip and more) in a traveltime range of 0.5 - 2.2 s.

Figure 36 shows the planned processing sequence of this 3-D survey and the relational structures between seismic data and controlling databases in the form of a generalized flow chart.

The circular symbols at the top of the figure characterize the magnetic tapes supplied by the contractor. The thin-framed rectangles represent the mathematical procedures to apply, and the broad arrows at the right indicate the flow of all seismic data from the field tapes to an interpretable 3-D data block.

The thick-framed rectangles symbolize the basic data files stored on disk (seismic data and controlling databases) and the broad bidirectional arrows indicate the relational structure, e.g. the pre-stack database has access to the pre- and post-stack data, and the post-stack database has also access to the pre- and post-stack data.

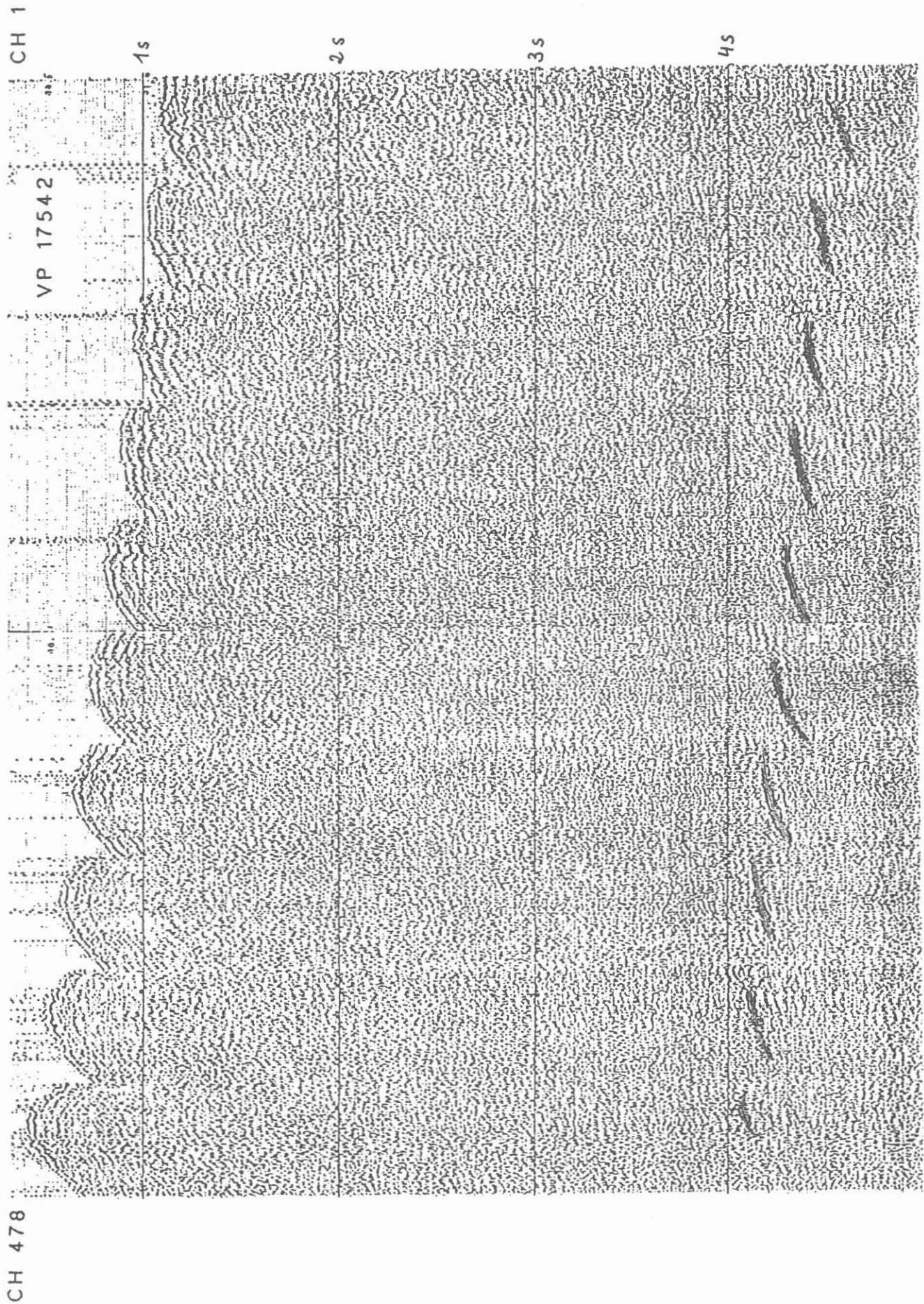


Fig. 35: Example of raw data (shot point 17542) with evaluated reflections of the Erbendorf structure

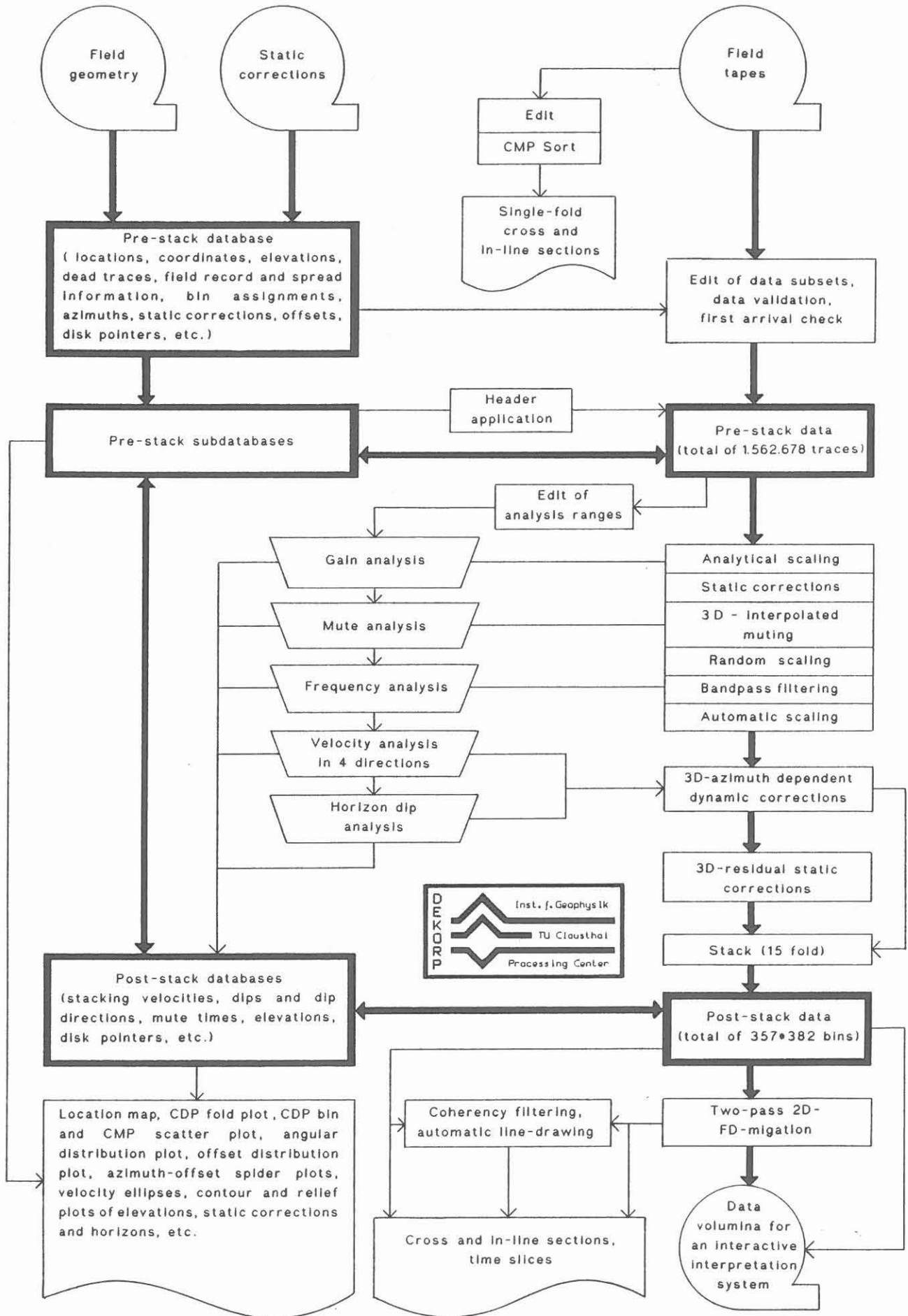


Fig. 36: Flow chart of the planned 3-D processing sequence

The trapezoids in the center of Figure 36 represent the analyses necessary for the determination of optimum processing parameters, and the paper symbols at the bottom of the figure characterize the plots available for evaluation.

The final processing of this extensive 3-D survey will last until spring 1991 at least, however, unmigrated data volumina will be fed to an interactive interpretation system at an earlier stage facilitating geo-tectonic predictions before the start of the drilling of the main KTB borehole.

References:

DEKORP Research Group (1988); Results of the DEKORP 4/KTB Oberpfalz Deep Seismic Reflection Investigations. J Geophysics 62: pp 69-101

Körbe M. (1988); Diskussion der geplanten Schuss-Geophon-Aufstellung für die KTB-3D-Messung 1989. Studienarbeit, Institut für Geophysik, Tech. Univ. Clausthal

Seismograph Service (England) Ltd.; Land 3-D Survey Processing System User's Guide (Release 9.2A). Holwood, Keston, Kent, Great Britain

Stiller M., Thomas R. (1989); Processing of Reflection-Seismic Data in the DPC Clausthal. In: Emmermann R., Wohlenberg J.; The German Continental Deep Drilling Program (KTB). Springer, Berlin Heidelberg New York, pp 177-232



Experiment "Durchschallung"
Calculation of Static Corrections from
Seismic Borehole Records Using the
Vibrator Signals of the 3-D Seismic
Reflection Survey within ISO 89

J. Albrecht
D. Teichert



Experiment "Durchschallung"

Calculation of Static Corrections from Seismic Borehole Records Using the Vibrator Signals of the 3D Seismic Reflection Survey within ISO89

Jörg Albrecht and Dietmar Teichert

Abstract

During the 3D seismic reflection survey within the project Integrated Seismics Oberpfalz 1989 (ISO89) the vibroseis source signals were recorded simultaneously with five three-component geophone borehole chain SEKAN5 or a single three-component borehole geophone, respectively, in the KTB pilot hole. The aim was to measure the traveltimes of direct waves in the depth range between 3220 and 3420 m in order to deduce spatial velocity inhomogeneities between surface and recording depth from traveltime residuals in the surroundings of the KTB. These data shall be used for improved static corrections if distinct from statics obtained by short refraction lines and first arrival analysis of surface data. A short description of the method is given which is based on approximation by least square fitted planes. Data examples and preliminary results are presented.

Authors' address: DEKORP Processing Center, Institut für Geophysik der Technischen Universität Clausthal, Arnold-Sommerfeld-Str. 1, D-3392 Clausthal-Zellerfeld

1. Introduction

The huge amount of source signals generated during the 3D seismic reflection survey within IS089 was predestinated to provide additional information on spatial velocity inhomogeneities in the vicinity of the KTB drill site by observation of the direct seismic waves in the borehole in depth as great as possible. These data should enable better resolution of traveltimes than surface data due to the almost noise-free recording conditions at greater depth. The travelttime anomalies are analyzed and shall be transformed into static corrections. By comparison with the static corrections obtained by conventional methods (i.e. short refraction lines and first arrival analysis of surface data) it will be decided whether these data will contribute to improved corrections essential for the quality of the 3D seismic results.

2. Survey Geometry

2.1 Intended Scheme

The vibrator positions used for this experiment resulted from the survey geometry of the 3D reflection seismics elaborated at the DEKORP Processing Center (DPC), TU Clausthal (REHLING and STILLER, 1990).

The survey area extends over a square of about 20 km side length with the KTB pilothole at its centre. The deployment scheme of the vibrator positions comprises 21 traverses of about 100 source points each. The interval between these points is a recurring sequence of 100m, 200m, 300m, 200m. Sixty percent of the source points, (position numbers 21 to 80) are to be used two times corresponding to a total of 3360 vibrator points, nominally. For recording of the vibrator signals a borehole chain consisting of five three-component

geophones with 25m spacing (SEKAN5) should be used (1 vertical and two horizontal traces per geophone). This tool is a development of PRAKLA-SEISMOS AG, Hannover (MYLIUS et al., 1990). Since a two-fold vibroseis signal excitation was designed in the central part of each traverse it was intended to record the signals in two different depth positions of the geophone chain thus extending the observed depth range. For vibrator point numbers 1 to 60 of each traverse the depth range of 3320 to 3420m was scheduled and for numbers 21 to 100 the depth range of 3220 to 3320m.

2.2 Actual deployment

Due to technical difficulties the SEKAN5 borehole geophone chain had to be replaced several times by a single three-component borehole geophone (MYLIUS et al., 1990, and REHLING and STILLER, 1990). The recording depths of the single geophone are 3220m and 3420m, respectively. However, some data could not be recorded at the intended depths because the chain and the single geophone, respectively, could not be sunked appropriately. Table 1 presents to which extent the vibrator signals of the 3D seismics could be recorded within the pilothole.

Table 1

Depth range (m)	Geophone chain (%)	Single geophone (%)	Deficit (%)
3220-3320	18.27	60.48	21.25
3320-3420	59.05	36.19	4.76

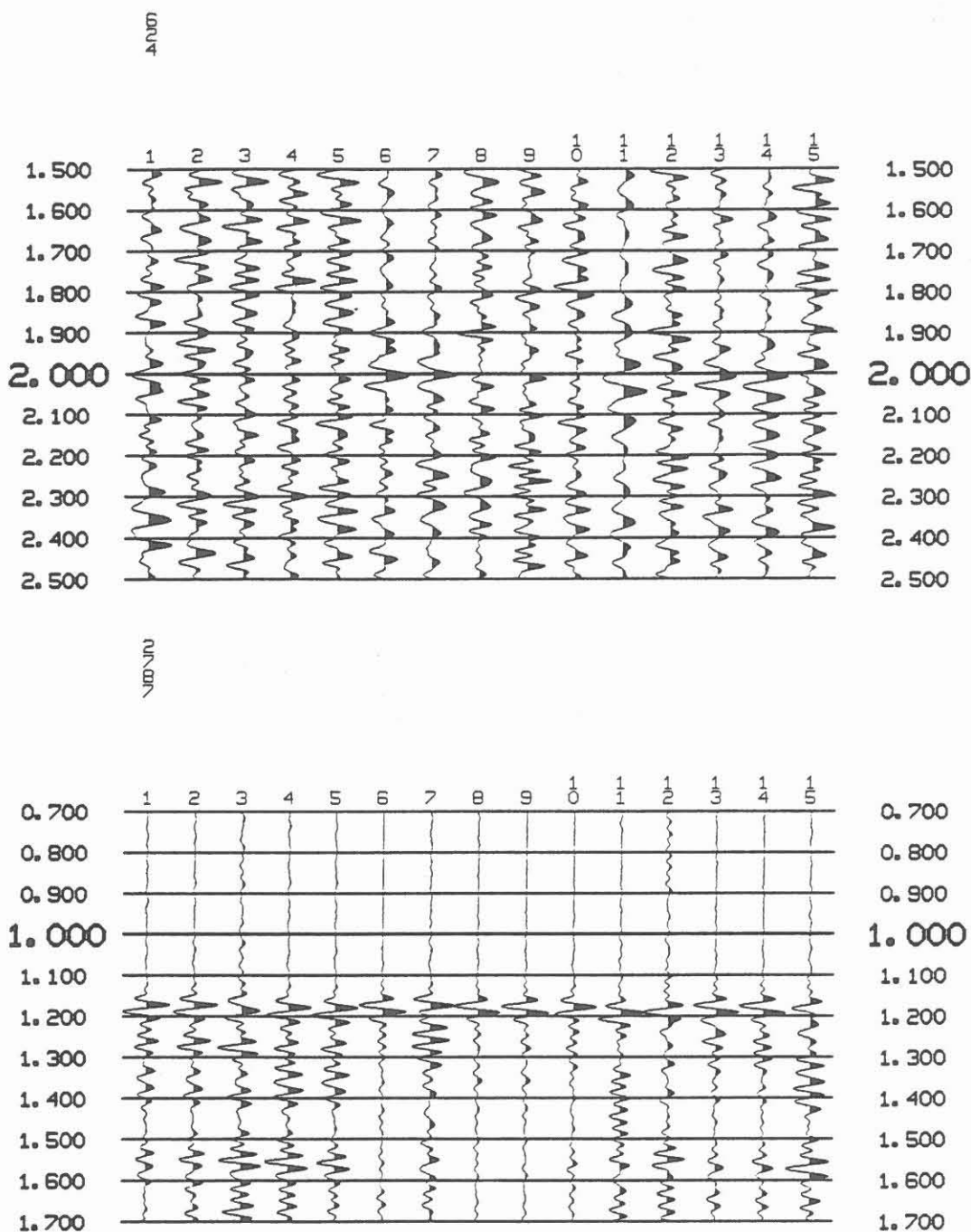


Fig. 1

Record no. 624 (upper panel) and no. 2787 (lower panel)
Traces 1 to 5: vertical components
Traces 6 to 10: 1. horizontal component
Traces 11 to 15: 2. horizontal component
Vertical scale: traveltme in seconds

3. Data base and processing

In order to deduce static corrections from the observed data the picking of direct traveltimes in the records with reference to a particular depth is necessary. Fig. 1 shows two selected records of the geophone chain at 3220 to 3320m and 3195 to 3295m depth, respectively. For the initial processing steps a reference depth of 3220 m was selected corresponding to traces 1, 6 and 11 for record number 624 and to traces 2, 7 and 12 for record number 2787 in fig. 1.

In order to obtain exact traveltimes even if the signal to noise ratio is strongly decreased (e.g. record number 624) the three components of the identical recording depth were scaled, squared and summed within the time window from 0 to 3.5 s (fig. 2). The subsequent picking of first arrivals was carried out with an appropriate computer programme developed at DPC. The output consists of a total of 1296 traveltimes for the reference depth of 3220m corresponding to about 98% of the data recorded at that depth.

4. Methodological approach and initial results

In order to take into account large-scale inhomogeneities in the space under study the spatial traveltime plane of the first arrivals was approximated segmentally through 2nd-order planes described by the equation:

$$a_{11}x^2 + a_{22}y^2 + a_{33}z^2 + 2a_{12}xy + 2a_{23}yz + 2a_{31}zx + 2a_{14}x + 2a_{24}y + 2a_{34}z + a_{44} = 0$$

Its coefficients were calculated by least square fitting. Figure 3 shows the picked traveltimes along three neighbouring traverses indicated by vertical bars and the traveltimes from the least square fitted plane indicated by continuous lines. The residuals between the observed and the fitted traveltimes

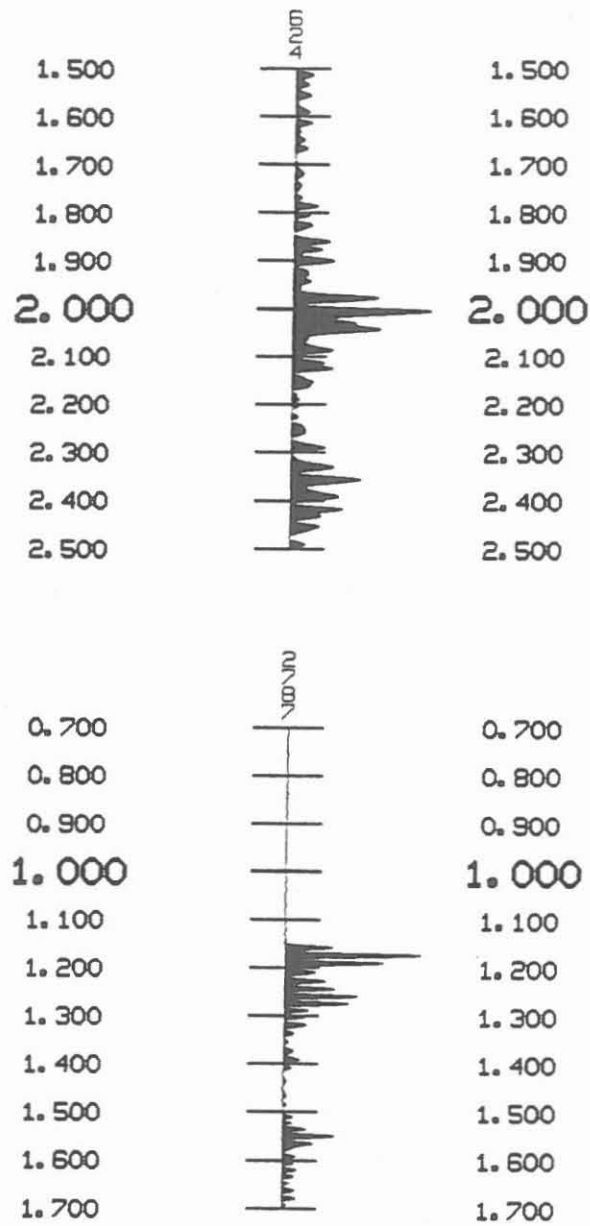


Fig. 2

Traces at 3220 m depth after pre-processing of the corresponding traces of figure 1. Note that the signal to noise ratio of record no. 624 has been improved considerably. For further explanation see text.

contain the effect of small-scale inhomogeneities in the space under study and, of course, the influence of the respective elevations at the source points. The residuals will be used for the calculation of static corrections for reflectors below the recording depth of 3220m, in this case (fig. 3).

During the next processing steps which are not terminated, yet, the static corrections (concerning elevation and thickness of the weathering zone) calculated conventionally thus far shall be compared with the results obtained by our method. If differences can be recognized they must be related to inhomogeneities below the reference level of the conventional static corrections. Then, the application of the respective residual static corrections should provide better stacking results of the 3D seismic data. Moreover, the results are expected to indicate lithological variations in specific domains.

Further data evaluation, e.g. the calculation of the remaining partial plane coefficients is still in process, and therefore must be reserved for future publications.

References

- Mylius, J., Nolte, E., Scharf, U. (1990):
Use of the Seismic Receiver Chain SEKAN5 within the Framework of Integrated Seismics in the Oberpfalz.- KTB Report 90-6b, Niedersächsisches Landesamt für Bodenforschung, Hannover.
- Rehling, J.G., Stiller, M. (1990):
3-D Reflection Seismic Survey of the Area around the Continental Deep Drilling Project Site.- KTB Report 90-6b, Niedersächsisches Landesamt für Bodenforschung, Hannover.

3-D ESP-Experiment of the
Integrated Seismics Oberpfalz 1989

H. Wiederhold



3D-ESP - EXPERIMENT OF THE INTEGRATED SEISMICS OBERPFALZ 1989

Helga Wiederhold

ABSTRACT

The comprehensive field investigations of the Integrated Seismics Oberpfalz 1989 (ISO 89) were carried out by the DEKORP group at the German Continental Deep Drilling (KTB) Site from late July to late November 1989. A 3D-expanding-spread experiment (3D-ESP) was involved utilizing the source signals of the 3D seismic survey in such a manner that the common midpoints fall into a small area with the KTB at its centre. 189.460 seismic traces have been recorded. The source-receiver configurations comprise offsets from 0 to 24 km and azimuth angles from 0 to 180°. Thus best conditions for velocity analyses in 3 dimensions for the area around the KTB are given. The layout and the field parameters of the 3D-expanding-spread experiment are shown. The subsurface area covered ca. 40 fold has an extension of about 2650 m x 3800 m. Details of the recorded data material are demonstrated.

Niedersächsisches Landesamt für Bodenforschung
Stilleweg 2
D-3000 Hannover 51

INTRODUCTION

The 3D-expanding-spread experiment (3D-ESP) is part of the Integrated Seismics Oberpfalz 1989 (ISO 89) and is directly connected with the 3D seismic reflection survey (REHLING and STILLER, 1990). The basic idea, first suggested by the Geophysical Institute of Technical University of Clausthal, is to record all source points of the 3D seismic survey with an additional geophone spread in such a way that the subsurface reflection point is constant vertically below the KTB location. With this configuration reflections within a wide source-receiver offset and azimuth range are obtained with best chances to determine detailed average and interval velocity information in 3 dimensions for the area around the KTB and depth down to Moho. In the following an overview of the field investigations and the collected data material is given.

FIELD INVESTIGATIONS

The field investigations took place in August/September 1989. As seismic source the Vibroseis signals of the 3D seismic survey were used. The planning, preparation and realization of the 3D seismic survey is described in detail by REHLING and STILLER (1990). For the 3D-expanding-spread experiment a DFS-V recording unit with 120 channels operated by the DEKORP group was used. In order to integrate this experiment into the 3D seismics the geophone locations were chosen to be the same as used for the 3D seismics; thus no extra locations needed be surveyed. That means, the geophone spread had to be along the geophone lines of the 3D seismic survey. The spread for one shot included two parallel lines with 60 channels each, a geophone group spacing of 100 m and a distance of 400 m between both lines. A sketch of the geometry is given in Fig. 1. While, for example, the 3D seismic survey was on swath 4 the 'expanding spread' was on geophone lines 5 and 6 of swath 1, and correspondingly, while the 3D survey was on

swath 3 the 'expanding spread' was on lines 15 and 16 of swath 2. The midpoints of the geophone spread and the vibrator traverse are symmetrical to the KTB. The spread has been kept fixed for one vibrator traverse (= 40 shotpoints). With the change of the vibrator traverse (800 m distance) the geophone spread moved by 8 geophone positions (= 800 m) in the opposite direction, thus the covered area remains always the same.

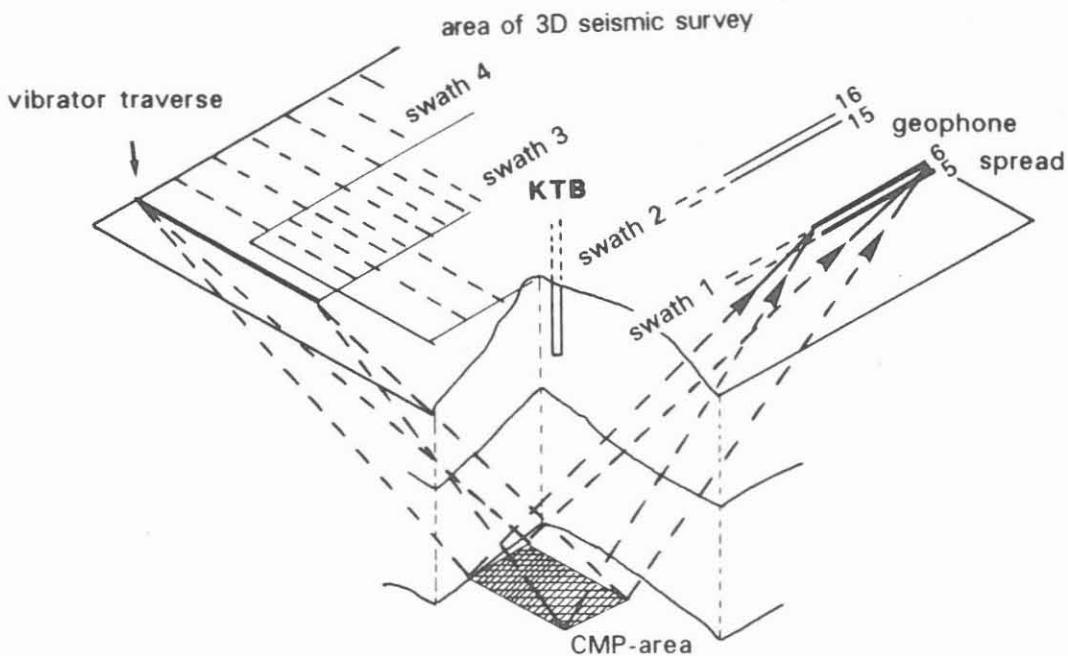


Fig. 1: Sketch of geometry of the 3D-expanding-spread experiment.

By this procedure a subsurface area is set-up with the following parameters (theoretically): The geophone spacing, 100 m at the surface, means 50 m subsurface distance. The vibrator spacing is irregular but in the mean 200 m, giving 100 m subsurface interval. With each second traverse the vibrator points are permuted and the subsurface reflection points fall in the intermediate space and we get a 10-fold, respectively 11-fold coverage with 50 m interval for the 21 traverses of one swath. By the second geophone line the coverage is dou-

bled and we get a coverage of 21. With the second swath it is doubled to 42. Due to budget restrictions only two of the 4 swaths of the 3D survey were observed in this way. So theoretically a coverage of 42 for each 50 m x 50 m bin was obtained.

The field parameters are specified in Table 1.

<u>Method</u>	Vibroseis
<u>Equipment</u>	DFS-V (DEKORP), 120 channels
sampling rate	4 ms
recording time	33.7 s
reflection time	13.7 s
source signal	upsweep 12-48 Hz, 20 s
vertical stack	5 - 8 fold
data format	SEGB, multiplexed
<u>Receiver geometry</u>	
layout	in a plane, 2 receiver lines with 60 geophones, 400 m line interval, 100 m receiver interval, center of receiver spread and center of vibrator traverse are symmetrical related to KTB.
<u>Source parameters</u>	same as 3D-seismics
vibrators	5 VVEA (16 to)
pattern	48 m
interval	alternating: 100-200-300-200-100 m, 40 source points per traverse und receiver spread in total 21 vibrator- traverses, subdivided into 2 swaths.
<u>Coverage</u>	42 fold (theoretical)
<u>CMP interval</u>	50 m
<u>CMP area (1 fold)</u>	3550 m x 4150 m (theoretical) 4050 m x 4200 m (actual)
<u>CMP area (ca. 40 fold)</u>	2350 m x 3750 m (theoretical) 2650 m x 3800 m (actual)

Table 1: Field parameters for the 3D-expanding-spread experiment of the Integrated Seismics Oberpfalz 1989.

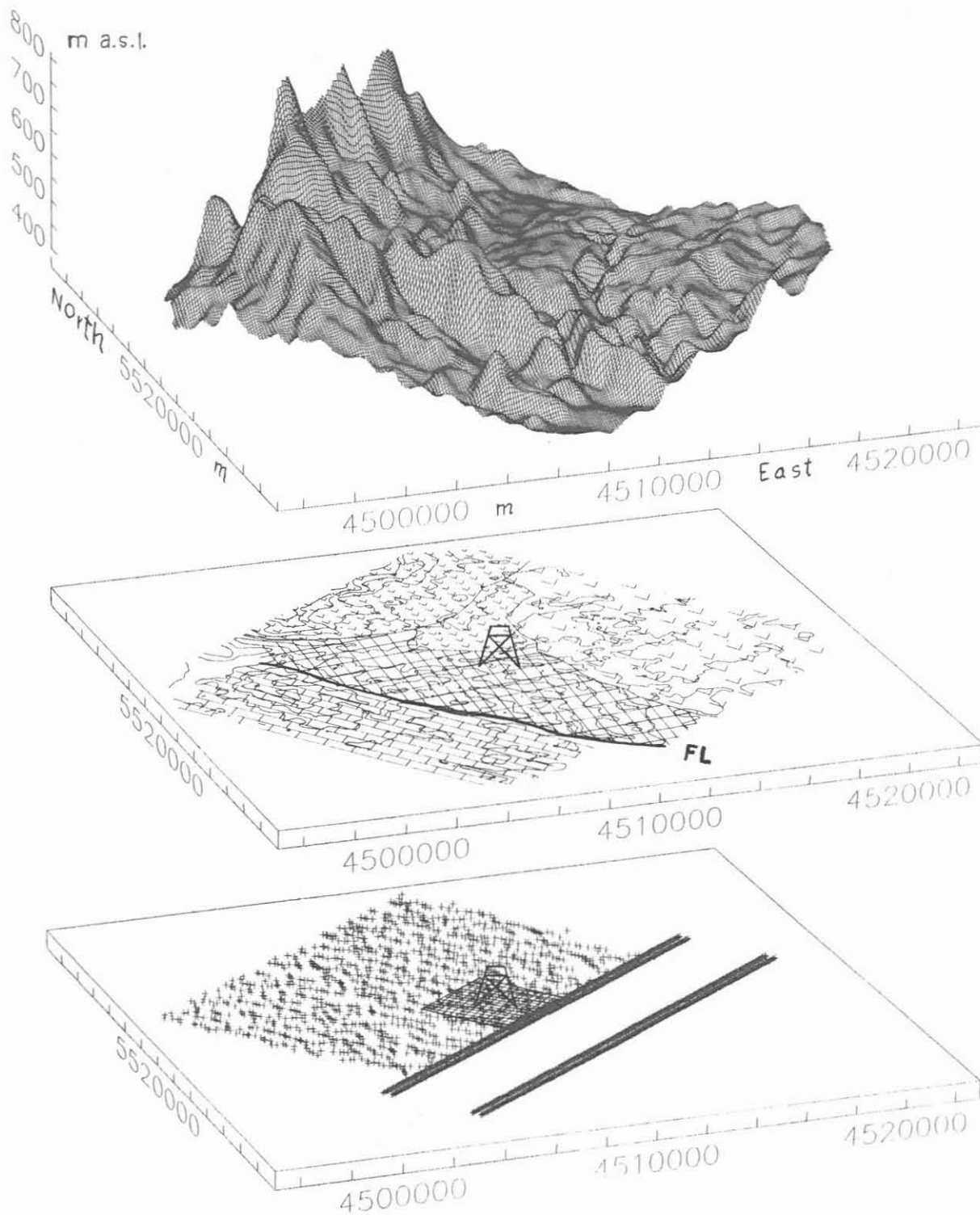






Fig. 2: Surveyed area of the Integrated Seismics Oberpfalz 1989 with the KTB drillhole in its centre. Top: Topography (vertical exaggeration: 20); centre: Contour lines and main geological units:  Steinwald granite massif,  Falkenberg/Friedenfels granite massif,  gneisses and amphibolites,  sediments. FL=Franconian Line. Bottom: Situation map of actual vibrator points (scattered) and geophone lines. The covered subsurface area is marked.

DATA MATERIAL

Fig. 2 gives an overview of the surveyed area. In the upper part the topography is shown. The Franconian Line in the foreground is striking as well as the Steinwald granite massif in the northern part with up to 800 m height above sea level. In the middle part the main geological units are sketched as there are the Variscan granites (Steinwald G., Falkenberger G., Friedenfelser G.), the ZEV (= zone of Erben-dorf-Vohenstrauss) with metabasitic gneisses and amphibolites, the Franconian Line and the sediments northwest of it.

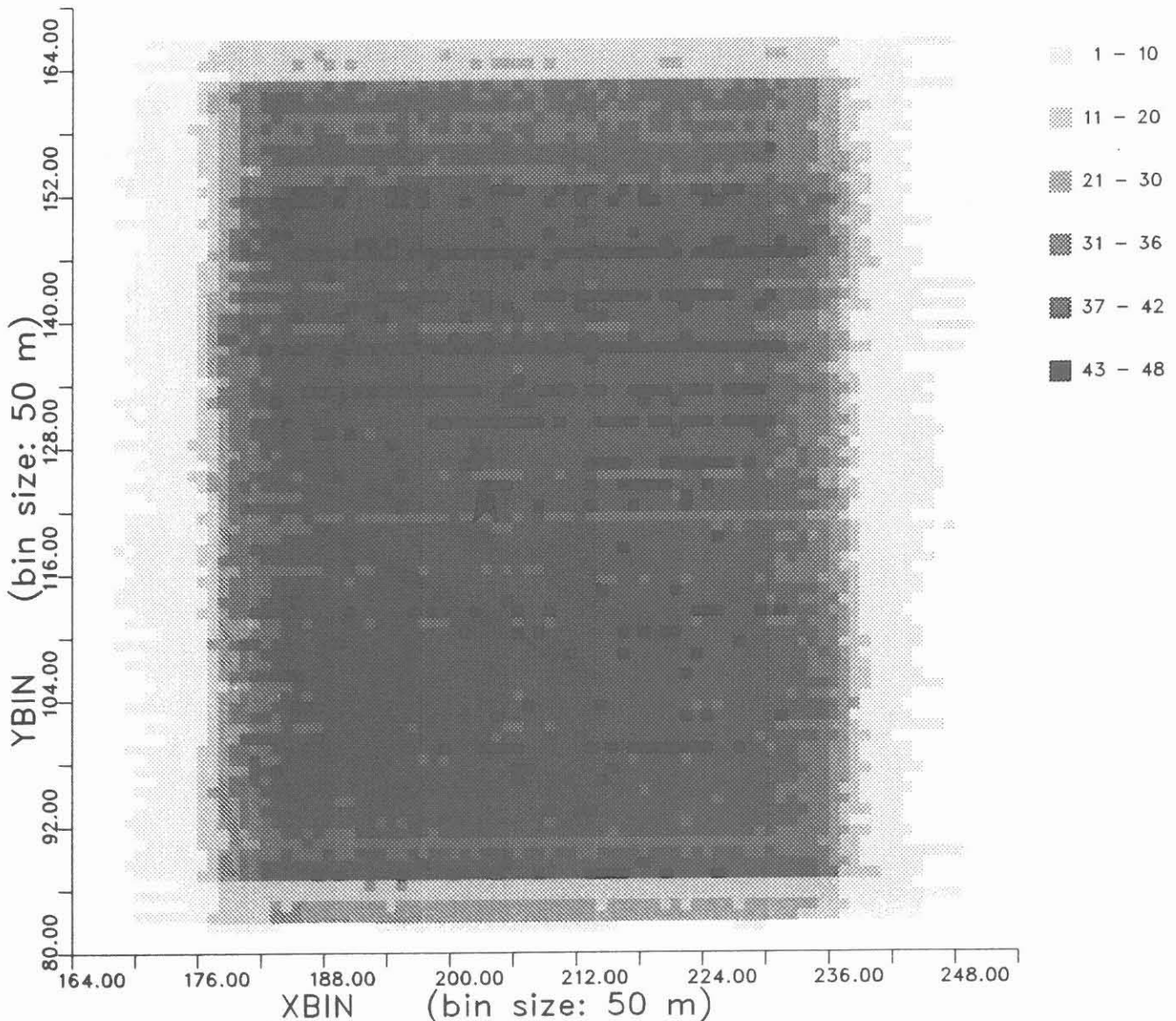


Fig. 3: Total subsurface coverage for 3D-expanding-spread experiment.

The lowest part of Fig. 2 shows the actual vibrator points and geophone locations. A total number of 189,460 seismic traces has been recorded. The area covered in the subsurface is marked. It has an extension of 4050 m x 4200 m. Fig. 3 shows the actual total coverage. The direction of XBIN corresponds to the direction of the geophone lines and YBIN to the vibrator traverses. A maximum coverage of 48 has been achieved, the mean coverage is 37 to 42-fold per 50 m x 50 m bin. The border zone with poorer coverage is caused by the fact that with the first and last vibrator traverse the geophone spread could not be shifted by 8 geophones necessary

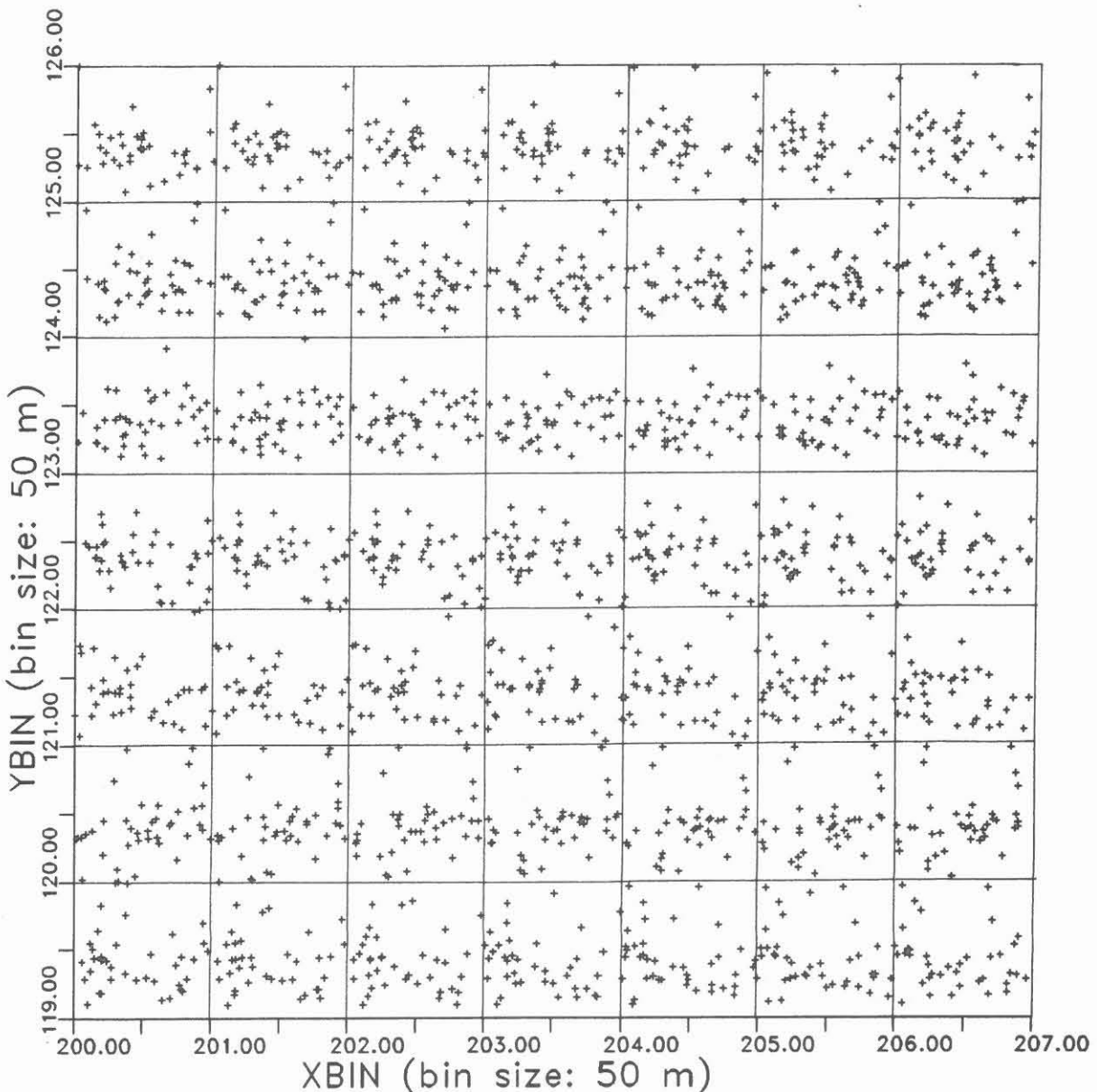


Fig. 4: Common midpoint distribution within several bins (bin size: 50 m x 50 m).

for symmetry, because the geophone lines had been surveyed for the 48 traces of the 3D survey. Dead traces are not considered up to now.

An example of the common midpoint distribution in single bins is shown in Fig. 4. Fig. 5 gives examples for the azimuth and offset distribution in single bins. Taking all subsurface points together we get the offset distribution shown in Fig. 6: Offsets from 0 to 24 km are achieved, offsets in the range 2 km to 22 km 160-fold, the range 7 km to 18 km ca. 800-fold and offsets of about 15 km about 1600-fold. Compared with the 3D seismic survey itself with a maximum offset of 6.5 km we have good conditions for velocity analyses. But we

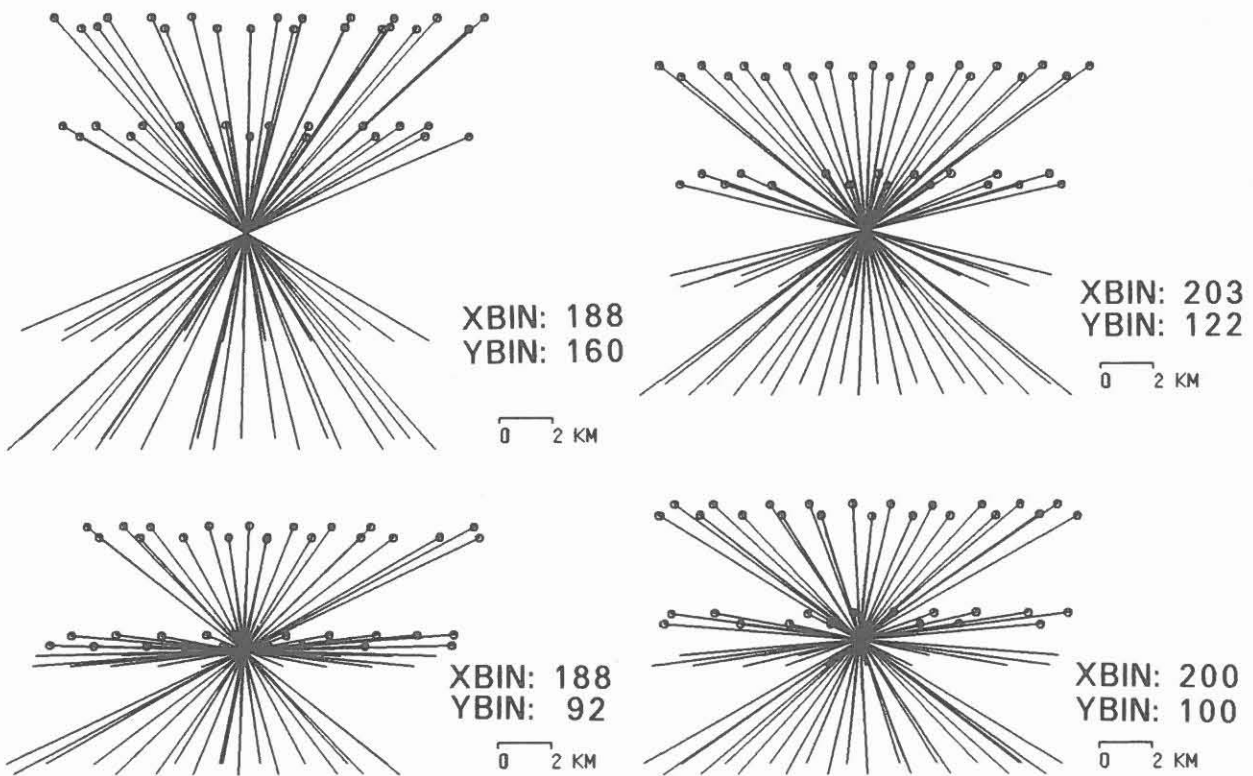


Fig. 5: Source-receiver geometry for single bins; o = source point.

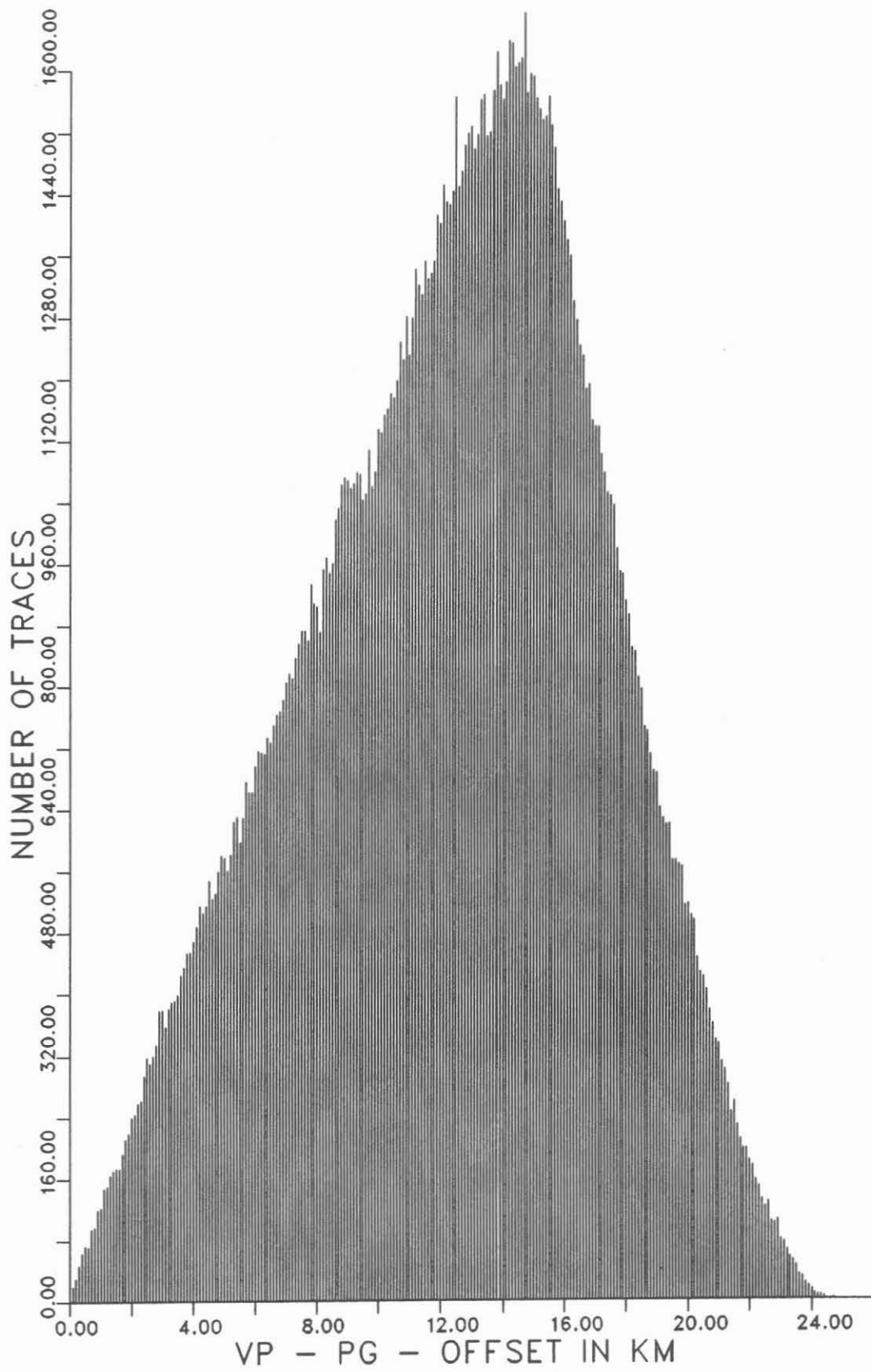


Fig. 6: Offset distribution including all traces.

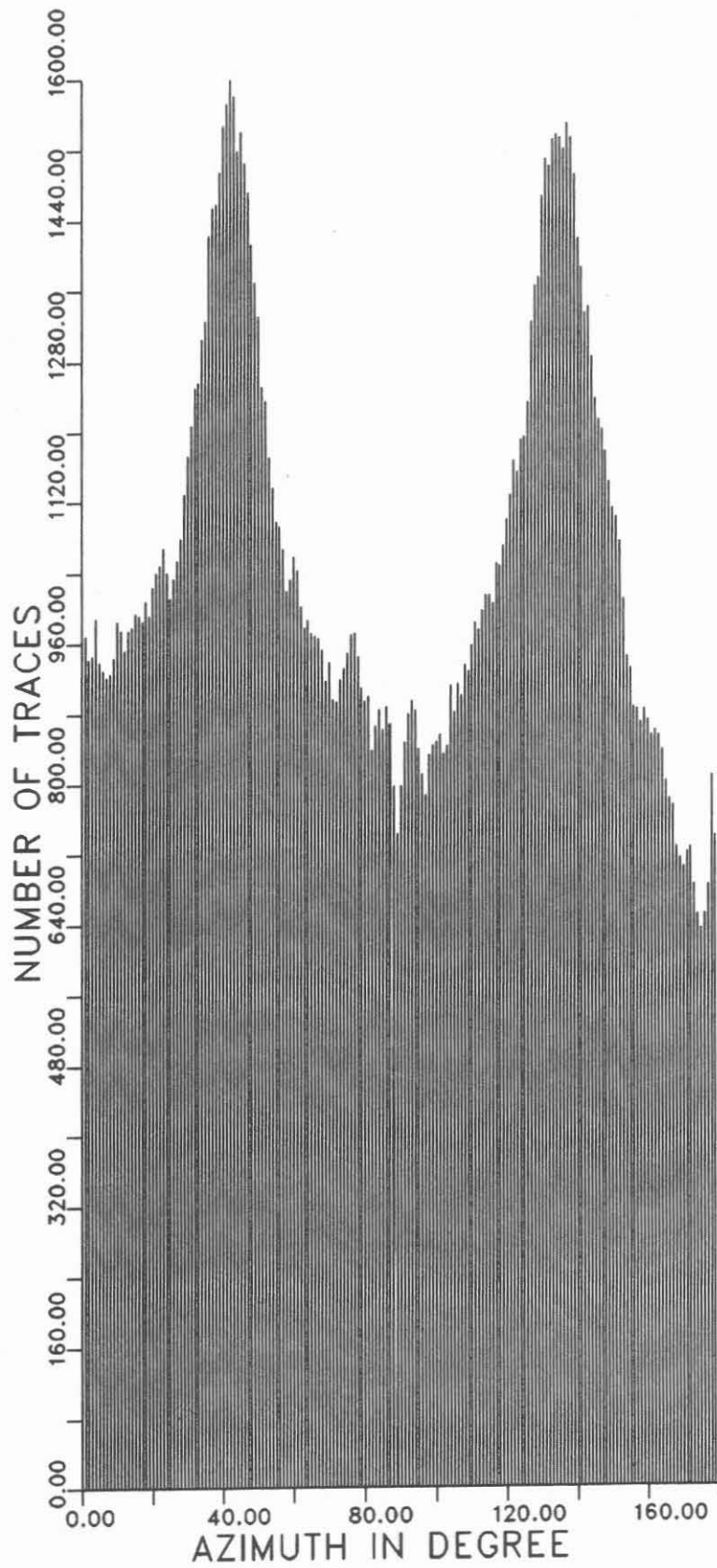


Fig. 7: Azimuth distribution including all traces.

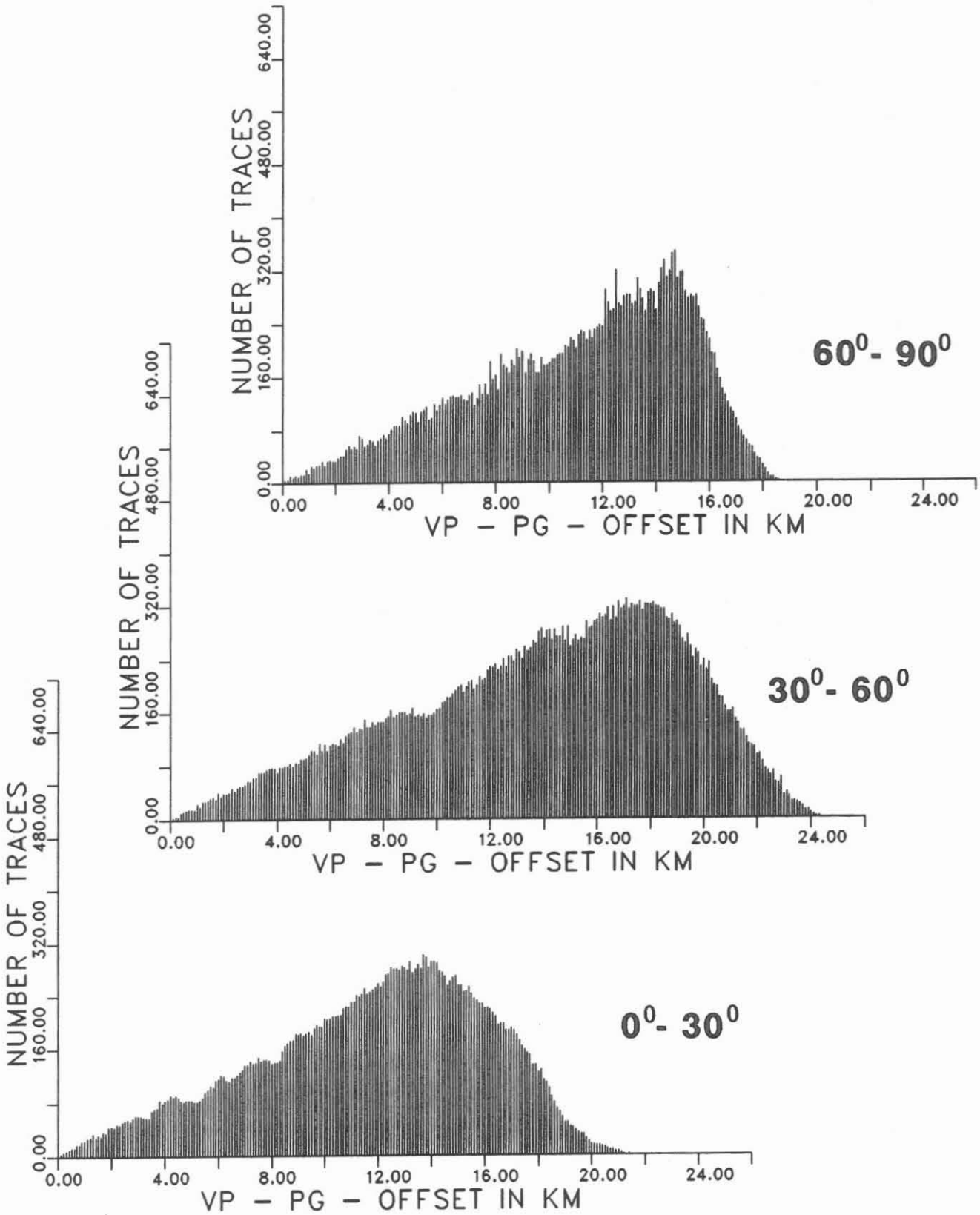


Fig. 8: Offset distribution for 30° azimuth ranges. The range 90° - 180° is covered in an analogous manner.

must be aware that this distribution includes all source-receiver azimuths ($0^{\circ} - 180^{\circ}$), so a velocity analysis based on this data set would lead to an average velocity only without considering seismic anisotropy. The coverage for the whole azimuth range is shown in Fig. 7. An azimuth of 0° respectively 180° corresponds to the direction of the geophone lines. A mean coverage of 800 is achieved for the whole range, maximum coverages of 1600-fold are obtained for angles of 45° and 135° . The offset distributions for single azimuth ranges, in 30° steps, are shown in Fig. 8 and listed below:

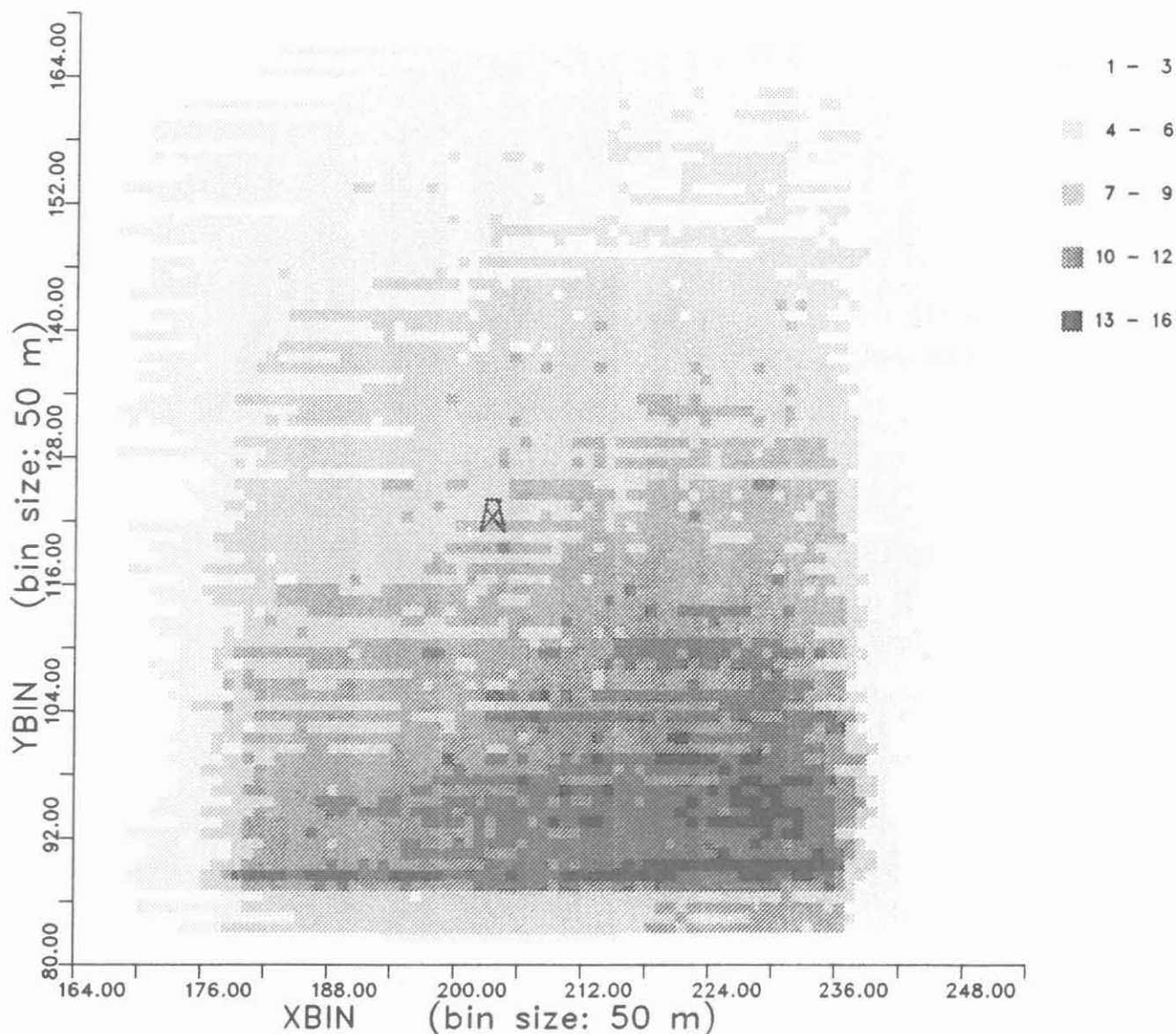


Fig. 9: Subsurface coverage for source-receiver azimuths restricted to $0^{\circ} - 30^{\circ}$.

00°-30° azimuth: 4-18.5 km: 80-fold; 8-18 km: 160-fold
30°-60° azimuth: 4-22.0 km: 80-fold; 8-21 km: 160-fold
60°-90° azimuth: 4-17.0 km: 80-fold; 8-16 km: 160-fold

The range 90°-180° is covered in an analogous manner. The small offsets are generally less covered. These distributions are valid for the entire area and Figs. 9 - 11 show the coverage in the area restricted to different azimuth ranges. The maximum coverage reached for these sections is 16-fold. The highly covered bins are restricted to smaller areas.

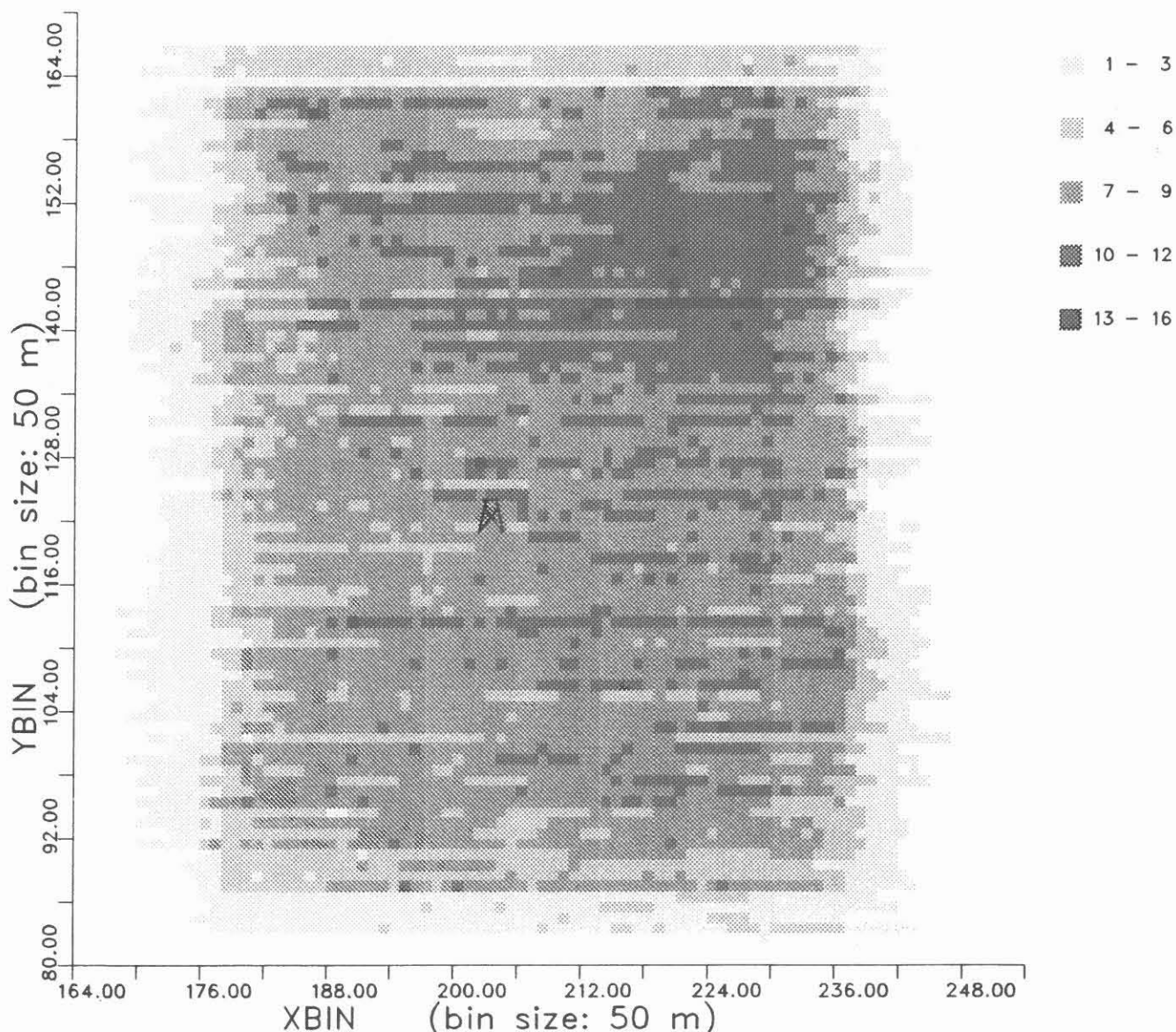


Fig. 10: Subsurface coverage for source-receiver azimuths restricted to 30° - 60°.

An example of the data material is given in Fig. 12 where a common shot gather with the two parallel geophone spreads of 60 geophones each and an interval of 400 m is shown. The first break is in the range 1.8 s to 2.8 s. At about 4-5 s a strong reflection respectively reflection band is observed corresponding to approximate vertical reflection times of 3.5-4 s.

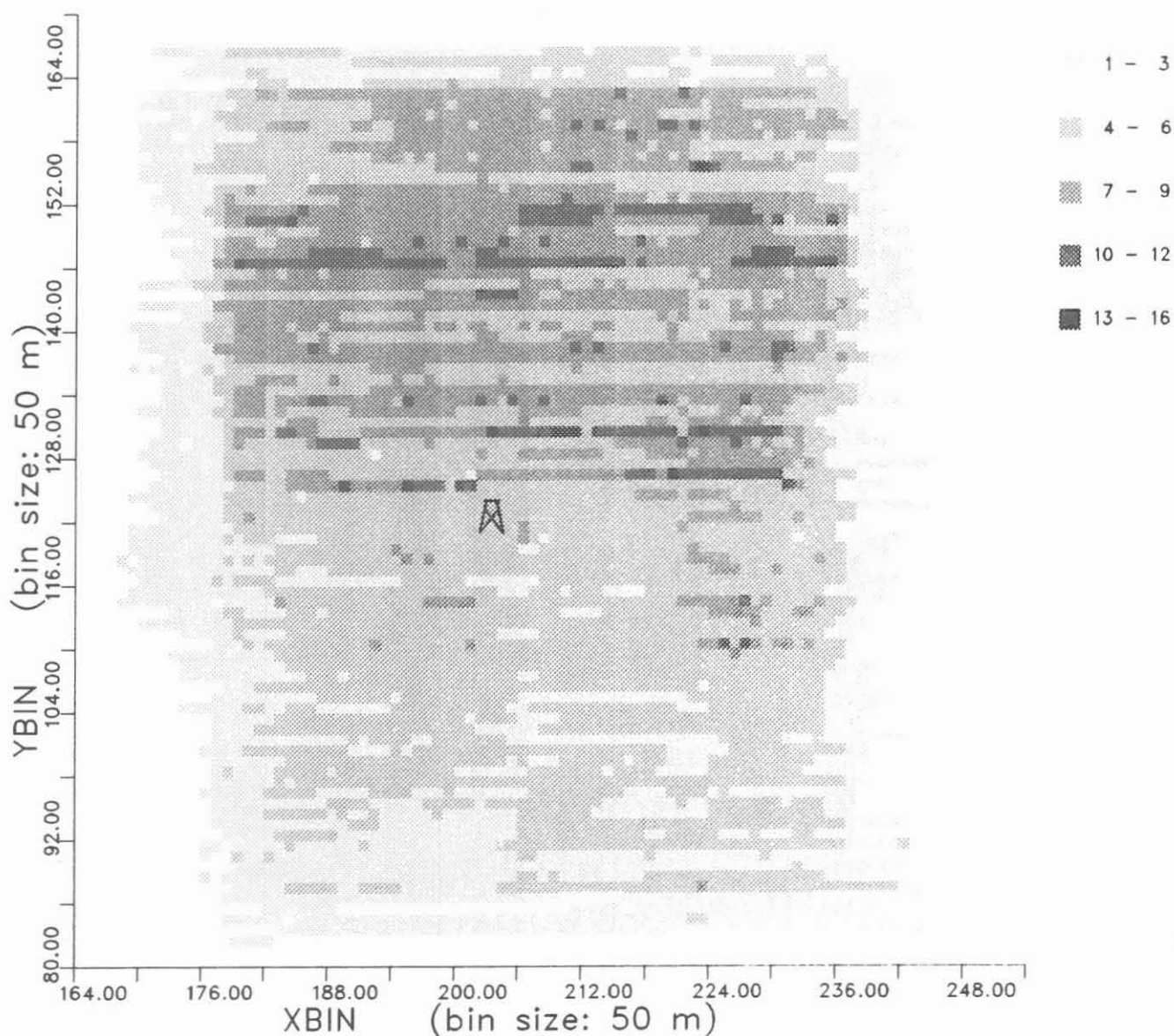


Fig. 11: Subsurface coverage for source-receiver azimuths restricted to 60° - 90° .

OUTLOOK

The data material described above is expected to give a strong basis for a detailed velocity model throughout the crust for the area of the KTB. First static corrections have to be implemented. As it is known that the rocks are seismically anisotropic, the velocity analysis has to be restricted to distinct azimuth ranges. Preliminary values of the velocities can be obtained by normal moveout corrections, constant velocity stacks or x^2/t^2 diagrams. Problems may arise applying hyperbolic normal moveout functions at large offsets. Further problems are due to dipping reflectors and the complex geology. So for example the influence of the Franconian Line is unknown. However, by means of the results of the 3D survey and all the other experiments of the ISO 89 experiment a detailed picture of the velocity field will be obtained. Various types of raytracing modelling will be used, and from all these we hope that ISO 89 will make a substantial contribution to the understanding of the complex geologic situation.

REFERENCES

- REHLING, J.G., STILLER, M., 1990: 3D Reflection Survey of the Area around the Continental Deep Drilling Project Site.
- NLfB, Hannover, KTB-Report 90-6B.

Integrated P- and S-Wave Borehole Experiments
at the KTB-Deep Drilling Site

E. L. Lüschen
W. Söllner
A. Hohrath
W. Rabbel



INTEGRATED P- AND S-WAVE BOREHOLE EXPERIMENTS AT THE KTB-DEEP DRILLING SITE

E. Lüschen*, W. Söllner*, A. Hohrath*, W. Rabbel**

ABSTRACT

Data are presented from integrated special experiments which have been performed in conjunction with a seismic 3D reflection survey within the framework of IS089 (Integrated Seismics Oberpfalz 1989) coordinated by DEKORP (German Continental Seismic Reflection Program) between July and November of 1989.

The main objective was to study the nature of P- and S-wave reflections and velocities, the Poisson's ratio and the seismic anisotropy in a medium of crystalline rocks around the KTB site (Continental Deep Drilling Program), where the borehole has reached a depth of 4000 m. A digital 5-unit geophone chain with 25 m spacing and three components was used for downhole recording.

The program described here consists of:

- 1) shearwave 2D reflection profiling (SCMP) with two 10-12 km long lines crossing the KTB-site, source: 2 horizontal vibrators with different orientations, 3-component recording;
- 2) shearwave moving source profiling (S-MSP); downhole recording of the source points of the SCMP;
- 3) vertical seismic profiling (VSP) down to 3660 m with different source azimuths and offsets (zero-offset, 4 km, 8 km); P- and S-wave sources: explosives, horizontal and vertical vibrators, and horizontal hammer techniques.
- 4) multiple azimuth shearwave experiment (MASE) with 4 km and 8 km offset and horizontal vibrator sources (radial and transversal orientation).

The VSP surveys display steeply dipping reflections, increasing in number below 3000 m depth. Horizontal structures, preferentially seen in the surface profiling, are the exception. Polarization analysis of shearwaves shows dominant azimuths in shearwave splitting which correlate with maximum horizontal stress (N 158° E) and with azimuth and dip of foliation.

* Geophysikalisches Institut, Universität Karlsruhe, Hertzstrasse 16, D-7500 Karlsruhe 21, F.R.G.

** Institut für Geophysik, Universität Kiel, Olshausenstrasse 40-60, D-2300 Kiel 1, F.R.G.

INTRODUCTION

The interpretation of standard 2D-reflection profiling data collected in crystalline areas often suffers from the lack of direct calibration. Deeper crustal reflections (e.g. DEKORP Research Group, 1988; Lüschen et al., 1987) differ significantly from those known from industrial sedimentary basin surveys. Although they are often very bright, reflections from crystalline rocks appear discontinuous and of chaotic or, in the lower crust, of laminated character.

The German Continental Deep Drilling Program (KTB) offers a unique opportunity to study seismic reflections of the crystalline basement and their nature in more detail. An integrated seismic survey has been designed under the auspices of DEKORP to provide an extensive data base which is comparable to the techniques used in hydrocarbon exploration, including 3D-reflection surveys and vertical seismic profiling (VSP). This program has been extended by the inclusion of many non-standard experiments, particularly using wide-angle, downhole and shearwave techniques.

Shearwave observations, by means of their polarization and by determination of the seismic anisotropy (Helbig and Mesdag, 1982, Crampin, 1987a,b), in combination with standard P-wave measurements, possess the potential to obtain additional information on lithology and structure, crack and microcrack distribution. Experimental studies by Nur and Simmons (1969) have shown that velocity anisotropy can be induced by the stress field. Laboratory measurements on crystalline samples (Kern, 1982) demonstrated that the V_p/V_s ratio can be a very useful lithological indicator. The KTB offers a direct link between experiments on core samples, well-logging, and seismic illumination by downhole surveys and surface seismic measurements. Thus, seismic images of the crystalline environment can be calibrated by findings in the borehole and, on the other hand, the regional significance of lithological and structural features in the borehole can be tested.

This article describes a package of four special field experiments, completed within the Integrated Seismic Program between July and November of 1989. They focus on application of shearwave and downhole techniques in order to derive information which complements standard P-wave techniques. We used a series of standard and non-standard field configurations, described in the next chapter, as well as supplementary experiments with different source techniques. The basic principles of these techniques, which came into use in industrial hydrocarbon exploration in the eighties, are provided by several excellent review and introductory articles, e.g. Hardage (1985) and Danbom and Domenico (1986).

Our intention was to illuminate the target area around and below the borehole (maximum depth 4000 m) with seismic waves of different resolution characteristics for different angles and raypaths addressing the problem of distinguishing lateral inhomogeneities from seismic anisotropy. The experiments described in this article should not be regarded as stand-alone experiments. Their full resolving power is expected during integration of all experiments, particularly in conjunction with the contemporarily completed 3D seismic survey.

The processing is not yet completed. Particularly, polarization studies require a systematic approach in the future. Therefore, this paper describes the present stage of the data base after completion of most of the standard processing sequence. First noteworthy results are also outlined. Figure 1 shows the area of main interest indicated by a frame of 15 km side length and 15 km depth around the projected KTB-hole. Figure 2 shows the same target area represented by the SW-NE reflection profile KTB 8502 (DEKORP Research Group, 1988), where the KTB-hole is located in its centre. Reflections of almost discontinuous character can be recognized below 0.7 s TWT. The most prominent group of reflections is found between 3 and 4 s TWT, which define the so-called Erbendorf body (Franke, 1989).

THE EXPERIMENTS

Figure 3 represents a location map of all the experiments to be described in this chapter. It covers nearly the same area which has been surveyed by the 3D reflection technique. Figure 4 shows the basic principles applied to each corresponding experiment. All field operations were performed under the technical management of field crew Schwanitz of Prakla-Seismos AG, Hannover, in close cooperation with the authors from DEKORP and with the KTB logging group. SCMP and S-MSP experiments were conducted in July 1989 in the starting phase of the ISO89-program before the 3D-survey. All the others were performed during holidays and weekends of the 3D field crew until late November 1989.

I) Shearwave 2D reflection profiling (SCMP)

The SCMP-experiment has been designed analogous to standard P-wave 2D reflection profiling using the common-midpoint (CMP) stacking method. We were interested in the near-vertical shearwave response of crustal structures (down to the crust-mantle boundary) known from previous P-wave profiling during the reconnaissance phase (DEKORP Research Group, 1988). The Erbendorf-body, characterized by pronounced P-wave reflectivity and relatively high velocities between 3 and 4 s P-wave two-way traveltime (or approximately 9 to 12 km depth), was of particular interest.

Since it could not be expected to exceed the lateral und vertical resolution of P-waves, this experiment was designed to produce multifold CMP-coverage for two short perpendicular profiles, each approx. 5 km long. CMP-stacking in this case is expected to enhance the shearwave signal to noise ratio and to allow for velocity analyses. The field configuration of the two lines was closely adapted to the previous P-wave profiling of 1985. Its design benefitted from a pilot study in the Black Forest (Lüschen et al., 1990) concerning the efficiency of shearwave generation by the Vibroseis method and by explosions. A comparative study is under preparation.

The layout of the three-component receivers was asymmetric to the source points (see figure 3) in order to enable velocity analysis for greater moveouts and to better balance between the energy of first arrivals and late reflections, which is of crucial importance when using the Vibroseis technique. The deployment of three-component receiver stations,

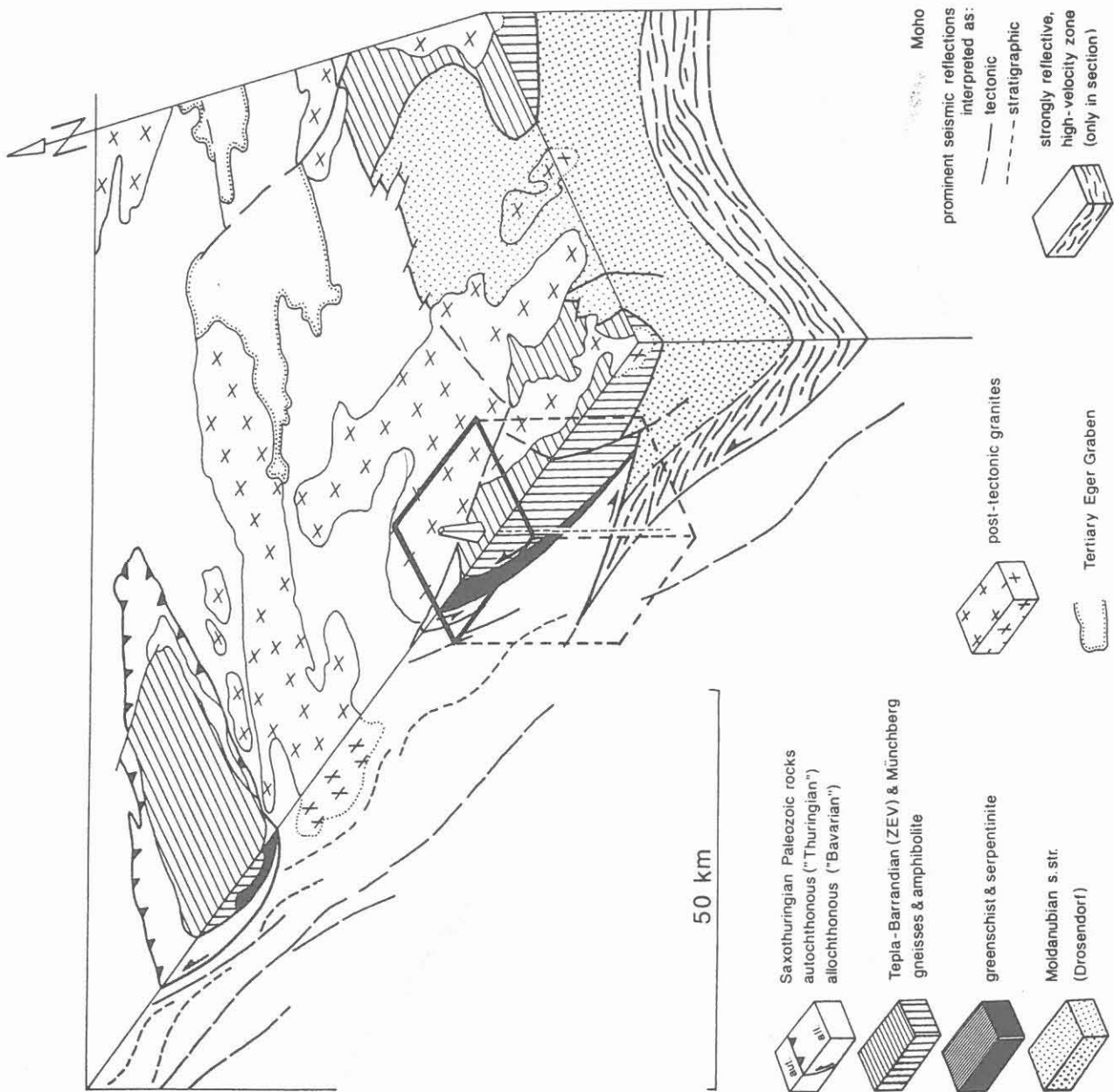


Figure 1: Study area marked by a frame of approximately 15 km side length and 15 km depth. Interpretive 3-D representation of the crustal structure around the KTB drill site derived from surface mapping and 2-D reflection profiling during pre-site investigations (from Franke, 1989). The surface of the marked target area corresponds also to location map of figure 3.

Figure 2: Central part of the stack section KTB 8502 from a pre-site survey (DEKORP Research Group, 1988). Length of section: 12 km, shown are the first 5 s TWT corresponding approximately to 15 km depth. Processed by DEKORP Processing Center Clausthal. Location of KTB is indicated.

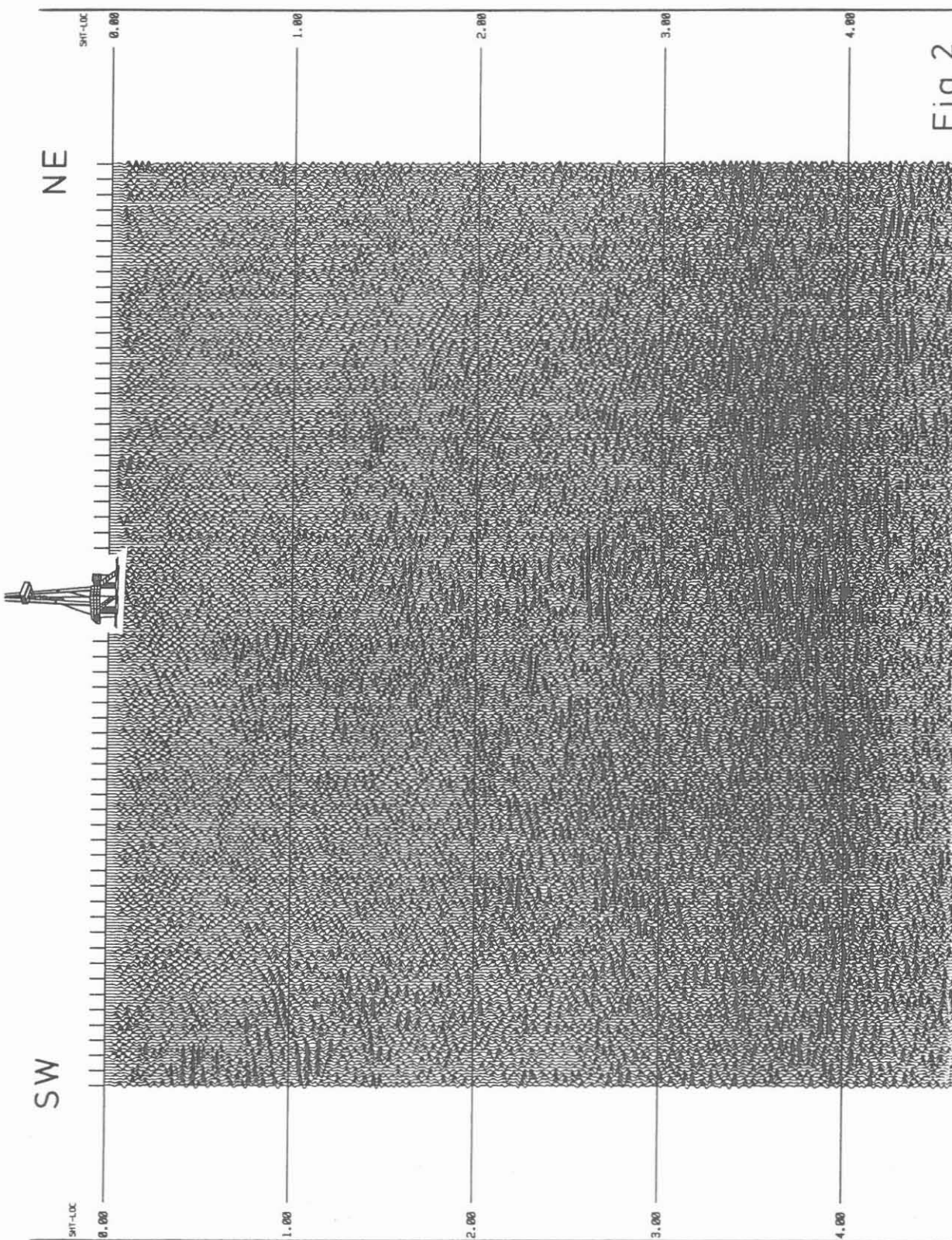


Fig 2

Fig 2

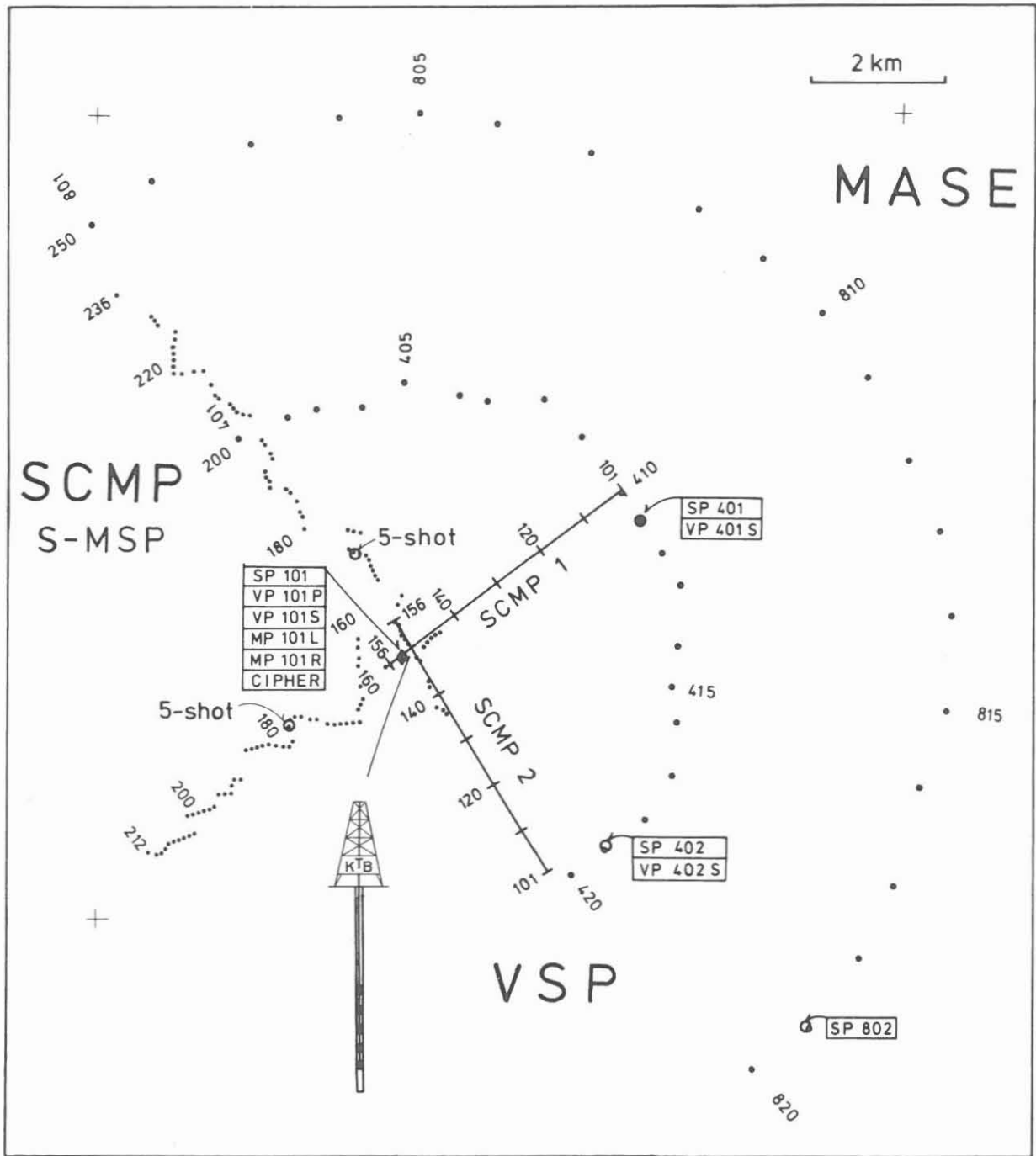


Fig 3

Figure 3: Location map of the study area, reduced from scale 1:25000.
 SCMP: Shearwave 2D reflection profiling, line SCMP1: locations 101-212 (NE-SW), line SCMP2: locations 101-250 (SE-NW), dots are vibrator points, solid lines are stationary 3-component receiver spreads;
 S-MSP: Shearwave moving source profile, simultaneous recording of all SCMP source points with a 3-component downhole geophone unit at 3400 m depth;
 VSP: Vertical seismic profiling, 4 source points: 101 (zero offset), 401 and 402 (4 km offset) and 802 (8 km offset),
 SP: explosive source, VP (P): vertical vibrator, VP (S): horizontal vibrator, MP (L) Marthor source (hammer, left), MP (R) Marthor, right, CIPHER: circular polarized horizontal excitation.
 MASE: Multiple azimuth shearwave experiment, vibrator source points 401-420 (4 km offset) and 801-820 (8 km offset).

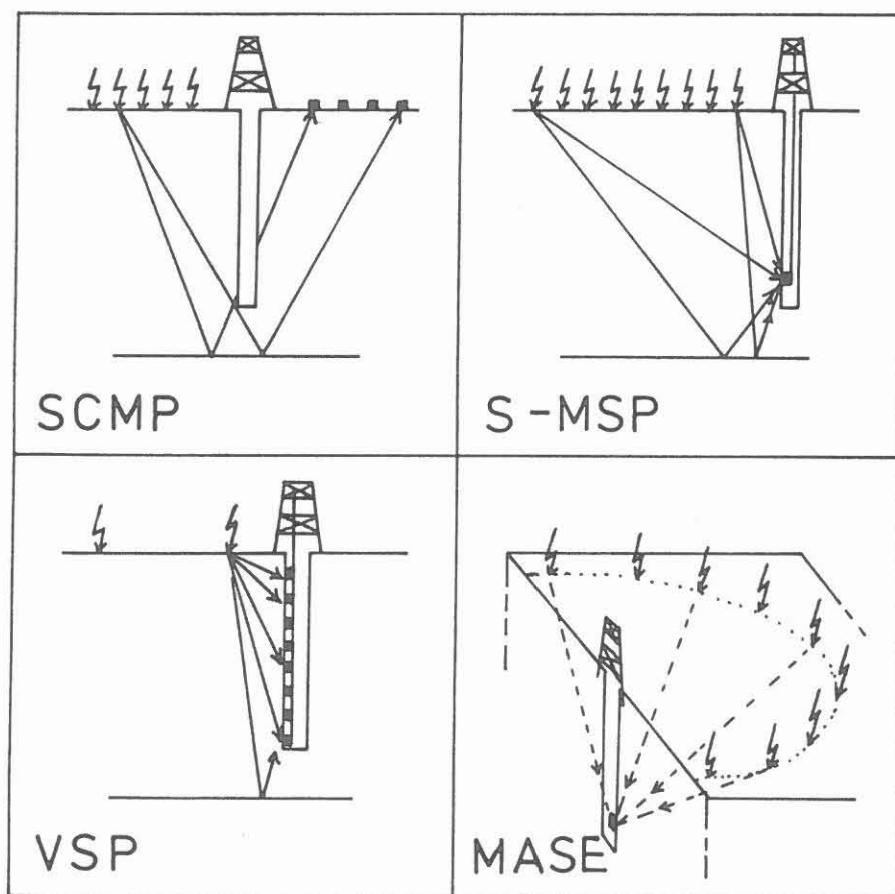


Figure 4: Schematic diagram with the basic principles of the SCMP, S-MSP, VSP and MASE experiments.

particularly of the horizontal geophone strings, needs special care concerning ground coupling and orientation. Therefore we decided to deploy them only once, and rechecked the layout frequently, keeping it in a stationary position, while the source moved along the line. The maximum coverage is therefore produced on a sector with the KTB-hole in its centre and decreases towards the ends of the lines.

The recording was done by two DFS V systems of the DEKORP group at NLFb, Hannover, and the University of Karlsruhe, with a total number of 168 channels, equipped also with stacker and Vibroseis electronics. The spread on each line (SCMP 1 and SCMP 2) consisted therefore of 56 3-component stations (locations 101-156) with a spacing of 80 m.

Two horizontal vibrators (type VVCS, Prakla-Seismos AG) were used as shearwave source. They moved in 80 m intervals from location 144 to 212 (SCMP 1) and from 136 to 250 (SCMP 2). After a start-up sweep test an upsweep of 9 to 43 Hz and 30 s length was chosen, since it turned out to be impossible to generate signal frequencies significantly above 40 Hz. Most vibrator-points were situated in meadows with a relatively hard ground, so ground coupling of the wedge-shaped baseplates was highly efficient, without any ground-damage, and enabled good force and phase control. The orientation of the horizontally vibrating baseplates was transverse (Y) to the line on all points. Additionally, on every third point we also used Y-45° and Y+45° orientations.

In contrast to explosive techniques, vibrators offer the possibility to apply well-defined stresses to the ground regarding their frequency and their orientation. On the other hand, the energy of shearwave generation is not always, except for some favourable cases, comparable to explosive sources and sometimes not predictable. This may be caused by non-optimum ground coupling and by effects occurring within the weathering zone. This apparent drawback was expected to be compensated during multiple vertical and horizontal (CMP) stacking.

Additionally to the Vibroseis survey, explosives were used on one shotpoint on each line, to produce a single-fold shotgather with the site of the KTB-hole in the centre of the coverage (compare figure 3, shots are labeled with '5-shot'). These shotpoints consisted actually of 5 distinct holes (20-25 m deep, spacing 5 m, one hole in the centre, each one charged with 25 kg dynamite), which were fired, the centre shot first, and recorded separately. According to the three-hole technique (or Camouflet method, Edelman, 1985), the central shot produces a zone of weakness or a lateral inhomogeneity. The other shots, adjacent to this zone, therefore produce stronger horizontal stresses which then propagate as shearwaves. These shearwaves may be further enhanced when the records of the two opposite shots are stacked after inverting the polarity of one of them. In our case we modified this three-hole method by an additional pair of shots.

For static corrections, a short-refraction survey with a 12 channel signal-enhancement system and an oblique hammer device (VAKIMPAK) for shearwave generation was used on selected parts of the two lines. Additionally, the other experiments, especially the S-MSP, are expected to provide static corrections for shearwaves.

Table 1 lists all important field parameters (Vibroseis survey). The operation was performed in a 2 week campaign at the end of July 1989 during the starting phase of the 3D survey.

Source	2 vibrators VVCS (Prakla-Seismos) 170 kN Peak Force, force control wedge-shaped baseplates spacing 80 m signal (upsweep) 9 - 43 Hz 30 s length orientation transversal (Y) (on each third point: Y, Y-45o, Y+45o)
Receiver	three components horizontal components: Sensor SM 6, 8 Hz vertical component: Sensor SM 4, 10 Hz group spacing 80 m geophones per group 12 no specific geophone pattern (5-10 m)
Recording	TI-DFS V 120 Channel (DEKORP, Hannover) TI-DFS V 48 Channel (University Karlsruhe) both with I/O-MSP Stacker and Pelton Vibroseis electronics 2 uncorrelated records per vibrator point and orientation 5-fold vertical stack of each record sample interval 4 ms length of recording 34 s , 37 s pre-amplifier 42 dB low-cut 5 Hz or out high-cut 62 Hz format SEG B
CMP coverage (after processing)	50-70 decreasing towards the endpoints of the line

Table 1: Field parameters used in shearwave 2D reflection profiling (SCMP)

II) Shearwave moving source profiling (S-MSP)

A moving-source-profile (or walkaway survey, compare figure 4) was gathered at the same time as the SCMP survey. This was achieved by recording all SCMP sources simultaneously by a downhole tool. A digital 5-unit geophone chain (SEKAN 5, Prakla-Seismos AG), which very recently has been developed for KTB purposes (Mylius et al., this volume), was placed in a stationary position between 3590 m and 3690 m depth, the spacing being 25 m. Each unit

consisted of 3 components oriented in cartesian coordinates, each component consisted of 2 detectors connected in series. Sensor 10 Hz geophones were used. The signals were filtered on-site, pre-amplified (by switchable gains), A/D converted and transmitted in multiplexed form to the surface. Each unit was equipped with a magnetic compass for orientation.

Recording was done at the KTB-site with a 24-channel ES 2420 EG&G system, borrowed from the Alfred-Wegener-Institut, Bremerhaven. 15 channels were needed for downhole recording. This microprocessor-controlled system allowed for quick preprocessing (e.g. correlation, stacking, filtering etc.) and quality control. The quality of the SCMP source points thus could be evaluated immediately. Recording in slave operation was triggered by the master-DFS V system of the SCMP. Recording parameters were essentially the same. Field data format is SEG D.

For purposes of inspection and repairs the digital chain had to be replaced by an analogue single 3-component unit after the first week. Line SCMP 2 was therefore recorded with this unit.

III) Vertical seismic profiling (VSP)

Vertical seismic profiling provides the closest link in interpretation between reflections observed in 2D and 3D surface reflection profiling and the lithology in the borehole. Its application in hydrocarbon exploration has been widely established during the eighties (Hardage, 1985).

P-wave sources as well as S-wave sources were applied. In order to cover a maximum range of frequencies and corresponding resolution characteristics, different source types for each wave type were also used (see table 2).

The Marthor (trademark of IFP) was used additionally to the vibrator source in order to compare zero-phase signals (after correlation) with minimum-phase (impulsive source) regarding polarization analysis. Since the source was located on very hard ground, higher signal frequencies were expected with the Marthor, but frequencies lower than 40 Hz were actually generated, lower than using the vibrator. Also energy of the Marthor source turned out to be lower than in case of the vibrator. Therefore it was decided to continue with the vibrator technique in the subsequent MASE experiment where a good shearwave signal to noise ratio was of crucial importance.

Four different source locations were used (compare figure 2). Although a high-quality zero-offset VSP already existed (with a dense receiver spacing of 12.5 m, completed in winter 1988/89, actual offset 200 m, see following chapter), another dynamite zero-offset profile (labeled SP 101) was repeated with an offset of 60 m. The reasons for this were, firstly that the processing quality of the old profile (Schruth et al., 1990) has been hampered by the combination of two different datasets, and secondly that borehole-guided waves (e.g. Stonley-waves) could be expected additionally from a source point closer to the borehole. We preferentially considered these wave types relevant for fracture and stress analysis. The S-vibrator VP 101 S was located at the same place, while the other zero-offset sources VP 101 P, MP 101, and CIPHER were located at 160 m, 200 m and 320 m offset. The other three source points 401, 402 and 802 were located at 4 km and 8

km offset, respectively, and in different azimuths (see figure 3). They were considered to provide a link to the MASE-Experiment and to illuminate the target area with a wider range of different raypaths, which is important for inversion techniques and for anisotropy studies.

P-wave sources: -----

- a) dynamite (SP): single charges of 0.5 - 1 kg in 20 m deep holes, which were used multiple times, tamped with water, actual firing depth was variable: 5-20 m, base of weathering zone near 5 m depth, a monitor geophone at 60 m depth was used for signal control.
- b) vertical (standard) vibrator (VP (P)): Type VVEA, Prakla-Seismos, 19 t, Upsweep 10 - 80 Hz, length 20 s, vertical stack 5-10-fold, recorded without correlation.

S-wave sources:

- c) horizontal vibrator (VP (S)): Type VVCS (see table 1) Upsweep 9 - 47 Hz, length 30 s, stacked 10-fold (5-fold per record), recorded without correlation, orientation: transverse with respect to source-hole azimuth.
 - d) Hammer, MARTHOR (MP): Type M 3, Institut Francais du Petrole, 10 shots on each side (left (L), right (R)) were stacked and recorded separately to allow for inverted stack during processing, orientation mostly transversal with respect to source-hole azimuth (SW).
 - e) CIPHER : Circular polarized shearwave excitation, new method in test, based on Vibroseis technique Edelmann and Lüschen (1990).
-

Table 2: Listing of seismic source techniques used in the vertical seismic profiling (VSP)

The downhole tool was the same as described above (SEKAN 5). The chain of 5 units (spacing 25 m) first was moved to a defined depth position, then all source points and all sources were recorded subsequently, before the chain was moved by 125 m to the next position. Maximum depth was 3660 m, since in 3766 m a whipstock was set during drilling which could not be passed. Recording of the whole sequence took about 45 to 60 min and moving the downhole chain was accomplished in another 10 min (including reading of the magnetic compass). Recording was done again with the 24-channel ES 2420 EG&G system already mentioned above. Parameters, such as sampling rate, length of record, stacking, correlation etc., often had to be changed from record to record. Sampling rates of 1 ms were used for dynamite sources and the Marthor, 2 ms for the P-wave vibrator and 4 ms for the S-wave vibrator.

A first set of profiles was acquired during August 1st-4th working 18 hours each day: profiles SP 101, VP 101 S, MP 101, SP 401 and VP 401 S. Signal to noise ratio was found to be relatively low in this time period. Inspection

of the downhole chain indeed revealed damages to cables and electronics due to corrosive borehole fluids.

Within a second time period, from October 30th to November 3rd, the profiles VP 101 P, SP 402, VP 402 S and SP 802 were recorded with the cable material of the downhole unit replaced by more resistant materials. Data quality has improved considerably, particularly regarding the signal to noise ratio of the data behind the first arrivals.

The CIPHER experiment (see table 2, Edelmann and Lüschen, 1990), testing a special vibrator configuration to generate circular polarized shearwaves, was conducted shortly after the MASE experiment (see next chapter) on 6th September. A vertical profile from 2800 m to 3400 m depth was recorded with the SEKAN 5 downhole tool during this experiment. This shearwave source was also applied on selected vibrator points of the SCMP and S-MSP experiments.

IV) Multiple azimuth shearwave experiment (MASE)

Shearwave sources were distributed over half-circles around the KTB-hole, with special emphasis on the analysis of azimuth-dependent anisotropy. Two circles of 4 km and 8 km radius, respectively, were selected, starting NW over E to SE, each one with 20 source points (see [figure 3](#)). The far-offset source points of the VSP were also located on these half-circles.

After a comparative study between the Vibroseis and the Marthor source during the first VSP-experiment, mentioned above, we favoured the vibrator for shearwave generation because of its higher energy. One vibrator (VVCS) was used for radius 4 km and 2 vibrators for radius 8 km. Additionally, at a radius of 2 km, 5 vibrator points (separated by 45°) were recorded with one vibrator (not shown in [figure 3](#)). At each point the transverse (Y, with respect to source-borehole azimuth) orientation of the baseplate movement was recorded first and then the radial (X) orientation. An upsweep of 9 to 47 Hz was used with a length of 20 s. Two uncorrelated records were generated per point and per orientation, each one with 5-fold vertical stacking and 32.7 s length.

The downhole tool of 5 geophone units (SEKAN 5) was located at 3300-3400 m depth, with 25 m spacing, during the whole experiment. Thus 15 channels were recorded, three components for each of five units. Recording was done again with the 24 Channel ES 2420 EG&G system. For reference purposes, in order to control the quality of the downhole equipment by checking the reproducibility, a sweep of a stationary vibrator nearby the borehole was recorded from time to time. This experiment was conducted from the 2nd-6th of September. While one vibrator was operating at a radius of 4 km, the others at a radius of 8 km were moving to their next position and were operating alternately with the first vibrator.

At each source point an extensive shallow shearwave refraction survey was conducted by a group from Kiel University. The object was to correct static effects on time delays and anomalies in polarization caused by the near-surface weathering layer. Horizontal geophones were deployed at intervals of 2 m along 200 m long lines. A manual hammer was hit horizontally on an

iron bar clamped to the ground. Recording was done by a 24-channel microprocessor-based system (own construction).

Additionally, a near-surface polarization experiment (NESPE) was conducted at several source points of the MASE. Its objective was to study anomalies in polarization caused by near-surface effects. Single down-sweeps of 41 to 11 Hz and 61 s length were recorded. The vibrator was rotated in several steps of 45°. The analysis will be based on first arrivals.

DATA PROCESSING AND FIRST RESULTS

The present stage of processing is described and first results and phenomena are outlined. The sequence of experiments is the same as in the previous chapter. The processing is being performed with a CONVEX C1 super-computer and DISCO software at Karlsruhe University.

I) SCMP

The field layout was planned to enable CMP-processing as a tool to enhance signal to noise ratio of deep S-wave energy. Because the spread was not rolled (stationary), the highest CMP coverage is achieved near the center of the two lines, close to the borehole. Crooked line processing has to be applied. Major problems are expected from the topography and from highly variable near-surface velocities and weathering thickness. We therefore consider static corrections as a very crucial processing step. If this is not appropriately done, the quality of CMP stacking will decrease drastically inspite field records with a relatively high signal to noise ratio.

Since static corrections are not yet available, we present single vibrator-point gathers regarded as typical from both lines. Figures 5 and 6 show 3-component gathers of vibrator-point 170 of line SCMP1 and VP 197 of line SCMP2, respectively (compare figure 3). Processing only consisted of demultiplexing, correlation, vertical stacking of 2 field records, combining records of DFS V 48 channel and 120 channel systems. No further processing has been applied, the data show true amplitudes.

P-wave onsets of the direct wave can be seen on the vertical component, while the horizontal components reveal stronger S-wave first arrivals. Although the source orientation was transversal (Y), the energy of the recorded S-waves is shared by all three components. This indicates strong heterogeneities in the subsurface which cause seismic energy scattering and complex changes in polarization of S-waves. The direct waves of lines SCMP1 (SW-NE) and SCMP2 (NW-SE) are characterized by different phase velocities (table 3). Although the offset range is slightly different in the two VP-gathers, there is first indication of a pronounced seismic anisotropy.

Line	Azimuth	Vp	Vs	Vp/Vs
SCMP 1	N 225	5050 m/s	2950 m/s	1.71
SCMP 2	N 135	5950 m/s	3300 m/s	1.80

Table 3: Phase velocities derived from direct P- and S-waves

Travelling in NW direction, both wave types show increased velocities and an increased Vp/Vs ratio of 1.8 (crustal average is 1.73). These values are representative for a depth range of approximately 1 - 2 km around the KTB site. The difference in Vp is 16 %, in Vs 11 %. This is confirmed independently by a velocity evaluation of the S-MSP data (compare next chapter). A possible relationship of this azimuthal anisotropy with the recent stress field and/or the fracture orientation must be considered. An alternative explanation in terms of lateral heterogeneities, e.g. the granite-gneiss contact, is less likely. The raypaths considered here pass the ZEV (Zone Erbendorf Vohenstrauss) body consisting of gneisses and amphibolites (see [figure 1](#)).

Both records also reveal distinct seismic energy on the horizontal components, particularly at 7 s TWT, presumably S-wave reflections. There is no energy seen on the vertical component. The subsurface covered by reflections is nearly identical in the center of the spreads, but different in azimuth. The reflected energy therefore corresponds to the same structure. The signal characteristics are different. On line SCMP1 ([figure 5](#)) there is a 0.4 s long band of energy, on line SCMP2 ([figure 6](#)) distinct phases, one on each component, can be recognized. Obviously, these elements are different in polarization by 90 degrees. We argue that these phases might be split shearwaves, propagating through an an-isotropic medium above the reflecting structure. This must be substantiated by further polarization analysis of the complete dataset.

[Figures 7 and 8](#) show comparative results of the S-wave Vibroseis (10-fold vertical stack) and the dynamite source for both lines. The field configuration is nearly identical, for comparison see [figure 3](#). Both figures present the raw shot gather in their lower panel, a low-pass filtered version (according to the sweep frequencies used for Vibroseis) in the middle panel and the Vibroseis data of [figures 5 and 6](#) in the top panel. Although the dynamite data reveal better signal to noise ratio of the first arrivals, the later S-wave reflections seen on the Vibroseis horizontal components seem to be of higher quality. On the other hand, the vertical component of the dynamite data show very pronounced P-wave reflections between 3 and 4 s TWT. These reflections correspond to the previously defined 'Erbendorf'-body (see [figure 2](#)). Assuming an average Vp/Vs-ratio of 1.73, these P-wave reflections correspond also to the S-wave reflections at 7 s TWT mentioned above. A more detailed study of Lüschen et al. (1990) aims at quantitative comparisons between the spectra of

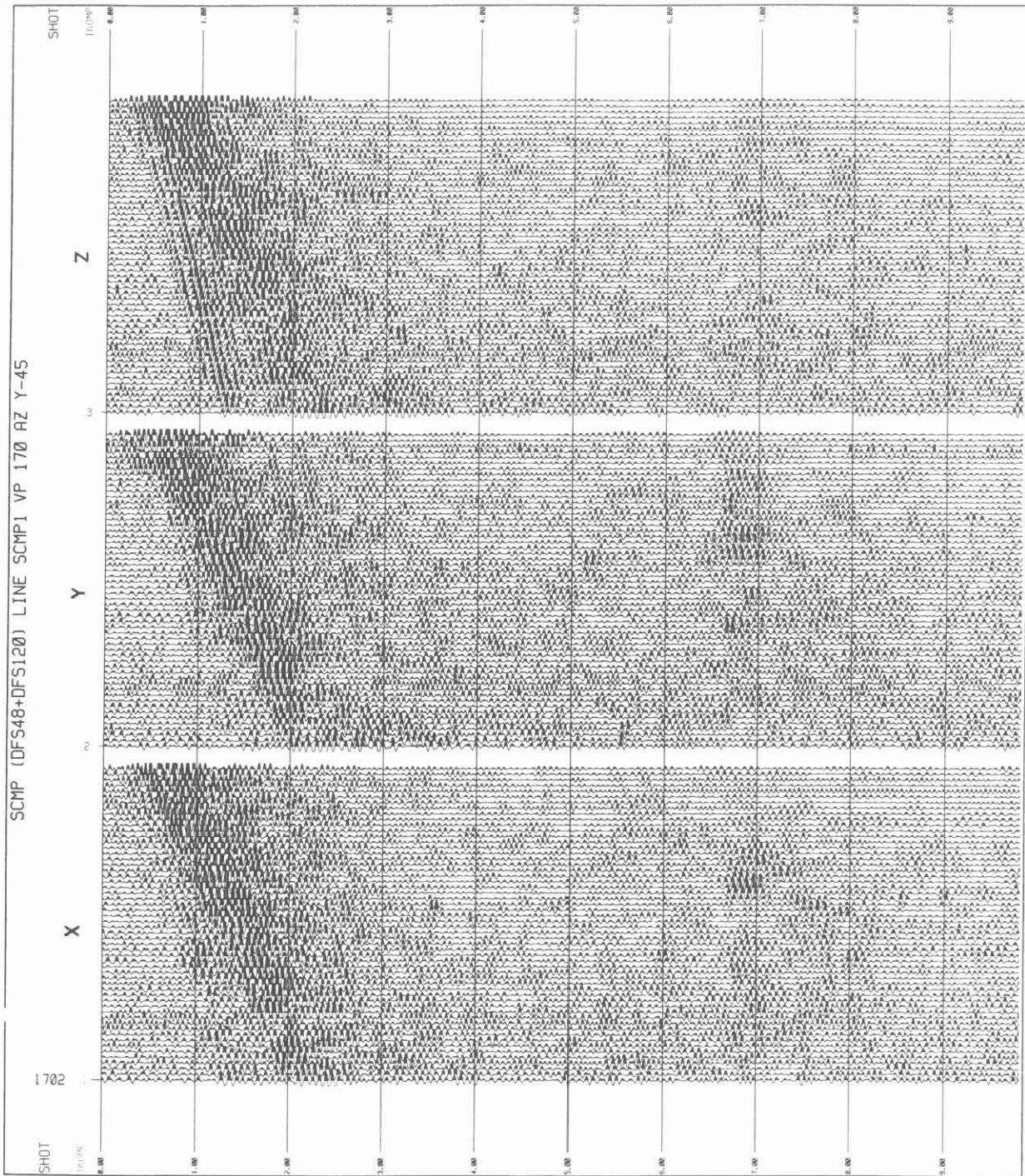


Fig 5

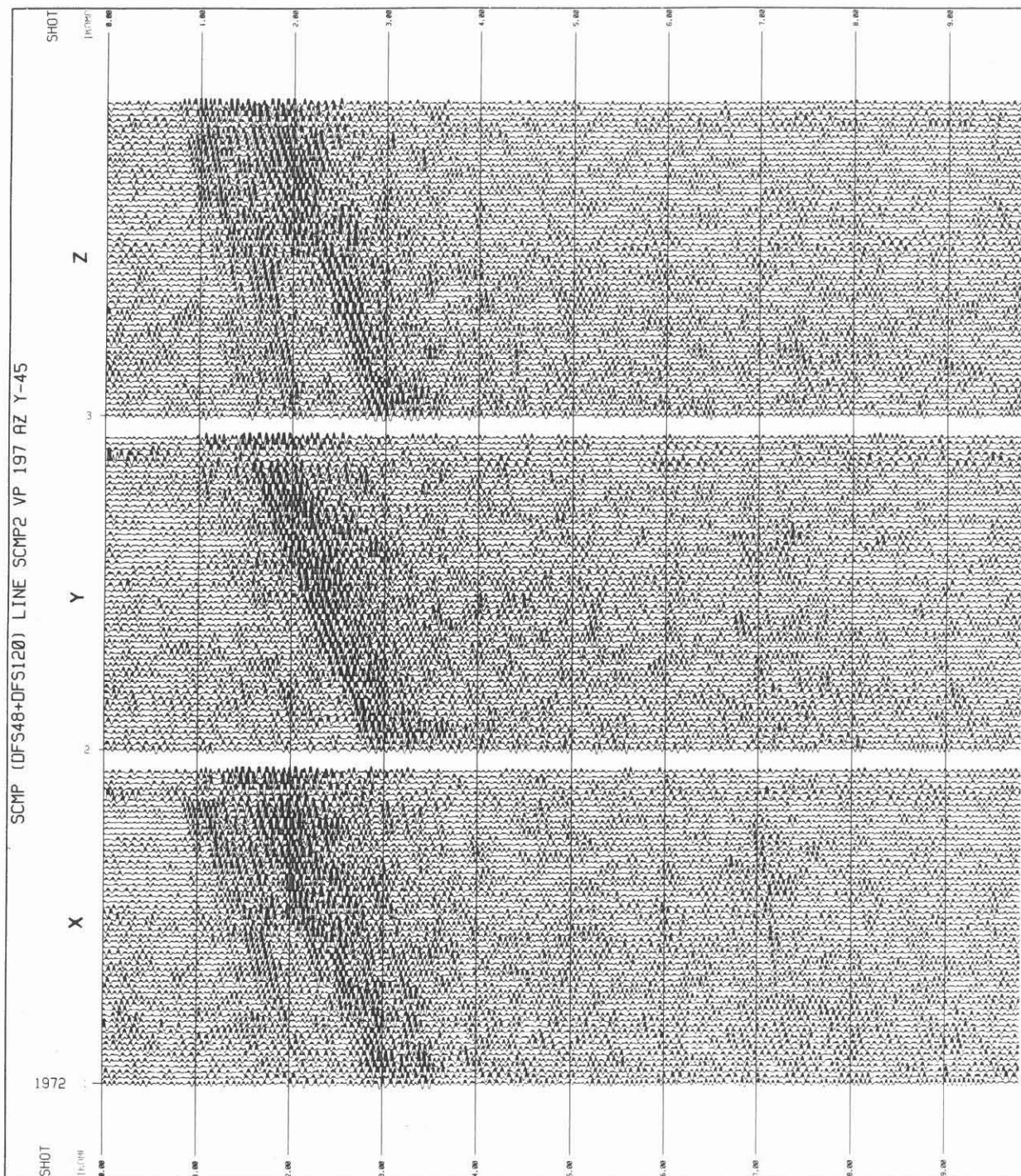


Fig 6

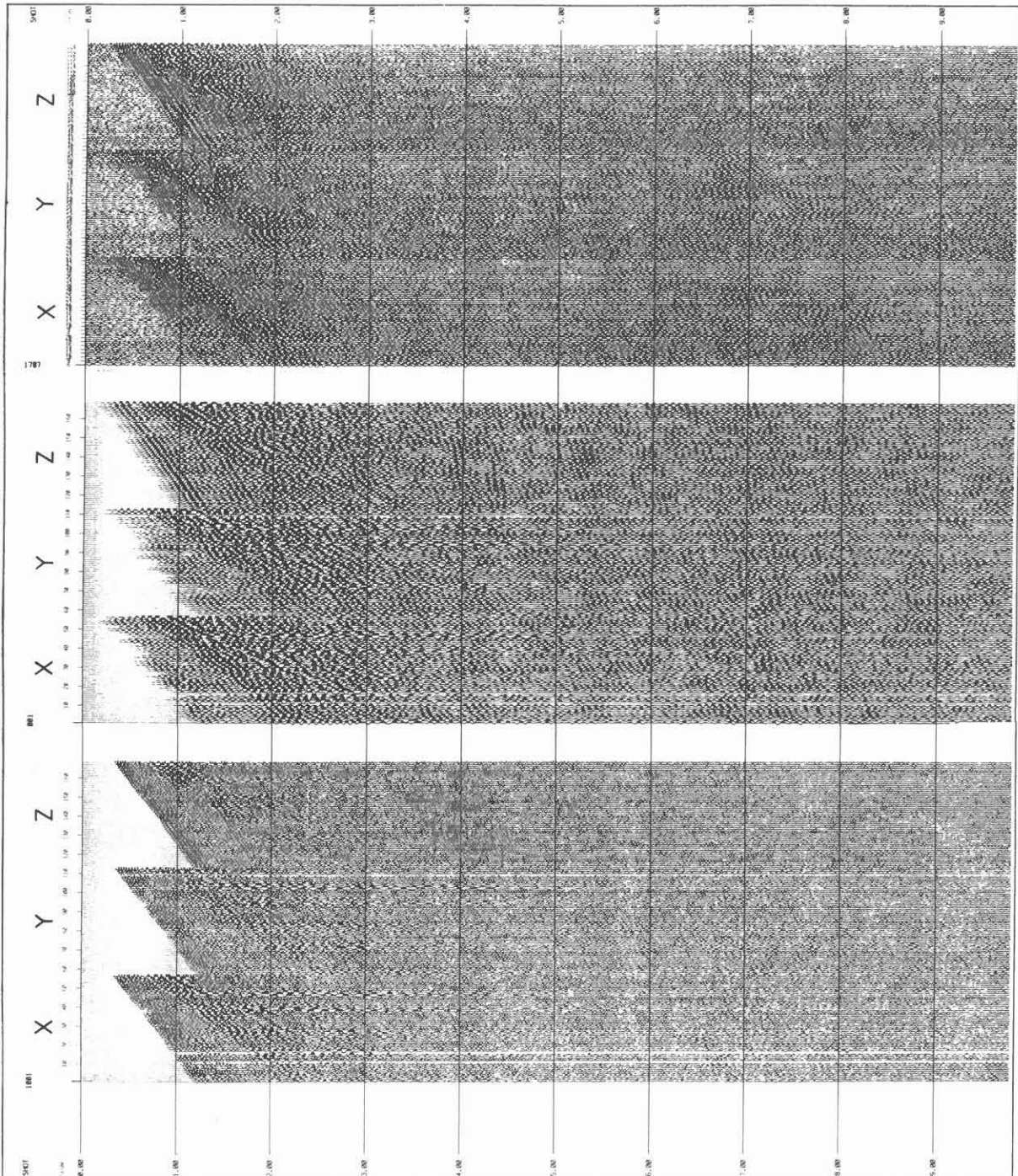


Fig 7

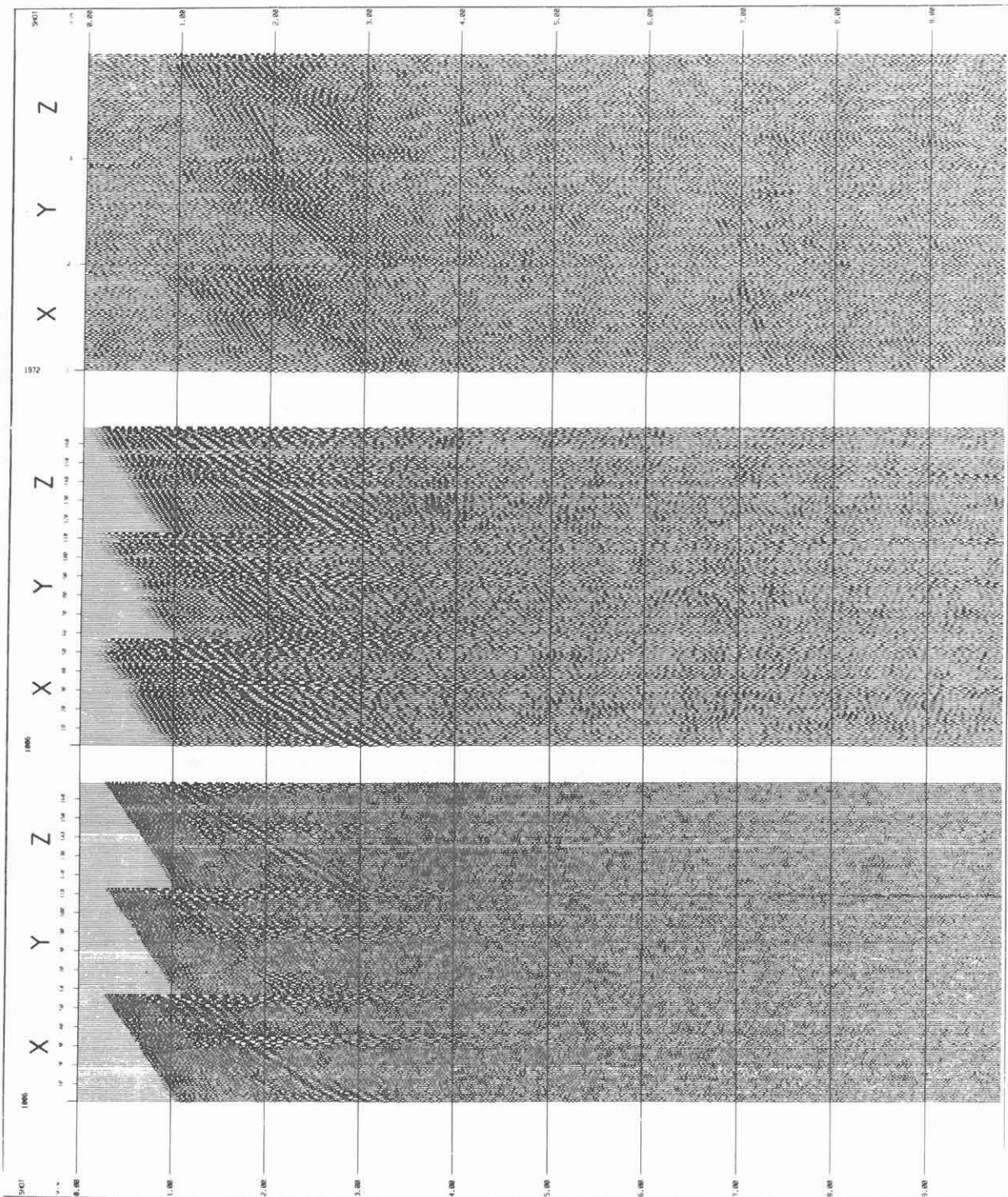


Fig 8

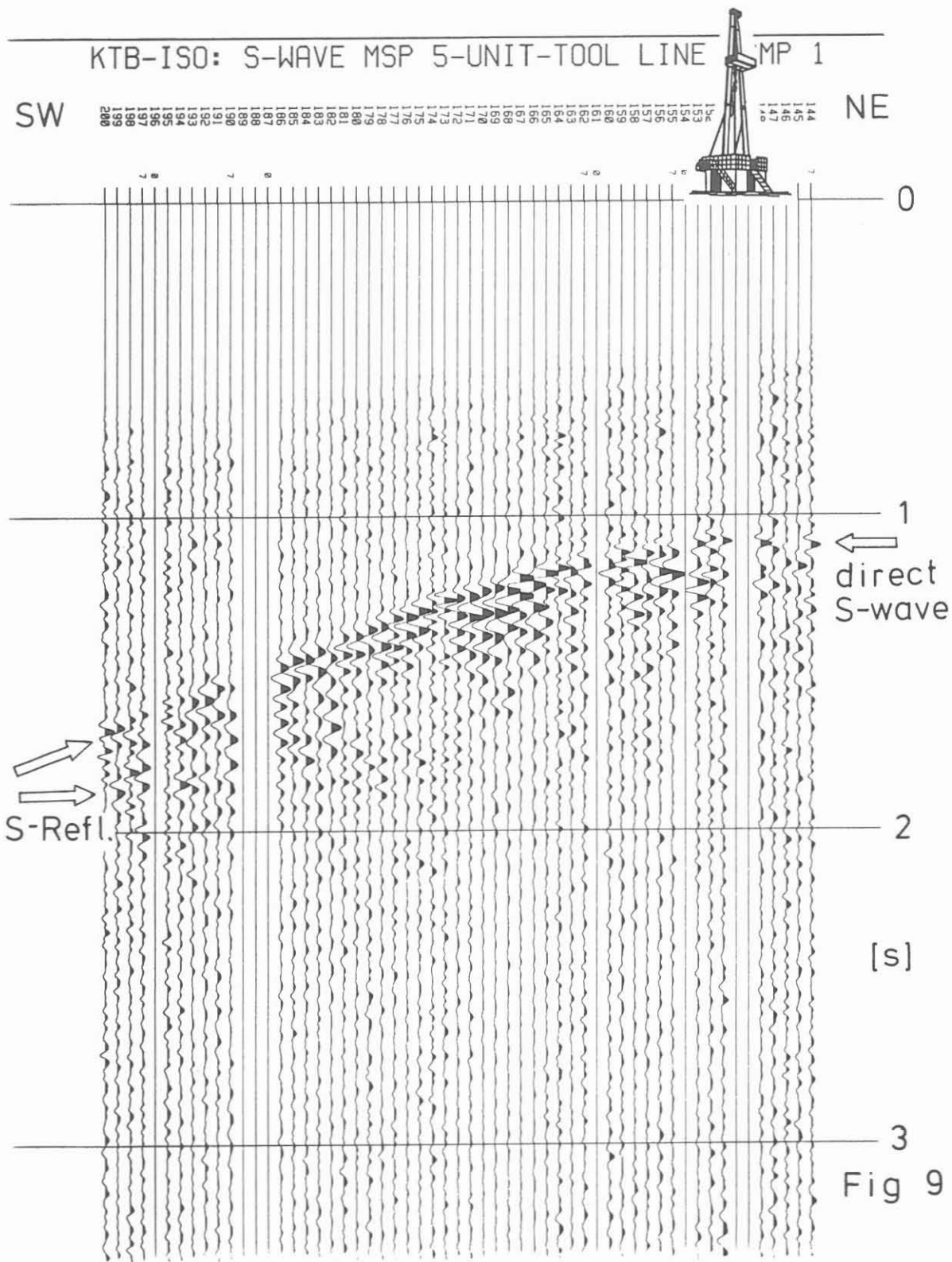


Figure 5: Vibrator gather of VP 170 of line SCMP 1. 56 stationary channels for each component. Offset range is from 1.2 km to 5.6 km. Orientation of the vibrator baseplate is transverse (Y). Data were demultiplexed, correlated (extended correlation), 10-fold vertical stack (2 field records). No further processing. True amplitudes. Note highly correlated P-wave first arrivals on the vertical component and less correlated direct S-wave onsets on the horizontal components. S-wave reflections at 7 s TWT.

Figure 6: Vibrator gather of VP 197 of line SCMP 2. Offset range is 3 km to 7.4 km. See figure 5 for more details.

Figure 7: Dynamite-Vibroseis comparison for line SCMP 1. left: raw dynamite data, 25 kg, 1 hole 25 m deep, offset range 1.8 km to 6.2 km.
middle: low-pass filtered version of dynamite data, 9 - 43 Hz.
right: Vibroseis gather of figure 5, 10-fold vertical stack.
Compare P-wave reflections at 3-4 s TWT and S-wave reflections at 7 s TWT.

Figure 8: Dynamite-Vibroseis comparison for line SCMP 2. For details see figure 3 and 7.

Figure 9: Moving source profile (or walkaway) with the shearwave sources of the SCMP survey. The traces are recorded with a horizontal component (H1) located in 3665 m depth (selected from 5 units, located between 3590 and 3690 m, with 3 components each). Note hyperbolic-like direct S-wave arrivals and later arrivals marked in the figure. True relative amplitudes.

different source techniques used in this program. The three-hole technique, taking all shots of one shotpoint into account, provides even better signal to noise ratio for the first arrivals, particularly a better S-wave to P-wave energy ratio, and eliminates the surface waves (Raileigh-wave, seen on X- and Z-components). Quality of deeper reflections could not be enhanced with this technique.

II) S-MSP

The shearwave moving source profile (or walkaway survey) was accomplished during the SCMP survey, recording the vibrator source with a stationary downhole geophone chain. Figure 9 shows an example of the first line representing a horizontal component (H1) of the second unit (of 5 units), located at 3665 m depth with an azimuth of N 2° (H2 at N 92°). The traces correspond to the vibrator location moving from NE (location 144) over the KTB-site to the SW (location 200).

The processing consisted (analogue to data presented in figures 5 to 8) of demultiplexing, vertical stacking of two records, correlating, trace selection one per record. Amplitudes in this presentation are conserved, no further processing has been applied. Zero traces for missing vibrator locations have been added. Since the downhole tool was an array of five 25 m spaced units, each one with 3 components (oriented arbitrarily), 15 datasets of this kind are available for the line SCMP 1 (line SCMP 2: 1 unit with 3 components only). Because of cross-feed during recording by the pilot sweep channel, which produce autocorrelations of the sweep on each seismic channel after correlation, the first 500-700 ms of the record have been muted.

The direct shearwave arrivals seen between 1 and 2 s traveltime, form a typical hyperbola-like curve. Based on the CMP-concept, this allows for a velocity analysis similar to the move-out analysis in surface reflection studies. Such an analysis gives a shearwave velocity of 3130 m/s for line SCMP1 (figure 9) and 3240 m/s for line SCMP2. These velocities must be regarded as average velocities for the medium around the borehole between surface and downhole receiver. The discrepancy confirms the findings from the SCMP direct waves mentioned above. After normal move-out correction of the arrival times, short-period deviations can be used advantageously for calculating static corrections for the SCMP survey. Also, later S-wave arrivals are seen on the traces of the southwestern vibrator locations behind the direct arrivals (marked in figure 9). Arriving nearly at the same time from about 25 vibrator positions (arrivals are aligned horizontally), they may be interpreted as reflections from a steep (40-60°) structure dipping to the east.

III) VSP

The processing first had to account for differing recording parameters, such as recording length, sampling rate and number of recorded channels, in the sequence of field records. During the field experiment, the downhole tool was kept in a fixed position while recording all source locations and source types successively, then moved to the next position. The basic processing is as follows. During demultiplexing (format SEG D,

multiplexed), the data were sorted into their appropriate profiles. In case of Vibroseis, the data were vertically stacked (2 records) and then correlated (in two versions: zero-phase correlation, minimum-phase correlation). The correlation length was extended by adding zero samples at the end of the uncorrelated records.

Figure 10 demonstrates the problems related to application of dynamite sources. Shots were repeated in the same hole several times. Therefore coupling conditions as well as the depth of the charge vary along the profile. The upper panel shows the variation of source signature as well as delays in arrival times recorded with the monitor geophone located at 60 m depth beneath the source. The same characteristics can be recognized in the middle panel representing raw first arrivals recorded downhole which have been time shifted in order to be aligned horizontally. Signal signature as well as arrival times change drastically. Application of spiking deconvolution (lower panel) can compensate for these artificial variations of the signal characteristics.

Vibroseis as well as Marthor data were not affected by this problem. On the other hand, the dynamite data contained much higher frequencies enabling higher resolution. At about 1100 m depth, seen in the raw data, a tube wave starts downward. Its origin marks the position of a major breakout in the borehole wall known from caliper logs.

Figure 11 describes the next major processing step which is typical for 3-component VSP processing: the rotation of components (e.g. Toksöz and Stewart, eds., 1984). This is demonstrated in figure 12 on the data of VP 402 (S-wave vibrator, 4 km offset). The 5 downhole units were orientated arbitrarily during recording and movement in the borehole. The upper panel of figure 12 represents the raw original data set for far-offset VSP 402 (compare figure 3 for location). Consistent and correlating phases can be recognized on component Z (labeled IKOMP = 1). The shearwave energy is dominant, also weaker P-wave energy can be seen.

The middle panel of figure 12 shows the three components after rotation (see e.g. DiSiena et al., 1984; Benhama et al., 1988) according to the compass readings. Component 1 (right) is still vertically orientated, component 2 (formerly H1) now is northward, and component 3 (left, formerly H2) now is eastward orientated. Shear-wave phases now show good correlation on all three components. Since the azimuth of the raypath is NW, P-wave energy is distributed on all three components of this North-East oriented cartesian coordinate system.

The lower panel shows the components in a different coordinate system, which is orientated according to the raypath direction. Component 1 is now the radial one (parallel to source-receiver direction). P-wave energy is now concentrated on this component, as theory predicts. Component 2 is horizontal radial (HR) and component 3 is horizontal transversal (HT). This rotation can be performed automatically using two methods (after DiSiena et al., 1984; Kanasewich, 1981; Benhama et al., 1988):

- 1) Maximizing the energy. First, P-wave energy is maximized within the horizontal plane, searching for the rotation angle which maximizes the P-

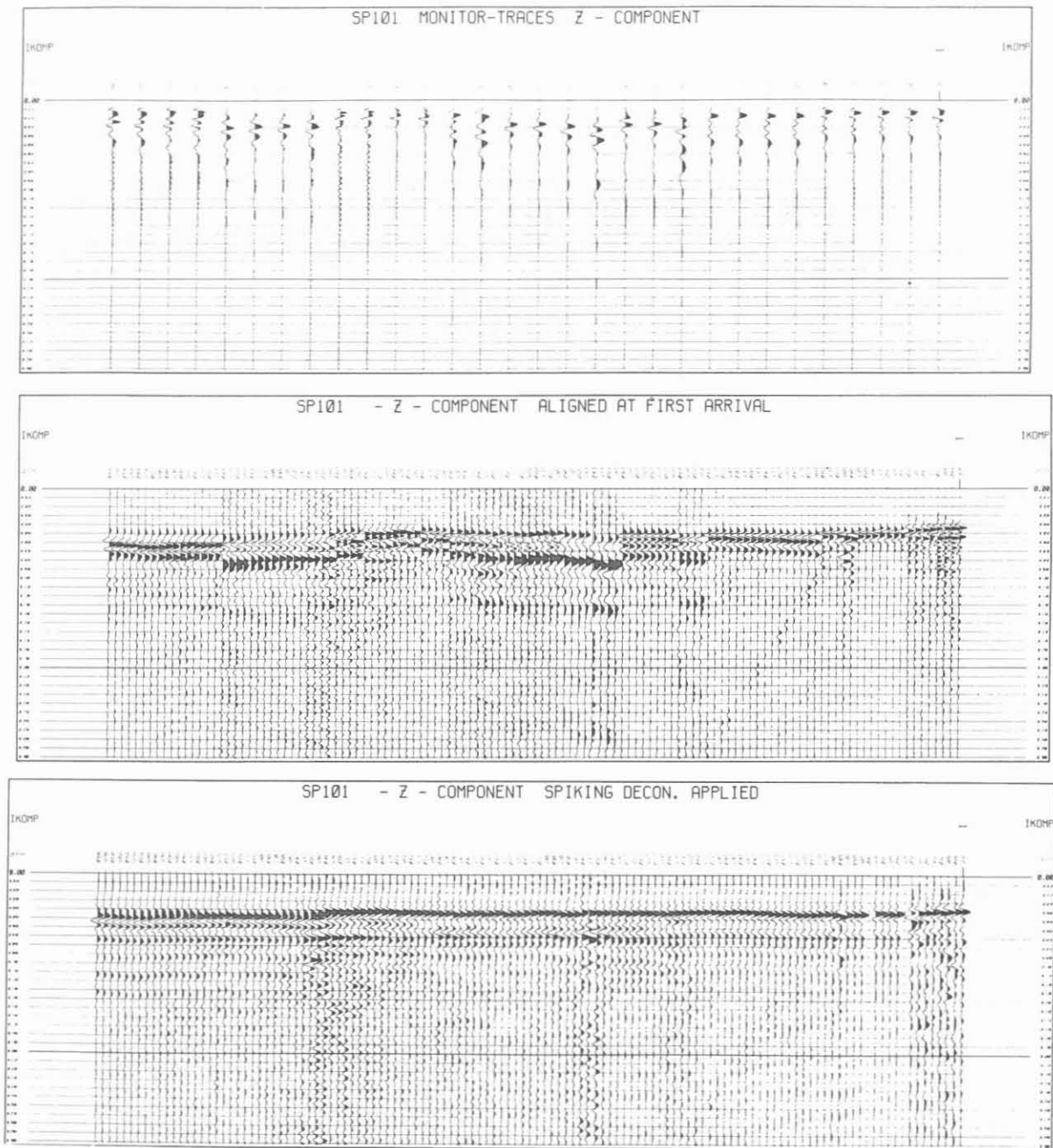


Fig 10

Figure 10: Zero-offset VSP SP 101 (dynamite, z-component): Comparison between monitor traces (upper panel) with downhole geophone traces (middle panel). Note strong variations in signal signature and arriving times. Traces of the downhole record are shifted upward to be aligned horizontally. Note the tube wave starting at 1100 m depth. Lower panel: downhole data after application of spiking deconvolution.

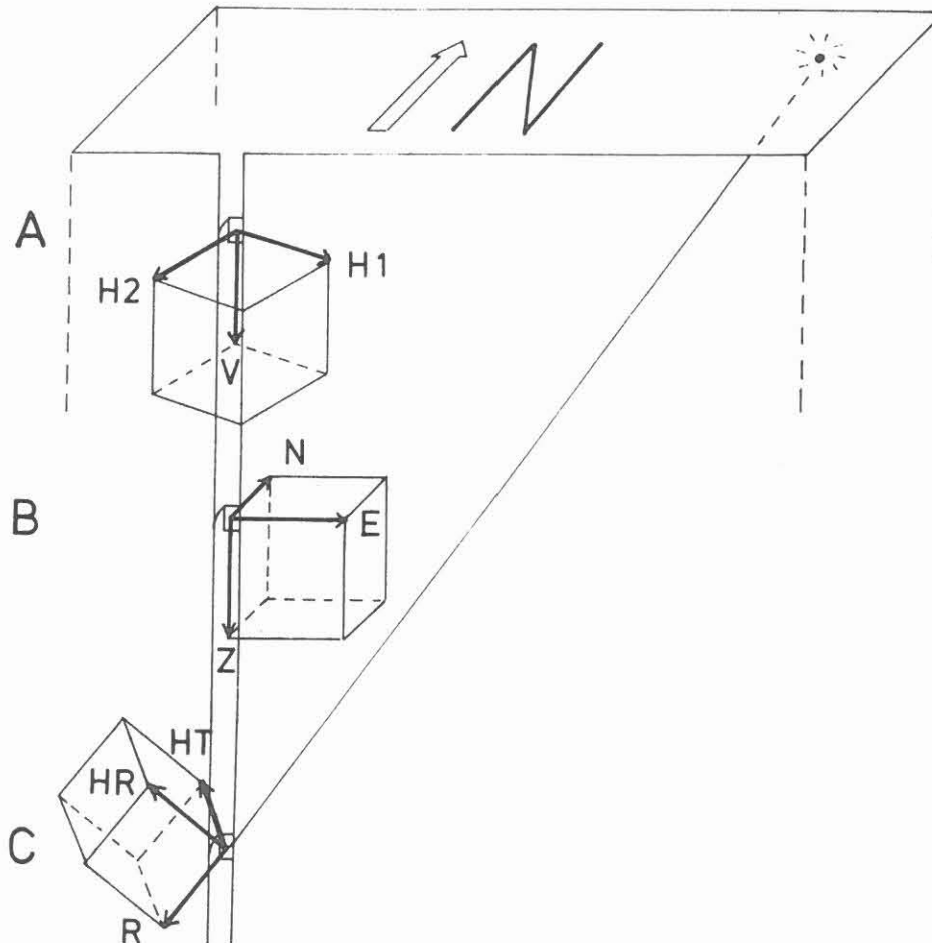


Figure 11: Schematic diagram of different coordinate systems used for rotation of the recorded wavefield. A: original arbitrary coordinate system, B: rotated system according to compass readings, C: rotated system using automatic procedures described in the text.

Figure 12: Far-offset vertical seismic profile VP 402. Source offset 4 km, source: 1 S-wave vibrator, source azimuth SE. Top: three components of raw data, original receiver orientation (not orientated). 1=Z, 2=H1, 3=H2. Middle: rotation according to compass readings, 1=Z, 2=N, 3=E. Bottom: rotation using the covariance matrix, 1=R, 2=HR, 3=HT.

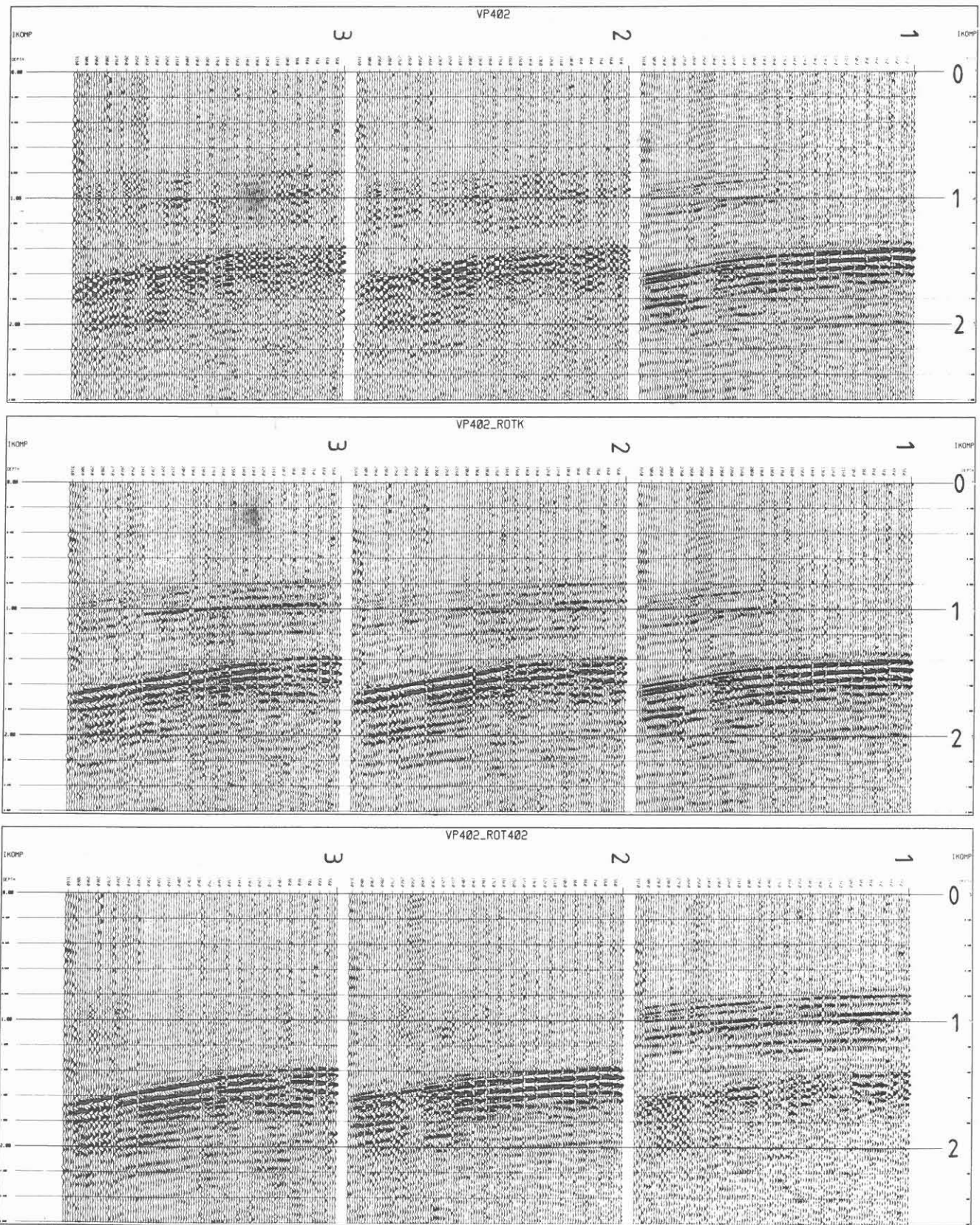


Fig 12

wave energy on the horizontal radial component (H1 -> HR). Then this procedure is repeated for the HR-Z-plane (Z -> R).

2) Covariance matrix. From the covariance matrix the minimum variance is determined instead of maximizing the energy.

Both methods are basically related to each other, and produce practically the same results. For automatic rotation we use the method with the covariance matrix. This method additionally provides the degree of rectilinearity of the polarization. It is used simultaneously with the rotation after compass readings, depending on the individual problem to be studied. The automatic rotation requires that P-wave energy is present on all components. In contrast to earlier suggestions, figure 12 also shows that the compass provides reliable readings.

The next crucial processing step is **deconvolution**. This is of particular importance for all zero-offset VSPs. The Vibroseis data in this case need to be transformed from zero-phase to minimum-phase signals, which in our case is done during correlation. An operator of 1000 ms length is applied to the downgoing wavefield first. The antifilter is then applied to the complete wavefield. Thus the resolution of the signals is enhanced and multiples are suppressed.

Figure 13a presents the original wave field of all available zero-offset VSPs in a compressed and comparative form. First, all traces have been shifted down by a constant time, then the traces were individually shifted upward according to the traveltime of the direct S-wave. For better comparison, this procedure aligns the shearwaves horizontally. On top of figure 13a the data of the previous VSP 3600 (Bram, 1988, Kästner et al., 1989, Hohrath, 1990, Schruth et al., 1990) is also plotted. This data was recorded with a smaller spacing of 12.5 m instead of 25 m and its source signature provides higher resolution, particularly in the case of S-waves.

Thus, five different zero-offset VSPs are now available. It can be clearly recognized, that the S-wave energy and signal frequencies change drastically between the different source types. Additionally, several P to S conversions are visible starting at the P-wave branch of the direct arrivals, particularly on the VSP 3600 (figure 13b). The direct S-wave, which originates at the surface, is propagating in different phases of their own velocity. This is a first manifestation of shearwave splitting according to seismic anisotropy. The slowest phases also could be interpreted as Stoneley waves (borehole guided wave). But this interpretation is very unlikely, because the amplitude decay is typical for body waves and because there are no such waves reflected from the bottom of the borehole. Although the vibrator and the Marthor source were oriented transversely with respect to the source-borehole azimuth, the recorded S-wave energy is not restricted to the HT-component. This indicates that polarization of the signal is changing along its raypath due to the complexities and the anisotropy of the medium. In case of the dynamite sources, the S-wave generation is most likely due to conversion of the P-wave at the surface or at lateral inhomogeneities near the source (Fertig, 1984). In case of the first VSP with 200 m offset (explosive source, top of figure 13a), the slowest shearwave phase cannot be traced upward back to the origin in time and space. It starts with a delay of approx. 150 ms. We

suggest that it is generated by the arrival of the surface wave (Rayleigh wave) at the borehole mouth. For the vibrator and the Marthor, the shearwaves can be regarded as originating directly at the source.

The data shown in figure 13a reveal different S-wave wavelengths and frequencies covering a wide range (10 to 100 Hz). This allows for analysis of the polarization as a function of the frequency. Figure 14 presents a blow-up of VP 101 P. The two split shearwaves can clearly be recognized. Hodograms of the corresponding signals, presented in figure 15, clearly show, that the faster and the slower shearwave are different in polarization by 90 degrees. This means that the S-wave with particle motion in NW direction is faster than the other. Because of the dramatic difference in character between the two phases, the slower one could be interpreted alternatively as a tube wave. But no reflection from the borehole bottom confirms this interpretation. Further systematic analysis of polarization of all our data for more details is necessary to verify these statements.

Figure 16 shows raw data of the CIPHER experiment, represented as a vertical seismic profile with a limited depth range from 2800 to 3400 m. After rotation according to the compass readings, the data show very pronounced and several distinct shearwaves. The P-wave is discernable on the vertical component. Because of better signal to noise ratio, we consider this technique as a powerful tool for generating shearwaves. A detailed study describing the field procedure and the results are under preparation by Edelmann and Lüschen (1990).

Figure 17 and figure 18 show the far-offset VSPs in comparison between the dynamite and the S-vibrator source (see figure 3 for location). P-waves as well as S-waves show the characteristic bending of the first arrival curve, which is due to the larger offset. S-waves are of remarkable quality, especially on the VP 402 S (figure 18). There are several remarkable details to interpret. In SP 401 (figure 17, top), SP 402 (figure 18, top) and SP 802 (figure 18, bottom) there are oblique events between first P-waves and first S-waves, propagating with an almost constant phase velocity, starting when the first P-wave arrives at the borehole mouth. A possible interpretation of this feature is due to a reflection of the direct P-wave at a steeply dipping structure, which outcrops near the borehole site. The reflected wave then propagates vertically along the borehole. Interpretation as a tube wave is unlikely because of the high phase velocities (> 5000 m/s).

In case of zero-offset VSP wavefield separation techniques can be applied to suppress the downgoing wavefield (direct waves) and to enhance the upgoing reflections (e.g. Hardage, 1985). Usually, f-k filter or median filters are applied for this purpose. For interpretation purposes, the traces are then time shifted according to the two-way-traveltime correction. After performing a corridor stack, the VSP now can be compared directly with a surface reflection profile. On the other hand, these seismic measurements now can be calibrated by the borehole measurements. Up to this processing stage the data are presented in this paper. Table 4 provides a listing of typical standard processing steps, in this case for the dynamite-VSP SP 101.

SP - 101

UPGOING WAVEFIELD (P)
FILTER 40 - 110 HZ

FIELD EXPERIMENT

- 1 SOURCE: DYNAMITE (0.5 - 1 KG)
IN 5 - 20 M DEEP HOLES
OFFSET 50 M
- 2 RECEIVER: 5-UNIT-DIGITAL 3-K CHAIN
S E K R A N
(PRAKLA-SEISMOS AG)
SPACING 25 M
- 3 3-K MONITOR GEOPHON IN 60 M DEPTH
- 4 RECORDING UNIT: EG&G GEOMETRICS 2420 (24CH)
- 5 FIELD PARTY: SCHWANITZ / PRAKLA-SEISMOS AG
LUESCHEN / KARLSRUHE UNIVERSITY
- 6 DATE: AUG. 1ST-3RD, 1990

DATA PROCESSING HISTORY

PROCESSED BY: WALTER SOELLNER, EHALD LUESCHEN
ACHIM HOHRATH, MARTIN WIDMAIER
CONVEX-DISCO TEAM UNIVERSITY KARLSRUHE

DATE: FEB. 20TH 1990

SOURCE FILE: /MNT/WALTER/PROC/SP101/SP101NPROC.DAT

DATA FILE: /SCRATCH/WIDE/SP101_NSPIKE_UP.DAT

- 1 DEMUX (FIELD TAPES UNSORTED IN SEGO MULTIPLEXED)
- 2 BAD TRACE EDIT
- 3 DEFINITION OF IKOMP DEPTH AND TYPE
- 4 SORT (INTO PROFILE-IKOMP GATHER)
- 5 POLARITY EDITING AND ADDITION OF MISSING TRACES

SOURCE FILE /SCRATCH/WALTER/SP101_NSPIKE_UP.DSK 6000

DATA FILE /MNT/EHALD/VSPHASE/VSP_READ_PLOT.DAT

- 6 ROTATION OF COMPONENTS ACCORDING TO DIRECTION OF DOWNGOING P-WAVE
- 7 DECONA SPIKE OP. LENGTH 500 MS , DESIGN-GATE 1000 MS
- 8 F-K FILTER (UPGOING WAVEFIELD PASSING)
- 9 NOTCH FILTER 50 HZ 100 HZ
- 10 FREQUENCY FILTER:
TIME RANGE LOW CUT HIGH CUT
SECONDS HZ HZ HZ HZ
ALL 25 40 110 140
- 11 MUTE: 625/112 3660/618
- 12 GAIN: EXPONENTIAL GAIN CORRECTION
- 13 AGC 300 MS
- 14 PLOTTING INFORMATION: 6.25 MM PER TRACE
15 CM PER SECOND
POLARITY: POSITIVE PEAKS SHADED
SETAMP: PEAK
GAIN: 3

UNIVERSITAET
KARLSRUHE

KTB OBERPFALZ VB
VSP DATA PROCESSING

UNIVERSITAET
KARLSRUHE



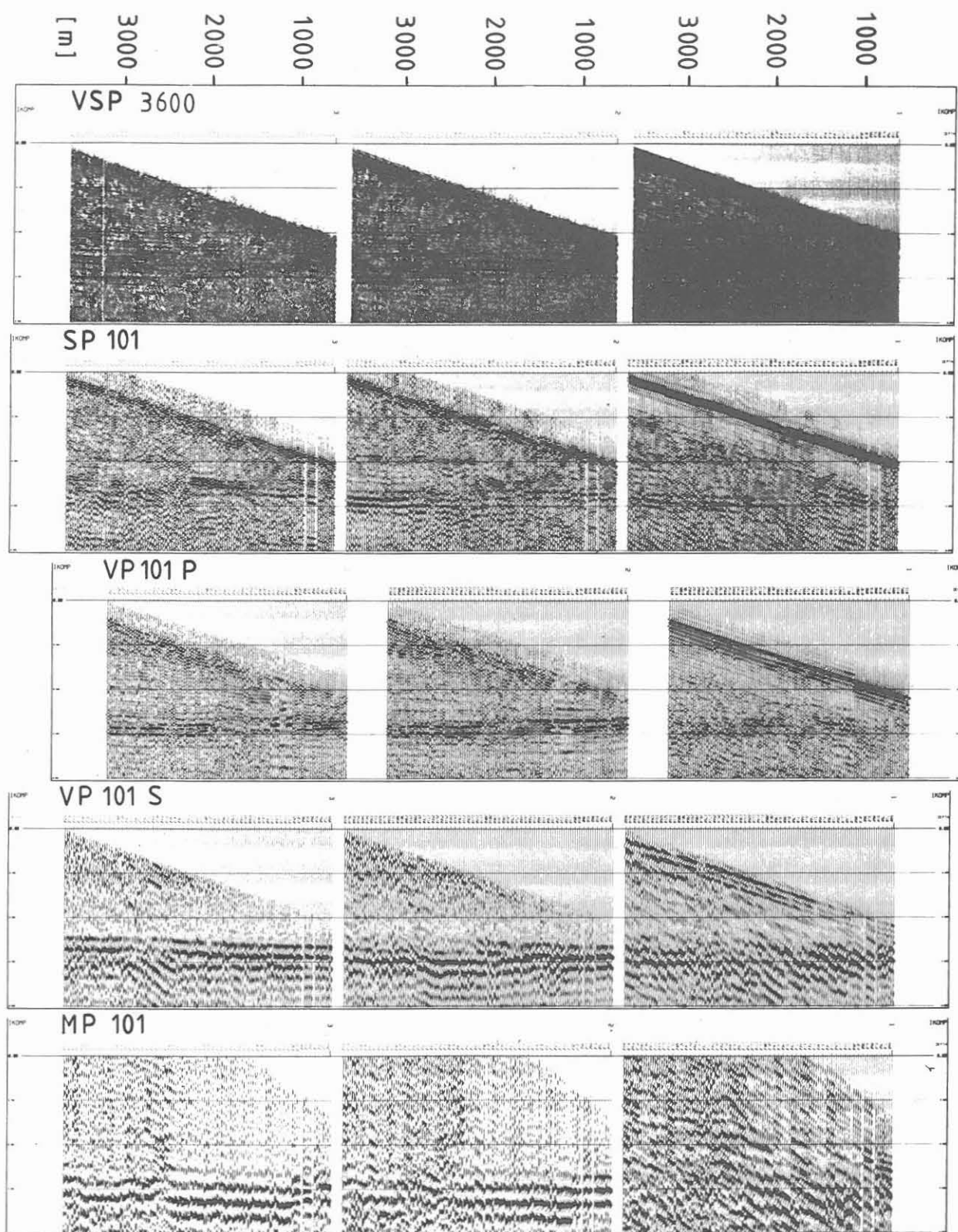


Fig 13a

2

VSP 3600

660
710
760
810
860
910
960
1010
1060
1110
1160
1210
1260
1310
1360
1410
1460
1510
1560
1610
1660
1710
1760
1810
1860
1910
1960
2010
2060
2110
2160
2210
2260
2310
2360
2410
2460
2510
2560
2610
2660
2710
2760
2810
2860
2910
2960
3010
3060
3110
3160
3210
3260
3310
3360
3410
3460
3510
3560
3610

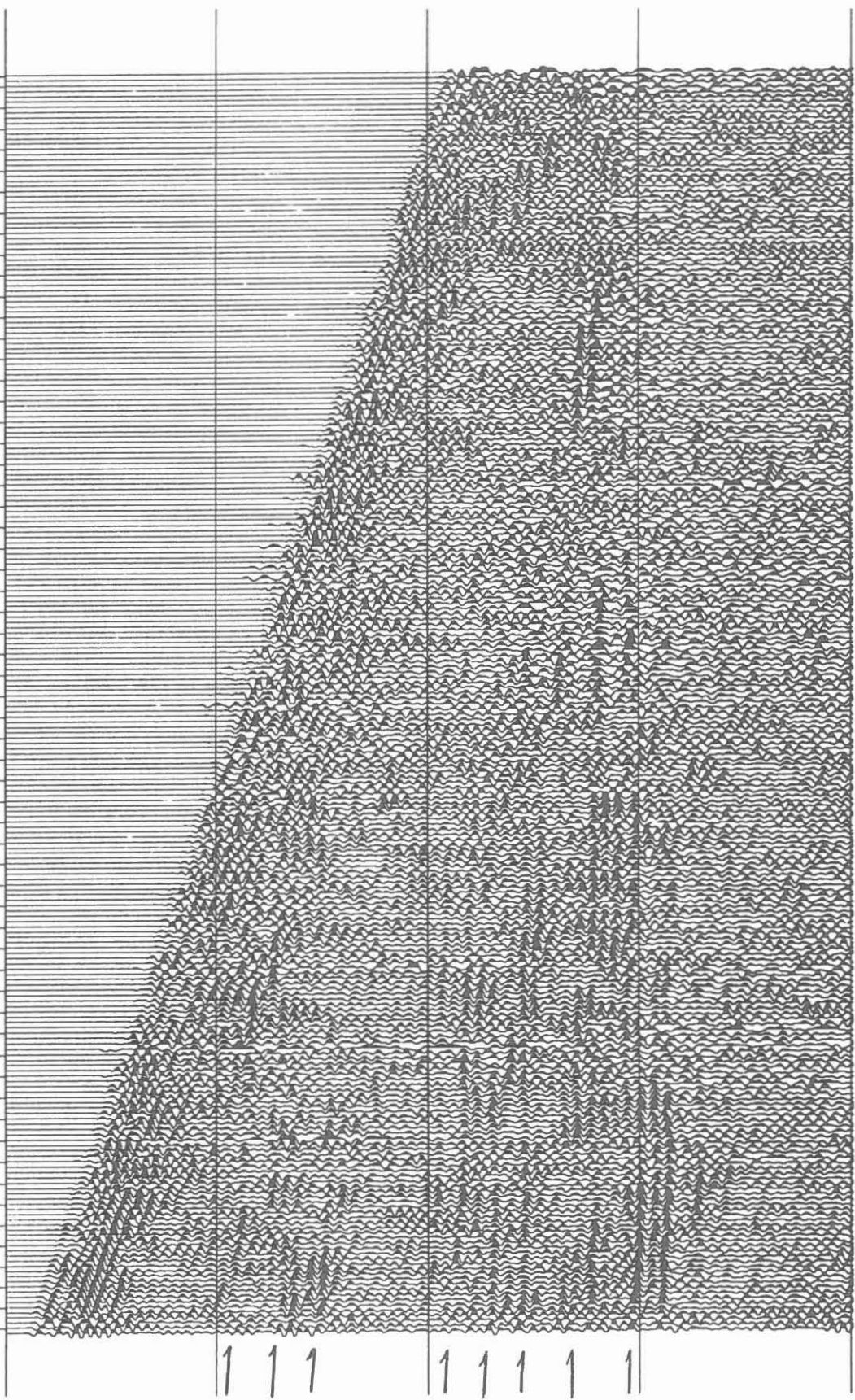


Fig 13 b

VP101P_ROTK.DSK

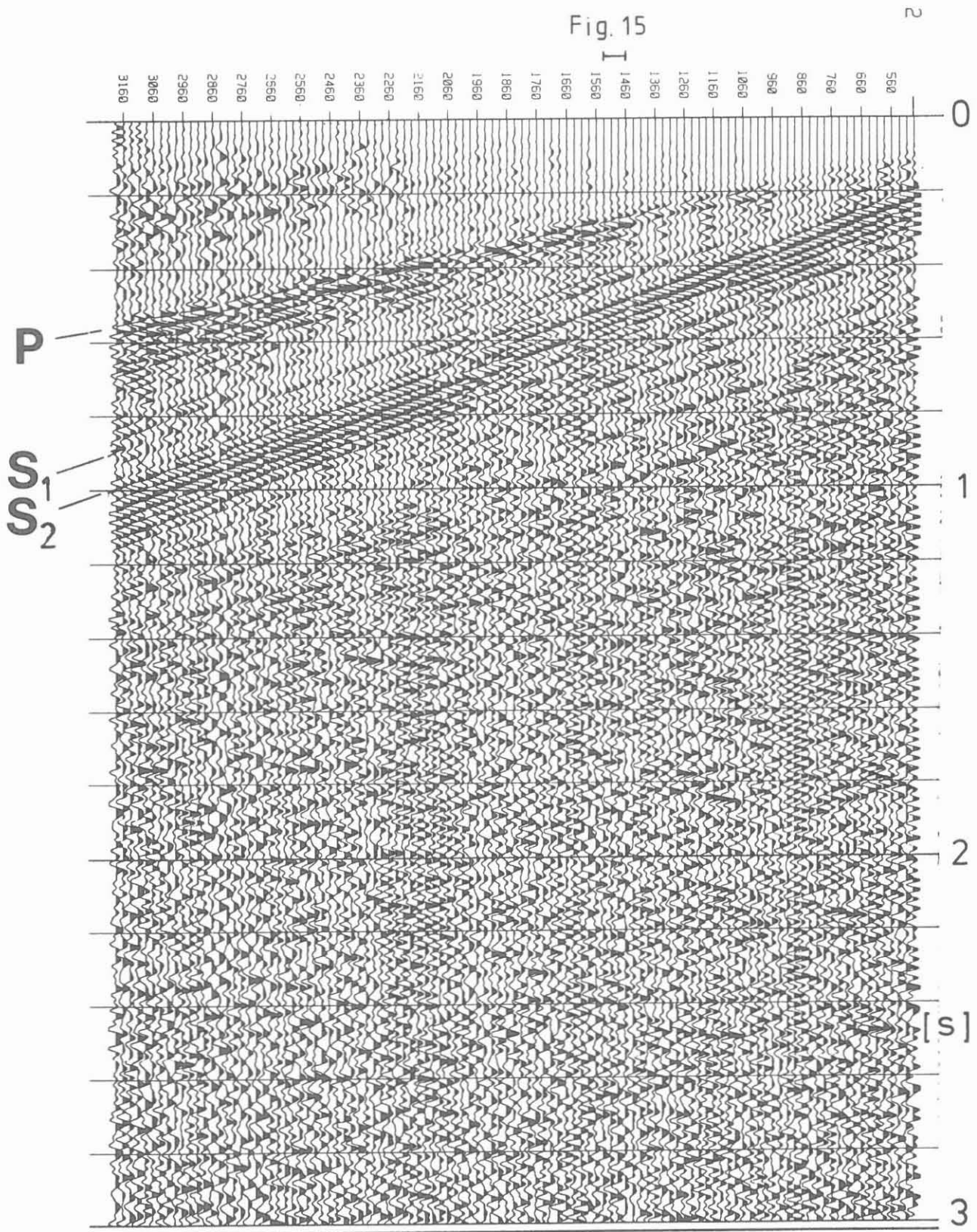


Fig 14

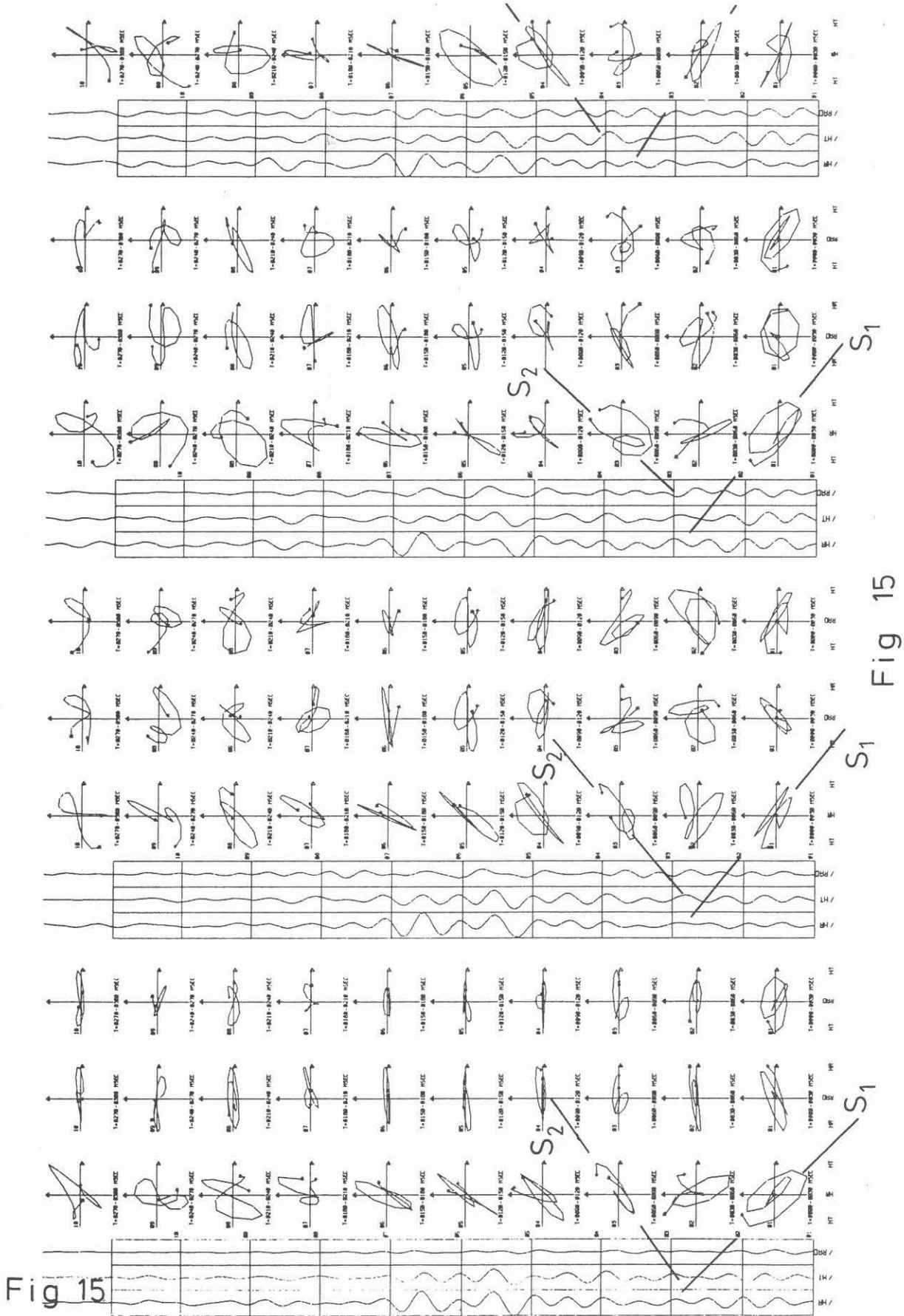


Fig 15

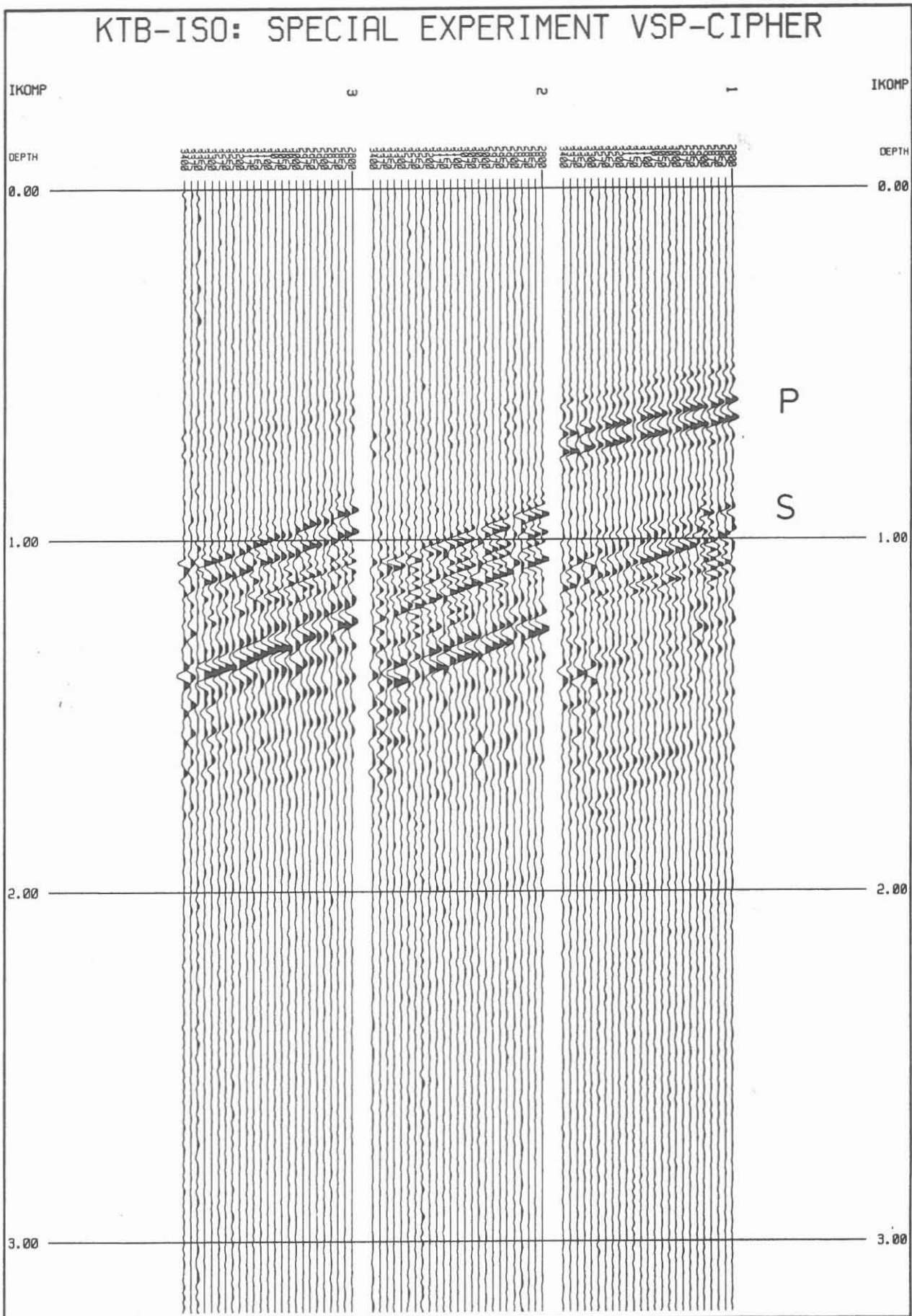


Fig 16

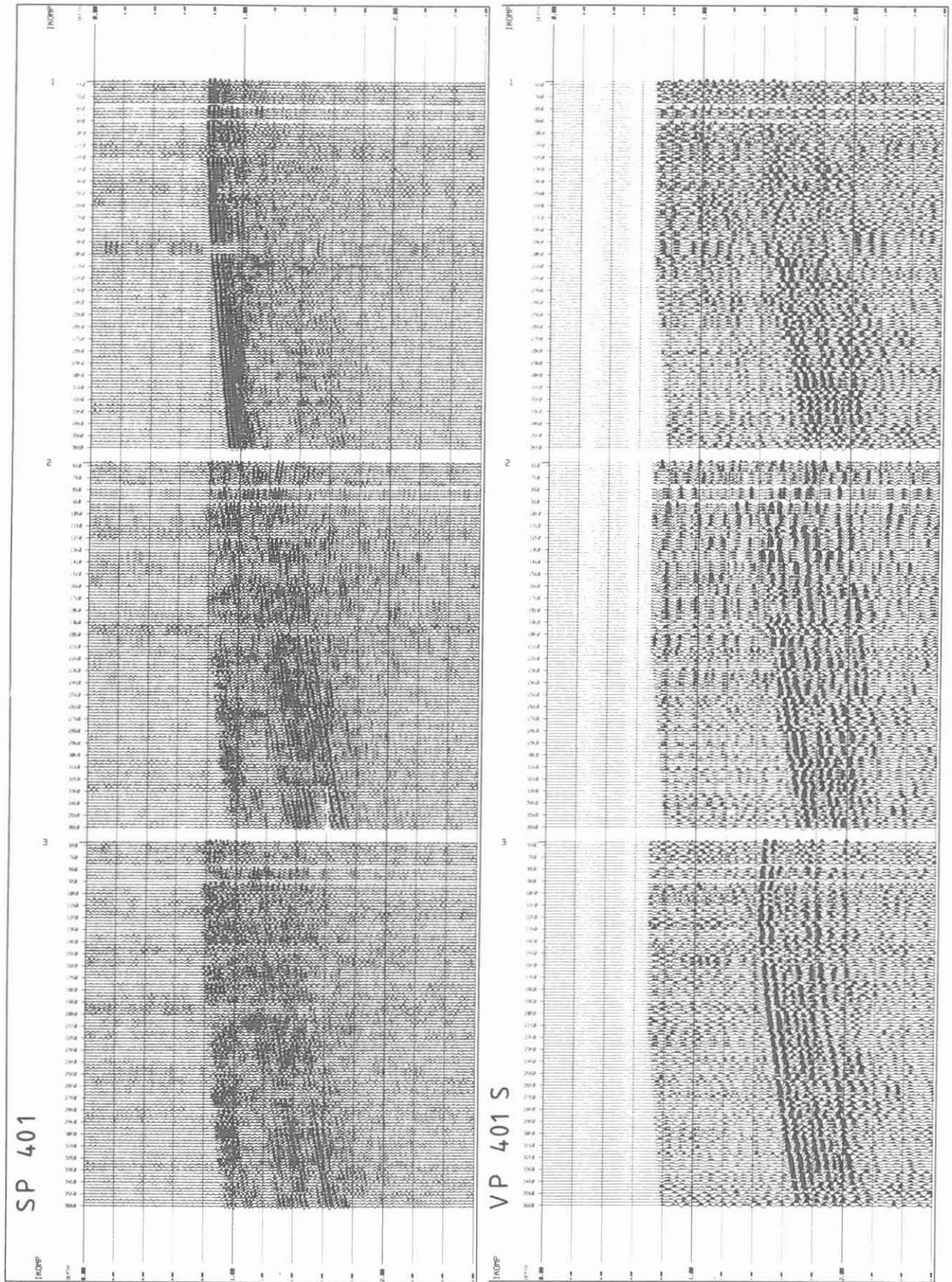


Fig 17

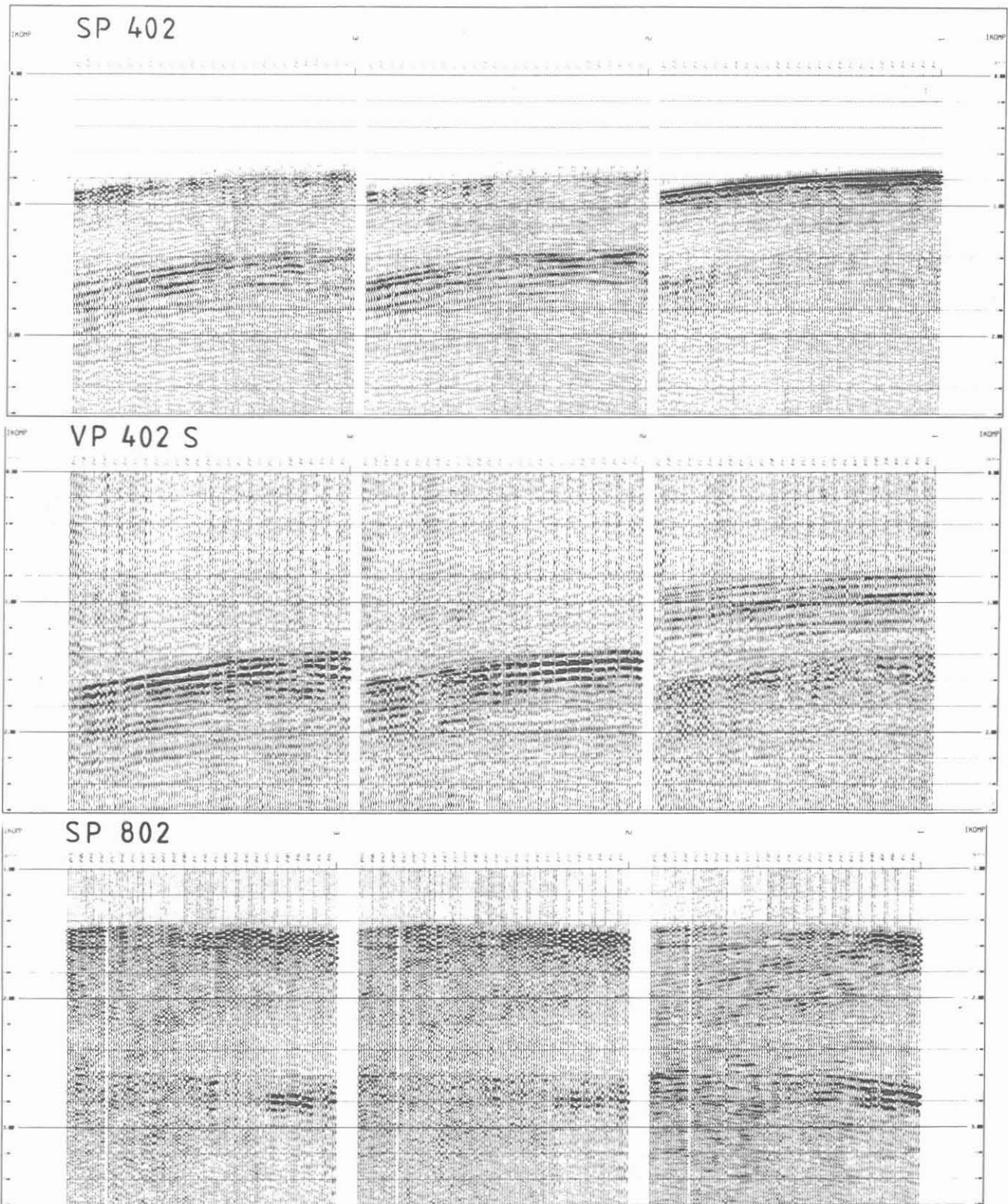
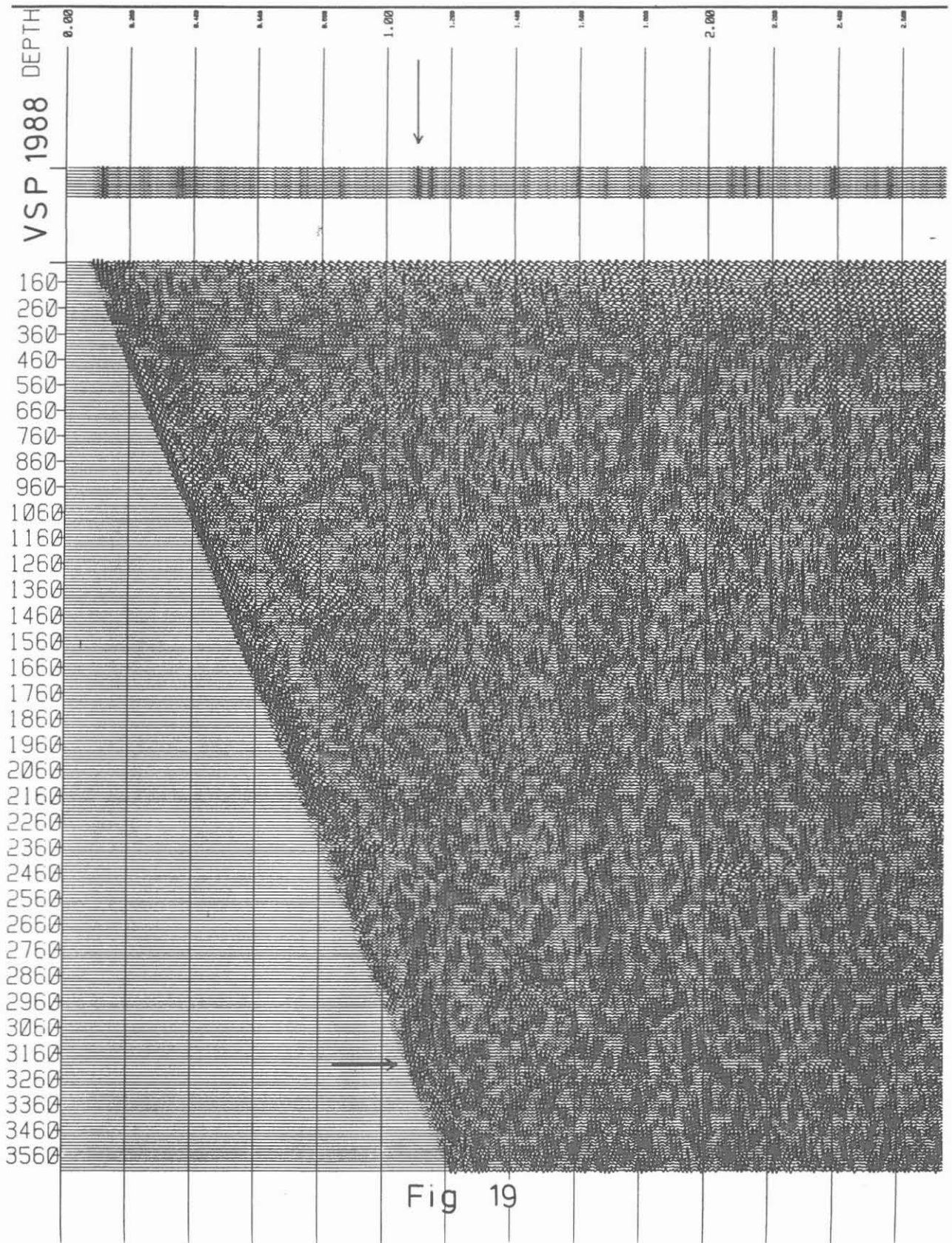


Fig 18



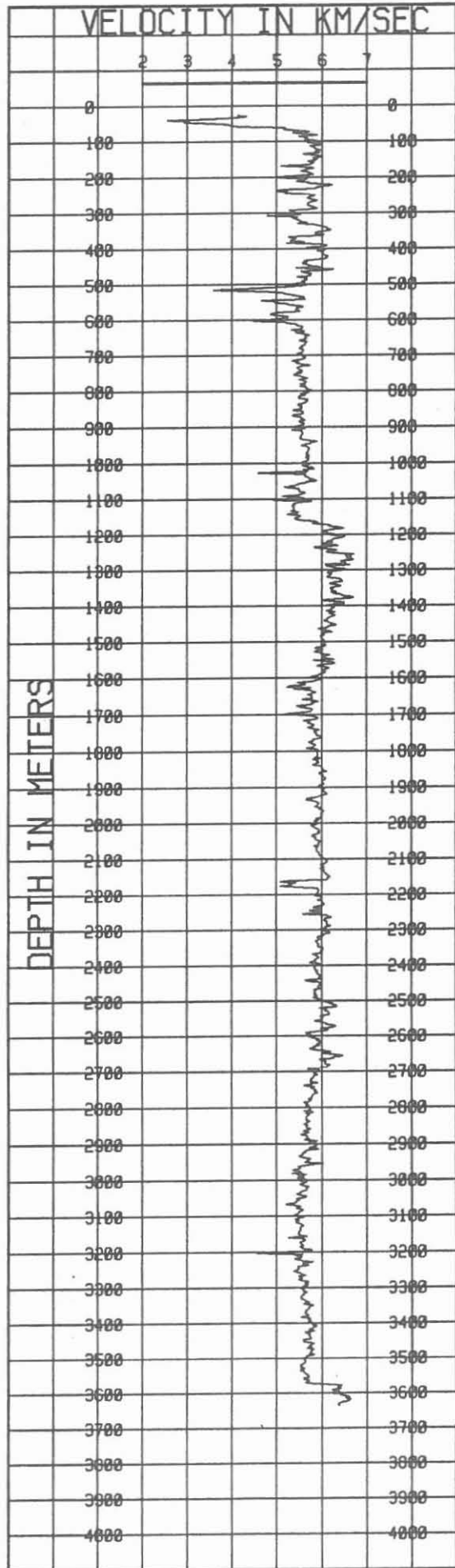


Fig 20

SP101 COMPONENT R UPGOING WAVEFIELD

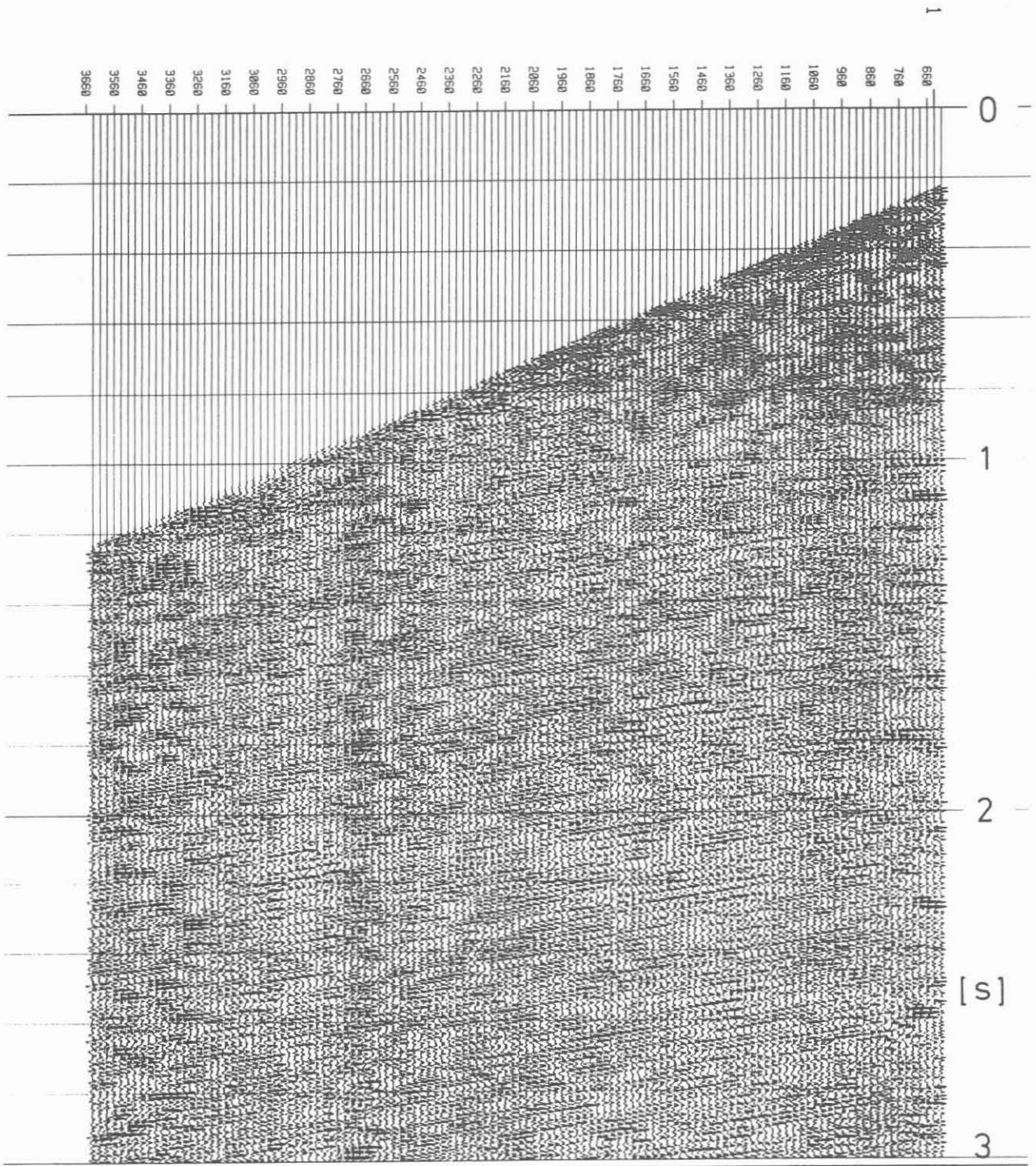


Fig 21

VP101 HR RAUFLAUFENDES WELLENFELD TWT

VP101 COMPONENT HR UPGOIN

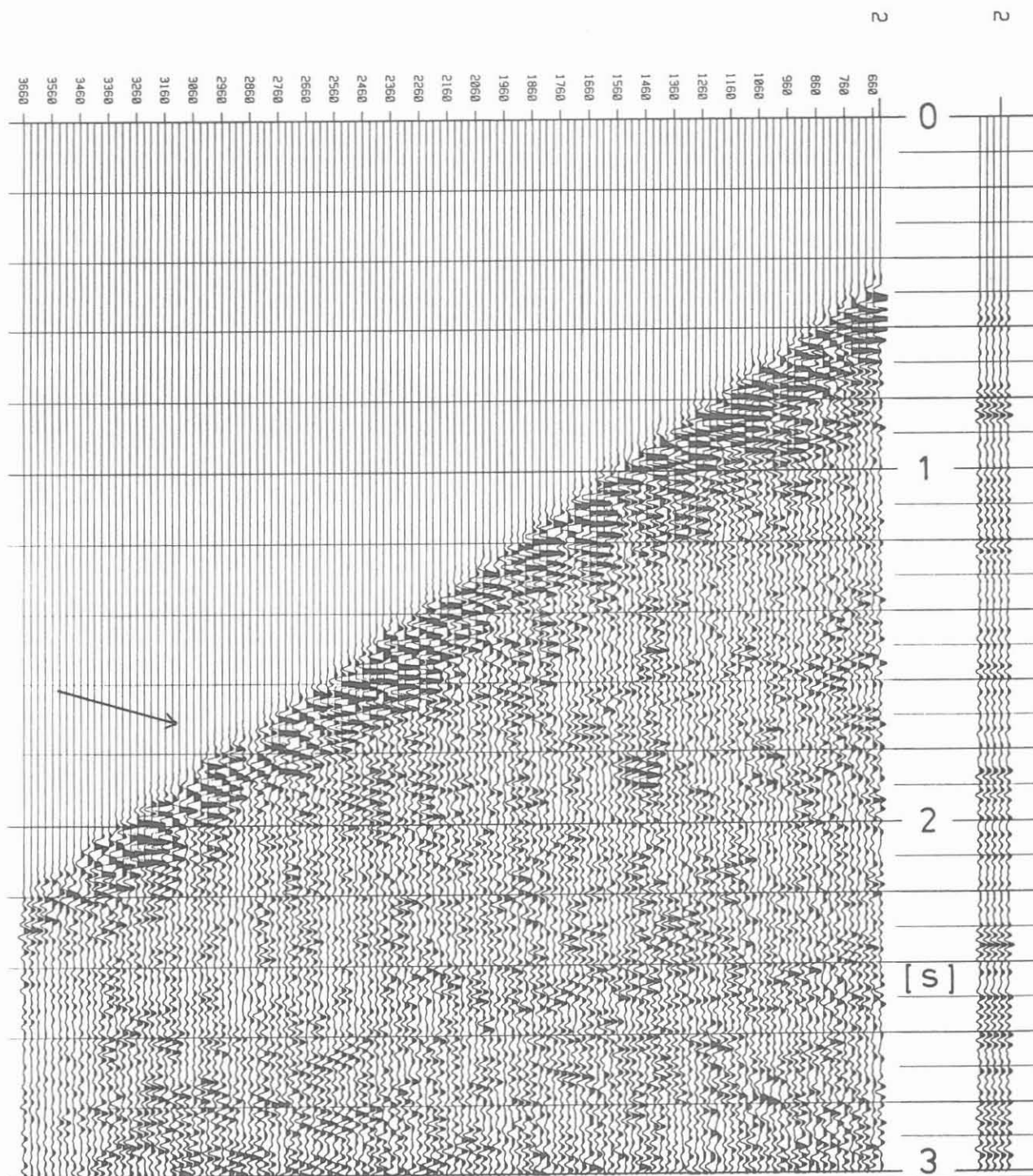


Fig 22

Figure 13a: Zero-offset vertical seismic profiles in comparison. Components are: 1=R, 2=HR, 3=HT (rotation with covariance matrix). Processing also includes deconvolution. Plotting is with AGC of 300 ms. Traces are time shifted in order to align S-wave first arrivals horizontally. From top to bottom: dynamite VSP 3600, dynamite SP 101, vertical vibrator VP 101 P, horizontal vibrator VP 101 S, Marthor MP 101 (after inverted stacking of left right shot). Note different energy of shearwaves and different frequencies. Timing lines in intervals of 200 ms.

Figure 13b: Blow-up of VSP 3600 (component HR). Compare figure 13a.

Figure 14: Enlarged section of VSP VP 101 P (vertical vibrator), N-component, AGC with 300 ms window length. Two splitted shearwaves are marked.

Figure 15: Particle motion diagrams (hodograms) for selected adjacent 3-component traces of figure 14. The hodograms correspond to the trace windows of 30 ms length marked on the left. Note that direction of particle motion changes from NW-SE to SW-NE within 60 ms.

Figure 16: Special experiment CIPHER. Raw data for a VSP between 2800 and 3400 m depth. Components 1=Z, 2=N, 3=E, rotated using compass readings.

Figure 17: Far-offset vertical seismic profiles, source location 401: 4 km offset, azimuth NE. Dynamite source SP 401 (top), bandpass 15-40 Hz, horizontal vibrator VP 401 (bottom), bandpass 18-35 Hz. Rotated with covariance matrix: components 1=R, 2=HR, 3=HT. No amplitude scaling, horizontal balancing applied.

Figure 18: Far-offset vertical seismic profiles, source location 402: 4 km offset, azimuth SE. Dynamite source SP 402 (top), bandpass 15-40 Hz, horizontal vibrator VP 402 (middle), bandpass 18-35 Hz. Source location 802: 8 km offset, azimuth SE, dynamite source SP 802 (bottom), bandpass 15-40 Hz. For rotation see figure 17, but the method was not successful in case of SP 802 (bottom).

Figure 19: Upgoing wavefield of VSP 3600 after f-k filtering, radial component, in two-way-traveltime representation. Trace interval 12.5 m. For processing steps see text. Bandpass 40-90 Hz, AGC with 300 ms window for plotting. Summed traces (horizontal stack of all traces) on the right. Muting after f-k filtering along first arrival traveltime curve.

Figure 20: Sonic log of December 7th, 1988, provided by KTB logging group

Figure 21: Upgoing wavefield of SP 101 after f-k filtering. Trace interval 25 m. Bandpass 40-110 Hz. See figure 19 for more details.

Figure 22: Upgoing wavefield of VP 101 (shearwave vibrator) after f-k filtering, HR component, in TWT representation. Trace interval 25 m, Bandpass 18-35 Hz, AGC with 500 ms window for plotting. Summed traces (horizontal stack of all traces) on the right. The arrow marks an example of an upgoing tube wave (Stoneley wave, see text).

Figures 19, 21 and 22 correspond to the upgoing (reflected) wavefield after f-k filtering of the zero-offset profiles. We show examples from the 1988 experiment (Bram, 1988, Hohrath, 1990) in figure 19, the SP 101 for comparison (figure 21), representing the reflected P-waves, and VP 101 (figure 22), representing the upgoing S-waves. Processing is as described above. Figure 20 presents the sonic log for comparison.

In the VSPs of the crystalline environment fundamental differences are discernible compared to data from sedimentary strata. Instead of long continuous reflected branches, numerous shorter segments are visible. Only a few of them form long consistent branches, although often interrupted. We attribute this to a generally lower energy of reflections, hence a lower signal to noise ratio, which is caused by energy losses due to numerous small scale impedance contrasts. The wavefield therefore must be considered as an interference pattern or back-scattered energy from numerous single reflections.

Reflections from horizontal structures would show up parallel to the depth axis. Only one horizontal reflection is visible in figures 19 and 21, originating at 3200 m depth. The horizontal stack (see right side of figure 19) enhances this reflector, having a two-way-traveltime of 1.2 s. The sonic log (figure 20) shows a pronounced low-velocity peak at this depth, where a fracture zone is known from other borehole measurements and from coring, - but it is characterized by a strong dip. Curiously, at the same depth in the VSP another reflection originates which is oblique to the depth axis, indicating a pronounced dip. It also reveals a curvature typical for reflections from dipping structures. It must be assumed that the fracture is responsible for the dipping reflector. The question arises about the nature of the horizontal reflector.

Consistent reflections are relatively poor above 2000 m, although shorter segments correlate with variations in the sonic log. Below 2000m depth, the intensity of the reflection pattern is generally increased. Inclined reflections showing the characteristic dip and a slight bending are dominating at all depth ranges. All possible dips are present, the steepest reflectors are visible in unfiltered versions, represented by downgoing waves behind the direct wave. In figure 21 most features of the VSP 3600 are confirmed, the dominance of dipping reflections (typically 30-40°) is drastically enhanced. The horizontal stack of all traces (see figure 19) selects the horizontal reflectors only, e.g. at 1.2 s, while all the inclined reflectors have been cancelled by this procedure. The 1.2 s reflector can be identified in the surface 2D section (see figure 2), while all the included reflections tend to be suppressed during standard CMP processing which emphasizes horizontal layering of structures. With this information from the VSPs, processing of 2D and 3D surface measurements could focus on dipping reflections using modified stacking velocities or dip move-out (DMO) stacking techniques.

In the S-wave VSP (figure 22) the upgoing wavefield is also characterized by dominating inclined events. Horizontal reflections are not recognized. Shearwave reflections from dipping structures (regardless of their strike) must be inclined toward the origin of the diagram. There are several events

with the opposite inclination. These can be interpreted unequivocally as borehole-guided waves (tube waves, Stoneley waves), because of their low phase velocity. All other upgoing wave types have to align horizontally (reflected S-wave from horizontal structure) or obliquely towards the origin at the surface. Borehole-guided waves bear the potential of information about the recent stress pattern and crack orientation. From systematic inspection of all down-going and upgoing wavefields of different types (after appropriate f-k filtering) we expect to characterize the medium and its impedance contrasts by mapping the P-reflections, P to S converted waves (down, up), S-reflections, S to P converted waves (down, up) and tube waves.

IV) MASE

The processing of the multiple azimuth shearwave experiment is basically the same described in case of the S-MSP (see above). Figure 23 displays the traces recorded with the vertical component of unit 2 in 3375 m depth. It is selected as an example out of 5 units located in 3300 to 3400 m depth, each one with 3 components. The traces represent the vibrator positions starting in the NW moving around the KTB-site on two different radii. The first group of traces (labelled 4 T, lefthand) are from transversal orientation of the S-wave vibrator on the 4-km-circle, the second group (4 R) from radial orientation, the same with the 8-km-circle. Static corrections have been applied which account for slight variations in the source-receiver distance. The reference distance is 5300 m for the 4-km-circle and 8700 m for the 8-km-circle. Variations in travelpath length (calculated with 3D coordinates of receiver and source) are reduced with an average S-wave velocity of 3070 m/s.

The shearwaves are the dominant phases on figure 23. The first S-wave clearly displays a traveltime anomaly consistently on both radii and both source orientations. As expected from azimuthal anisotropy, this anomaly has a sinoidal behaviour as a function of the azimuth. Conclusions in terms of anisotropy can be drawn after application of additional static corrections for near-surface effects. This is not yet available.

DISCUSSION

Systematic analysis of the polarization using variable source as well as three receiver components is expected to provide a quantitative image of seismic anisotropy, which may be caused by the recent stress pattern (Nur and Simmons, 1969), or by orientated fracture systems (Crampin, 1987b), by texture and foliation of the rock. The MASE provides observations variable in azimuth, but constant in offset. The S-MSP on the contrary allows for observations constant in two azimuths, but variable in offset. The VSPs complete the observation scheme with data variable in depth.

The initial results presented in this paper show a remarkable correlation with the orientation of the most compressive stress in the KTB deduced from televiewer observations (Mastin et al., 1990). The orientation of this stress field is almost N 160°. The azimuthal difference in P- and S-wave velocities observed in the SCMP survey (see table 3), the fastest waves

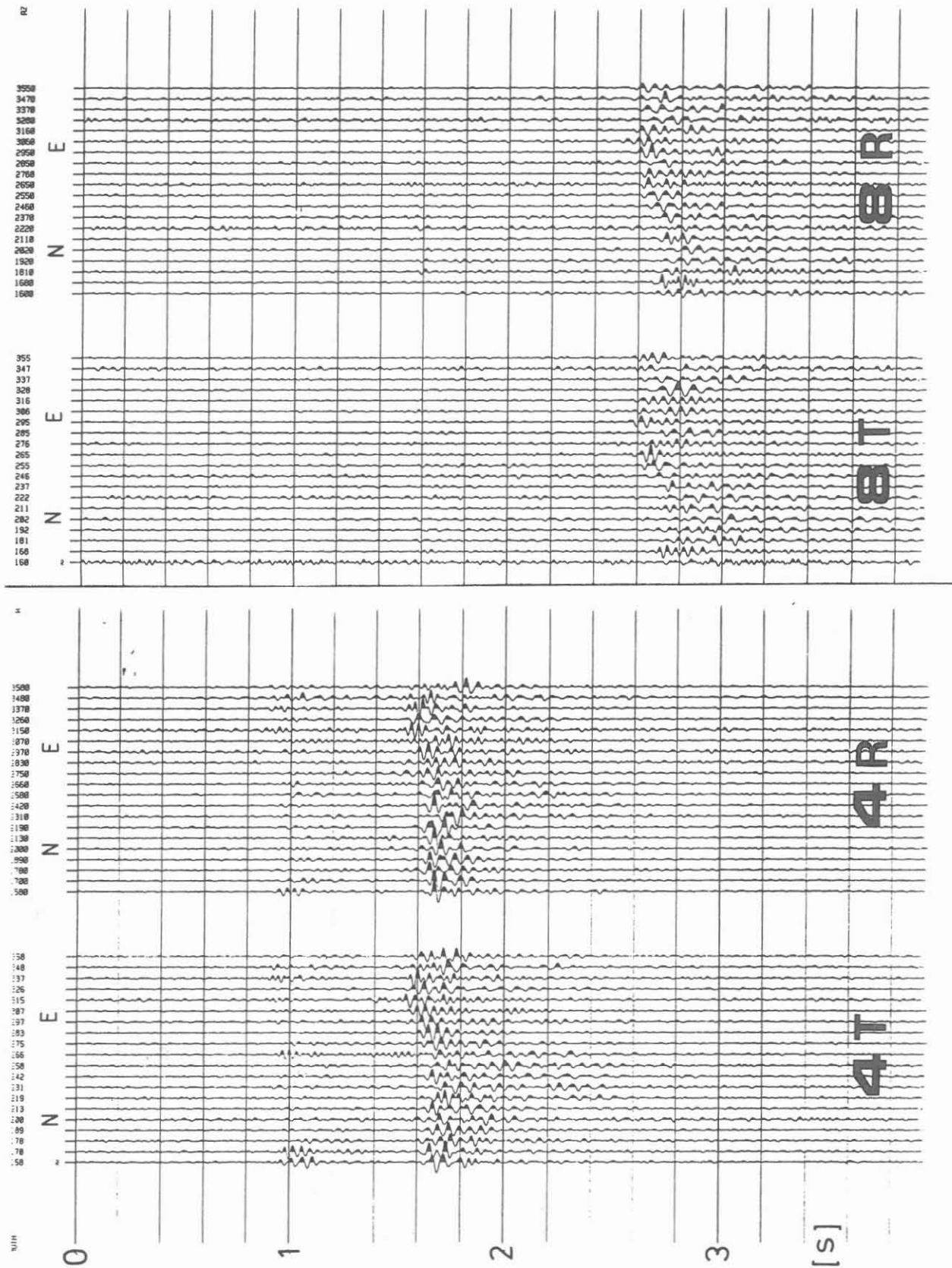


Fig 23

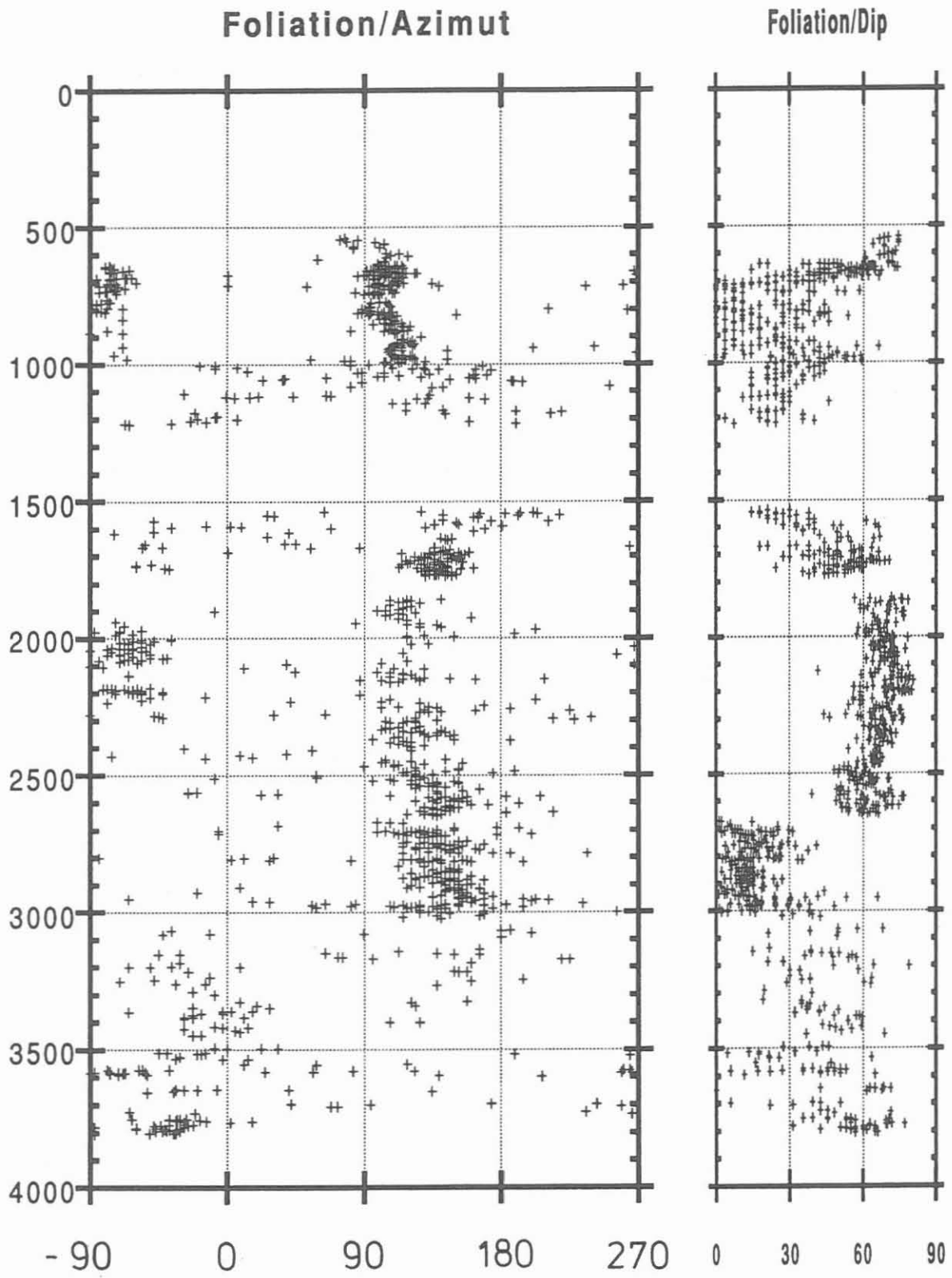


Fig 24

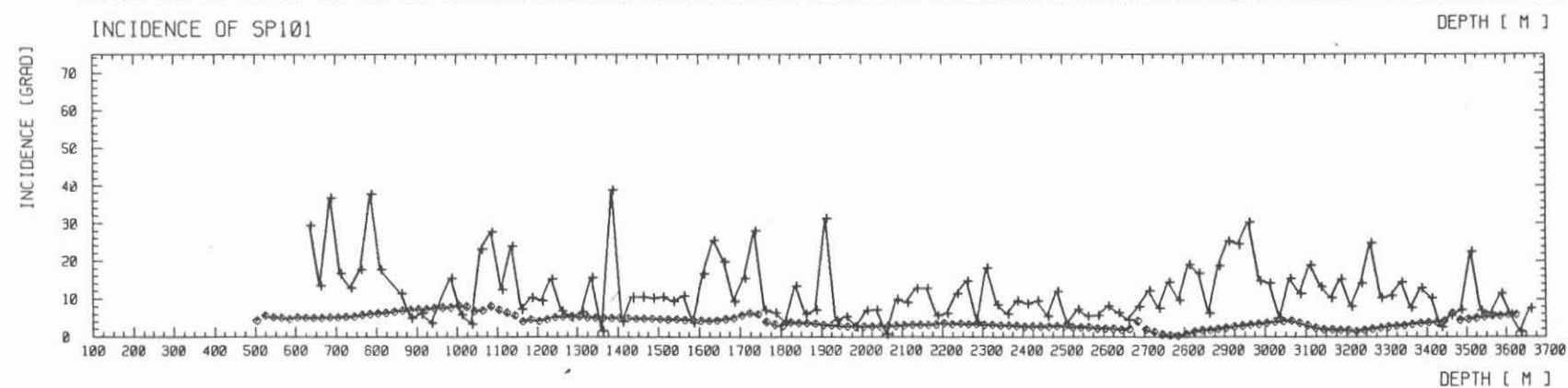
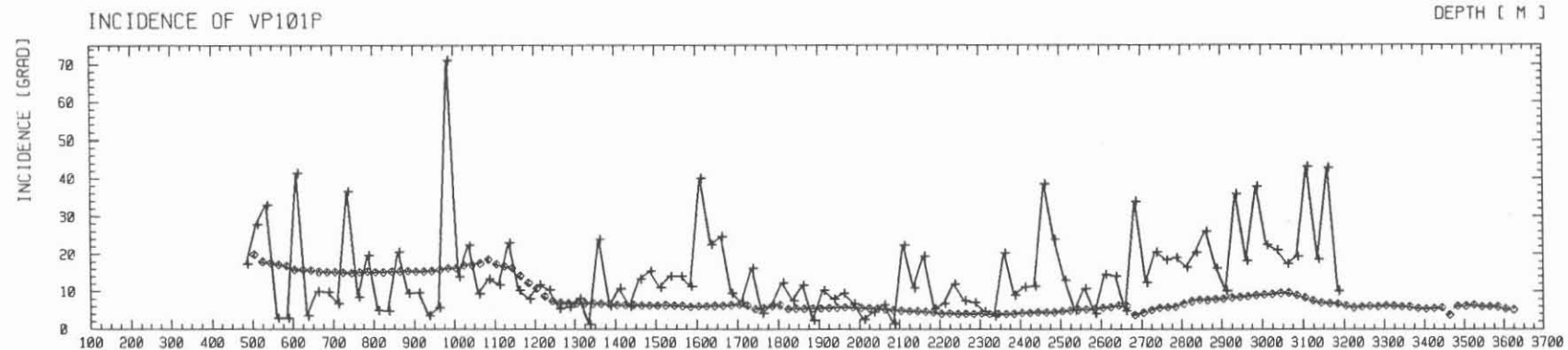
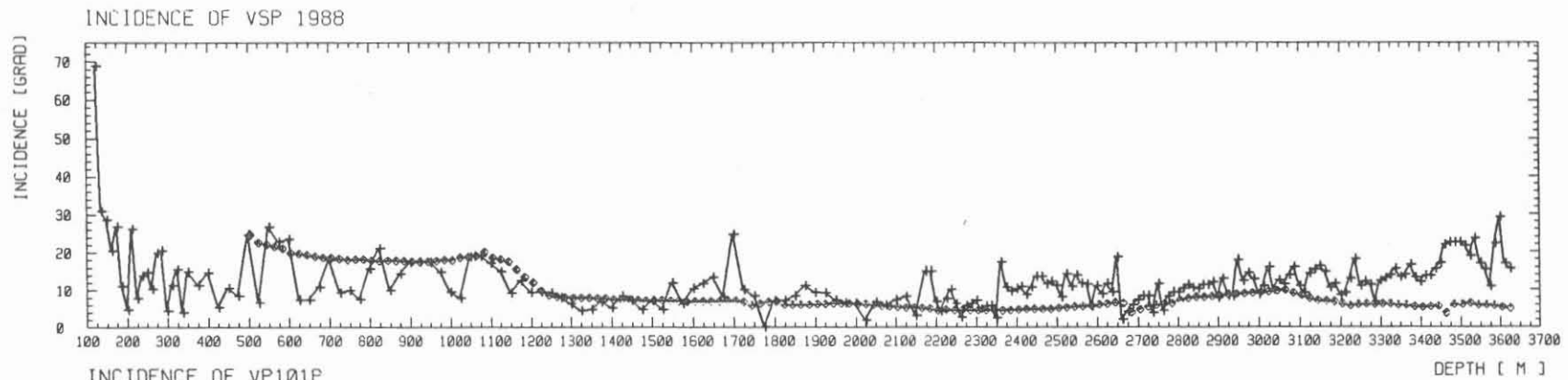


Fig 25

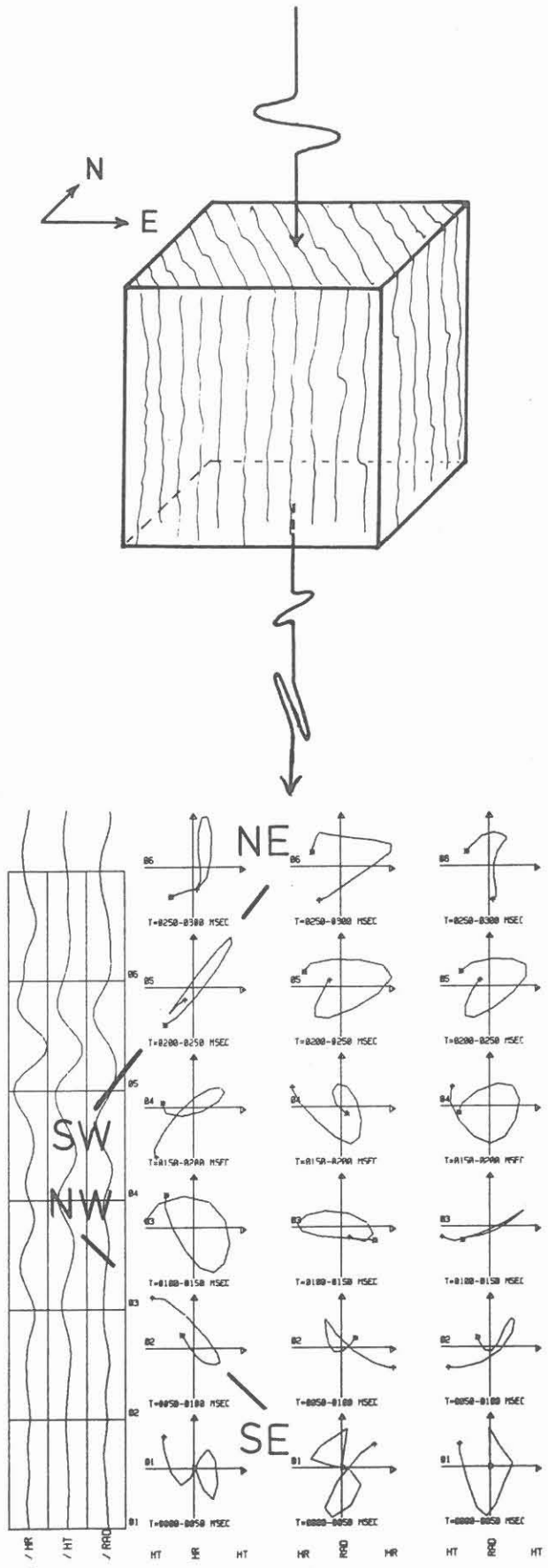


Fig. 26

Figure 23: Multiple azimuth shearwave experiment. All traces in this example are from Z component of the second downhole unit of SEKAN 5 in 3375 m depth. From left to right: 4 km offset with transverse source orientation, 4 km offset with radial orientation, 8 km offset with transverse orientation, 8 km offset with radial orientation. In each panel the traces start on the left with the source location in the NW. Static corrections include correction for distance, but no near-surface effects at the source. True relative amplitudes.

Figure 24: Azimuth (left) and dip (right) of foliation in the KTB-borehole derived from televiewer measurements (courtesy borehole study group at Geophysical Institute Karlsruhe). Note steep foliation at 1500-2700 m depth striking N 140°. This is believed to cause shearwave splitting demonstrated in figures 14, 15 and 24.

Figure 25: Incidence of the direct P-wave determined by the covariance matrix (crosses) and by geometrical calculation in an isotropic medium (squares) versus depth. Panels from left to right: SP 101 (dynamite), VP 101 P (P-wave vibrator), VSP 1988 (dynamite). The anomaly at about 1100 m depth corresponds to a deviation of the borehole.

Figure 26: Schematic diagram showing the suggested effect of the rock foliation on shearwave splitting. The lower part shows an example of the effect seen in particle motion diagrams of shearwave direct arrivals of VSP VP 101 S (S-wave vibrator). Motion is first in NW-SE, then in SW-NE direction with a delay of nearly 150 ms.

being observed in NW direction, may be attributed to the stress field and to the possible preferred orientation of cracks, which are related to each other. This is very likely for the uppermost 1 or 2 km. The velocities deduced from the first arrivals of the SCMP survey also correspond to this depth range.

Below the upper depth range, particularly between 1500 and 3000 m, we suggest that shearwave splitting observed in figures 14 and 15 is mainly caused by rock foliation. Figure 24 displays strike direction and dip angle derived from borehole televiewer measurements. In the depth range between 1500 and 2700 m, the dip is almost vertical, the azimuth is about 150 to 160 degree. Figure 25 shows the incidence of the direct P-wave determined by the covariance matrix and the incidence calculated in an isotropic medium using the direct raypath. This theoretical incidence is corrected for the borehole deviation. The VSP 1988 data is to a high degree rectilinearly polarized whereas the VP 101 P and SP 101 data show lower rectilinearity, due to effects caused by the weathering zone. Deviations between the two functions are expected to be related to interference of the direct P-wave with P to S converted and reflected wave modes as well as to deflections due to foliated rocks. Remarkable are the anomalies of the measured incidence angle below 2300 m in the VSP 1988, which might be caused by the increased number of reflections (see upgoing wavefield, figure 19) and variations in the foliation (figure 24).

Figure 26 the suggested relation between foliation and shearwave splitting is shown qualitatively. Cracks and microcracks with the same orientation can produce the same effects (Crampin, 1987b) and cannot be excluded here. Petrophysical investigations of Kern and Schmidt (1990) on core samples indicate that there is considerable velocity anisotropy dominated by crystallographic preferred orientation of major minerals (texture), in particular biotite and hornblende.

From systematic analysis of the polarization in the future, taking into account the variation of source orientations, offsets and azimuths at the surface and depth variations of the seismic wavefield, we expect more quantitative results on seismic anisotropy, its nature and its distinction from lateral heterogeneity. Further evaluation will be accomplished with reference to the other results of IS089. The intention of this paper was to present the design of the field experiments and the presently existing data base.

REFERENCES

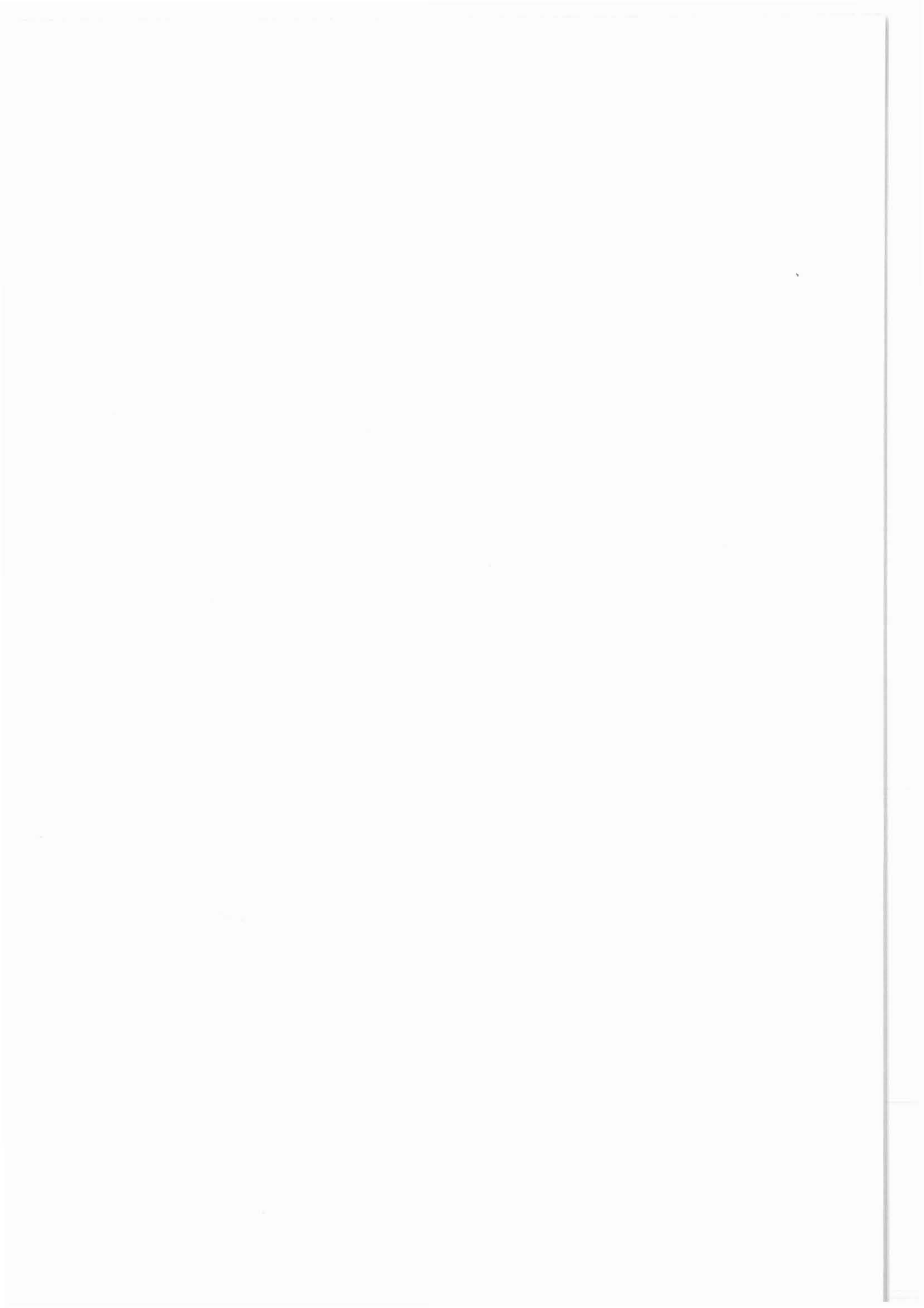
- Benhama, A., Cllet, C., Dubesset, M. (1988): Study and applications of spatial directional filtering in three-component recordings. *Geophysical Prospecting*, 36: 591-613.
- Bram, K. (1988): VSP-Messungen in der Bohrung KTB-Oberpfalz. In: Draxler and Haenel (Eds.), *Grundlagenforschung und Bohrlochgeophysik (Bericht 5)*, KTB-Report 88-7.
- Crampin, St. (1987a): Geological and industrial implications of extensive-dilatancy anisotropy. *Nature*, 328: 491-496.

- Crampin, St. (1987b): Crack porosity and alignment from shear-wave VSPs. in: S.H. Danbom and S.N. Domenico (Editors), Shear-wave Exploration, Geophysical Developments, SEG Special Publ., 1, 227-251.
- DEKORP Research Group (1988): Results of the DEKORP4/KTB Oberpfalz deep seismic reflection investigations. *J. Geophys.*, 62: 69-101.
- Danbom, S.H. and Domenico, S.N. (Editors) (1986): Shear-Wave Exploration. Geophysical Development Series, Vol.1, Society of Exploration Geophysicists, Tulsa, Okla., 274 p.
- DiSiena, J.P., Gaiser, J.E. and Corrigan, D. (1984): Horizontal Components and shear wave analysis of three-component VSP data. in: Toksöz, M.N. Stewart, R.R. (Editors), Vertical Seismic Profiling, Part B: Advanced Concepts. Geophysical Press, London, p. 177-188.
- Edelmann, H.A.K. (1985): Shear-wave energy sources. in: G. Dohr (Editor), Seismic Shear Waves, Part B, Applications. Geophysical Press, London, pp. 134-177.
- Edelmann, H.A.K. and Lüschen, E. (1990): New shear wave technique first applied for deep crustal studies, in preparation.
- Fertig, J. (1984): Shear waves by an explosive point-source: the earth surface as a generator of converted P-S waves. *Geophysical Prospecting*, 32: 1-17.
- Franke, W. (1989): The geological framework of the KTB drill site, Oberpfalz. In: R. Emmermann, J. Wohlenberg (Eds), The German Continental Deep Drilling Program (KTB), Springer Verlag, Berlin, pp. 37-54.
- Hardage, B.A. (1985): Vertical seismic profiling, Part A: principles. *Handbook of Geophysical Exploration*, Vol. 14A, Geophysical Press, London, 509 p.
- Helbig, K. and Mesdag, C.S. (1982): The potential of shear-wave observations. *Geophysical Prospecting*, 30: 413-431.
- Hohrath, A. (1990): VSP-Processing anhand einer Drei-Komponenten Registrierung im KTB. Diploma Thesis, University of Karlsruhe.
- Kästner, U., Bram, K., Hubral, P., Kiefer, W., Königer, Ch., Macdonald, C., Merz, J., Rühl, Th., Sandmeier, K.-J. (1989): Seismische Untersuchungen an der KTB-Lokation. KTB-Report 89-1, 169-210.
- Kanasewich, E.R. (1981): Time sequence analysis in geophysics. The Univ. of Alberta Press, Winnipeg, pp. 480.
- Kern, H. (1982): P- and S-wave velocities in crustal and and mantle rocks under the simultaneous action of high confining pressure and high temperature and the effect of the rock microstructure. In: W. Schreyer (Editor), High-Pressure Researches in Geoscience. Schweizerbartsche Verlagsbuchhandlung, Stuttgart, pp. 15-45.
- Kern, H., Schmidt, R. (1990): Petrophysical investigations on KTB core samples at simulated in situ conditions. Poster presented at KTB-Kolloquium, Giessen, 28.2.-2.3.1990.
- Mylius, J., Nolte, E., and Scharf, U. (1990): Use of the seismic receiver chain SEKAN 5 within the framework of integrated seismics in the Oberpfalz, this volume.
- Lüschen, E., Wenzel, F., Sandmeier, K.-J., Menges, D., Rühl, Th., Stiller, M., Janoth, W., Keller, F., Söllner, W., Thomas, R., Krohe, A., Stenger, R., Fuchs, K., Wilhelm, H. and Eisbacher, G. (1987): Near-vertical and wide-angle seismic surveys in the Black Forest, SW Germany. *J. Geophys.*, 62: 1-30.

- Lüschen, E., Nolte, B. and Fuchs, K. (1990): Shear-wave evidence for an anisotropic lower crust beneath the Black Forest, southwest Germany. *Tectonophysics*, 173: 483-493.
- Lüschen, E., Durrheim, R., Feddersen, J., Hopp, O. and Edelmann, H.A.K. (1990): A comparison of controlled shear-wave sources for crustal studies in southern Germany. In preparation for submission to *Geophysical Prospecting*.
- Mastin, L., Heinemann, B., Krammer, A., Fuchs, K., Zoback, M.D. (1990): Stress orientation in KTB Pilot hole determined from wellbore breakouts. submitted to *Scientific Drilling*.
- Nur, A., Simmons G. (1969): Stress-induced velocity anisotropy in rock: an experimental study. *J. Geophys. Res.*, 74, 6667-6674.
- Schruth, P., Bram, K., Hohrath, A., Hubral, P., Kästner, U., Lüschen, E., Rühl, T., Söllner, W. (1990): Auswertung und Interpretation der VSP-Messungen in der Bohrung KTB-Oberpfalz VB bis zu einer Tiefe von 3600 m. KTB-Report, in press.
- Toksöz, M.N. and Stewart, R.R. (editors, 1984): *Vertical Seismic Profiling, Part B: Advanced Concepts. Handbook of Geophysical Exploration, Vol 14B.* Geophysical Press, London, 419 p.

Moving Source Profiling
A Link between KTB-Borehole Data
and Seismic Surface Measurements

H.-P. Harjes
M. Janik
M. Kemper



Moving Source Profiling A Link between KTB-Borehole Data and Seismic Surface Measurements

H.-P.Harjes, M.Janik and M.Kemper

Abstract.

The moving source profiling (MSP) measurements are done by moving seismic sources along a surface line crossing the well site while a chain of geophones, placed within the well bore at a certain depth, records the seismic response. A multifold coverage of the subsurface can be obtained by repeating the source profile for a number of different geophone depths.

This idea of altering the conventional vertical seismic profiling (VSP) geometry to allow illumination of subsurface structure away from the well is an attractive idea because it is designed to better locate horizons below the drill bit. If these target horizons can be correlated with reflectors in usual seismic profiles, recorded on the surface, the latter can be calibrated by the MSP results.

Two MSP experiments were realized in the KTB pilot borehole. The first (MSP 1) included two N-S and E-W orientated source profiles of 10 km length and a single three-component geophone at 3585 m depth. Later a full MSP experiment (MSP 2) was run for one NE-SW orientated source profile and 20 different geophone depths. The source line was extended 7 km to the Northeast and 3 km to the Southwest of the well. A vibrator source produced seismic signals every 50 m. These shots were recorded by three-component geophones at depths from 3210 m to 3685 m with 25 m intervals resulting in a 20-fold coverage of the illuminated subsurface.

Due to the difficulties encountered in crystalline environments, different processing techniques were combined for interpretation of the MSP data set. Aside from comparing measured first-break times with theoretical ones to determine seismic velocities of the overburden an MSP-CDP transformation for migration were applied.

The steeply dipping boundary of the Falkenberg granitic intrusion was mapped as a distinct velocity contrast east of the KTB well. On the other hand, some remarkable seismic reflectors at depths between 4000 m and 10000 m are predicted to be hit by the future KTB main borehole.

1. *Introduction.*

In the past decade, sophisticated seismic data acquisition techniques have been developed which include the placing of geophones in downhole arrays. The importance of this method lies in its potential for detecting subsurface detail which is difficult to be obtained from conventional surface seismic data. The Vertical Seismic Profile (VSP) technique is normally executed with a single source position near the well head. Zero-offset VSP's provide subsurface information only within the Fresnel zone surrounding the well. In contrast, the Moving Source Profiling (MSP) data acquisition scheme (Brauner, et al. (1988)) where seismic signals are generated on a profile crossing the well site, allows the illumination of subsurface structure away from the well.

In an integrated seismic survey, like the ISO-89 experiment, the MSP-data might serve to calibrate reflections, recorded on surface profiles, to lithological information from borehole data.

As one can see from the schematic diagram of the MSP-experiment (figure 1), two different kinds of seismic waves travel to the downhole receivers : direct waves (dashed lines) from which the seismic velocity of the overburden can be deduced and reflected waves which will be used to accurately locate target horizons in the neighborhood of the borehole.

In view of the ultradeep KTB-borehole, the most challenging part of the MSP-experiment will be a prediction of discontinuities that should be hit when the drilling operation reaches depths below the pilot hole in which the geophones were placed during the MSP-survey.

Before we can start an interpretation of the experiment, the MSP-reflection response is to be reconstructed into the familiar co-ordinate system of surface seismic sections. As this experiment was - to our knowledge - the first test of the MSP-technique in crystalline environment, it is by no means evident that procedures developed for sedimentary structures are useful or to which extent the established processing steps have to be modified. Additionally, the data acquisition in itself in crystalline environment is a new frontier because the reflecting elements - as seen in pre-site surface seismic surveys - are very short and no specific target horizon was detected which could have been used for planning the MSP-layout.

2. *MSP-Experiments.*

A first MSP-experiment (MSP 1) was conducted in December 1988 to gain experience with the site-specific problems of data acquisition and processing in the KTB-area. It was planned to get a first insight into the geological structure at the location of the pilot hole and its extension to the neighboring site of the main deep drilling project planned at about 200 m distance. Additionally, the depth extension of the Falkenberg granitic intrusion east of the drill site should be explored. Figure 2 shows the two N-S and E-W vibrator lines of 10 km length. The E-W profile represents an asymmetric split-spread configuration which was extended to the east to include the Falkenberg granite. Along the vibrator lines combisweep signals (20 - 80 Hz) of 20 sec duration were produced at 50 m interval. 5 -10 sweeps were

stacked and correlated with an effective recording time of 7 seconds at a sampling rate of 4 msec.

A limitation of the first MSP-experiment was given due to the fact that data were recorded with only one three-component geophone at 3585 m depth. Additionally, a 120 trace geophone spread was laid out along both vibrator profiles (figure 2) to assist in tying the MSP-data to the existing surface seismic profiles, and in order to obtain reliable static corrections.

Within the ISO-89 experiment, a third MSP-profile (MSP 2) was recorded (figure 3). This time a receiver chain of 5 three-component geophones was used which were separated by a distance of 25 m. The deepest geophone position was at 3685 m. Then the receiver-chain was lifted 125 m and the vibrator profile was repeated.

Altogether, the vibrator line was run four times resulting in a 20-fold coverage of the cross section illuminated around the well (figure 4).

As one can see from the schematic map of the two MSP-experiments (figure 2 and 3), the orientation of the vibrator line for the multifold MSP-profile was changed to NE-SW direction to fit into the grid of the surface seismic data (3D-coverage) of the ISO-89 experiment.

3. *Data.*

A typical example of the raw data of MSP 2 is shown in figures 5a and 5b. The vertical and the H1-component is plotted for one depth position (3210 m).

The clearest coherent events can be associated to the direct P-wave and to the direct S-wave. The latter can be recognized by its larger moveout and also by its different spectral content. Obviously there is a long coda of the S-wave masking possible later reflection events. Without further processing it is very difficult to detect reflections even in the interval between the direct P- and S-wave arrival. The short-period multiples following both phases seem to originate from the weathering layer which is very pronounced at the surface of the Variscan crystalline outcrop forming the geology in the KTB-area. The varying thickness of the weathering zone together with the rough topography is also the reason for the incomplete static corrections.

Later phases can easier be detected in a "brute stack" of 20 depth positions which is shown for the vertical component in figure 6. Especially between the two direct waves some events emerge which could be interpreted as reflections from interfaces below the geophone positions.

Before we start to process these events further, the clear direct P-arrivals will be used to evaluate the velocity distribution of the overburden.

4. *Lateral variation of overburden velocities.*

From the split-spread E-W profile of the first MSP-experiment, arrival times of the direct P-wave were picked and compared to theoretical travel times, computed by ray-tracing method assuming a simplified geological model. A homogeneous half-space was compared to a model of two adjacent half-spaces, the latter one describing the intrusion of the Falkenberg granite (figure 7). Static corrections for topography and weathering layer were derived from a shallow refraction survey. In an iterative process, theoretical and measured travel times were adjusted by variation of velocities.

Figure 8 shows a comparison between measured first arrival times and the calculated ones for both models. Additionally the differential travel times are plotted at the bottom of fig. 8. The best fit is obtained for an average velocity of 5950 m/s in the western part of the profile approaching the well, whereas a lower velocity of 5580 m/s was found at the eastern end of the profile. This velocity decrease corresponds well with the granitic intrusion, on the other side, an average velocity of 5900 m/s was derived from the conventional VSP - measurements in the KTB pilot hole.

Some extrema in the differential travel times plotted in figure 8 occur independently from the model at offsets of 1.8 km, 2.5 km and 4 km. They reach the same magnitude as the model differences and have to be explained in terms of residual statics. Denser refraction lines are necessary to confirm this conclusion.

Despite these difficulties, it has been demonstrated that a tomographic evaluation of the MSP-data allows to verify lateral velocity changes in the overburden which is especially useful to locate steeply dipping interfaces like the gneiss/granite contact plane east of the KTB borehole.

5. *Predicting reflections ahead of the drill bit.*

Many uncertainties in surface seismic measurements are a result of having the source and the receiver on the surface, far removed from the target zone. In MSP's, however, since the receivers are located down the borehole, they are closer to the reflecting interfaces so the accuracy relative to surface measurements should be improved.

A KTB presite survey (Schmoll et al. (1989)) including two reflection seismic profiles exposed a series of reflections in the uppermost crust which were interpreted as indicating a nappe (ZEV = Zone of Erbendorf-Vohenstrauss). The depth of this old thrust fault was estimated between 4000 m and 5000 m. Since the geophone positions of the MSP-experiment covered a depth range from 3210 m to 3685 m, the base of the ZEV nappe should be imaged in the MSP-data in the time interval between 0.6 s and 1.2 s roughly corresponding to a depth range from 3.6 km to 5.4 km.

Before we can start to correlate coherent energy in the MSP-profile with reflections from surface seismic cross sections, the MSP-data have to be transformed into the familiar coordinate system of a surface seismic section. This migration-like mapping is especially important because the reflecting elements only show short lateral extension which is

characteristic for the seismic response of crystalline crust.

Figure 9 outlines the principle of the mapping technique for a constant velocity situation (Dillon and Thomson, 1984). The formulae simply transform a time on a trace to the x-z co-ordinates of a point in the subsurface. For a more complex velocity profile, ray-tracing techniques must be used. This mapping procedure is also known as "MSP-CDP - transformation" because it images the MSP-data into the CDP-domain, equivalent to a CDP-stacked section. To produce traces of constant CDP-increments, the MSP-data are mapped into a series of vertical strips which are referred to as bins, and then a trace is created for each bin by stacking the data that are mapped into that bin. The bin width must be chosen with care so as to achieve good signal quality without degrading resolution. Figures 10 and 11 show the result of the MSP-CDP- transformation for the vertical and horizontal component (H1) of the second MSP-experiment, respectively. Data from 10 depth positions are stacked. Using an average velocity of 5900 m/s derived from VSP-data, one can transform the one-way travel time into depth as marked on the right panel of both figures. A series of reflectors dipping to the east now clearly emerge in the depth section between 3500 m and 5000 m which seem to be terminated by steeply dipping faults. This hypothetical interpretation has to be taken with caution because the mapping procedure is only secure for horizontal events but it introduces errors for dipping reflectors.

To get an impression of the imaging of reflectors into MSP-data, a forward-modeling method was applied. Using a ray-tracing algorithm a reflector with an eastward dip of 10 degrees was modeled into a travel time curve as seen in a MSP-profile (figure 12). For the set-up of the MSP2-experiment (figure 3) we get an MSP-image as plotted in the lower half of figure 12. From this one can conclude that a coherent reflector of 1 km to 2 km lateral extension results from a discontinuity with a width of only 100 m. To obtain the true position of the target horizon, an iterative wavefront modeling should be performed until the resulting depth correlates with the corresponding MSP-depth conversion.

6. *Future work.*

At this stage, only preliminary results of the MSP-processing are available. The MSP-CDP transformation will be refined and true migration procedures will be applied to finally splice together the seismic surface profiles and the MSP-data. Two-dimensional filtering should help to separate the reflected wavefield from downgoing multiples. Last but not least, we want to make use of the information contained in the three-component recordings to identify wave-type and its bearing by polarization techniques.

7. *References*

Brauner,W., Duerschner,H. Koopmann,B., Marschall,R. and Peters,K.: Moving source profiling (MSP). *Geophys.Pros.*, 36,1, 6-21, 1988.

Dillon,P.B. and Thomson,R.C.: Offset Source VSP Surveys and their Image Reconstruction. *Geophys.Pros.* 32, 5, 790-811, 1984.

Schmoll,J., Bittner,R., Dürbaum,H.-J., Heinrichs,T., Meißner,R., Reichert,C., Rühl,T. and Wiederhold,H.: Oberpfalz Deep Seismic Reflection Survey and Velocity Studies, in Emmermann,R. and Wohlenberg,J. (eds.): *The German Continental Deep Drilling Program (KTB)*, 1989.

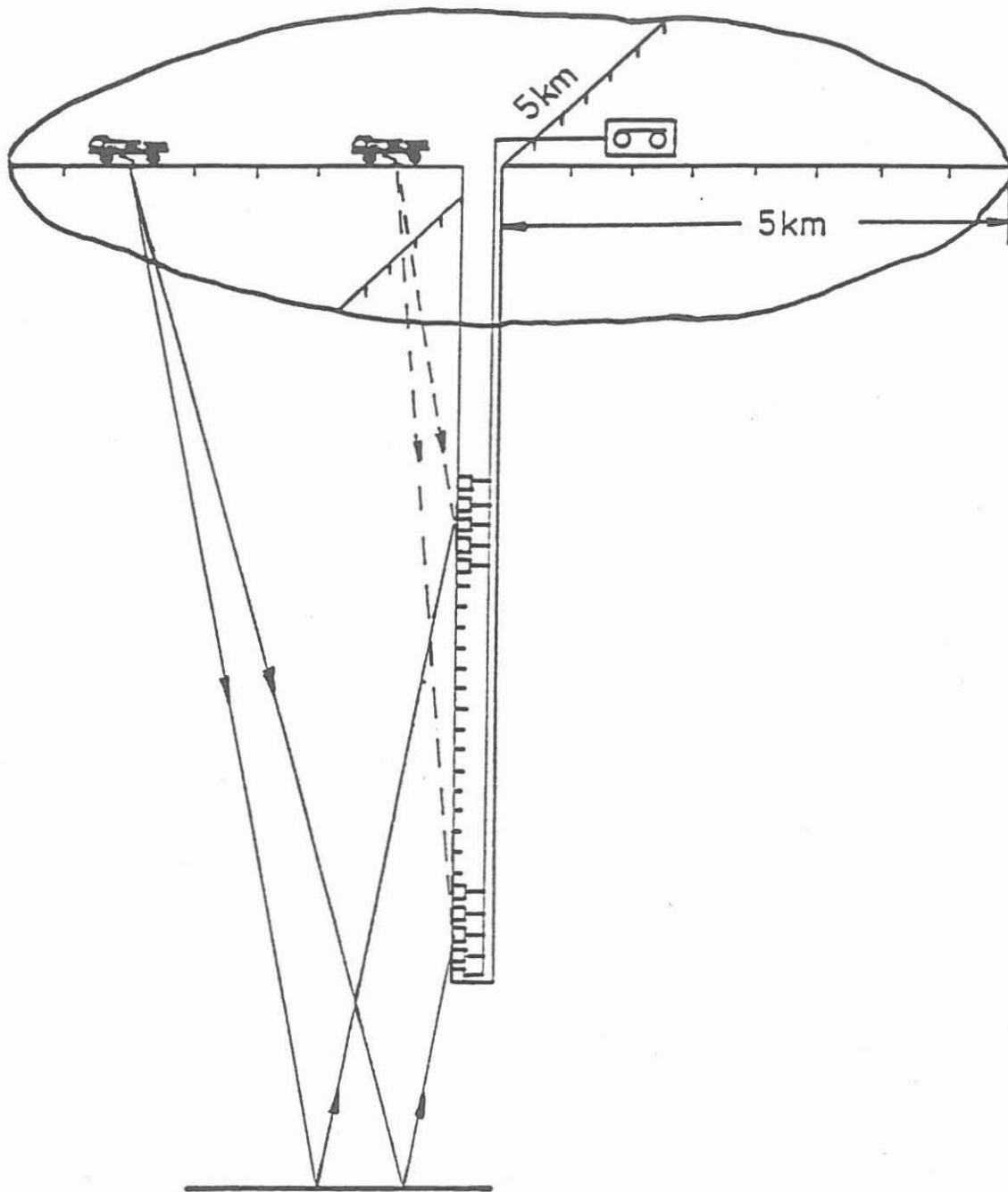


Fig. 1 Schematic diagram of the MSP-experiment.

MSP 1

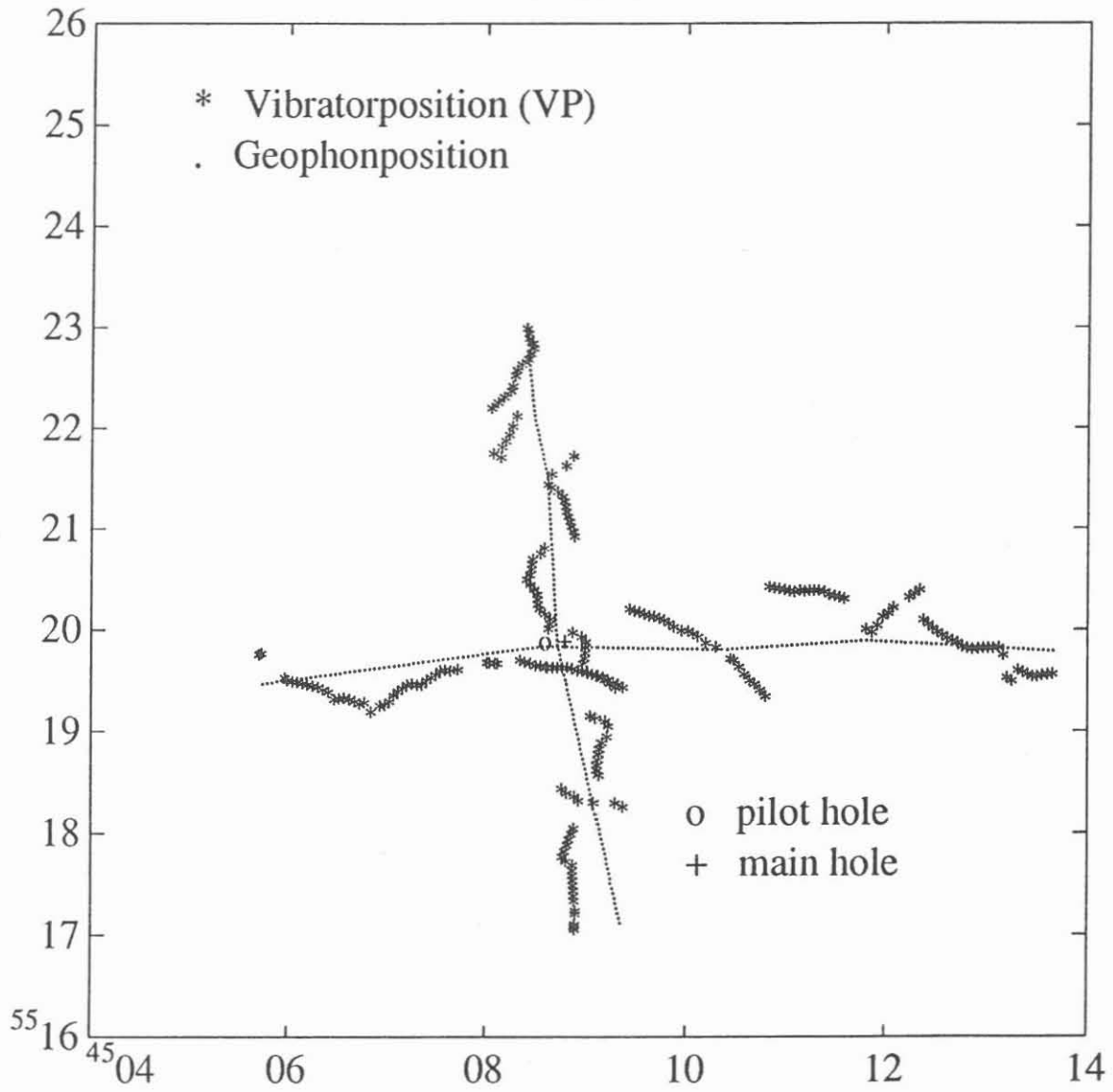


Fig. 2 Vibrator - and geophon profiles of the first MSP-experiment (MSP 1).

MSP 2

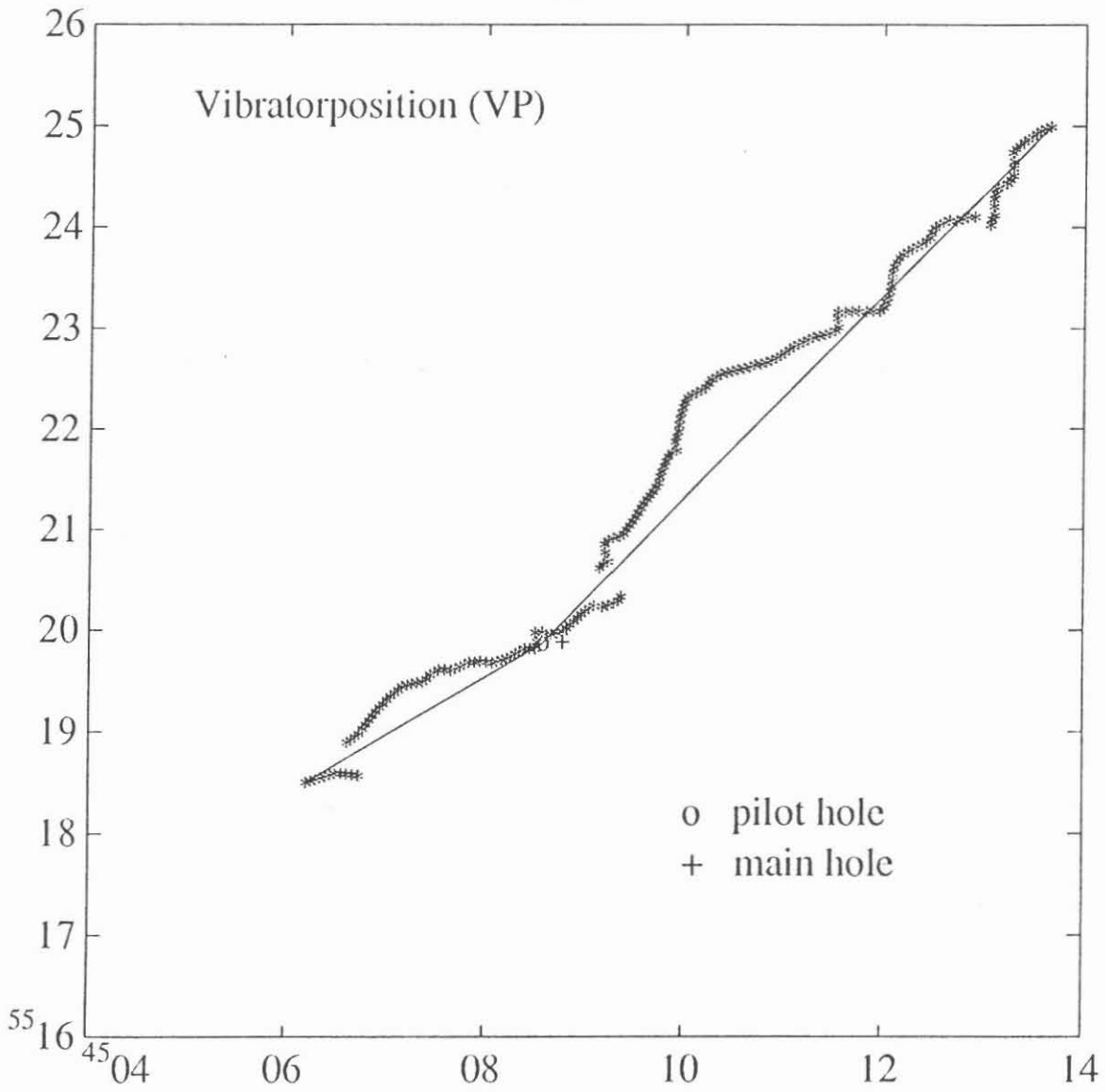


Fig. 3 Vibrator profile of the second MSP-experiment (MSP 2).

MAXIMUM FOLD : 20

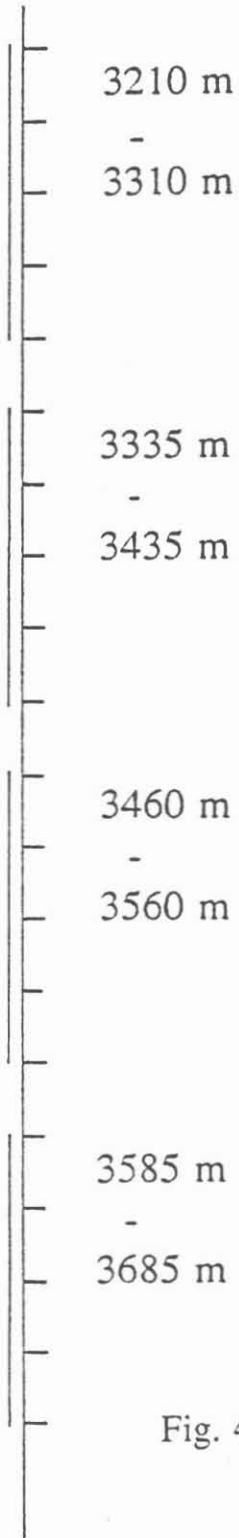


Fig. 4 Depth positions of the receiver chain, leading to a 20-fold coverage.

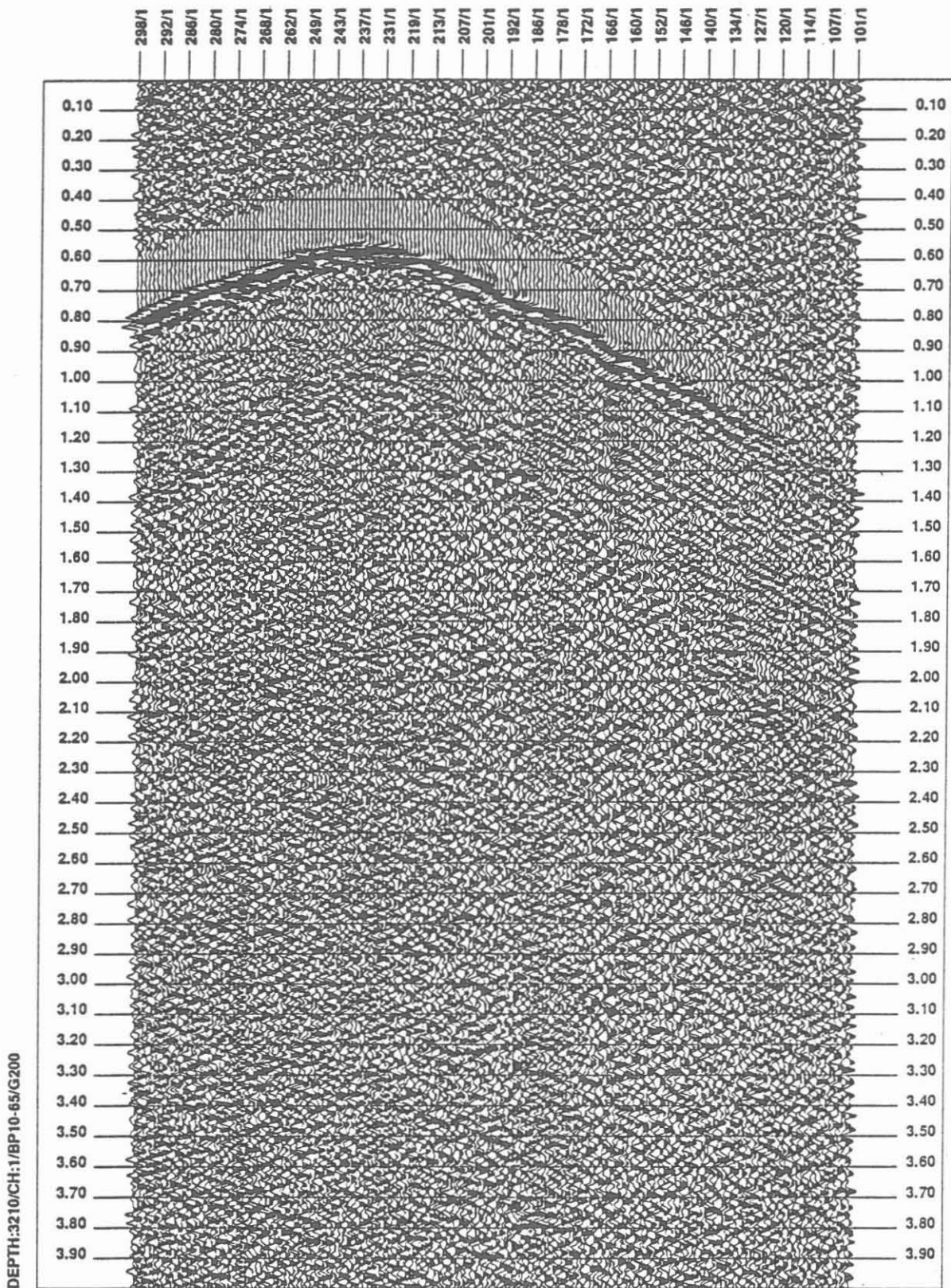


Fig. 5a Raw data from depth position 3210 m.
(Z-Component)

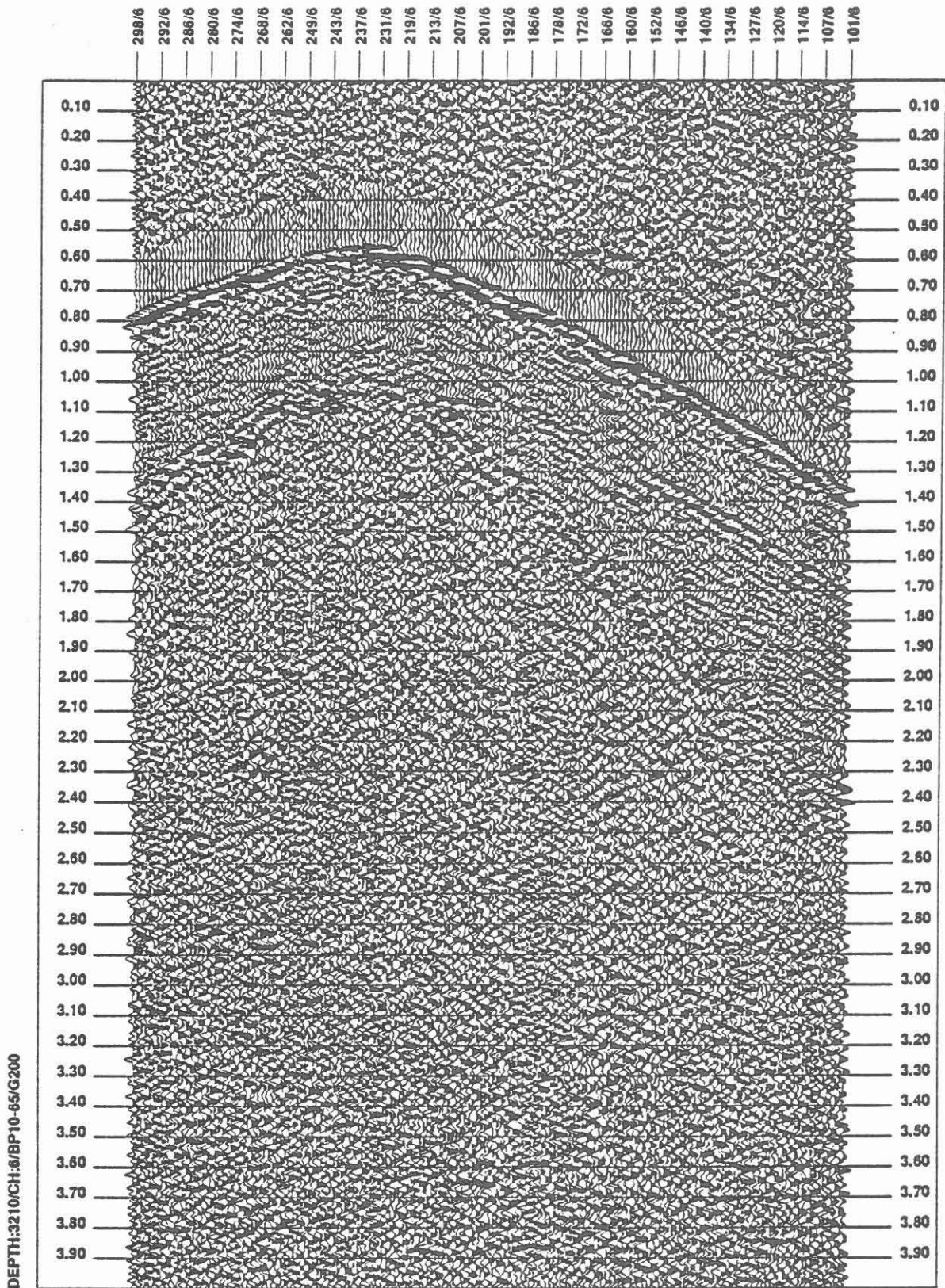


Fig. 5b Raw data from depth position 3210 m.
(H1-Component)

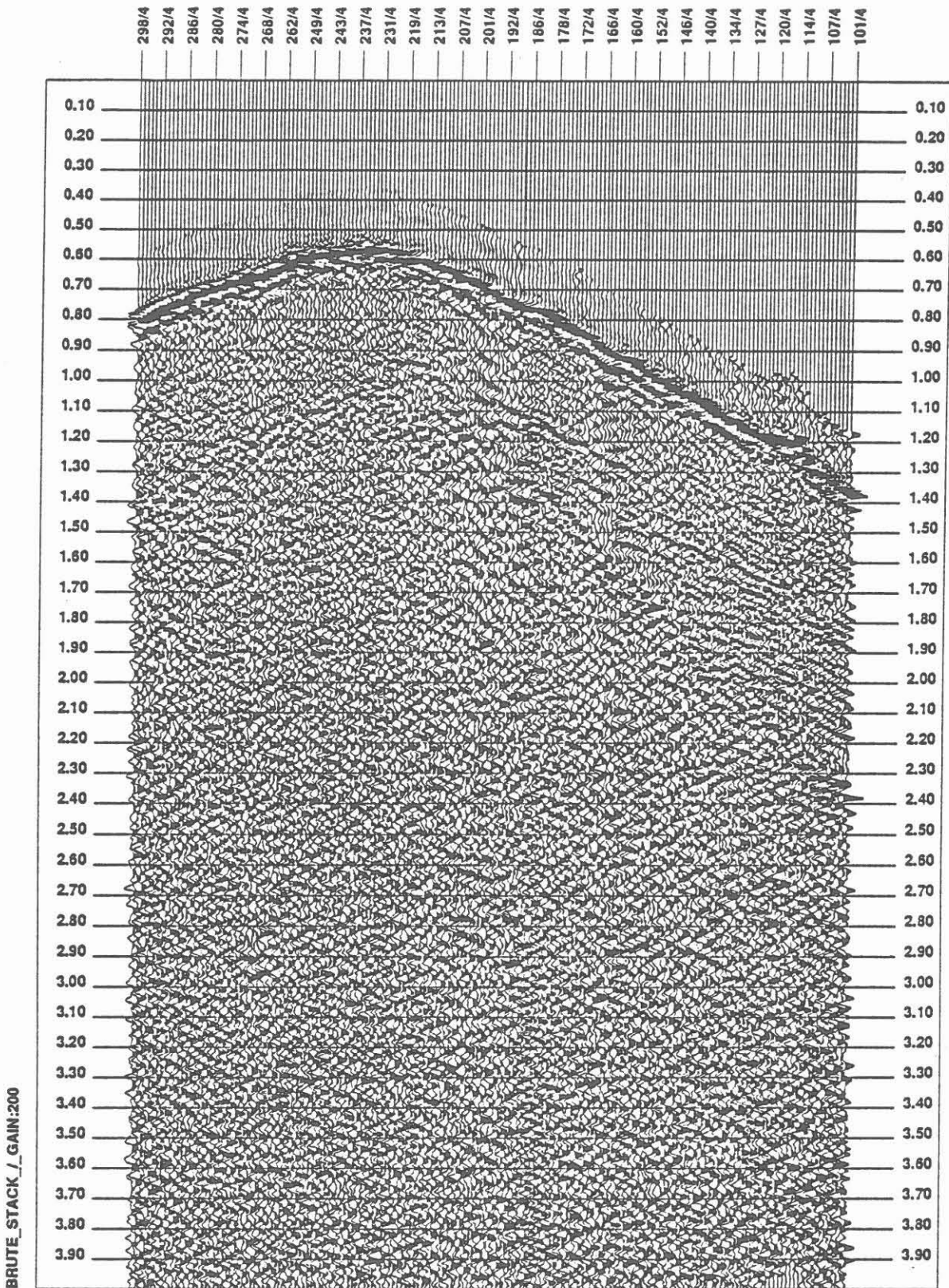


Fig. 6 Brute Stack, obtained by stacking all 20 MSP's after time correction for geophon spacing.

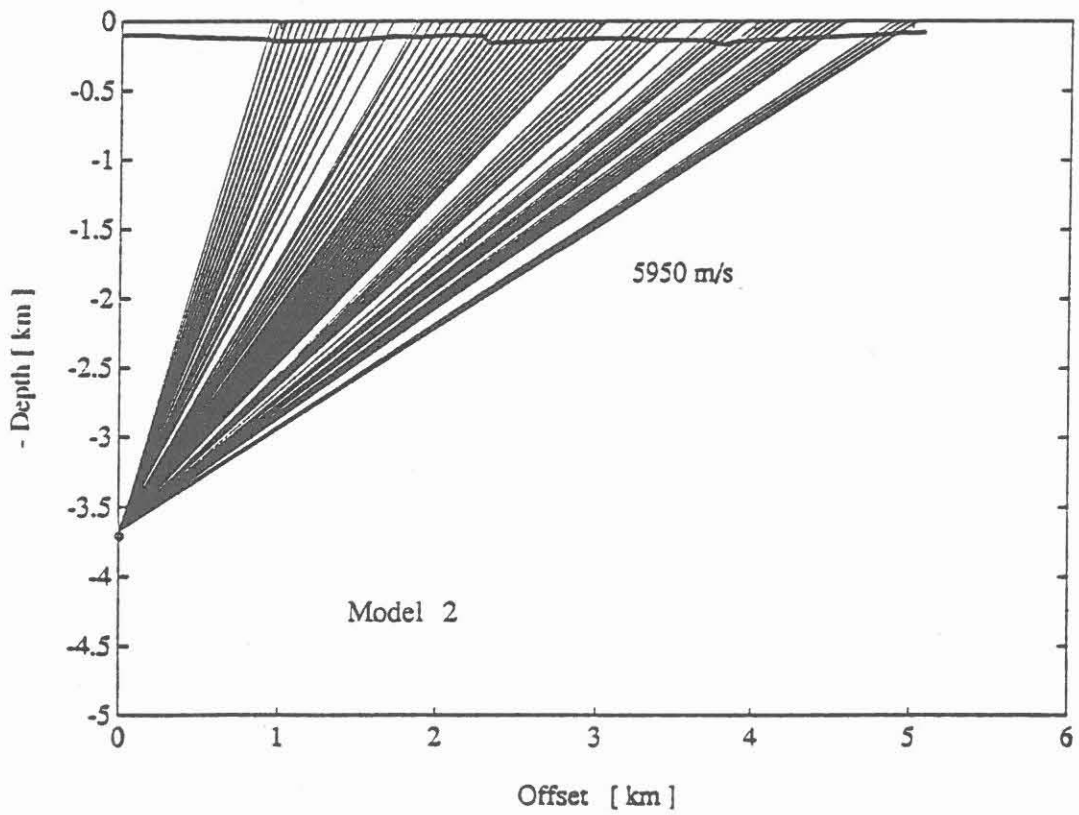
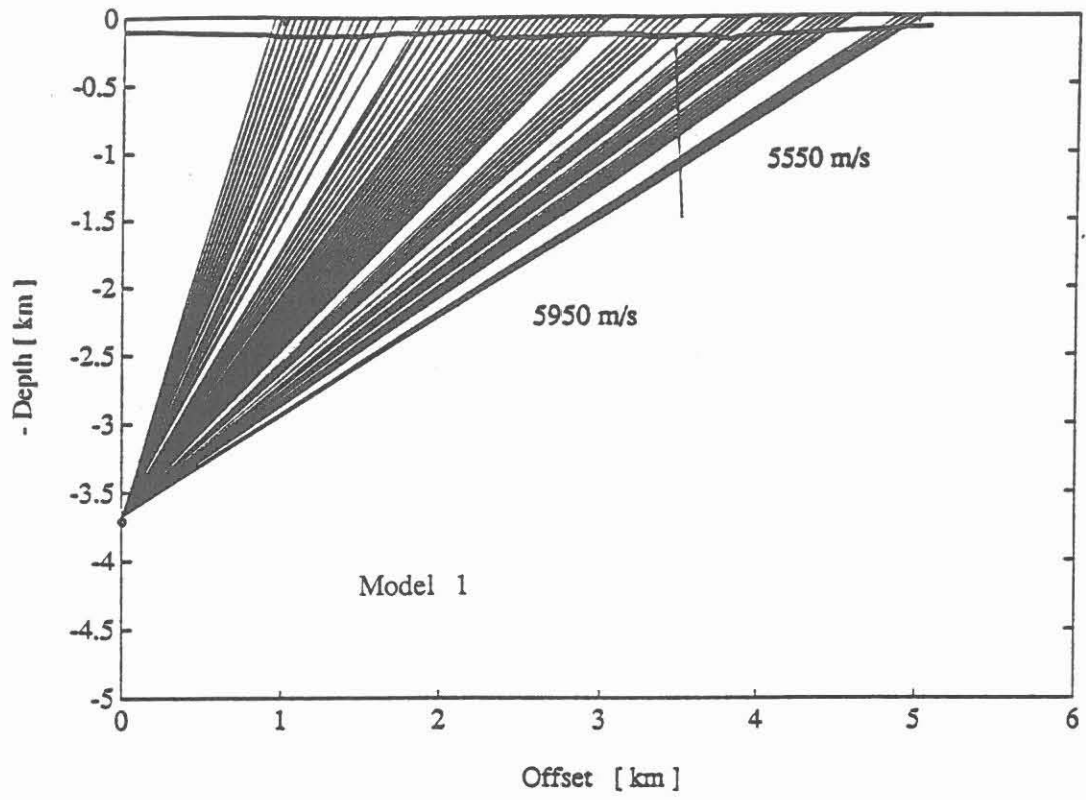


Fig. 7 Models used for first-break analysis. See text for further comments.

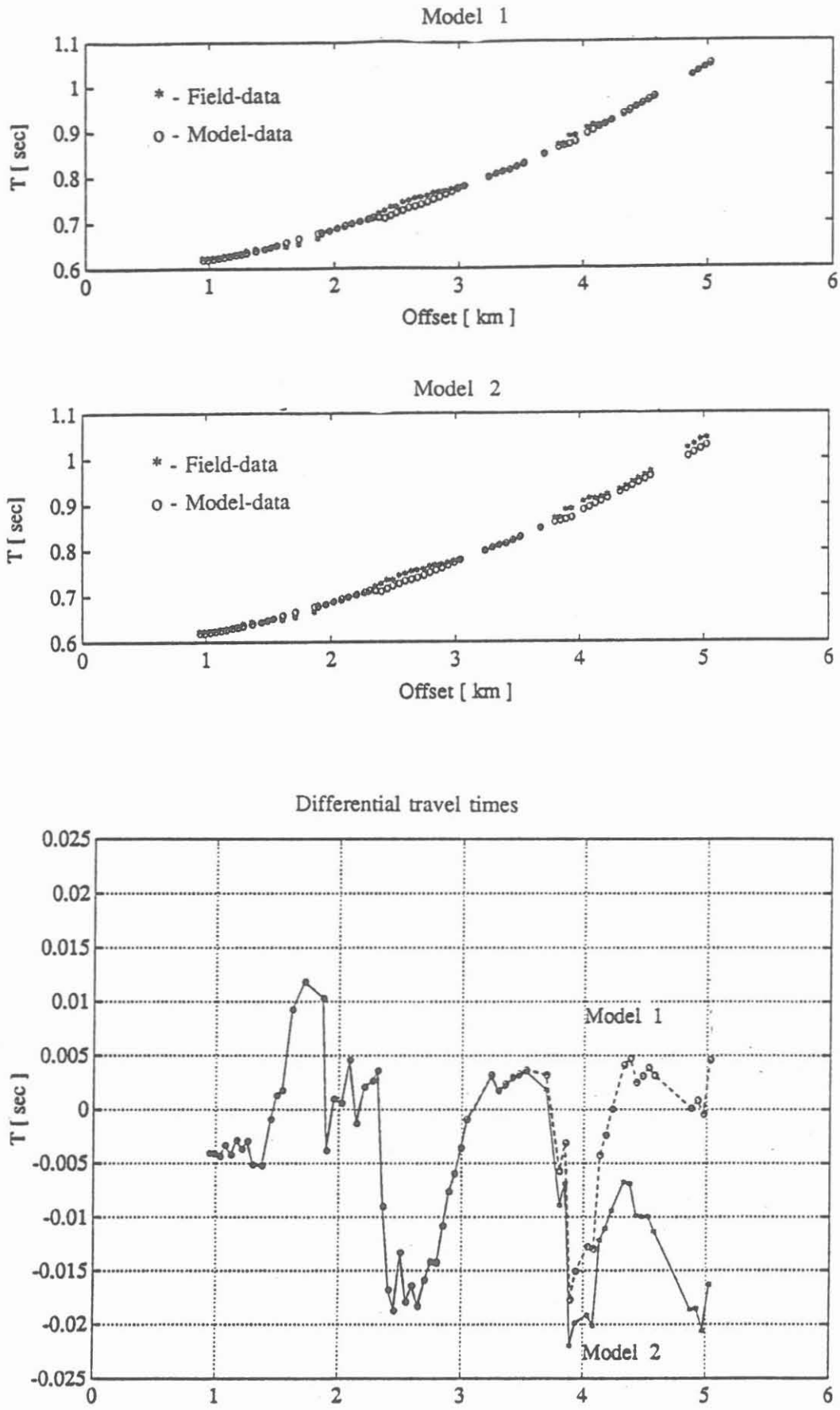


Fig. 8 Results of first-break analysis. See text for further comments.

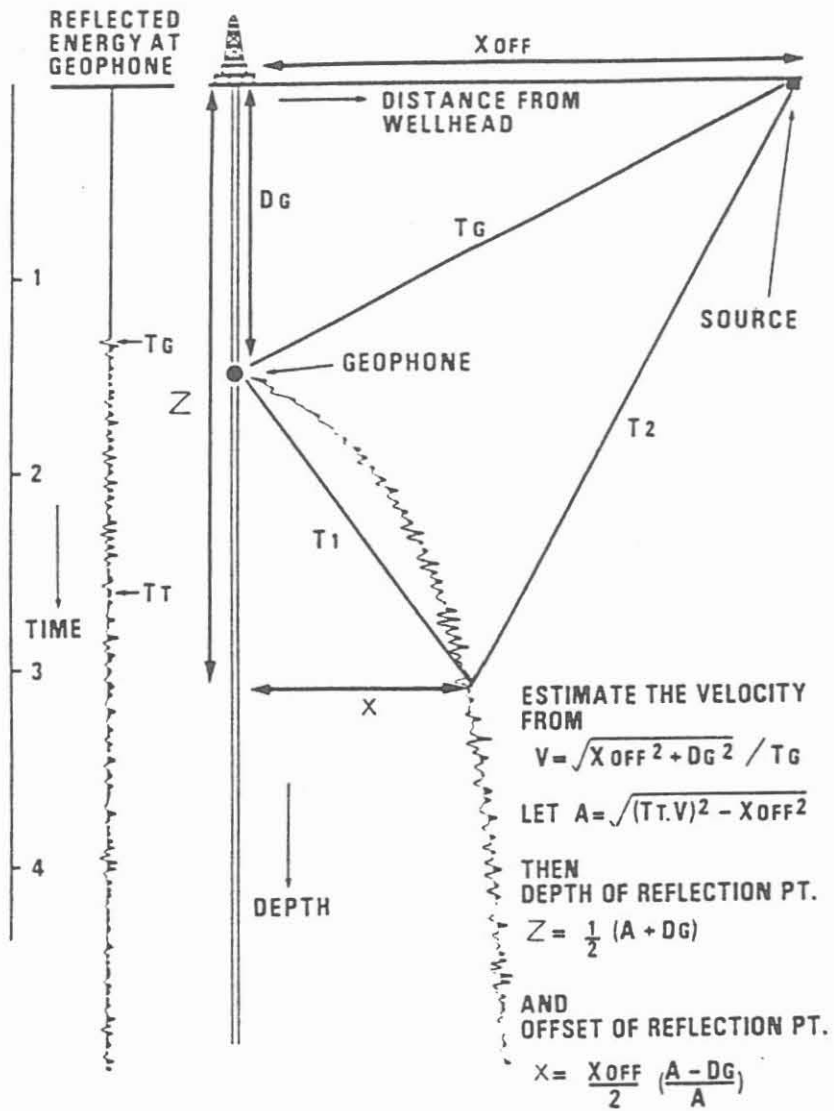


Fig. 9 Principle of MSP-CDP transformation. Every sample is shifted according to the formulas above.

CDP-TRANSFORMATION AND STACK

H1-COMPONENT 3210 M - 3435 M FOLD 10

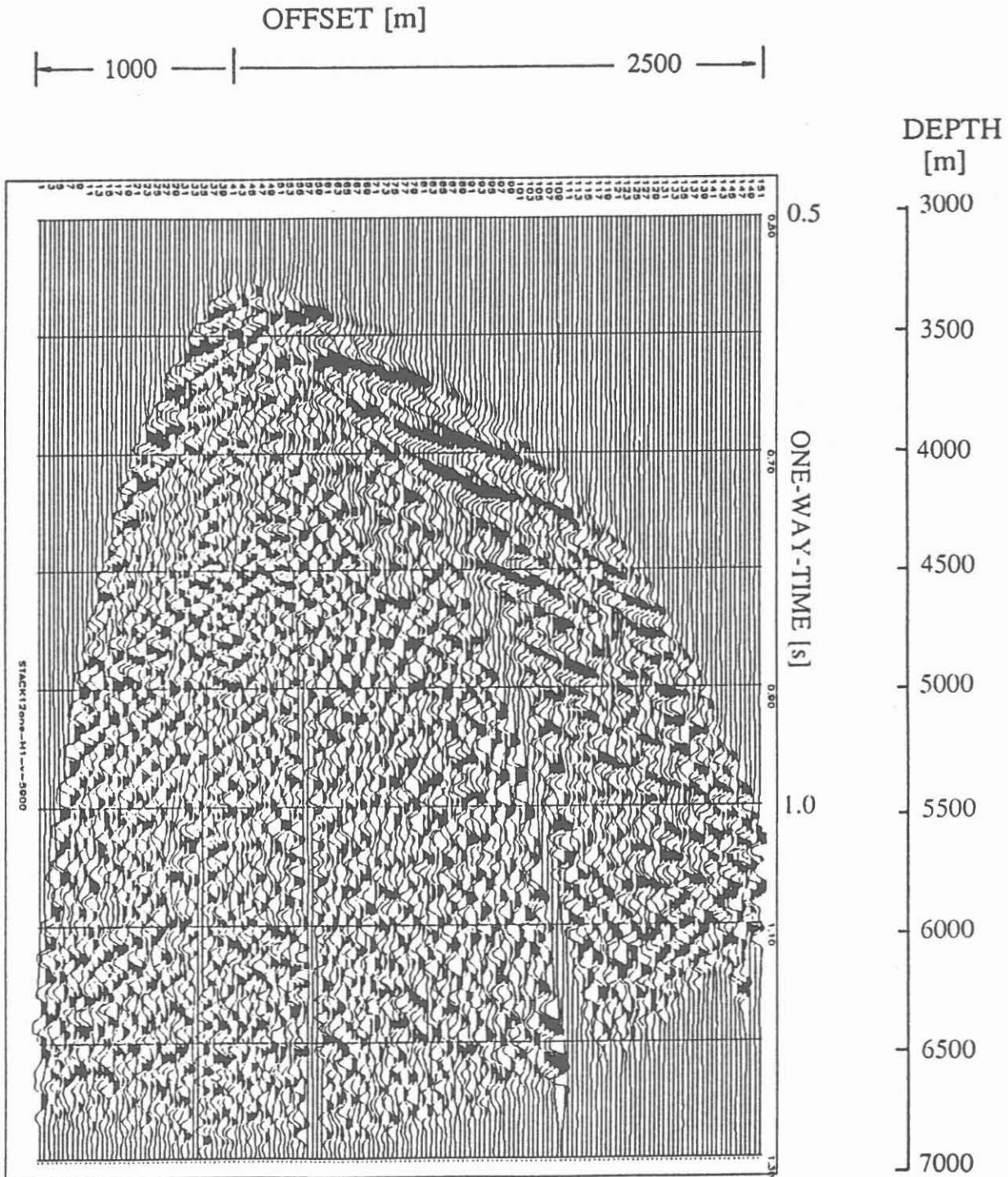


Fig. 11 Result of stacked CDP transformations.
(H1-Component).

CDP-TRANSFORMATION AND STACK

Z-COMPONENT 3210 M - 3435 M FOLD 10

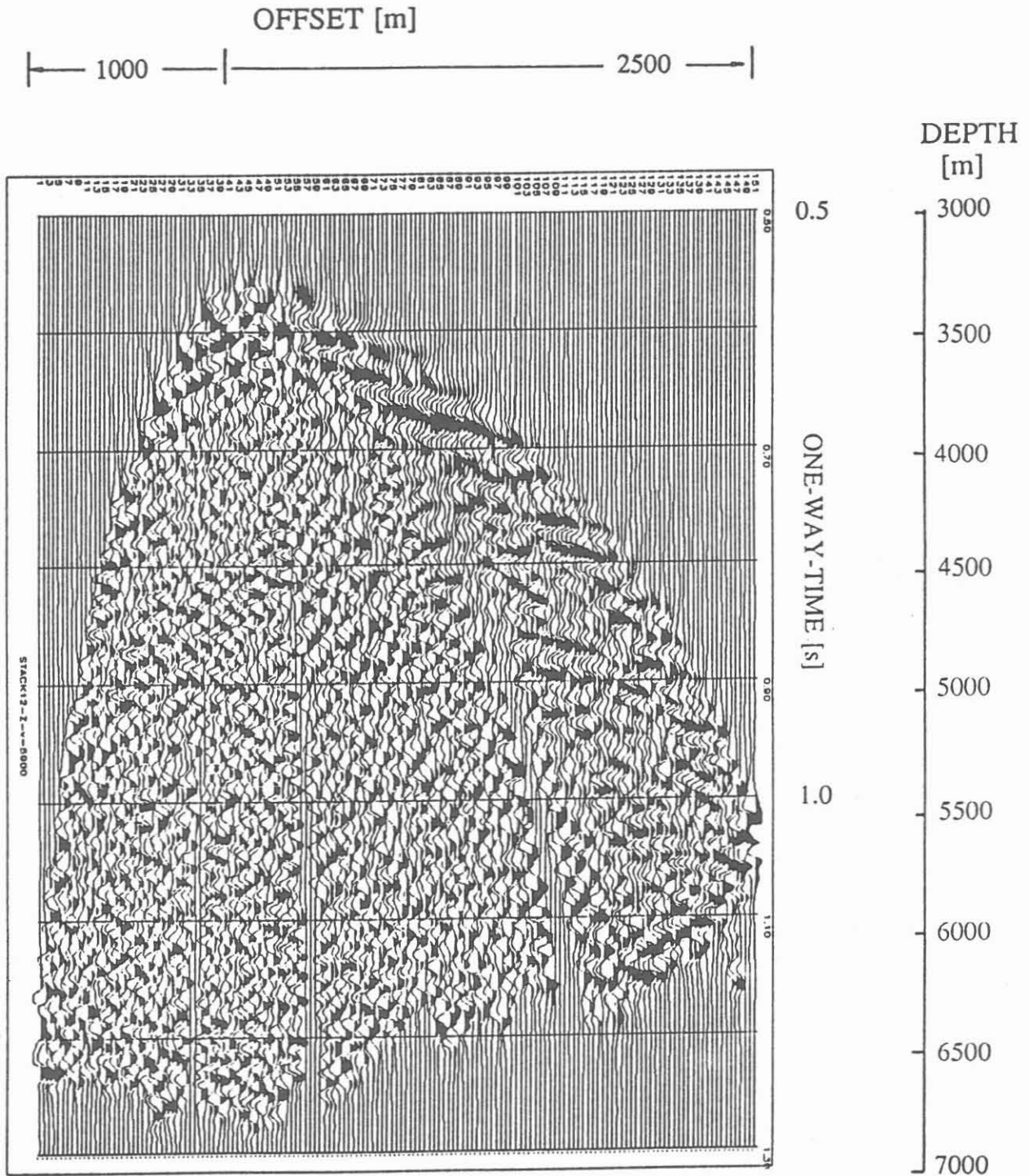


Fig. 10 Result of stacked CDP transformations.
(Z-Component).

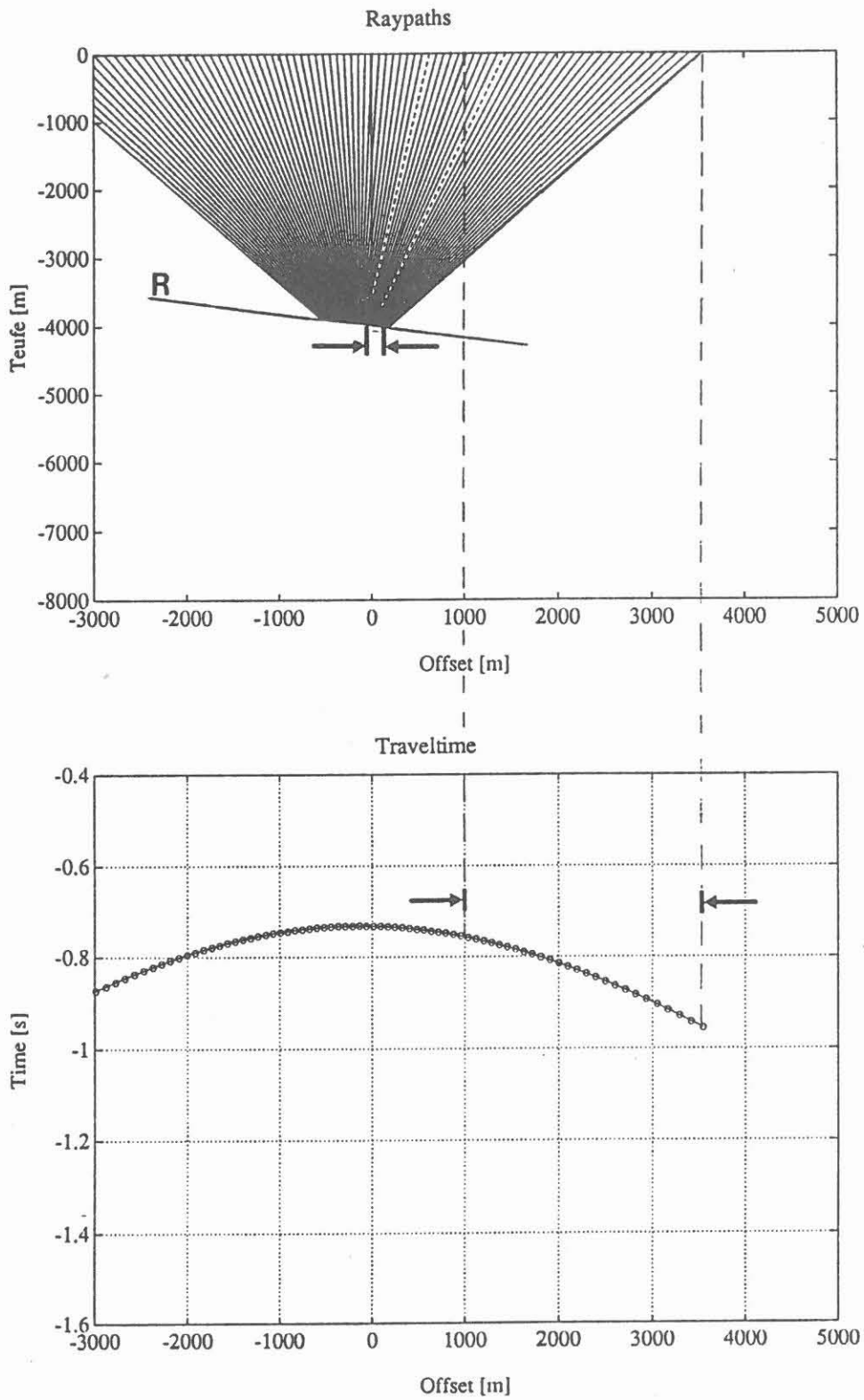
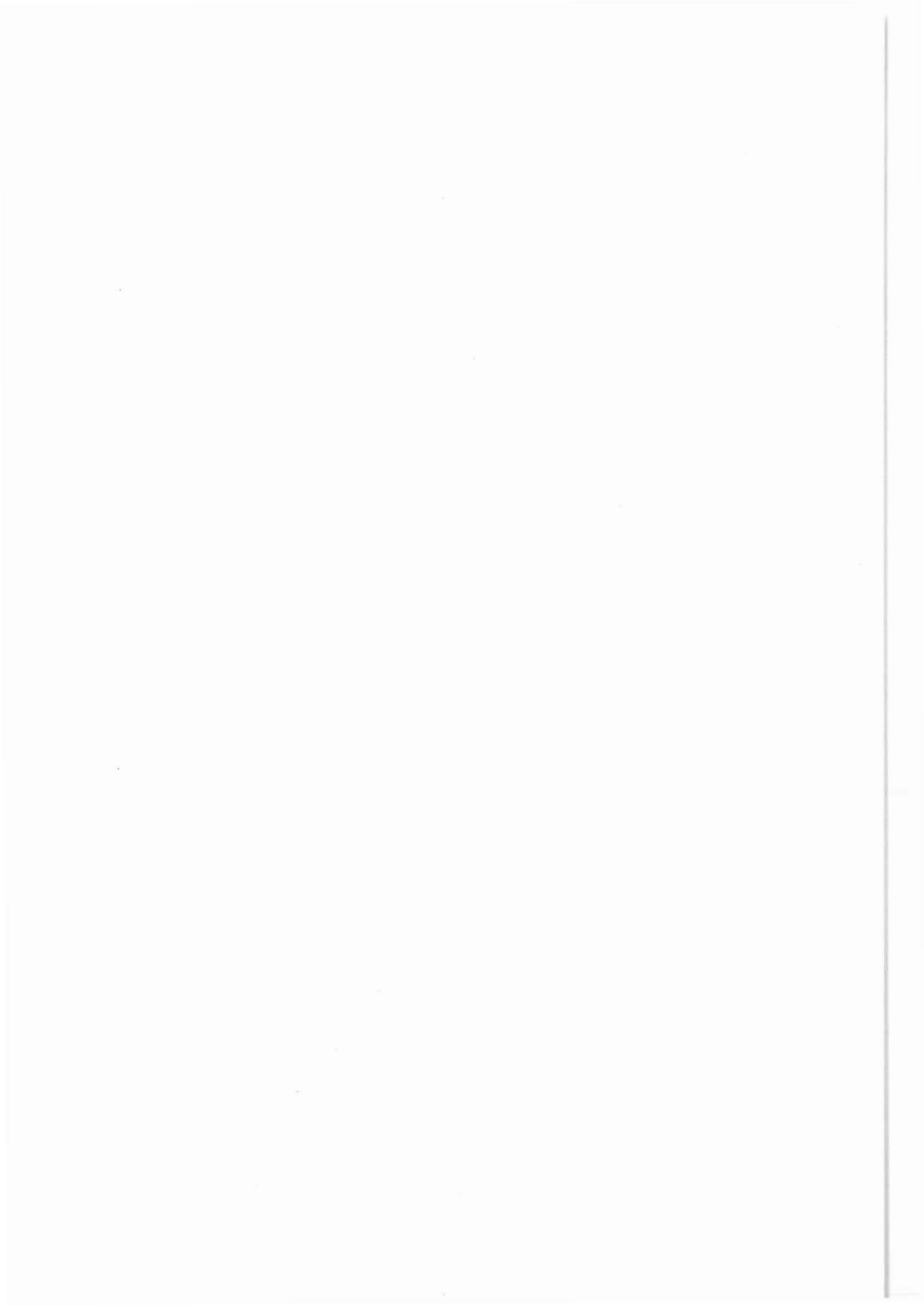
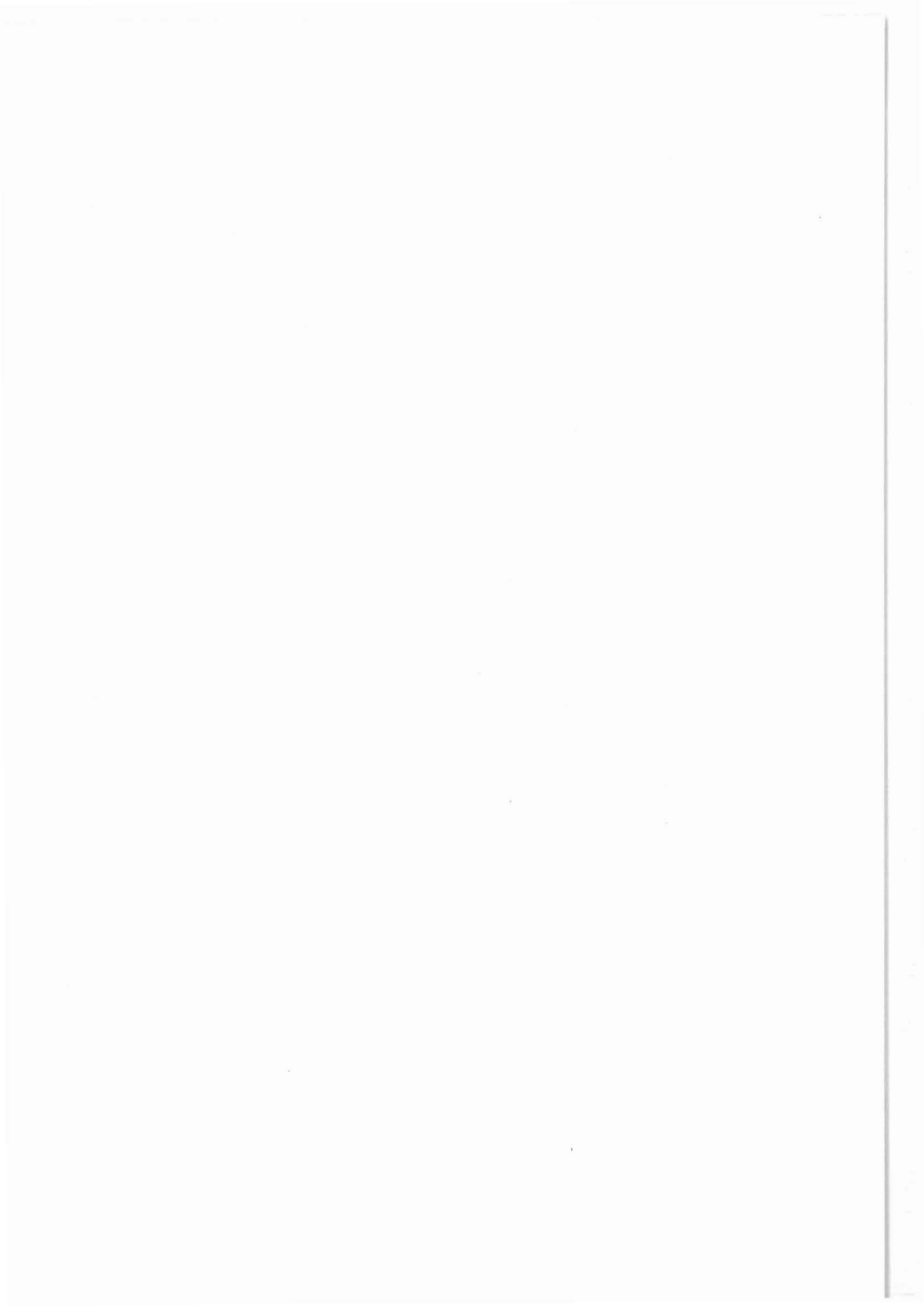


Fig. 12 Illumination of subsurface according to source offset.



Use of the Seismic Receiver Chain SEKAN 5
within the Framework of Integrated Seismics
in the Oberpfalz

J. Mylins
E. Nolte
U. Scharf



USE OF THE SEISMIC RECEIVER CHAIN SEKAN 5
WITHIN THE FRAMEWORK OF INTEGRATED SEISMICS
IN THE OBERPFALZ

Jörg Mylius*, Ernst Nolte*, Uwe Scharf*

S U M M A R Y

The tool chain SEKAN 5 developed and constructed by PRAKLA-SEISMOS was proved to be capable of withstanding long-term operation under the given pressure and temperature conditions in a chemically active Dehydrill HT mud in the KTB Oberpfalz VB 1A (350 bar, 110 °C, pH 10-11). The tool comprises five identical seismic receiver sondes which are equipped with a three-component receiver system, an electrically driven clamping unit and a magnetic compass system.

The results of the reference tests and the measured compass values were subjected to critical checks. For the observation period the reference tests on different days for each individual sonde indicated good agreement with respect to specific signal forms. The differences in orientation determined from the seismic data and the compass values are between -11 degrees and -26 degrees. The cause of the differences can be explained in that the wave paths lie outside of the observation plane.

1 INTRODUCTION

Within the framework of the DEKORP continental reflection seismic programme, PRAKLA-SEISMOS AG, Hannover carried out extensive seismic surveys from July to November 1989, centred on the pilot well of continental deep drilling project (KTB, Kontinentales Tiefbohrprogramm) in the Oberpfalz.

* PRAKLA-SEISMOS AG, Buchholzer Str. 100, 3000 Hannover 51

The survey comprised the following:

- a) 3D seismics over an area of 20 x 20 km (p-wave)
- b) 3D seismics in the wide angle range (p-wave)
- c) Expanding spread surveys (p-wave)
- d) Transmission measurements of mountainous area surrounding KTB pilot well
- e) Multiple offset VSP with p-waves and s-waves
- f) MSP for four tool chain positions (475 m covered area, p-wave)
- g) Two vibroseismic reflection lines in steep angle range connected with two MSP profiles (s-wave)
- h) Multi-azimuth shearwave experiment with p-wave and s-wave generation, the source points of which lie on concentric circles around the KTB pilot well, as well as two shearwave polarization experiments
- i) Short refraction surveys with p-waves and s-waves for static corrections

With the exception of the short refraction surveys all experiments were to be recorded in parallel with the SEKAN 5 chain during the entire survey period in the pilot well. The Tool chain could not be left in the well all the time because inspections and repairs had to be carried out.

The SEKAN 5 tool chain designed and constructed by PRAKLA-SEISMOS proved to be capable of withstanding the long time operation under existing pressure and temperature conditions in a chemically active dehydril HT drilling fluid in the KTB pilot well in the Oberpfalz (350 bar, 110 °C, pH value 10 to 11, HEROLD, 1989). Of course, application of the tool was not without its problems. According to our knowledge the SEKAN 5 is the only tool chain on the world market which is equipped with five receiver tools with three-component systems, mechanical clamping system and magnetic compass.

The long time operation demanded extremely durable materials and in fact led to the introduction of new materials and new technical solutions.

During the development of the tool chain PRAKLA-SEISMOS could refer to experience the company had made with an analog chain consisting of four receiver tools. From this experience a new concept was developed for a receiver chain based on the following requirements and conditions:

- use of the internationally accepted 7-core well cable
- digital transfer of the seismic data
- electronic circuits in just one tool (main tool) so as to enable the electronic components to be cooled effectively at greater depths and higher temperatures
- Application of sensors for magnetic, electric or radio-active detection of accurate depth determination
- Maximum tool diameter: 95 mm
- Maximum hydrostatic pressure: 1200 bar
- Maximum ambient temperature: 200 °C

Within the framework of a feasibility studie a maximum ambient temperature of 200 °C, which has to be expected at a depth of 6000 m, was presumed. At present available electronic components are not capable of functioning properly at this temperature and therefore require extensive cooling techniques which, however, in the course of the development works, proved to exceed the frame of the development project.

For this reason the tool chain was developed in two steps: Firstly for maximum temperatures of up to 125 °C and secondly for maximum temperatures of up to 160 °C. During the survey in the KTB pilot well the tool chain for temperatures of up to 125 °C was applied.

Finally an important practical aspect of the application of the tool chain should be noted. The tool chain can be installed in about one hour and can, depending on the drilling fluid, be lowered into the well at a half to a quarter of the speed of the individual tools (approx 25 m/min, 1000 m in 35 min). This means on the one hand application is restricted in VSP surveys with few survey points, but on the other MSP and VSP surveys with a lot of survey points and different source distances can be performed more economically and effectively, and additional possibilities can then be considered that previously had to be neglected owing to reasons of cost.

2 CONSTRUCTION AND COMPONENTS OF THE TOOL CHAIN

Figure 1 shows the schematic construction of the receiver chain. It consists of five similar seismic receiver tools which are equipped with a three-component receiver system, an electrically driven clamp arm and a magnetic compass system. The chain terminates at the top at the connection piece (main tool) and at the bottom at the pilot tool. The pilot tool has the job of monitoring the free run-in of the chain and serves as the carrier of the electric, magnetic or radioactive sensors. Just small changes of the load on a cable load sensor in the main tool indicate whether the pilot or receiver tool is beginning to set down and so enable complete setting down to be avoided.

The electric or magnetic sensors in the pilot tool serve the depth control.

The transfer or main tool contains the electronic circuits with which the analog seismic signals are converted into specific pulse code signals for the transfer via the well cable. It is not the state of the binary signal but rather the time interval between changes of state that are transferred. For this reason the control electronics are housed here in order to switch the receiver tools to the various functions - drive clamp arm, survey, read compass, transfer pilot tool.

The maximum diameter of the tools amounts to 88 mm; considering the effective length of the clamp arm, the borehole diameter should be 100 to 330 mm.

In the following the construction and the functions of an individual tool are described (see Fig 2).

The receiver tools of the chain are connected mechanically and electrically to one another by separate low torsion steel cable and multi-core cables.

Above every receiver tool, surrounded by a protective housing, is a pressure and watertight push-on connection incorporated in the main cable that forms the electrical connection to the receiver tool. The multi-core main cable runs to the main tool along the side of the secondary tools and is protected by a w-shaped section. The five seismic receiver tools are equipped with a three-component system comprising six oscillation-coil velocity receivers of type SENSOR SM4/UHT10 Hz natural frequency which are connected in series. To enable data control and effective data processing it is essential that all geophones that are

connected to the five receiver tools are almost identical with respect to their physical parameters. Particularly critical parameters are natural frequency, sensitivity and distortion. Figure 3 shows the natural frequency of 29 vertical and 48 horizontal receivers of the above described construction at 20 °C and 200 °C. The tolerance limit of 0.5 Hz at a resonant frequency of 10 Hz is exceeded by 0.1 Hz by two of the vertical receivers. The decrease of the medium resonant frequency at the vertical receivers is conspicuous and can be explained in a change of material characteristics of the springs which the coils are suspended from.

The sensitivity ($24.4 \pm 5\%$) lies within the tolerance limits; the above-mentioned applies to the decreased sensitivity of the vertical receivers.

The distortion shows that the vertical geophones are dependent on temperature to a greater extent than the horizontal geophones are. The maximum value is 0.2%.

The clamping arm reaches a maximum value of 750 N when clamping the tools and has a safety ratchet device which is released when the well cable is pulled.

Each receiver tool is equipped with a magnetic compass system in order to determine the tool orientation. The compass is to be explained more detailed, as the measured compass values are of particular significance. The compass needle is equipped with a mirror, being sampled by a circulating, well-focused beam. If the beam of the sampling device strikes the mirror the light is reflected into a photo diode which releases a voltage impulse. The time of these impulses referred to the circulation time gives the tool orientation.

Prior to running in the hole the technical deviation of the compasses of the individual tools are determined in the following way. Each receiver tool is freely suspended from a tripod made of non-magnetic material and screwed into a device at the bottom end which allows the tool to be precisely directed towards north; subsequently it is turned 360 degrees in steps of 15 degrees from north via east. After each step the compass reading is taken via the well cable and the tool control unit and the deviation from the given value determined.

Figure 4 shows the deviations of the compass of tool 5 on different days and in different places; at KTB (30.07. to 28.10.1989), at PRAKLA-SEISMOS, in Hannover (28.11.1989).

The x-axis depicts the required angle and the y-axis the deviation, the angle read from the tool compass minus the required angle. The maximum deviation for this compass amounts to +\ -20 degrees, if the deviation measurement of 30.07.1989 is ignored.

The deviation of the magnetic compass is caused by magnetic interference fields, which overlap the terrestrial magnetic field. They are due to various causes which are not to be discussed here.

In order to reduce interfering survey influences the average value of the deviation curves is taken, and the values read from the tool compasses are corrected by the average deviation value of each tool compass.

The compass values obtained in the well are to be discussed in chapter 4, Results.

3 EXPERIENCE

The operation periods of the tool chain and the dates of the deviation tests are listed in Table 1. The tool chain was in continuous operation for a maximum of 17 days at different depths and changing temperatures, thus proving its capability.

Main reasons for interruptions in the operation was a considerable wear of cables and push-on connections. After the first long time operation from 14.07. to 21.07.1989 (depth 3690 m, temperature 110 °C, pressure 370 bar) damages at tool connection cables, cable connections and the cable below tool 1 were discovered.

Elastomer-coated tool cables and push-on connections proved to be not suited for the purpose. The elastomer coat was partly swollen and showed holes and cracks which reached as far as the copper cores; polyurethane parts were almost completely decomposed. After termination of the first VSP survey the tool chain was equipped with new VITON-cables (special flourine caoutchouc) which show high chemical resistance and therefore are well-suited for the drilling fluid conditions of the KTB pilot well. Several technical changes have been carried out of which only one is important for compass measurements and should therefore be mentioned here. Owing to the tool construction the installed compasses were assumed to be subjected to deviation by the geophone magnets. For this reason geophone pairs, each with a different magnetic polarity, were installed for each single component. However, the deviation is still considerable and effective ways to avoid it have not been found yet.

The coupling of the individual tools at the measured depths was carried out without problems most of the time, as it can be realized in boreholes with a maximum diameter of 330 mm (13"). Although in depth ranges of about 1027 m and 1630 m there were narrow zones (approx 0.5 m) of > 330 mm according to a caliper, no coupling problems occurred.

Owing to the special conditions related to tool chain operations appropriate ways for obtaining control of all tool chain components over a longer period of time had to be found. During the survey with a tool chain or individual tool at the beginning of each survey day reference tests were carried out. For this purpose a p-wave or s-wave vibrator located at a fixed position about 150 m east of the pilot well was used for generating energy. Two to four reference shots were fired daily; the data form part of the respective experiments. The data were recorded with a GEOMETRICS ES 2420, correlated on the MicroMax on site with the software from ADVANCE and presented for control purposes.

3 RESULTS

The numerous experiments MASE, SCMP, VSP, MSP, 3D seismics, 3D expanding spread etc were recorded by the receiver chain or in case of break down via the individual tool. The results are not presented here.

In the following the results of the reference tests are presented. The measured compass values were subjected to critical checks.

Figure 5 shows reference generating during the period from 03.01. to 07.10.89 at depths of 3310 and 3435 m. (The depths refer to the lowest tool position.) The correlated seismic traces are sorted according to depth, receivers and components to enable observing the data quality at each tool in course of the time. The normalization of the seismic traces was effected on the amplitude maxima of the single traces in a delay time range of 0.5 s to 1.2 s. Looking at a depth of 3310 m and the vertical receivers of tools 1 to 5 the reference records from 04.10. to 07.10.89 are presented in left to right direction. During this time a shearwave vibrator was used for generating energy. In delay time ranges from 0.5 s to 0.7 s and from 0.9 s to 1.1 s the signals of the direct p-wave and direct s-wave respectively can be recognized. Comparing the signal forms and investigating the noise signals it becomes clear that the signals of direct p-waves and direct s-waves from generations on different days are to a great extent identical for each individual tool. Only tool 5 shows a higher noise level, the reason for which could not be found.

In conclusion a few remarks to the measured compass values: The compass values determined in the well have been corrected using the averaged deviation of every tool. The quality of the measured compass values can be checked by means of the seismic records, the reference tests or the results of the MSP surveys. Assuming the existence of a homogeneous, isotropic half-space and the absence of noise, the tool orientation, determined from the seismic data of the MSP survey, must be the same for all source points or show a phase difference of 180 °C for source points on this side and source points on the other side of the well.

The investigated MSP profile has 198 source points and the tool chain was kept at a constant depth of 3310 m.

The technique for determining the tools orientation from seismic data will not be entered into in more detail, however, it must be noted that the arrivals of the direct p-wave were used for calculation and that previously a filtering in the frequency range of the sweep (12 to 80 Hz) was applied.

Of course the assumptions are not fulfilled, however, knowing that the source points at the surface were on average 50 m apart it can be expected that the wave paths of adjacent points do not differ substantially from one another.

Figure 6 shows the result of the calculation of the tool orientation for the receiver tool 2 at a depth of 3285 m. The x-axis shows the vibrator points at equal intervals and the y-axis the determined angle. From VP (vibrator point) 101 to 253 or 254 to 298 the average amounts to -110 degrees (250) or 49 degrees respectively and the mean divergence is 7 degrees or 9 degrees respectively.

The phase shift from -110 degrees to 49 degrees becomes evident by the change in direction of the incidence of the signals. Theoretically the phase should be 180 degrees, however, it cannot be observed at any of the receiver tools; it varies between 158 and 223 degrees.

Depending on the incidence of the signals, two angles are obtained with a theoretical difference of 180 degrees. Considering the angles from VP 101 to 253 and VP 254 to 298, and supplementing the angles from VP 101 to 253 by 180 degrees the following result is obtained:

TABLE 2: Comparing the results of the orientation determination
(angle in degrees)

Tool	Depth (m)	Direction of the horizontal comp. H1 acc. to compass	Direction of the horizontal comp. H1 determined from seismic data		Differences	
			H1K	VP101-253	VP254-298	H1k-VP101
5	3210	119	155	145	-36	-26
4	3235	335	376	358	-41	-23
3	3260	256	310	267	-54	-11
2	3285	28	70	49	-42	-21
1	3310	242	285	256	-43	-14

The differences show the deviation in direction determined from seismic data on the one side and from compass data on the other.

The maximum difference amounts to -26 degrees, the minimum is -11 degrees. That means that there is general agreement in the calculated directions, however, the individual values are associated with errors of varying orders. The cause of the differences can be explained in that the wave paths lie outside of the observation plane.

5 BIBLIOGRAPHY

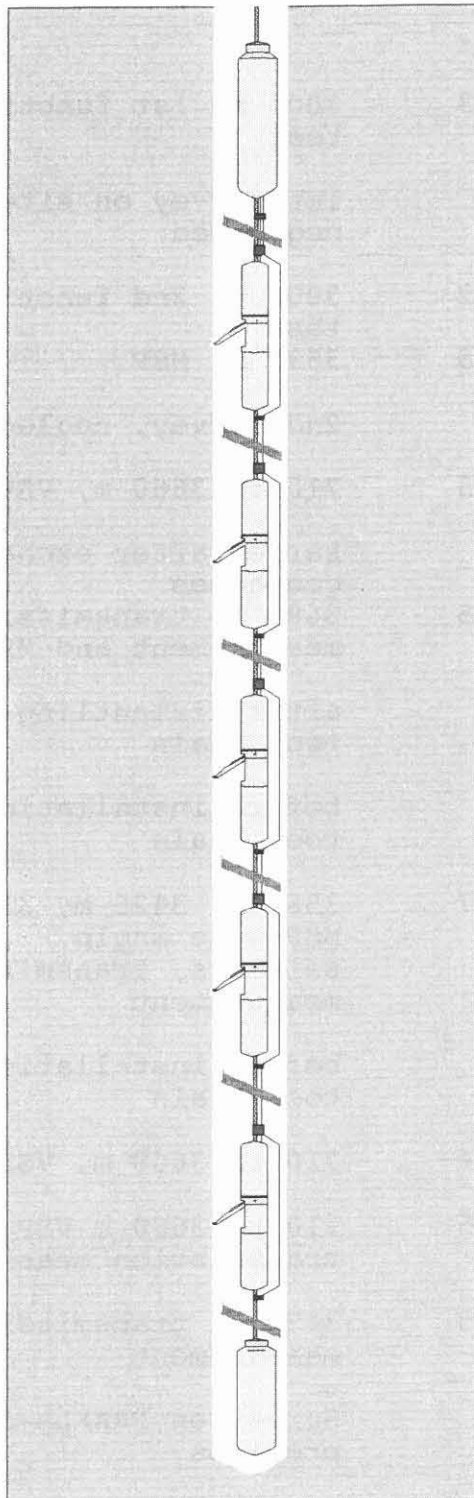
- 1 BURKHARDT, M, and others
Das Vorhergesagte und das gemessene Temperaturprofil
KTB-Report 89-3, page 216-242, 1989
- 2 HAGEDOORN, A L, and others
A practical set of guidelines for geophone element
testing and evaluation
1988, First Break vol 6, no 10, Oct, page 325-331
- 3 HEROLD, and others
Kontinentales Tiefbohrprogramm in der Bundesrepublik
Deutschland KTB-Spülungsdaten 0 to 3888.5 m
KTB-Report 89-3, page 245, 1989
- 4 LIPPMANN, E, and others
Gesteinsphysik im KTB-Feldlabor: Messungen und Ergebnisse
KTB-Report 89-3, page 120-129, 1989

TABLE 1

Dates of deviation tests	Survey time	Number of days	Remarks
	07.06.-09.06.	3	3000 m, 1st functions test
11.07.			1st survey on site, neglected
	12.07.-21.07.	2	3000 m, 2nd functions test
	14.07.-21.07.	8	3690 m, MSP
30.07.			2nd survey, neglected
	01.08.-03.08.	3	710 to 3660 m, VSP
31.08			survey after exchanging geophones
	31.08.-14.09.	15	3685 m, transmission measurement and MSP
14.09.			after dismantling of tool chain
01.10.			before installation of tool chain
	01.10.-17.10.	17	3560 m, 3425 m, 3310 m, MSP wide angle seismics, transmission measurement
28.10.			before installation of tool chain
	28.10.-31.10.	4	710 to 3660 m, VSP
	02.11.-06.11.	5	710 to 3660 m VSP, transmission measurement
	09.11.-21.11.	13	3420 m, transmission measurement
28.11.			Survey on PRAKLA-SEISMOS premises

The values refer to the depth of the lowest tool postions.
(Tool 1, tool interval 25 m.)

Diagramm of Seismic Receiver Chain for Deep Wells SEKAN 5



CABLE HEAD

TRANSFER TOOL
with A/D converter
and tension indicator

5th RECEIVER
TOOL

4th RECEIVER
TOOL

3rd RECEIVER
TOOL

2nd RECEIVER
TOOL

1st RECEIVER
TOOL

PILOT TOOL



Abb. 1

Schematic Presentation of Seismic Receiver Sonde BGCA with Carrier Cable and Electrical Cable Connected

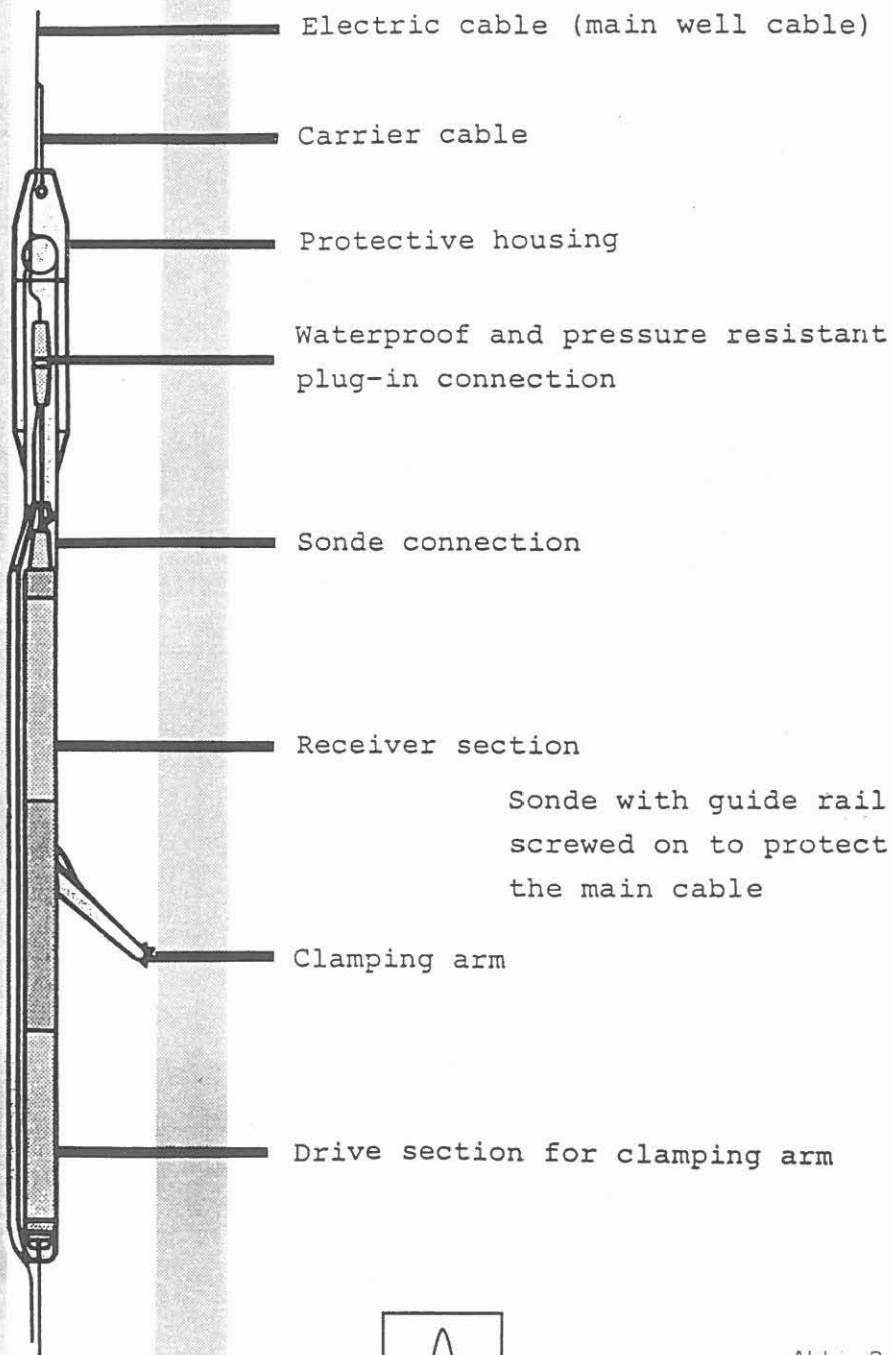
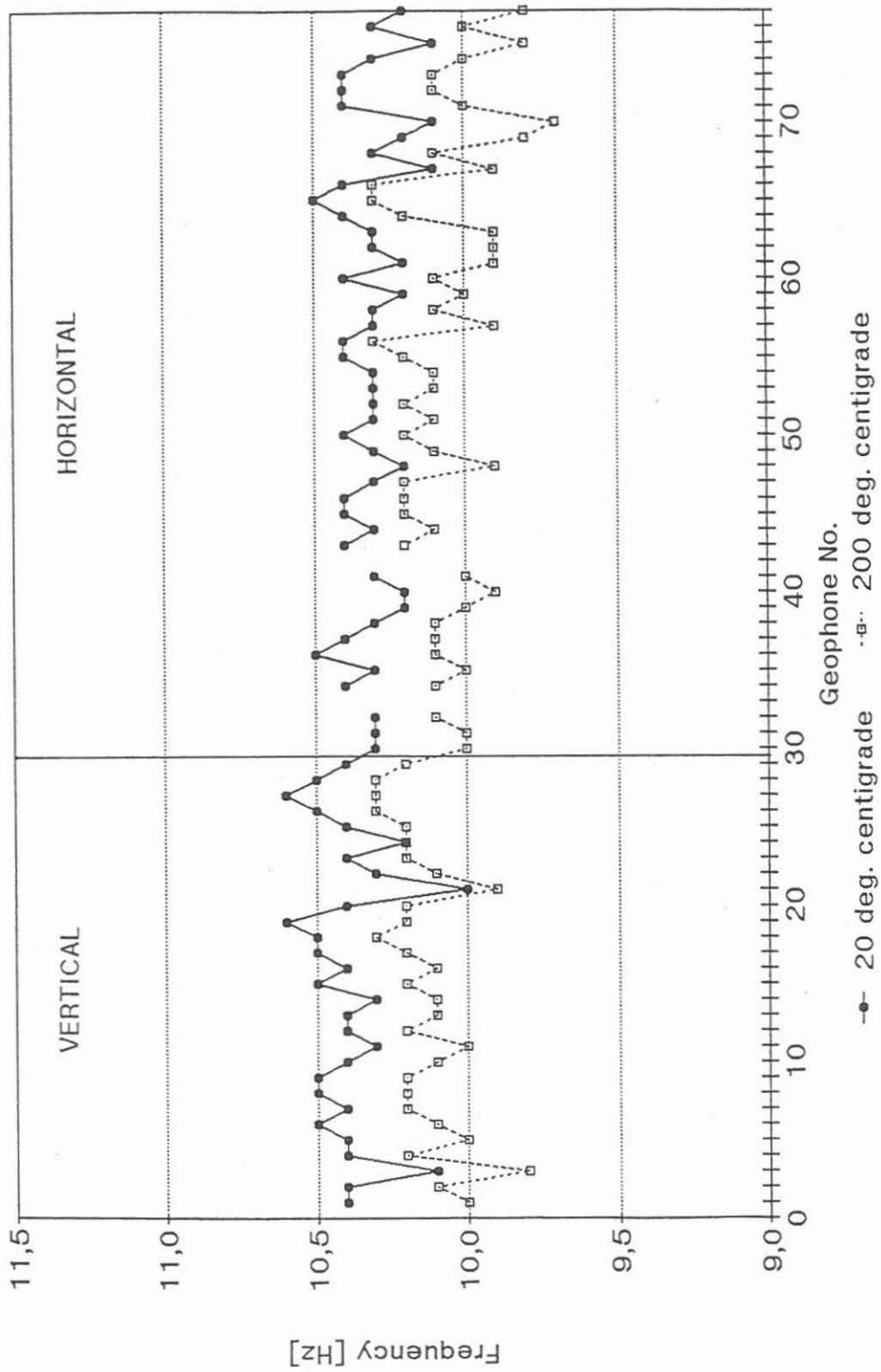


Abb. 2

GEPHONES SM4/10Hz HT
NATURAL FREQUENCY



PRAKLA-SEISMOS AG

Abb. 3

Deviation Sonde 5

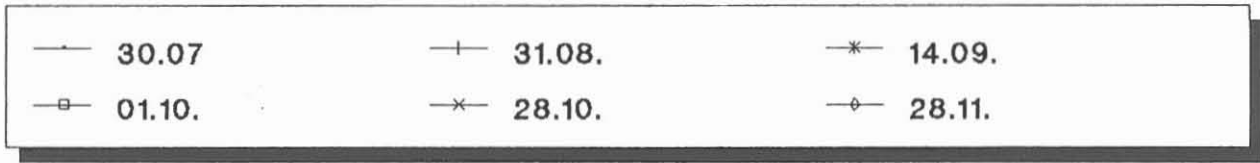
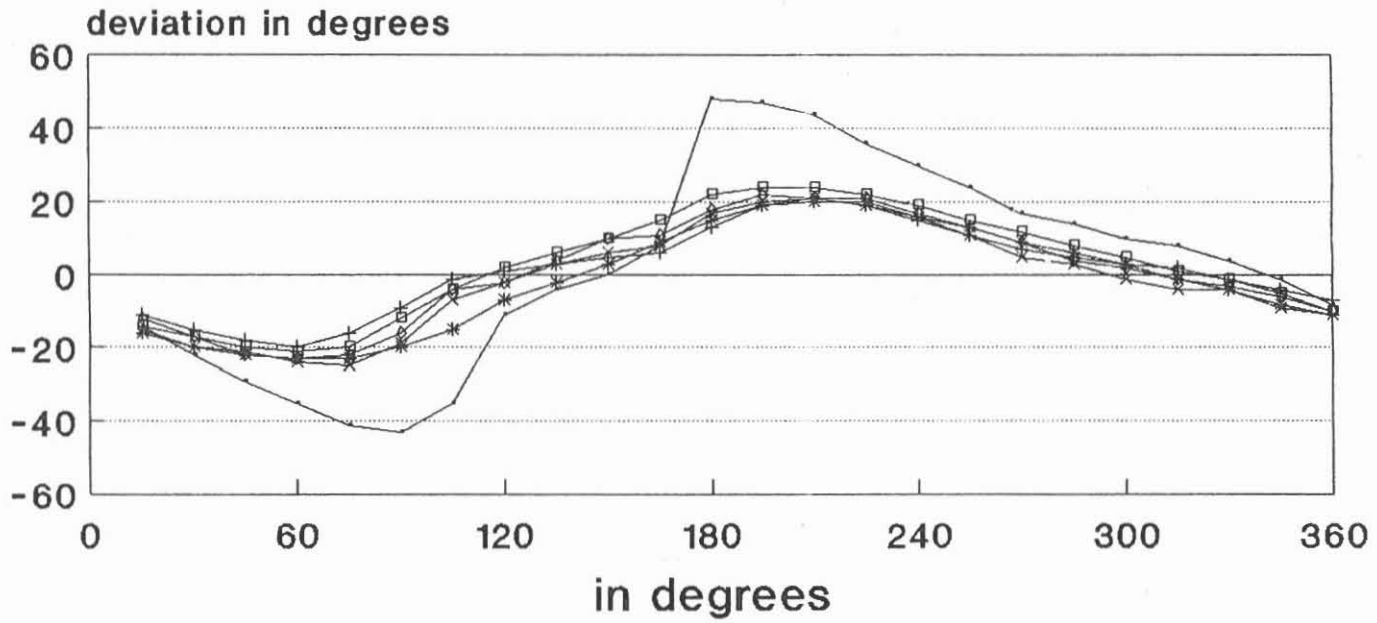
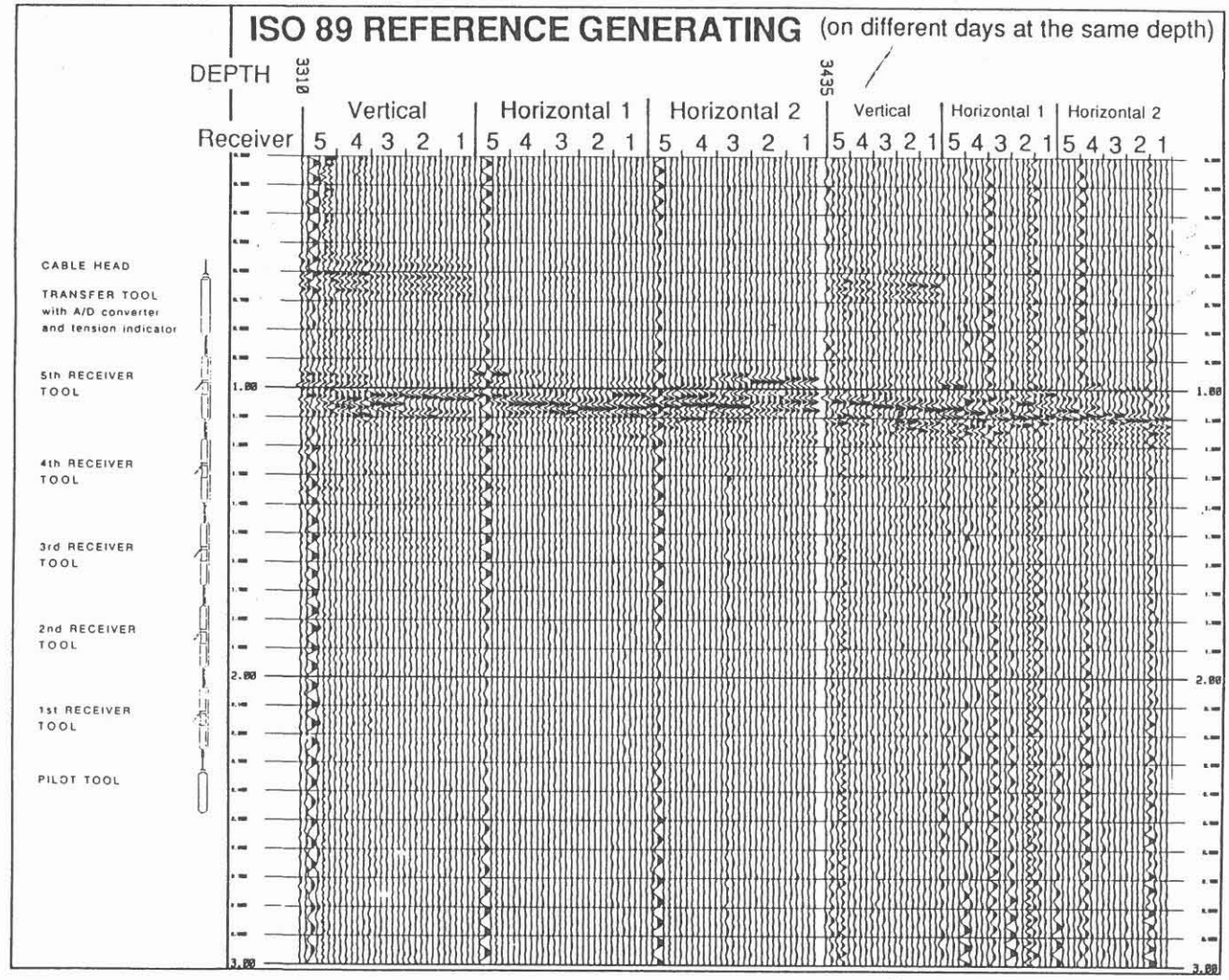


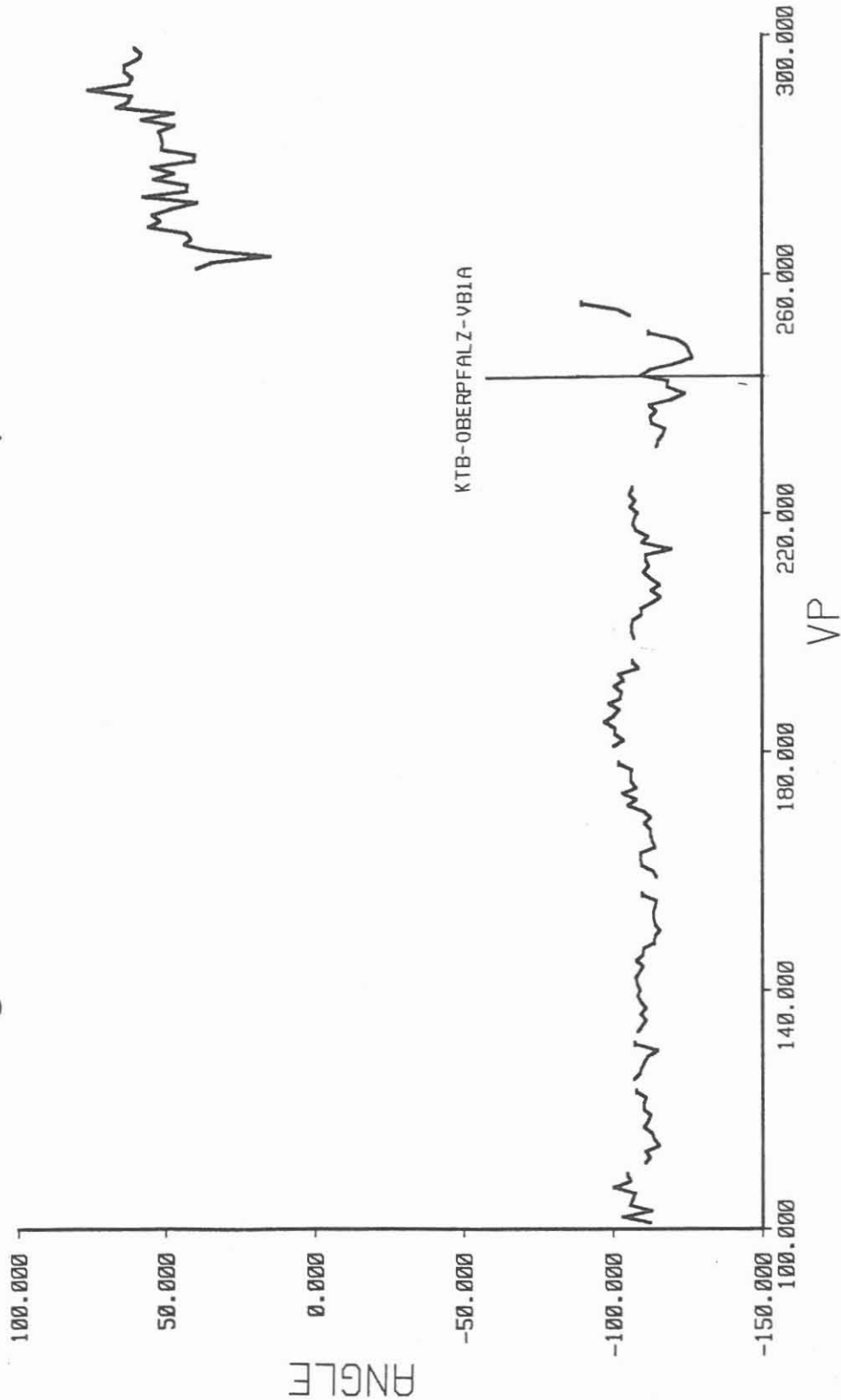


Abb. 5



ISO 89, MSP 3310, Satellite 2

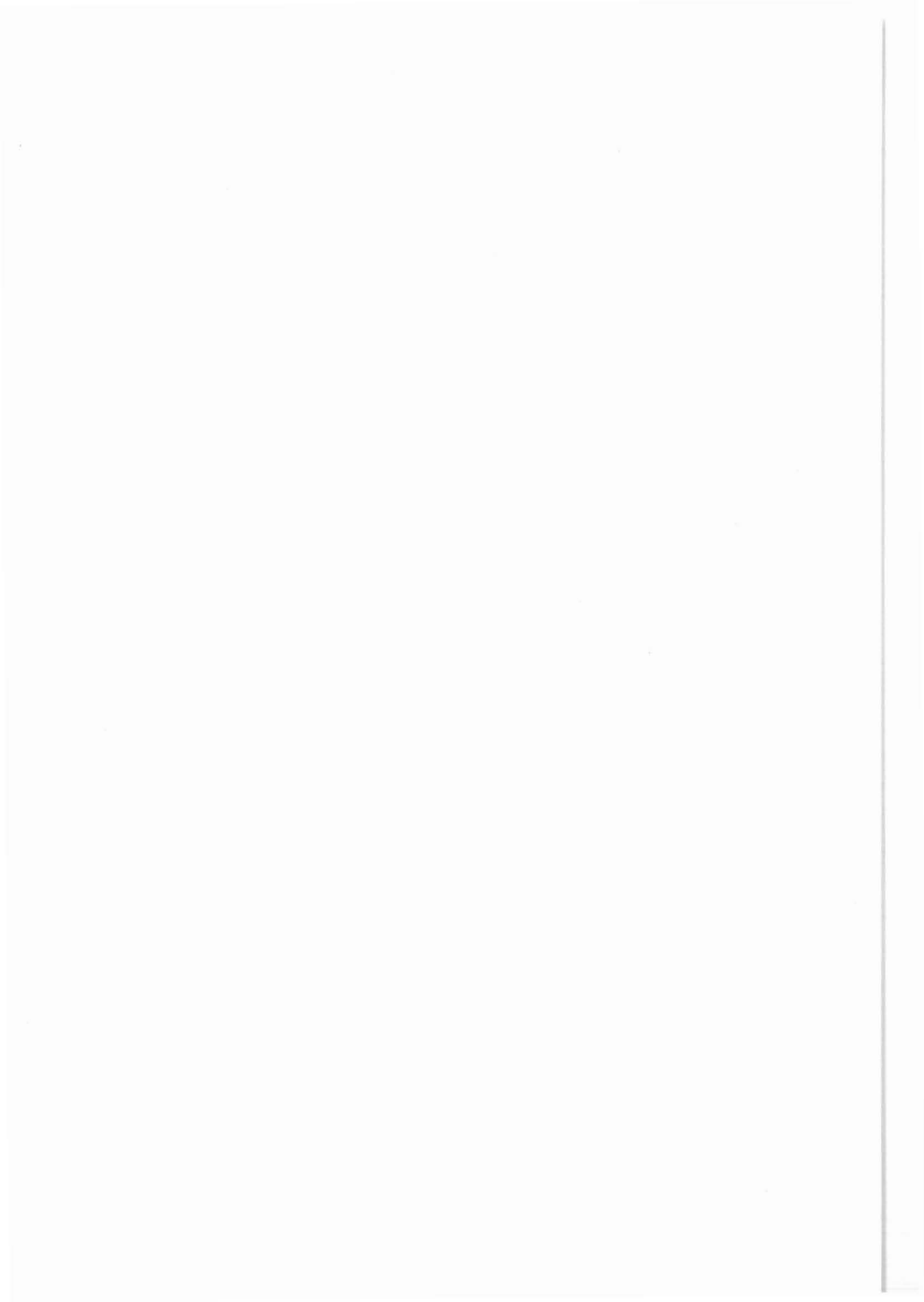
Rotation angle determined from direct p-waves



ANGLE

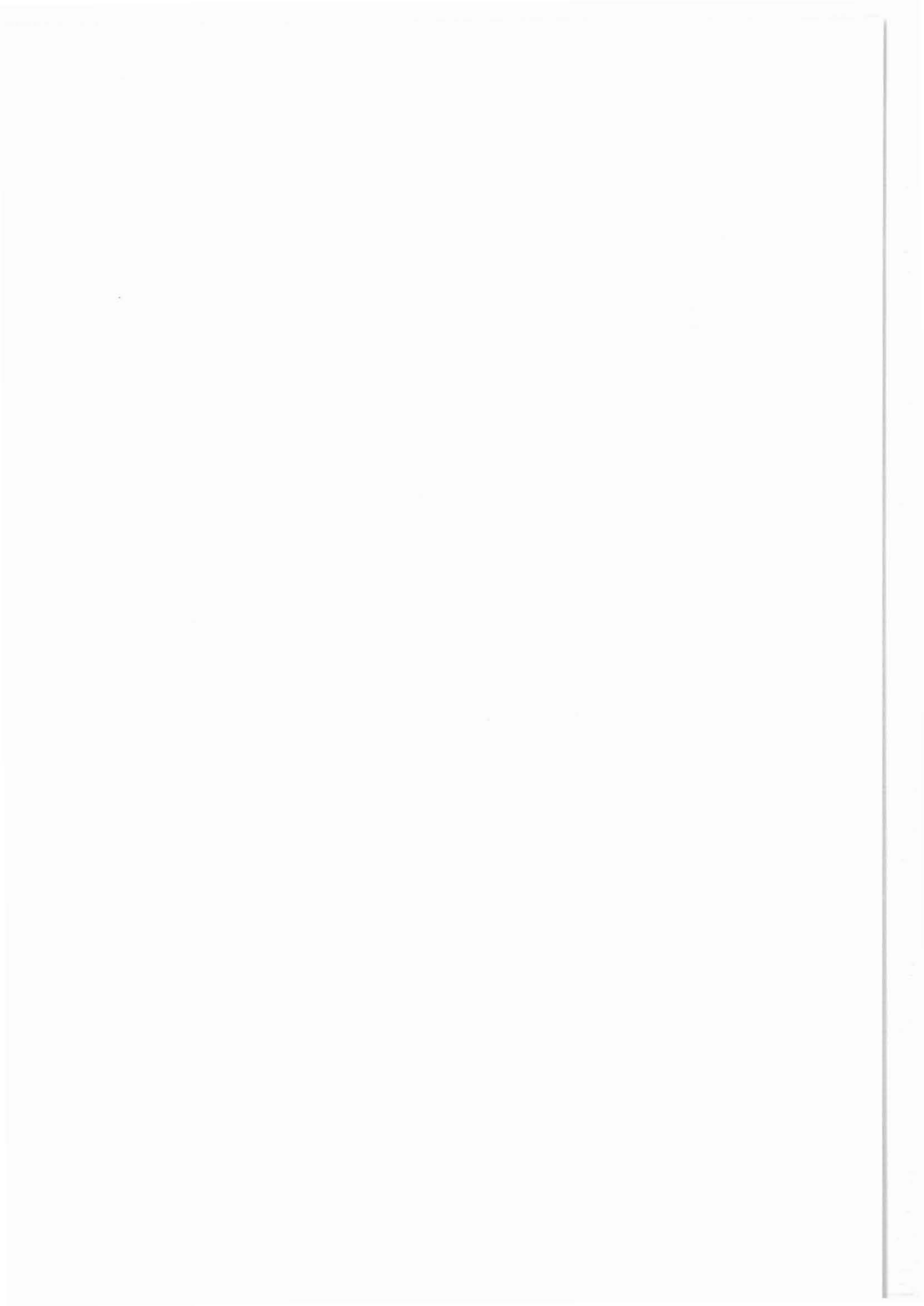


Abb. 6



3-D Wide-Angle Investigations in the
KTB Surroundings as Part of the
"Integrated Seismics Oberpfalz 1989 (ISO 89)"

H. Gebrande
M. Bopp
M. Meichelböck
P. Neurieder



3-D WIDE-ANGLE INVESTIGATIONS IN THE KTB SURROUNDINGS AS PART
OF THE "INTEGRATED SEISMICS OBERPFALZ 1989 (ISO89)"

H. Gebrande, M. Bopp, M. Meichelböck u. P. Neurieder *)

SUMMARY

The high reflectivity of the upper and middle crust of the Oberpfalz, both for near vertical and wide-angle reflections, was one reason for selecting this area as site for the German Continental Deep Drilling Program KTB.

A peculiarity in the middle crust beneath the KTB site is the so-called Erbendorf-Body (EB) giving rise to extremely strong wide-angle reflections. It deserves special interest because its position right on the border between the Saxothuringian and Moldanubian zones of the Variscan fold belt, the unusual high p-wave velocities (over 7.0 km/s) in its lower part at 11 to 14 km depth, and associated dipping reflectors suggest a possible lower crustal origin of the EB. A specially designed and so far unique wide-angle 3D-survey was carried out as part of the program "Integrated Seismics Oberpfalz 89" for investigating the spatial extent, the velocity distribution and the internal structure of the EB. The first results show clearly that the EB is not a local phenomenon beneath the DEKORP4 line, but that it exists, yet with remarkable complexities, beneath the whole covered area between the Franconian Line and the Falkenberg granite complex.

The wide-angle shots were also recorded by four 3-component geophones in the KTB pilot hole at 3195 to 3295 m depth and provided convincing evidence for s-wave splitting in the upper crust SE of the KTB location. This anisotropy effect seems to be related to the overall strike and dip of rock foliation in the zone of Erbendorf-Vohenstrauß (ZEV).

1. INTRODUCTION

It is one of the major goals of the Continental Deep Drilling Program KTB to contribute to a better understanding of the nature of seismic reflectors in the subsedimentary continental crust. The high reflectivity of the upper and middle crust at the KTB site, both in the vertical incidence as well as in the wide-angle domain (DEKORP Research Group, 1988), offers promising pre-conditions for this objective. The present report deals mainly with aspects of wide-angle reflectivity, seismic wave velocities and some fundamental observations of seismic anisotropy in the KTB surroundings.

*)Authors' address: Institut f. Allg. u. Angew. Geophysik,
Theresienstr. 41/IV,
D-8000 München 2, FRG

Except for some more general information on crustal structure of the Oberpfalz derived from large-scale seismic refraction measurements in the 1960's and early 1970's (Giese 1968, 1976; Peters 1974) most knowledge available before ISO89 originated from KTB pre-site surveys (DEKORP Research Group 1988, Gebrande et al. 1989, Schmoll et al. 1989). The most outstanding feature in the wide-angle domain is the so-called Erbendorf-body (EB), a high-velocity body at 11 to 14 km depth producing extremely strong reflections in the 40 to 60 km distance range. Detailed informations on its p-wave velocities, shape and NW-SE extent were provided by a systematic, multiply covered wide-angle survey along the DEKORP4 line in 1985.

The latest result of this survey is a wide-angle image of the Earth's crust in a NW-SE section through the KTB site (Fig. 1). It was obtained by application of the 2D isochrone-migration process on wide-angle data from the 41 to 90 km offset range (Schmidt 1990). 95 shot recordings of the contractor's 200 channel spread operated from 41 to 58 km offset and of 24 3-channel MARS stations operated by universities at 60 to 90 km offset were jointly and consistently processed to provide Fig. 1. In many respects (Moho, lower crust, SE dipping reflectors) the picture is conformable to the steep-angle migration result (Schmoll et al. 1989). In spite of the general weaker structural resolving power of wide-angle reflections, some special structures are imaged even more accentuated due to their incidence dependent reflection coefficients. This is true, e.g., for the EB, which is the conspicuous wedge-shaped body at 3.5 to 5 s two-way time (TWT) beneath the KTB site (Fig. 1). Different methods of velocity analysis and model calculations have consistently revealed p-wave velocities up to or even over 7.0 km/s in the lower part of the EB (DEKORP Research Group 1988, Gebrande et al. 1989).

These unusual properties of the EB, together with its likewise pronounced steep-angle reflectivity, have given rise to several speculations on its lithological composition and its geodynamic significance, which shall not be discussed here; in general the EB is expected to be a two-dimensional SW-NE striking structure marking the Saxothuringian/Moldanubian suture at depth (Franke 1989). On the other side, there are many indications, e.g., from older refraction lines (Gebrande et al. 1989) and from the KTB reflection lines (DEKORP Research Group 1988), that lateral heterogeneities perpendicular to the DEKORP4 line may be of similar importance like in-line heterogeneities. In principle it could even not be ruled out, from the solely one-dimensional measurements along DEKORP4, that the observed strong wide-angle reflection amplitudes of the EB may be partly due to focusing by off-line structures, and that the wide-angle image of Fig.1 may contain significant side effects.

Therefore, a consequent 3D wide-angle survey was planned and realized as part of the program "Integrated Seismics Oberpfalz 1989" devoted to a comprehensive seismic investigation of the KTB surroundings.

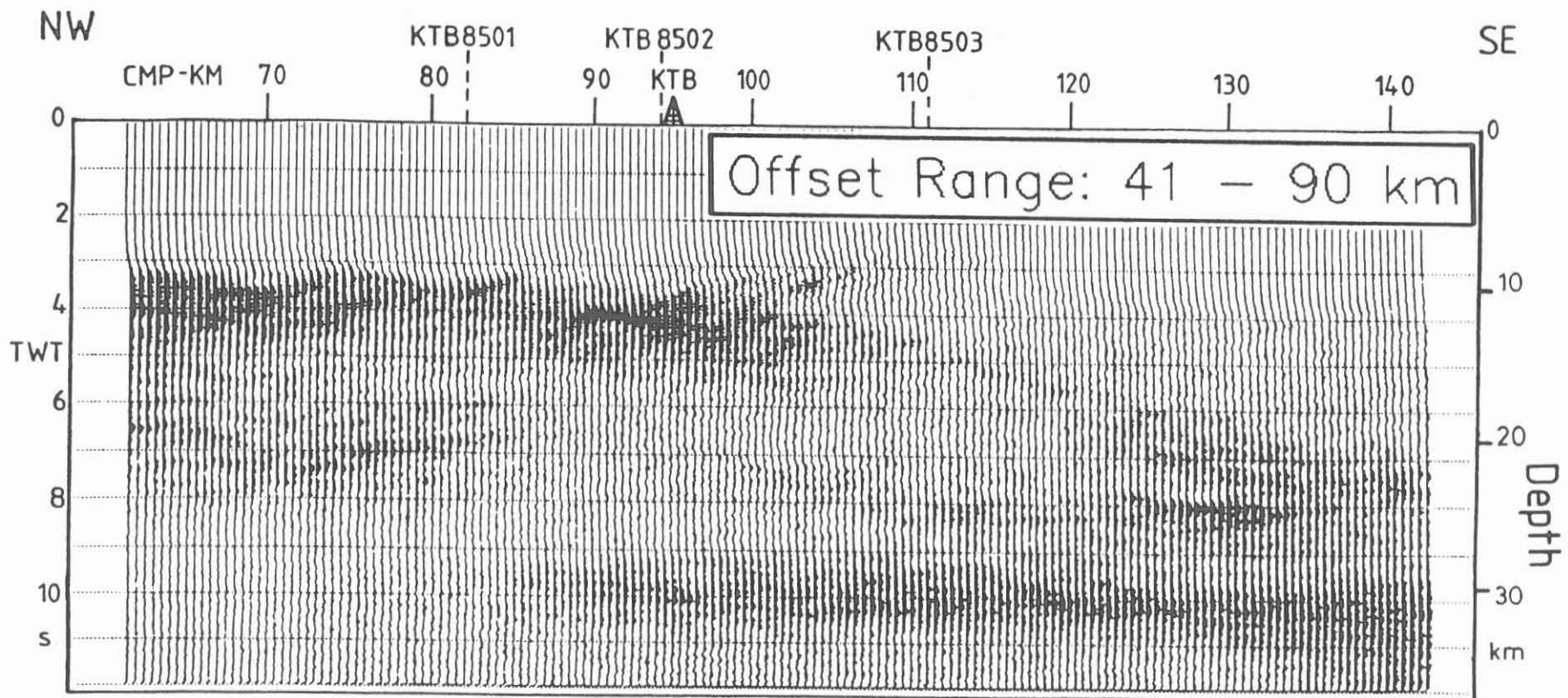


Fig. 1: Seismic image of the earth crust along a NW/SE-section through the KTB site obtained by 2D isochrone-migration of DEKORP4 wide-angle data from the 41 to 90 km offset range (after SCHMIDT, 1990). The Erbenndorf-body appears as a wedge-shaped structure in the middle crust beneath the KTB location.

2. LAYOUT AND REALIZATION OF THE WIDE-ANGLE 3D-SURVEY

The basic principle of the realized 3D wide-angle survey is shown in Fig.2. The scheme consists of a linear sequence of 20 shot-points with one km spacing and a transversely oriented receiver spread. It provides single coverage in a rectangle midway between shots and receivers, the edges of which are half as long as the shot and receiver spreads, respectively. It is advisable to choose the mean shot-to-receiver offset equal to the critical distance of the reflector to be mapped, which is about 40 km for the Erbandorf body. A supplementary in-line receiver spread has been added for improved velocity resolution.

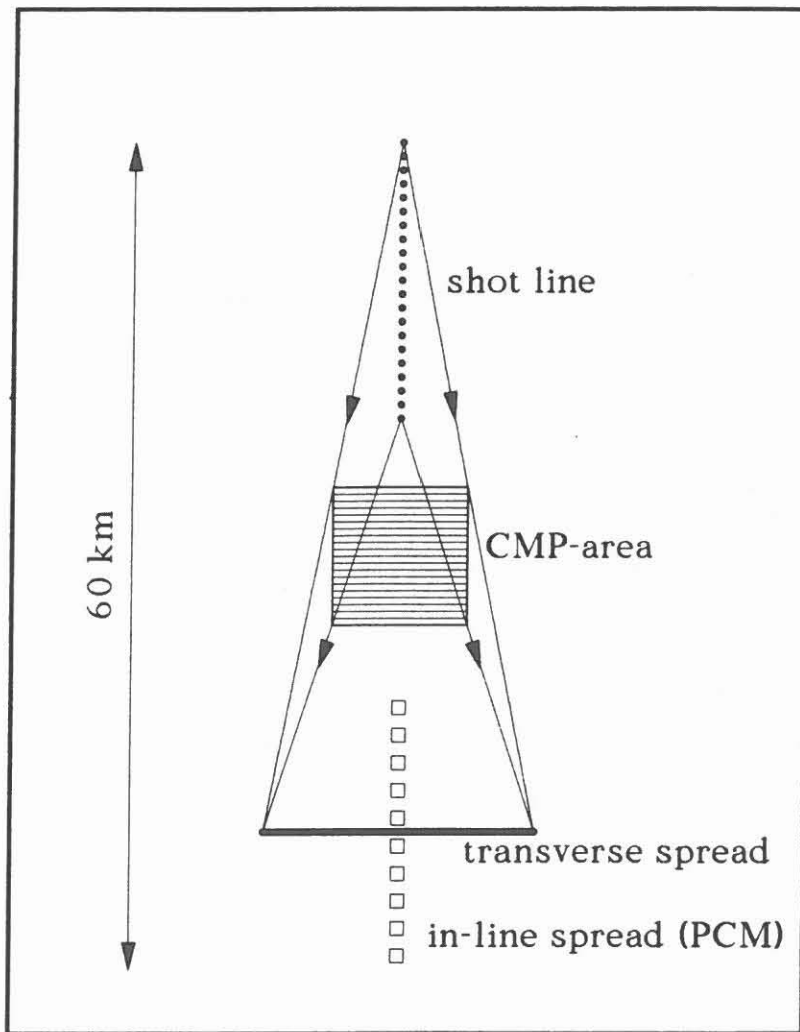


Fig. 2: Basic scheme for 3D wide-angle measurements: recording a linear shot series by a transverse oriented receiver spread of equal length at about the critical distance provides single CMP coverage in a square area in between. The supplementary in-line spread serves for improved velocity resolution.

The basic scheme of Fig.2 has been applied twice for the IS089 wide-angle survey, once in SE-NW direction with the shot-points 101 to 120 on the former DEKORP4 line (Fig. 3) and once in SW-NE direction with shot-points 201 to 221 near to the pre-site reflection line KTB8504 (DEKORP Research Group 1988). For the latter setting shot and receiver lines have been rotated by 90° with respect to Fig. 2. Both configurations cover the same CMP rectangle with the KTB drill site in its centre.

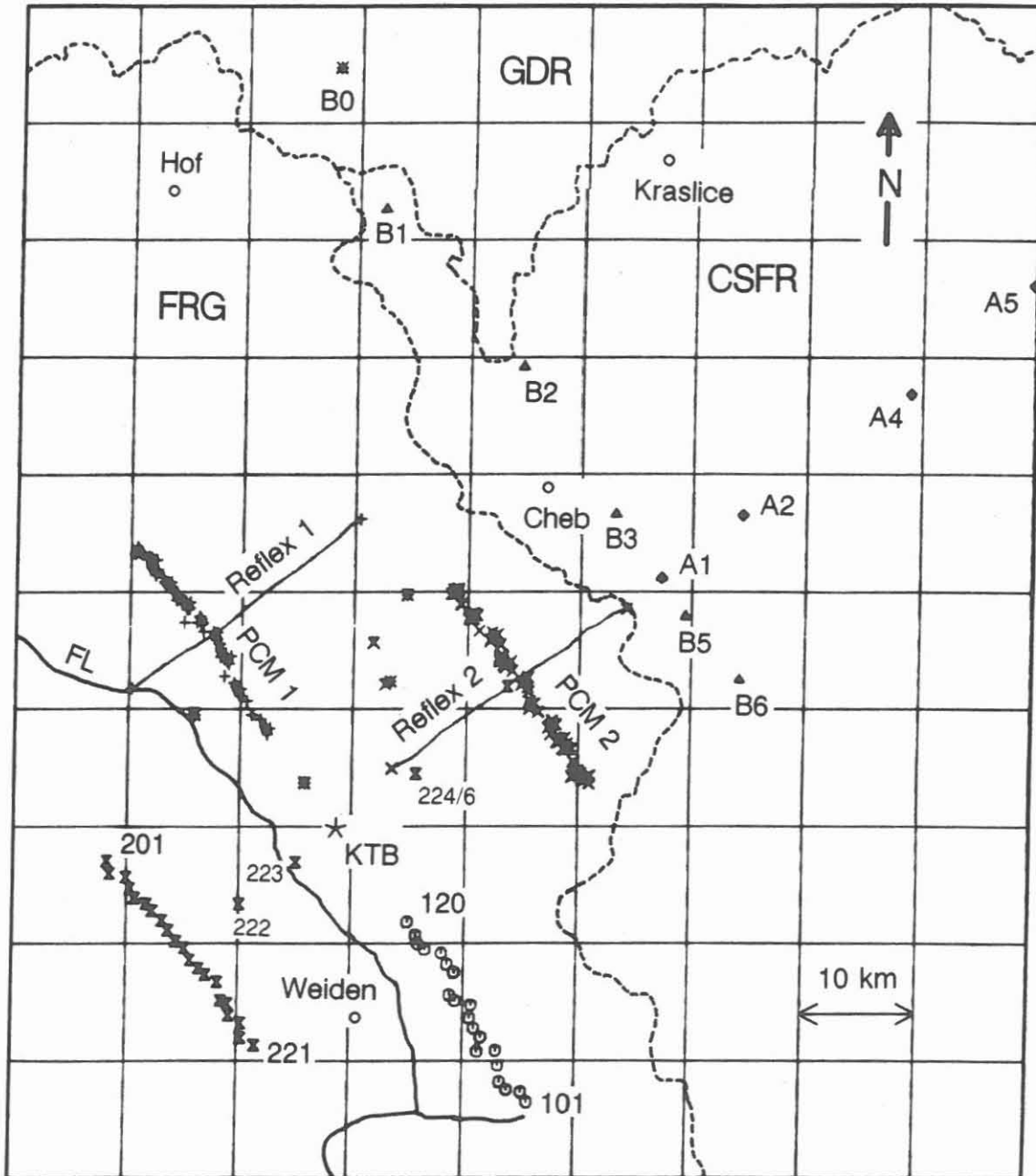


Fig. 3: Location map of IS089 wide-angle and refraction measurements: 101-120, 201-227 shotpoints in the FRG; B0 shot in the GDR; B1-B5, A1-A5 shotpoints in the CSFR; unnumbered symbols are locations of quarry blasts. Lines Reflex1 and Reflex2 are 312-channel receiver spreads formed by 5 university and DEKORP reflection units (Table 1); perpendicular spreads PCM1 and PCM2 consist of 20 PCM stations with a total of 120 channels.

The receiver spreads normal to the shot lines, termed Reflex1 and Reflex2 in the location map (Fig. 3), were observed by means of 5 university- and DEKORP-owned reflection instruments with a total of 312 channels and 80 m receiver group spacing. The perpendicular spreads PCM1 and PCM2 were formed by 20 PCM-stations with a total of 120 channels, half of which were used for three-component recordings. Details of the instrumentation are given in Table 1.

Field work was carried out from 9th to 21th October, 1989. It was integrated in the ISO89 3D steep-angle survey and closely coordinated and synchronized with a simultaneous refraction survey by GEOFYZIKA BRNO and ZIPE POTSDAM in the adjacent territories of the CSFR and the GDR. In that way, shots fired in the Oberpfalz could also be recorded in north-western Bohemia,

Table 1: Field recording instrumentation used for the ISO89 3D wide-angle survey and effective geophone parameters

Number&Type of Recording Devices	Channels & Components	Geophon- type and Bundling	Natural Frequency [Hz]	Damping- constant	Generator Constant [Vs/cm]
1 SERCEL 338B (Muenchen)	48 vert.	2*5 SM-6/B 3750hm	5.0	0.55	1.44
1 DFS-IV (Clausthal- Zellerfeld)	48 vert.	6 SM-6/B 3750hm	4.6	0.55	1.88
1 DFS-V (DEKORP)	120 vert.	6 SM-6/B 3750hm 710hm	4.6 "	0.95 0.78	1.65 0.80
1 DFS-V (Zuerich)	48 vert.	6 SM-6/B 710hm	4.6	0.78	0.80
1 DFS-V (Karlsruhe)	48 vert.	6 SM-6/B 3750hm	4.6	0.95	1.65
12 PCM-5800 (DEKORP,AWI)	8 1 3-comp. + 5 vert.	6 SM-6/A 1 MUC-3D	4.6 1.0/2.0	0.62	1.56 4.00/8.00
7 PCM-5800 (Aachen,AWI)	3 3-comp.	1 MARK-L4A 1 MUC-3D	1.0 1.0/2.0	0.62 "	1.00 4.00/8.00
1 PCM-5000 (Muenchen)	3 3-comp.	6 SM-6/A 3750hm	4.6	0.62	1.56
1 GEOMETRICS ES-2420 (AWI)	15/3 5/1 3-comp.	2 SM-4/UHT	10.0	?	?

southern Saxony and vice-versa. Altogether 64 borehole shots (47 in the FRG, 17 in the CSFR) and 10 quarry blasts (9 in the FRG and 1 in the GDR) were observed. The contractor's recording unit for the steep-angle 3D-survey recorded the shots as well and served as master unit for radio controlled shot release and remote start of the other reflection units.

In addition all shots were also recorded in the KTB pilot hole by 3-component geophones. A geophone chain with 5 active sensors was used during shot series 101 to 120, and a single 3-component sensor during the rest of the wide-angle experiment. Details on position and orientation are given in Table 2.

3. DATA PROCESSING AND FIRST RESULTS

3.1 Preprocessing

Due to the different recording instruments used in the wide-angle survey an extensive preprocessing was required to generate a homogeneous data set. As we had decided to process the whole data volume with the DISCO software package - partially modified and extended for wide-angle applications - some extra effort was necessary for the conversion of the non-standard PCM data into the internal Disco format. As a first step to this end, PCM data were already transformed during the experiment into a slightly modified ESSTF-format (European Standard Seismic Tape Format) and stored on computer-readable 9-track magnetic tape by means of the DEKORP PCM-playback computer, which was installed in the field headquarter; simultaneously generated analogue outputs were used for quality control.

For the straightforward input of the ESSTF data into the DISCO system an input-module "PCM" has been developed, which demultiplexes the block-multiplexed ESSTF data, converts them to DISCO format, cuts out the desired time windows from 0 to 32 s traveltimes, and adds 62 shot and receiver specific header informations to each seismic trace. Finally, data were resampled to 4 ms to become compatible with multichannel reflection data.

Editing was rather time consuming and included the following steps:

- correction of polarity reversals due to non-standard polarities of some borrowed geophones,
- despiking, especially for data from the first rainy week,
- elimination of dead or strongly disturbed traces,
- zeroing of strong transient disturbances, e.g. by cars crossing cables,
- mute until about 300 ms before first arrivals,

Furthermore the data were corrected for the different geophone parameters (Table 1) and an uniform receiver response (natural frequency 4.5 Hz, damping 0.62, generator constant 100 Vs/m) was simulated by recursive simulation filtering (Seidl 1980). Finally a 6 to 40 Hz band-pass filter was applied to all data. The efficiency of these processing steps is exemplified by Fig. 4, top and centre.

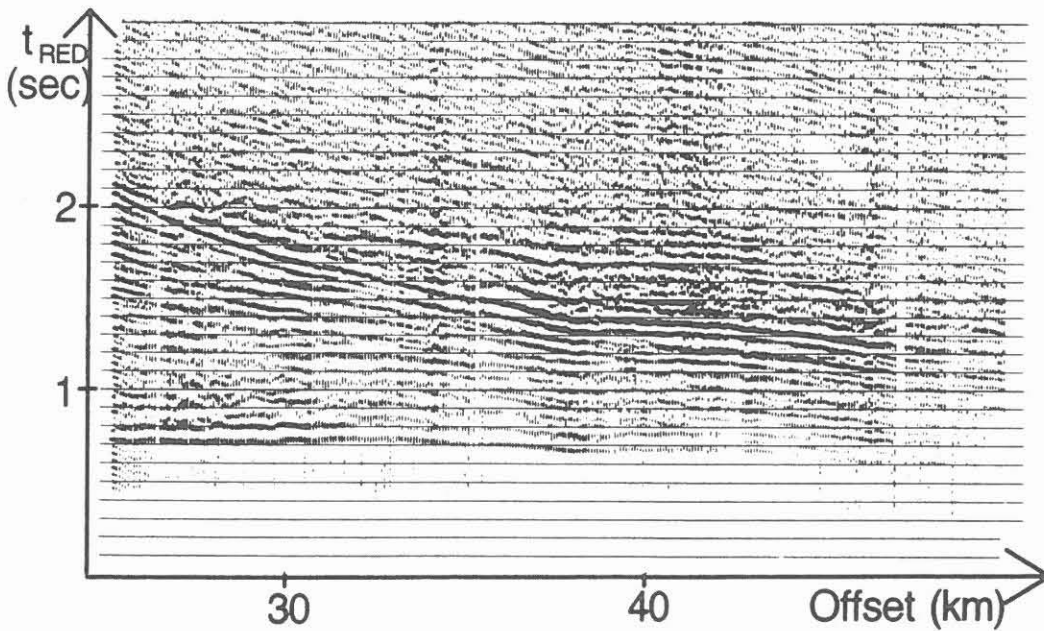
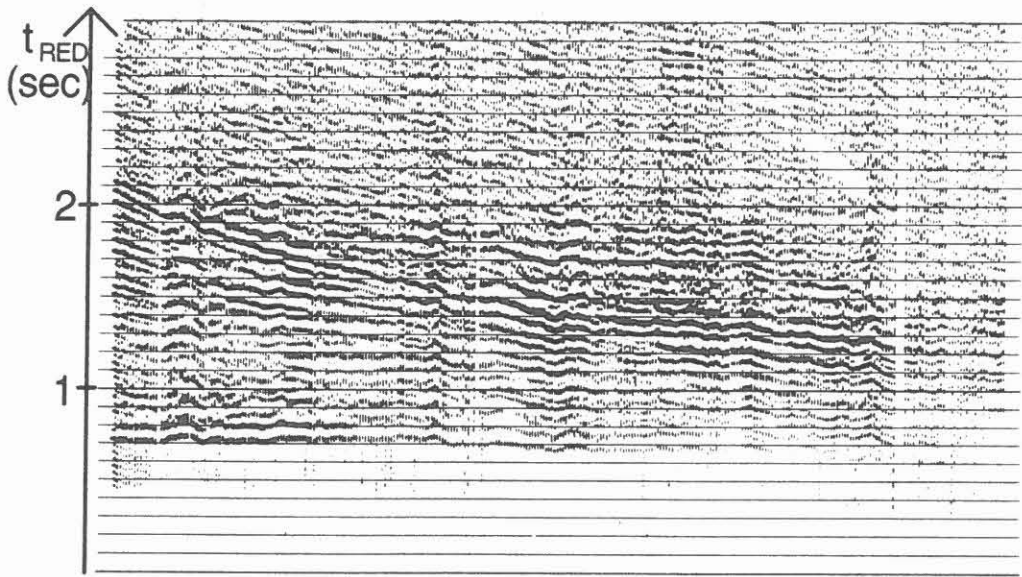
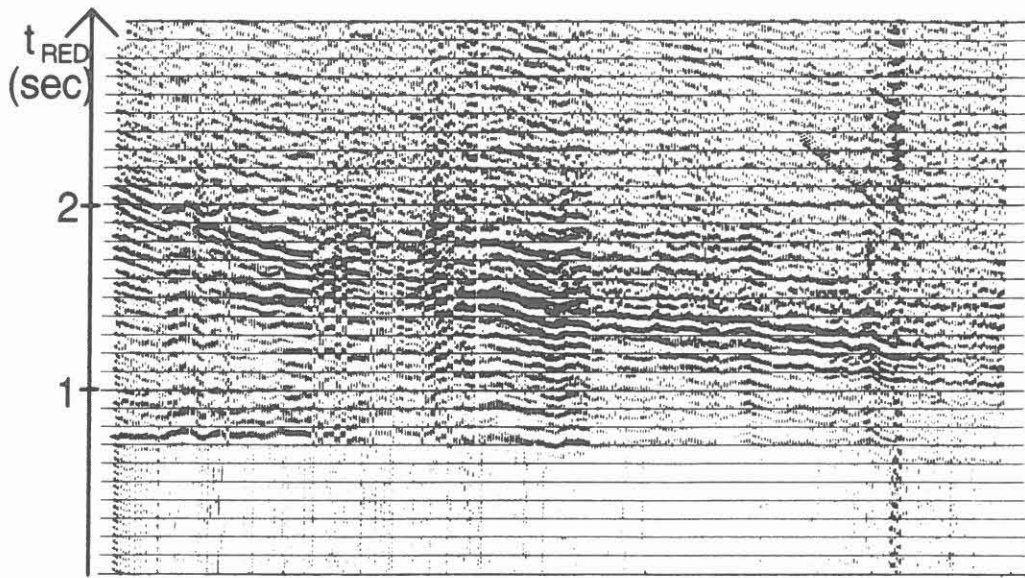


Fig. 4, centre, also reveals, and this is confirmed by comparative inspections of other shot records, that **static corrections** are a matter not to be ignored in wide-angle seismics. Because of missing nearby shots, however, they cannot be evaluated by standard refraction interpretation of first arrivals. Therefore we designed a two-step correlation method for the determination of short-wavelength statics and applied it, for the sake of higher resolution, to resampled data (from 4 to 1 ms). Based on 500 ms time windows around the first arrivals crosscorrelation functions of adjacent traces were stacked over 5 neighbouring shotpoints and a delay-time curve was defined along the spread by adding the individual delays of the correlation maxima picked by the interpreter. In this way 4 delay-time curves were obtained for each spread. After removal of a moving average over 5 km from each curve the remaining delay-time curves were in almost perfect agreement and their means were applied as first-order static corrections. After that, the procedure was repeated with a narrower time window of 100 ms and the resulting second-order delays were added to the first-order static corrections. The effect of applying these corrections is illustrated by comparison of Fig. 4, centre and bottom.

The general improvement of the signal-to-noise ratio from top to bottom in Fig. 4 is remarkable and will certainly increase the significance of the final results. That's why we feel it worth to do all the tedious preprocessing shortly described in this subsection.

As a typical shot record along spread Reflex2, Fig. 4 already anticipates qualitatively some main results of the present investigation:

1. The strong wide-angle reflections with 1 to 2 s reduced traveltimes, which were known so far only from the NW-SE-striking DEKORP4 line and by which the Erbendorf-Body (EB) was originally defined, appear also for SW-NE propagated waves over the whole length of spread Reflex2 (Fig. 3).
2. The EB wide-angle reflections show up again with large amplitudes and apparent velocities over 7.0 km/s.

This proves that the EB is not a narrow local feature beneath the DEKORP4 line and that its large reflection amplitudes and apparent velocities are not just the results of focusing by off-line heterogeneities. This conclusion is corroborated by all other ISO89 data processed and analysed so far.

3.2 Simulated Constant-Offset (COF) and Zero-Offset Sections

For a first qualitative assessment of horizontal structural variations we use simulated constant-offset sections. They are

on left page:

Fig. 4: Example for signal improvement by consecutive preprocessing steps. **Top:** raw data of shot 203 recorded by spread Reflex2. **Centre:** same data after editing, mute, restitution and 6-40 Hz band-pass filtering. **Bottom:** Same data as above with static corrections applied.

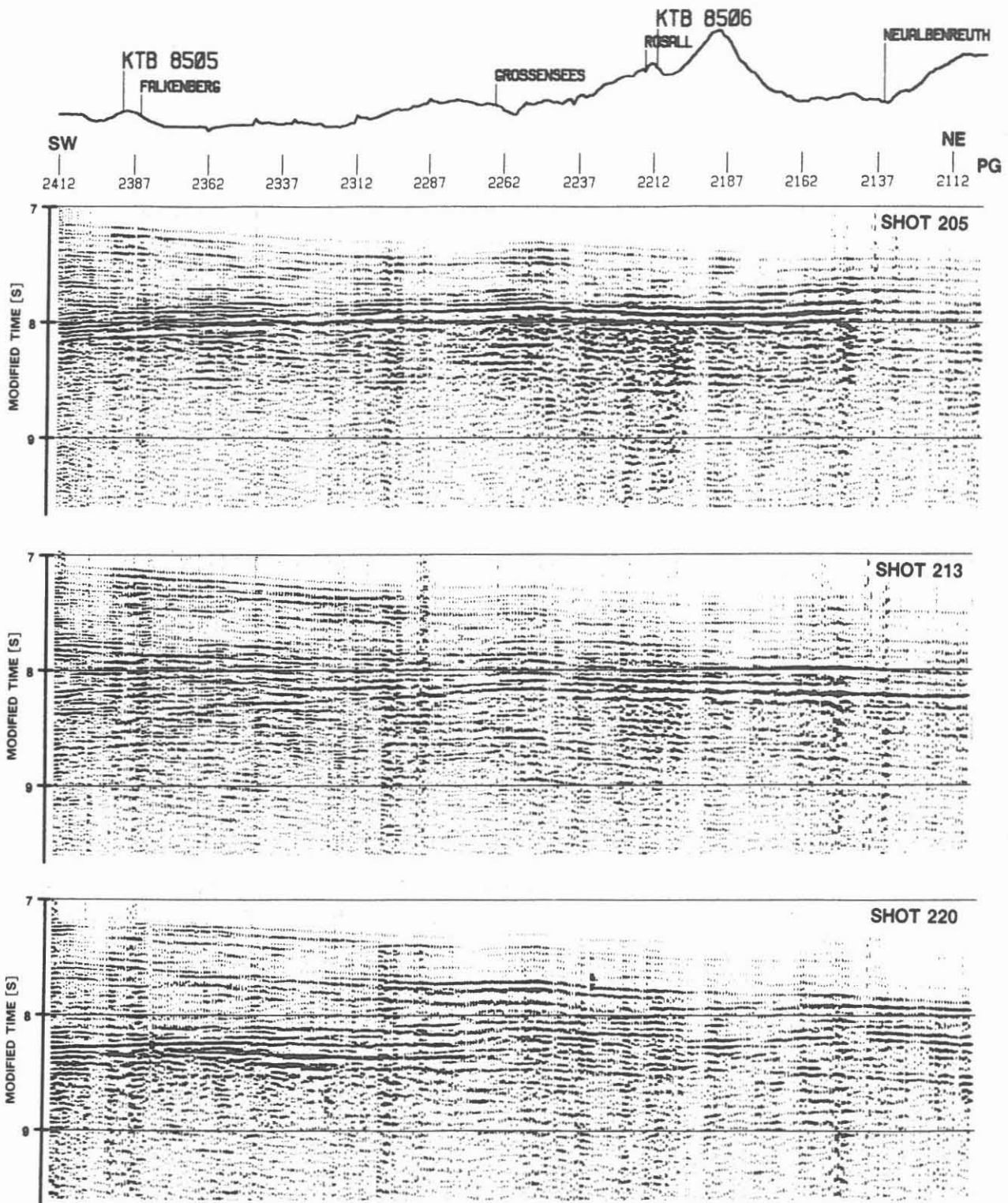


Fig. 5: Three shot records along spread Reflex2 transformed into constant offset sections (COF) by partial NMO-corrections; reference offset is 40 km. The typical wide-angle reflections from the Erbsdorf-Body appear around 8 s modified time. An increase in traveltime from NW to SE and a splitting up of reflections in the SE-part (shot 220) is observed.

obtained from single-shot sections or CMP gathers by partial dynamic corrections on to a specified target offset (e.g. 40 km in Fig. 5); traveltime differences due to variable shot-to-receiver offsets are thereby eliminated. We have implemented the COF-simulation process as an NMO-correction with a subsequent inverse NMO-correction on to the target offset.

In principle, any target offset would serve the purpose, but a reference value near to the mean shot-to-receiver offset has the advantages of least signal stretching and of smallest distortions in case of inaccurate NMO-velocities. For that reason 40 km has been used as COF target offset in Fig. 5. Examples are shown for three shots (205, 213, 220) recorded on spread Reflex2, which are representative for the whole series of shots 201 to 221, by which the KTB surroundings were scanned in SW-NE direction. For a first overview COF simulations were performed with a constant velocity of 5.95 km/s, which - according to the DEKORP4 wide-angle results - is the best estimate of the average v_p value down to the EB.

In Fig. 5 the wide-angle reflections from the EB appear around 8 s modified time with great amplitudes and widespread continuity. The latter is very surprising in view of the generally short reflection elements observed in the crystalline crust by steep-angle seismics, e.g. on profile KTB8502 (DEKORP Research Group 1988) which partially coincides with our spread Reflex2. The EB reflections form a band which broadens from NW to SE, i.e. from shotpoint 203 towards 220. In the SE-part (shot 220) the EB seems to split up in an upper, possibly overthrust and a lower segment, which descends to the SE.

Fig. 6 displays the same data as **simulated zero-offset (ZOF) sections**. A ZOF-section may be considered as the special case of a COF-section with total NMO corrections applied, i.e. with target offset zero. Simulated ZOF sections provide the benefit of direct comparability with steep-angle seismic results and of simple depth interpretation (with the risk of oversimplifications, however). If applied to far-offset wide-angle data, the inconvenience of serious signal distortion arises, because the NMO-corrections revoke the time-convergency of adjacent reflections with increasing offset and thereby yield considerable signal stretching at zero offset. The P_g -onsets which are most affected by stretching, and which moreover are kinematically not properly transformed by standard NMO-corrections, have therefore been suppressed in Fig. 6 by gradual muting. Structures with less than about 3.5 s zero-offset two-way time can not be resolved by our wide-angle observations starting at 25 km minimum offset.

The ZOF-sections are presented in Fig. 6 beneath a drawing of the receiver locations and their altitudes. According to the common-midpoint concept, however, the displayed reflections can be assigned to 12.5 km long, SW-NE trending midpoint lines beginning at about the Franconian Line and crossing the former DEKORP4 line 3.5 km NW, 1.0 km SE and 5.5 km SE, respectively, from the KTB location. In Fig. 6. the DEKORP4 line is situated

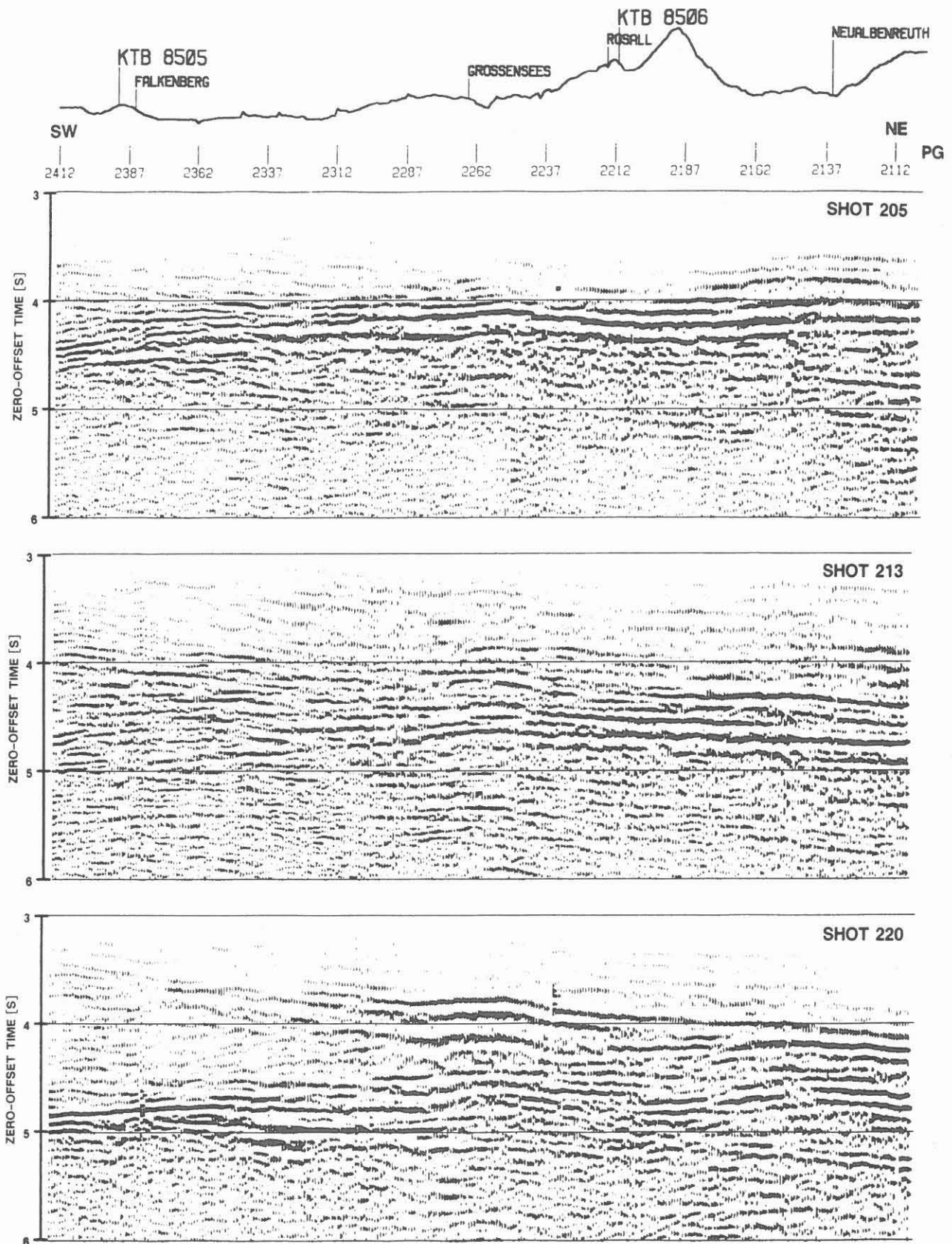


Fig.6: Simulated zero-offset sections for the same shot records as in Fig. 5 obtained by NMO-corrections with an average velocity of 5.95 km/s; P_G -onsets, being not properly transformed by NMO-corrections, have been suppressed by a ramp mute.

at PG no. 2290. Comparing the three ZOF simulations, again obtained with $v_{NMO}=5.95$ km/s, the dipping of the base of the EB towards SE and its bisection in the SE are clearly discernible.

Fig. 7 is an attempt to portray the NW-SE variations of the EB along the DEKORP4 line by a scenographic fence diagram of subsections cut out from all zero-offset transformed record

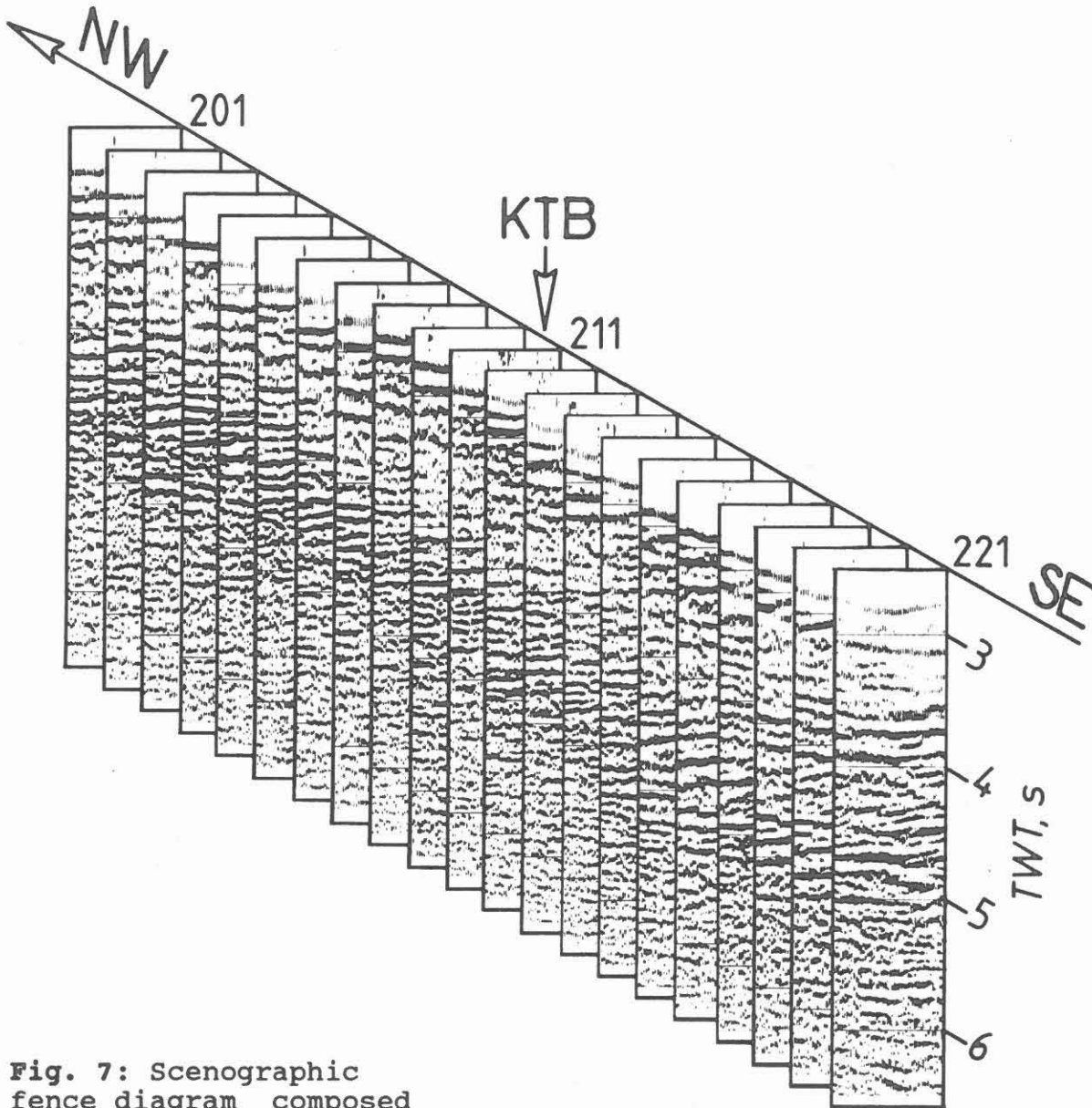


Fig. 7: Scenographic fence diagram composed of short zero-offset transformed segments (50 traces, 4 km) of IS089 shot records 201 to 221 with midpoints beneath the DEKORP4 line and the KTB location; the NW-SE extent of the covered stripe is 10 km. Strong reflections around 4 to 5 s TWT delineate the Erbendorf-Body and its intricate internal structure. Onsets around 3 s are P_g -waves not to be considered in simulated zero-offset sections.

sections of the shot series 201 to 221. Each of the transverse subsections represents a spread of 50 channels with 80 m spacing and shot-to-receiver midpoints around the DEKORP4 line. Altogether they cover a 10 km long and 2 km broad CMP-stripe with the KTB site in the centre. The P_g -waves forming the onsets at 2.8 to 3.1 s TWT in Fig. 7 have not been muted, in contrast to Fig. 6. The typical EB reflections are present in all subsections with strong amplitudes between 4 and 5 s TWT, in the bisected SE-part they somehow rise to less than 4 s. An intricate internal structure with pronounced horizontal variations is evident, which can, however, not be resolved in de-

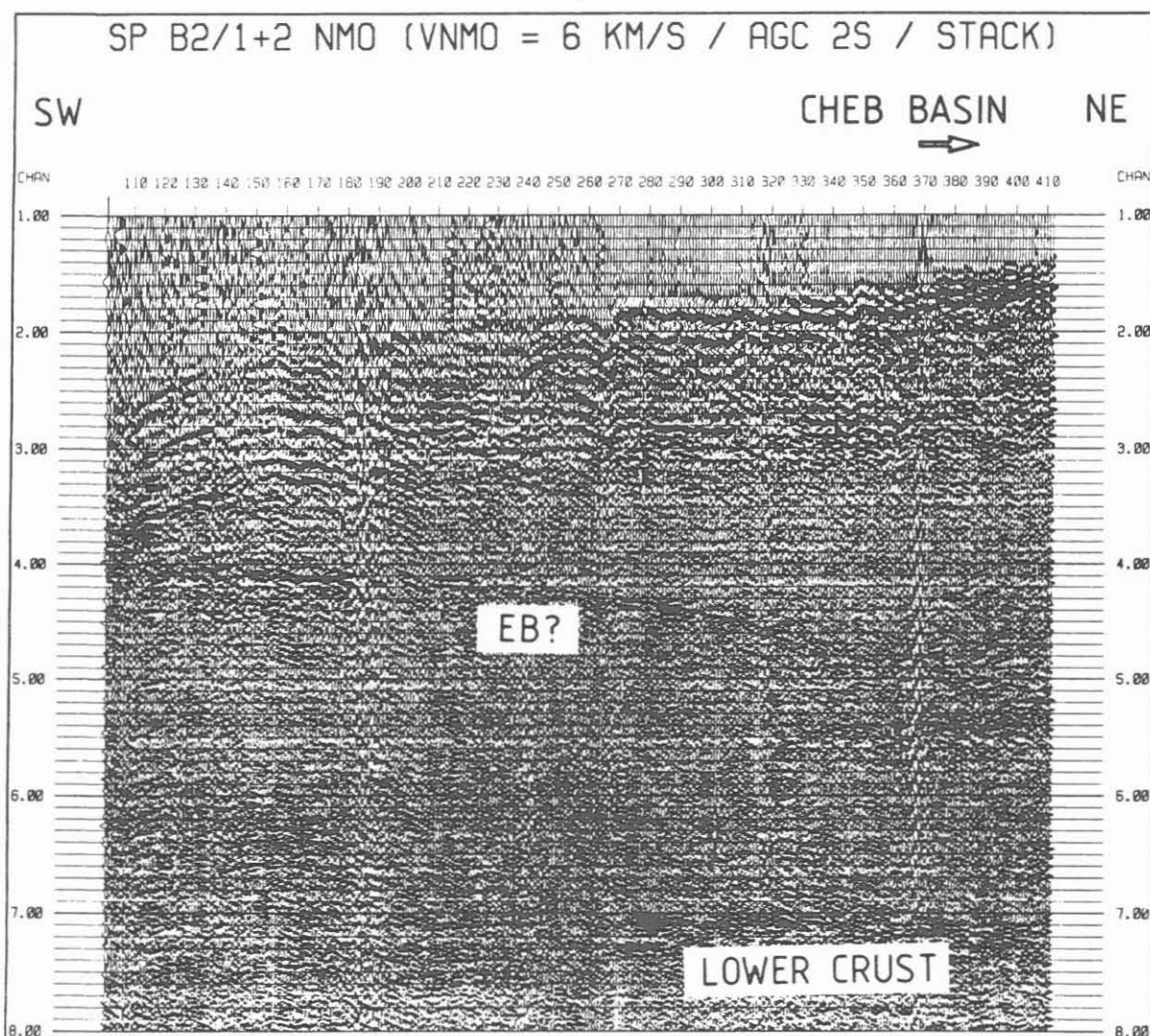


Fig. 8: Zero-offset-corrected stacked section of two shots from location B2 (CSFR) recorded along spread Reflex1. A very sharp wide-angle reflector with TWT comparable to the Erben-dorf-body appears under Reflex1 and seems to dip towards the tertiary Cheb basin; a change of crustal style in that direction is indicated by the appearance of strong reflections from the top of the lower crust.

tail with the simple approach of simulated ZOF-sections. The main point to be stressed by Figs. 5 to 7 is, that the EB reflections have been observed perpendicular to the DEKORP4 line in the whole area covered from the Franconian Line to the Falckenberg granite complex with the same characteristics as earlier parallel to DEKORP4.

ISO89 has also provided evidence that the EB is not a singularity in the middle crust of the narrow KTB surroundings. Similar bodies may exist in other places of the Saxothuringian/Moldanubian boundary zone. Fig. 8 shows a simulated ZOF-section of two stacked shots from shotpoints B2/CSFR recorded along spread Reflex1 (Fig. 3) with a very sharp wide-angle reflection of about the same TWT as the EB but with otherwise different signature. The reflector seems to dip from the SE margin of the Fichtelgebirge towards the tertiary Cheb Basin. Parallel in that a marked reflection from the top of the lower crust appears. This might indicate a tertiary regeneration of the Variscan crust at the transition to the Cheb Rift.

Simulated COF and ZOF sections are only very rough first approximations for imaging crustal structures by wide-angle reflections and should be interpreted cautiously. For a detailed and reliable imaging of strong horizontal heterogeneities the migration process is even more important in wide-angle seismics than it is in steep-angle seismics (Gebrande et al. 1989). A suitable 3D-version of the isochrone wide-angle migration method - Fig.1 is the result of a 2D-version - is presently being developed. For its hopefully successful application a comprehensive 3D velocity will be a prerequisite.

3.3 Velocity Analyses

The independent control or improvement, respectively, of the 2D velocity model derived from DEKORP4 data (DEKORP-Research Group 1988; Gebrande et al. 1989) and its extension to a 3D-model belong to the major targets of the ISO89 wide-angle survey. Seismic wave velocities are required for reliable structural imaging by steep- or wide-angle migration techniques as well as for the petrophysical, lithological and finally geodynamic interpretations.

We started velocity analysis of ISO89 data with spread Reflex2 because in this case the wide-angle data set includes observations down to zero offset, which are important for the velocity resolution in the upper crust. We used two independent methods:

- a special variant of the tau-p-inversion technique (Meichelböck 1988) and
- the so-called XTV-inversion (Gebrande et al. 1985), which is essentially a travelttime based stripping technique.

Fig. 9 shows an example for the tau-p method applied to stacked shot records 224 and 226 (Fig. 3). By means of an automatic picking algorithm manifold paths are traced through the slantstack transformed wavefield and converted to the v-z-

domain by the tau-sum method (Diebold et al. 1981). The stacked amplitudes are transferred from the tau-p into the v-z-domain and plotted as a filled-area contour-map, in which the dark crest is built up by the most coherent signals and thereby represents the dominant velocity-depth distribution half-way between shotpoint and receivers. Horizontal dark stripes marked by arrows in Fig. 9 may be due to subcritical reflections and indicate possible depths of first-order discontinuities.

The velocity-depth function picked by the geophysicist from Fig. 9 and controlled by forward modelling is shown, together with the result from the XTV-inversion of the same data, and with tau-p-inversions for shots 225/227 in Fig. 10. The tau-p-

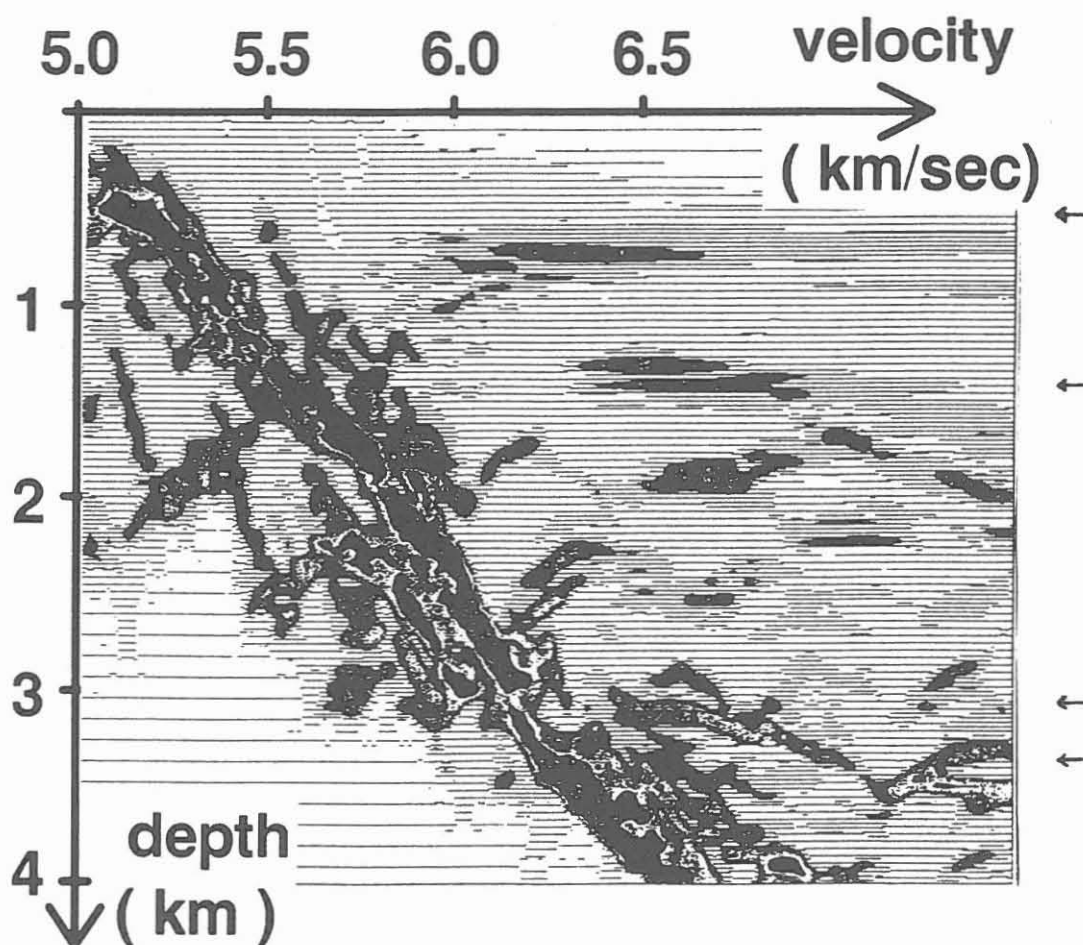


Fig. 9: Example for automatic velocity-depth determination by the modified tau-p wave-field transformation after MEICHELBOCK (1989). The dark crest is built up by the most coherent signal amplitudes of the shot records 224 and 226 and represents the dominant velocity-depth distribution for the area of the Falckenberg granite about 10 km NE of the KTB site. Arrows mark depths of probable undercritical reflections.

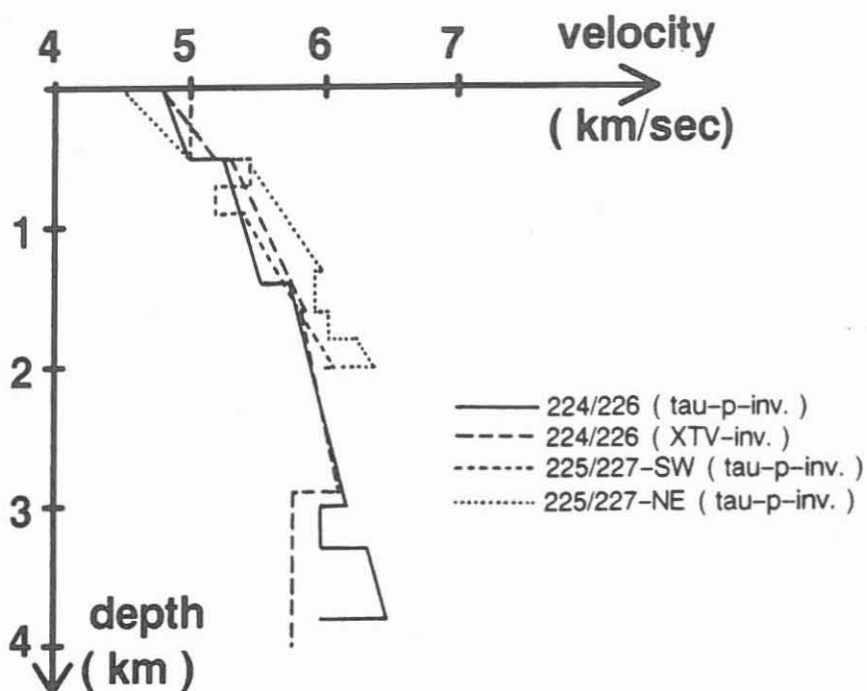


Fig. 10: Velocity-depth distributions derived by the tau-p and the XTV-method for the SW and the NE parts of line Reflex2.

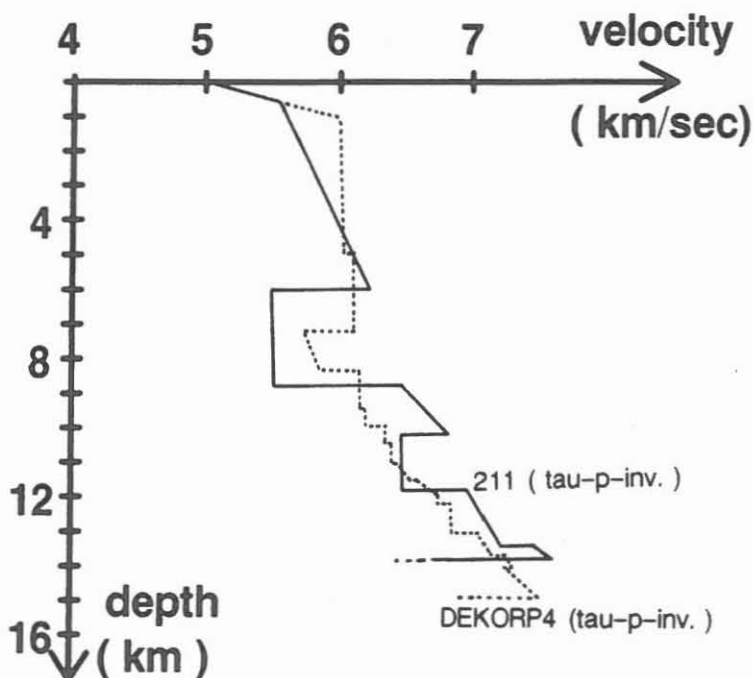


Fig. 11: Comparison of velocity-depth functions for the KTB vicinity, derived by the tau-p method from the single shot 211 recorded on line Reflex2 (SW-NE azimuth) and from CMP-sorted seismograms observed 1985 along DEKORP4 (NW-SE azimuth). The existence of p-wave velocities around 7.0 km/s at 12 to 14 km depth is corroborated by the IS089 data. Velocity resolution in the upper 5 km is poor due to the rather large offset minimum of 25 km.

and the XTV-method provide very similar results down to a depth of about 3 km, where a low-velocity layer is expected according to both solutions. The $v(z)$ function derived from shots 224/226 is expected to be valid for the area of the Falenberg granite complex about 10 km NE from the KTB site.

The shots 225/227 were situated in a split-spread position in the centre of spread Reflex2 near to a boundary between granites in the SW and mica schists in the NE and have provided significantly different $v(z)$ functions for both directions (Fig. 10). The depth of penetration is only 2 km for the split-spread data.

With regard to the EB the tau-p inversion of the shot 211, recorded on spread Reflex2 is of special interest, because the corresponding midpoints, to which the results of one-dimensional velocity determinations should be attributed, cross the KTB site (Fig. 11). The results are limited by missing observations in the 0 to 25 km offset range but, nevertheless, the $v(z)$ function seems to be well constrained at depths greater 5 km by clear first and later arrivals recorded on spread Reflex2. Allowance for sediments beneath the shotpoint was made by a static correction of 300 ms prior to the slantstack. P-wave velocities around 7.0 km/s in 12 to 14 km depth corroborate former results from the DEKORP4 line and confirm that they are not an artifact by some strange side-effect. The unusual high wave velocities as well as the high wide-angle reflectivity of the Erbsdorf-Body seem to be regional phenomena of the Earth's crust in the surroundings of KTB. The pronounced low-velocity zone obtained for the shot 211 is a surprise and needs further verification.

3.4 Polarization Analysis and Shear-Wave-Splitting

The operation of 3-component geophones recording nearly all seismic sources of the ISO89 project in the KTB pilot hole offered the unique possibility to analyze traveltime and wavefields of the wide-angle shots at depth. In view of convincing evidence for ultrasonic p- and s-wave anisotropy in almost all core samples from the KTB pilot hole (Lippmann et al. 1989; Zang et al. 1989) the question of large scale seismic in-situ anisotropy in the KTB surroundings calls for an answer. It's a question of fundamental interest going well together with the KTB project, but also a question of great practical importance, because significant anisotropy would require serious modifications in seismic processing.

The down-hole recordings from the first week of the ISO89 wide-angle measurements with shotpoints 101 to 120 are especially appropriate for an exploration of anisotropy effects because 4 (of 5) 3-component geophones were in perfect operation at that time. Details of geophone positions and orientation of components are given in Table 2.

As a first step we testet our two-dimensional isotropic velocity model derived from DEKORP4 wide-angle data against the

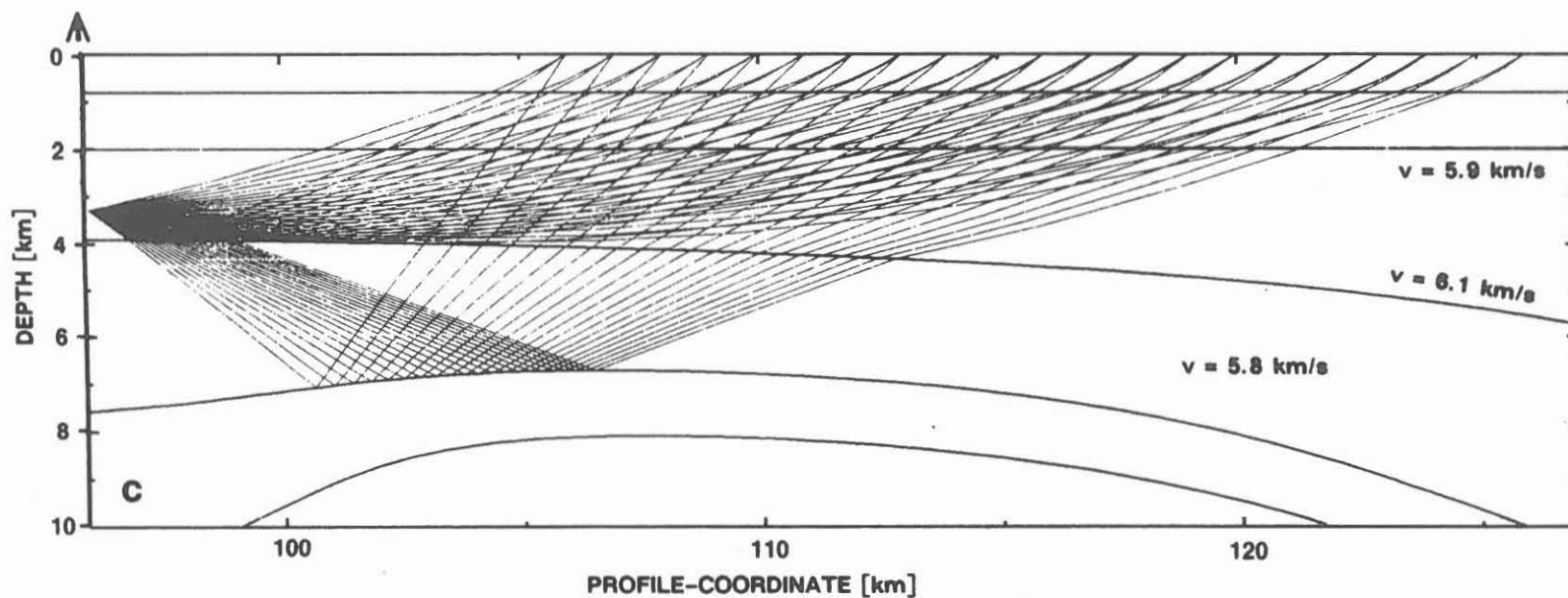
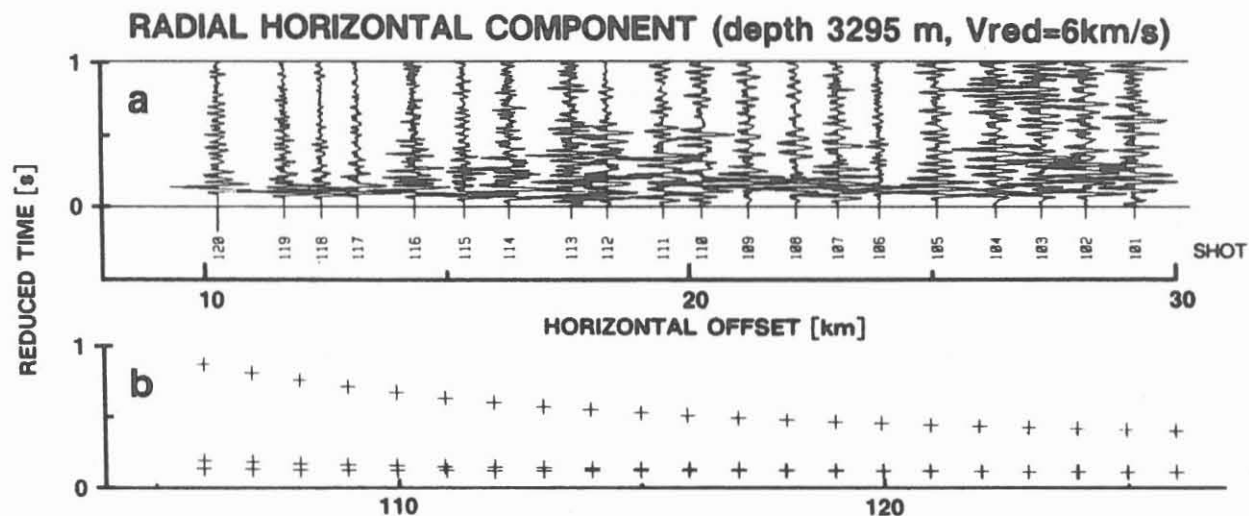
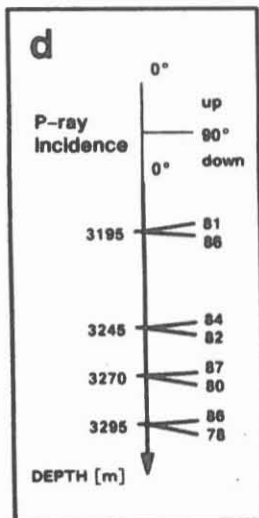


Fig. 12: Comparison of observed (a,d) and predicted (b,c) traveltimes and angles of incidence for 3-component down-hole measurements at 3295 m depth

ISO89 down-hole observations. Fig. 12a and b show the p-wave record-section in reduced time for the shot series 101 to 120 recorded by the geophone at 3295 m depth (a) in comparison with traveltimes (b) predicted from the model (c). The observed arrival times are about 0.1 s faster than predicted, but the average apparent velocities coincide rather well. The more or less horizontal incidence of the seismic rays predicted by the model calculations fits in with the results of polarization analyses of the 3-component recordings, which were performed by calculating the direction of the principal axis with the largest eigenvalue of the covariance matrix (Kanasevich, 1973).

Surprisingly the azimuth of the p-wave polarization proved to be in close agreement with the shot-to-receiver azimuth (Table 2). This means that either there is no significant p-wave anisotropy or the azimuth of wave propagation, i.e. the SE-NW direction, is close to a specific direction of pure longitudinal polarization in an anisotropic upper crust. Larger differences between p-wave polarization and propagation directions for other shotpoints, e.g. for quarries NNE from the KTB site, are in favour of the second explanation, and this becomes indeed evident by the investigation of shear-waves. In Fig. 13

Table 2: Receiver positions of the 3-component borehole geophone chain and orientation of its horizontal components according to compass readouts and p-wave polarization directions (assuming longitudinal particle motion)

sensor location number	depth [m]	component		horizontal receiver-azimuth [N°E]	
		code	type	from compass readout	from polarisation analysis
1	3195	111	vert.	---	---
		233	horz. H1	52	59 +/- 5
		333	horz. H2	142	149 +/- 5
2	3220	111	vert.	---	---
		233	horz. H1	---	---
		333	horz. H2	defectiv component H2	
3	3245	111	vert.	---	---
		233	horz. H1	19	26 +/- 4
		333	horz. H2	109	116 +/- 4
4	3270	111	vert.	---	---
		233	horz. H1	24	24 +/- 2
		333	horz. H2	114	114 +/- 2
5	3295	111	vert.	---	---
		233	horz. H1	248	249 +/- 4
		333	horz. H2	338	339 +/- 4

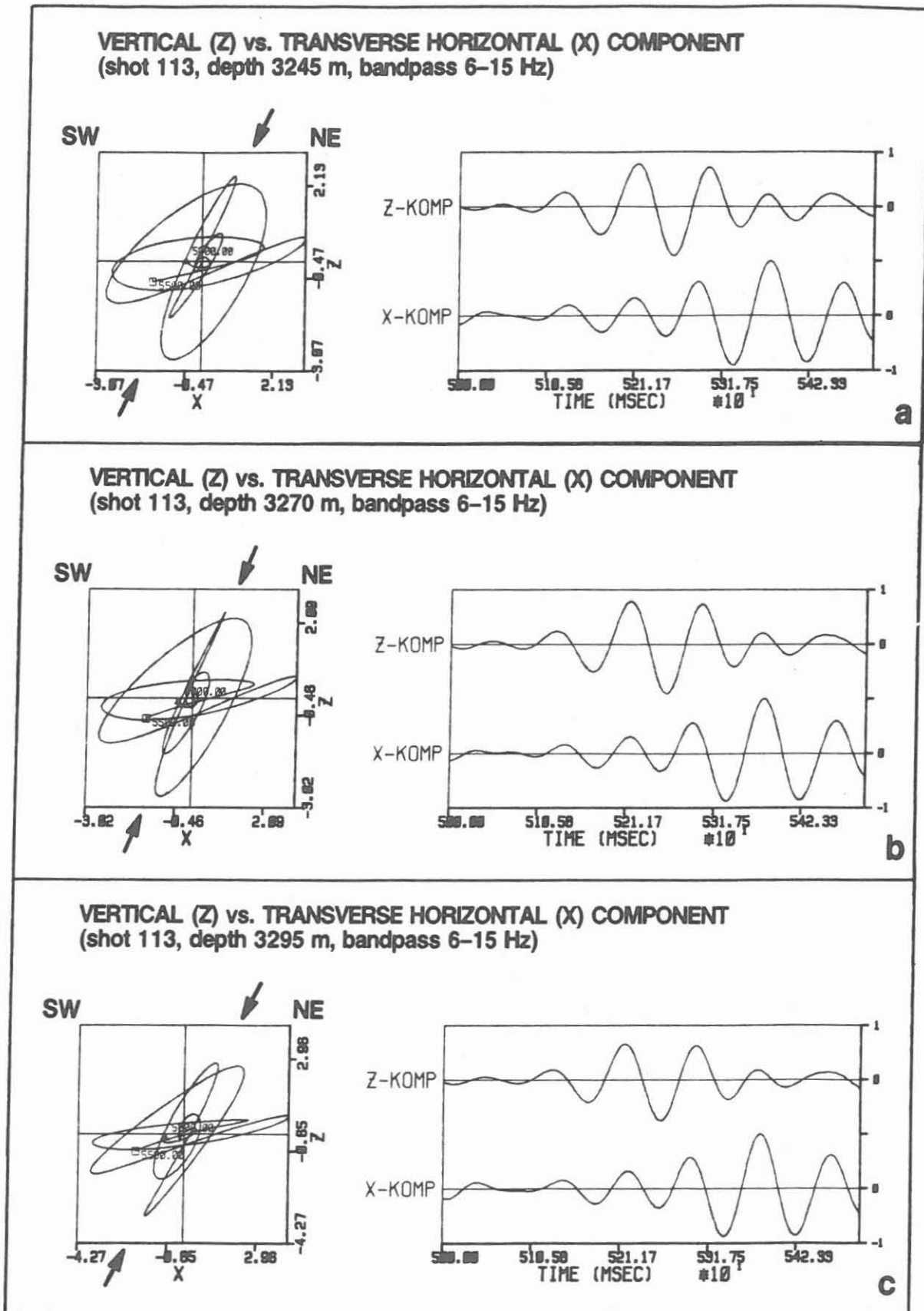


Fig. 13: S-wave components and s-wave hodographs showing s-wave splitting

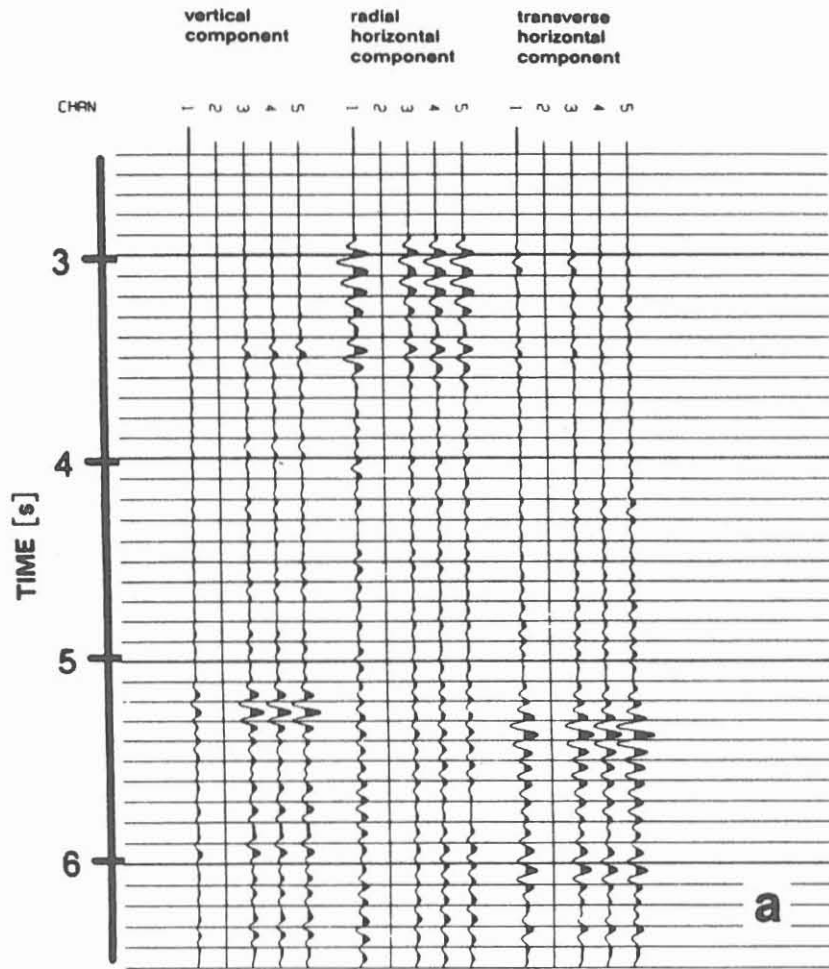
typical s-wave signals of a shot (no. 113) recorded in three different depth positions are plotted in the vertical plane normal to wave propagation and p-wave polarization. The components as well as the hodographs are displayed providing clear evidence for birefringence (shear-wave splitting). The s-wave trains start consistently with linear polarization dipping steeply (65 degree) to the SW and continue with more elliptical particle motion, which seems to be due to a superimposed orthogonally polarized shear-wave with slower propagation velocity. All records exhibit this general behaviour.

Decomposition of the 3-component seismograms into mutually orthogonal components parallel and normal to the p-wave polarization direction provides an almost perfect separation of p- and s-waves as demonstrated by Fig. 14a. By an appropriate additional rotation of the transverse components in the normal plane also the fast and the slow shear-waves can be separated. This is shown in Fig 14b for the four records of shotpoint no. 113. It becomes evident that the delay of the slow shear-wave is more than one period (about 100 ms) and this is also true for most of the other shot and receiver positions. This delay cannot be the result of a very local anisotropy, e.g. merely at the source or receiver. With a reasonable anisotropy coefficient of 5 to 10%, the waves must propagate through at least several km of anisotropic rocks to bring forth the observed delay.

Fig. 15 shows record sections of the decomposed fast and slow shear-waves for the total shot series recorded at 3295 m depth. Shear-wave splitting is evident, but there is no linear increase of delay-times with shot-to-receiver distances, as would be expected for a medium with constant anisotropy. Fluctuations seem to be of a scale of about 10 km; at the scale of seismic field experiments, however, they are not simply averaged out.

From comparison with laboratory investigations on KTB core samples and from theoretical considerations it is expected that rock foliation is the main cause for the observed anisotropy and that the polarization direction of the fast s-wave is in the plane of foliation. This would imply that the dipping polarization of the fast shear-wave reflects the dominant inclination of foliation in the zone of Erbendorf-Vohenstrauß SE of the KTB location. Shear-wave polarization is worth to be studied. With consequent methodical development it might become a diagnostic tool for the seismologist as useful as the polarization microscope is for the petrologist.

SHOT 113 (bandpass 6-15Hz)



SHOT 113 (bandpass 6-15Hz)

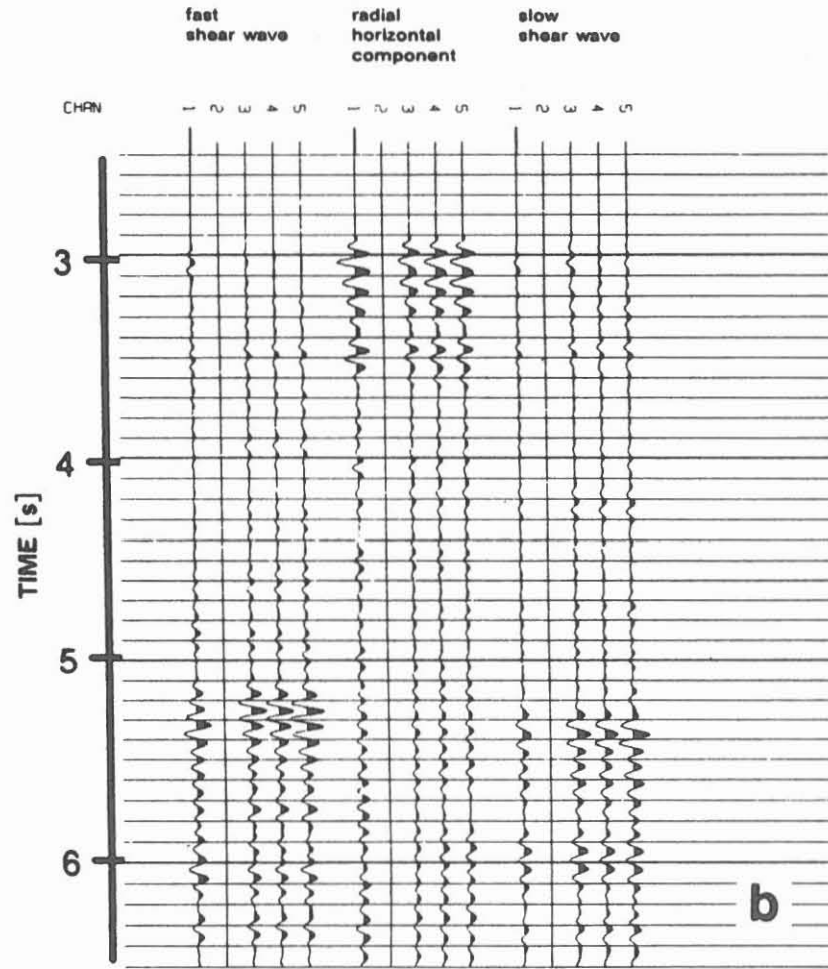
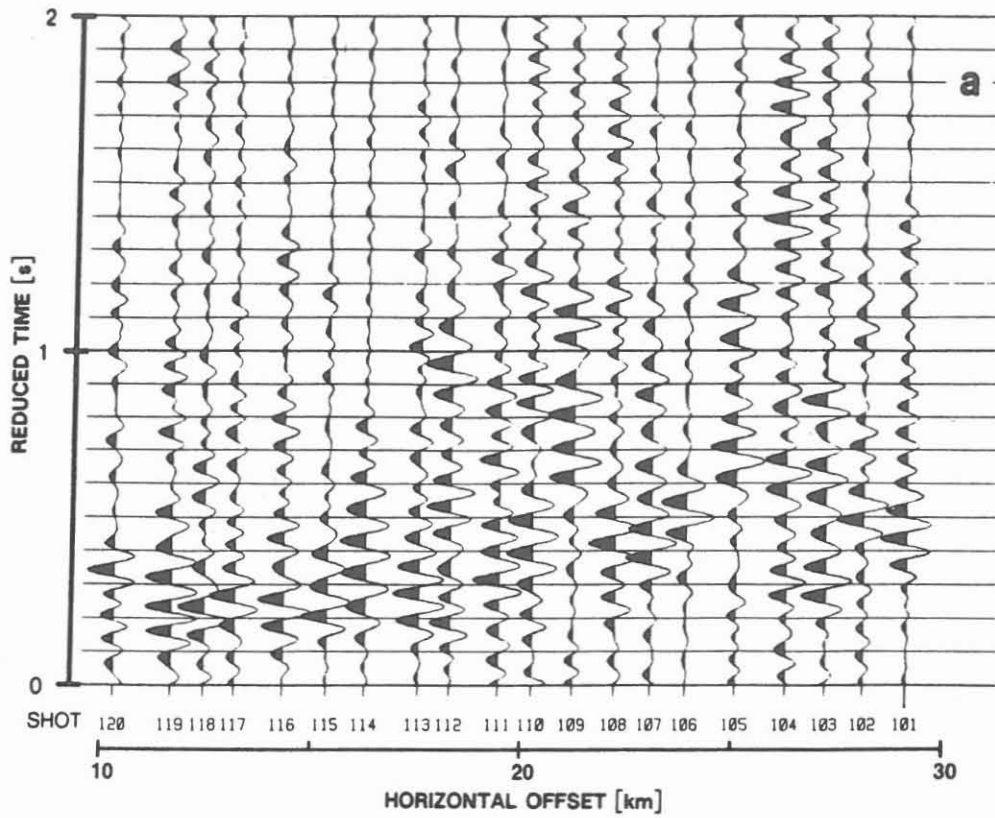
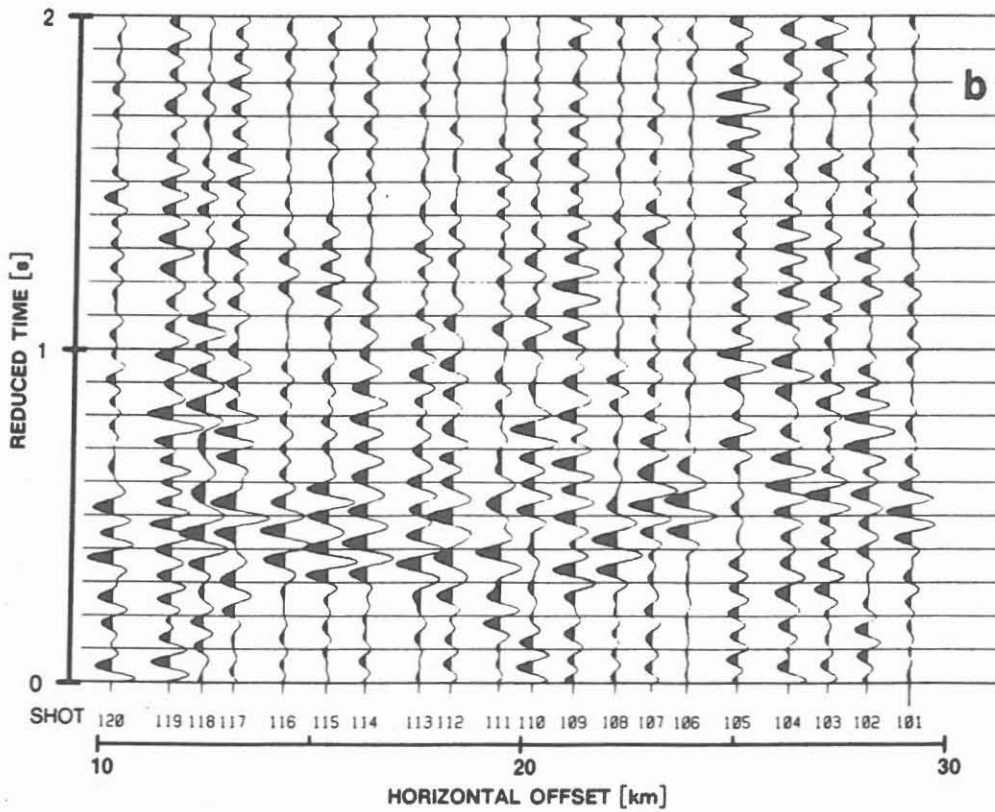


Fig. 14: Decomposition of four 3-component seismograms in (a) p- and s-waves and (b) p-, fast s- and slow s-waves by appropriate rotations



FAST SHEAR WAVE (depth 3295 m, bandpass 6-15Hz, $V_{red}=3.5\text{km/s}$)



SLOW SHEAR WAVE (depth 3295 m, bandpass 6-15Hz, $V_{red}=3.5\text{km/s}$)

Fig. 15: Comparison of the separated fast (a) and slow (b) shear-waves for all shotpoints recorded in 3295 m depth; shear-wave splitting is beyond all doubt.

Acknowledgments. The funding of the investigations by the Federal Ministry of Science and Technology (BMFT), Bonn, is gratefully acknowledged. We appreciate the continuous support by the DEKORP steering committee and by H. Soffel, director of the Institut für Allgemeine und Angewandte Geophysik, München. Thanks for excellent cooperation during field work are due to the teams from the Geophysical Institutes of Aachen, Clausthal, Karlsruhe, Münster, Zürich and München, from the Geological Survey of Lower Saxony, the Prakla-Seismos crew and to the colleagues from Geofyzika Brno.

References

- DEKORP Research Group: Results of the DEKORP4-KTB Oberpfalz deep seismic reflection investigations. *J.Geophys.* 62, 69-101, 1988
- Diebold, J.B., Stoffa, P.L.: The travelttime equation, tau-p mapping and inversion of common midpoint data. *Geophysics* 46, 238-254, 1981
- Gebrande, H., Miller H.: Refraktionsseismik. In: *Angewandte Geowissenschaften - Band II*, Bender, F., ed.: 226-260. Stuttgart: F. Enke Verlag, 1985
- Gebrande, H., Bopp, M., Neurieder, P. and Schmidt, T.: Crustal Structure in the Surroundings of the KTB Drill Site as derived from Refraction and Wide-Angle Seismic Observations. In: *The German Continental Deep Drilling Program (KTB)*, R. Emmermann and J. Wohlenberg eds.: 151-176, Springer-Verlag, 1989
- Giese, P.: Versuch einer Gliederung der Erdkruste im nördlichen Alpenvorland, in den Ostalpen und in Teilen der Westalpen mit Hilfe charakteristischer Refraktions-Laufzeit-Kurven sowie eine geologische Deutung. *Geophysikalische Abhandlungen* 1(2), 202 p., Freie Universität Berlin. Berlin: Friedrich Reimer Verlag, 1968
- Giese, P.: Results of data generalization. In: *Explosion seismology in Central Europe*, Giese, P., Prodehl, C., Stein, A., eds.: 339-346. Berlin: Springer Verlag, 1976
- Kanasewich, E.R.: *Time Sequence Analysis in Geophysics.* University of Alberta Press, 1973
- Lippmann, E., Bucker, C., Huenges, E., Rauen, A., Wolter, K., Soffel, H.C.: Rock physical properties: first results of the KTB-field-labratory. *Scientific Drilling* 1, 143-149, 1989

- Meichelböck, M.: Tau-P-Inversion, - mit Anwendungen auf DEKORP4-Weitwinkel- und Refraktionsmessungen. Dipl.-Arbeit, Inst. f. Allg. u. Angew. Geophysik der Ludwig-Maximilians-Universität München, 1988
- Peters, K.: Ergebnisse der Gravimetrie im Bereich der Münchberger Gneismasse und der Refraktionsseismik längs eines Profils über die Gneismasse. Diss. Ludwig-Maximilians-Universität München, 131 p., 1974
- Schmidt, T.: Seismisches Abbilden durch Isochronen-Migration von Weitwinkeldaten am Beispiel des DEKORP4-Profiles. Diss. Ludwig-Maximilians-Universität, in Vorbereitung, 1988
- Schmoll, J., Bittner, R., Dürbaum, J., Heinrichs, T., Meißner, R., Reichert, C., Rühl, T., Wiederhold: Oberpfalz Deep Seismic Reflection Survey and Velocity Studies. In: Exploration of the Continental Crust through Drilling IV, Emmermann, R., Wohlenberg, J., eds. Berlin: Springer Verlag, 1988
- Seidl, D.: The Simulation Problem for Broad-Band Seismograms. J. Geophys. 48, 84-93, 1980
- Zang, A., Wolter, K., Berckhemer, H.: Strain recovery, microcracks and elastic anisotropy of drill cores from KTB deep well. Scientific Drilling 1, 115-126, 1989

KTB-REPORTS



K T B R E P O R T S related to Borehole Measurements

already published:

KTB Report 87-2 (1987)

Grundlagenforschung und Bohrlochgeophysik. Beiträge zur Tagung der Deutschen Geophysikalischen Gesellschaft in Clausthal-Zellerfeld (31.3. - 4.4.1987). Hsg.: R. Hänel und R. Schopper

KTB Report 87-3 (1987)

Grundlagenforschung und Bohrlochgeophysik (Bericht 2). Arbeitsprogramm KTB-Bohrlochgeophysik sowie Bohrlochmeßprogramm KTB-Oberpfalz VB (1.9.87). Hsg.: R. Hänel

KTB Report 87-4 (1987)

Grundlagenforschung und Bohrlochgeophysik (Bericht 3). Bohrlochmessungen in der KTB-Oberpfalz VB - Intervall 0-478,5 m -. Hsg.: J.K. Draxler und R. Hänel

KTB Report 88-4 (1988)

Grundlagenforschung und Bohrlochgeophysik (Bericht 4). Bohrlochmessungen in der KTB-Oberpfalz VB - Intervall 478,5-1529,4 m. Hsg.: J.K. Draxler und R. Hänel

KTB Report 88-7 (1988)

Grundlagenforschung und Bohrlochgeophysik (Bericht 5). Bohrlochmessungen in der KTB-Oberpfalz VB - Intervall 1529,4-3009,7 m. Hsg.: J.K. Draxler und R. Hänel

KTB Report 88-11 (1988)

Grundlagenforschung und Bohrlochgeophysik (Bericht 6). Forschung und Entwicklung - Berichte laufender und abgeschlossener Vorhaben. Hsg.: P. Kehrer und W. Kessels

KTB Report 89-1 (1989)

Grundlagenforschung und Bohrlochgeophysik (Bericht 7). Auswertung von Bohrlochmessungen der KTB-Oberpfalz VB. Hsg.: R. Hänel

KTB Report 90-1 (1990)

Grundlagenforschung und Bohrlochgeophysik (Bericht 8). Bohrlochmessungen in der KTB-Oberpfalz VB - Intervall 3009,7-4000,1 m. Hsg.: J.K. Draxler

KTB Report 90-5 (1990)

Grundlagenforschung und Bohrlochgeophysik (Bericht 9). Hydraulische Untersuchungen in der Bohrung KTB-Oberpfalz VB. Hsg.: W. Kessels

KTB Report 90-6a (1990)

Grundlagenforschung und Bohrlochgeophysik (Bericht 10). Langzeitmeß- und Testprogramm in der KTB-Oberpfalz VB. Hsg.: K. Bram, J.K. Draxler, W. Kessels und G. Zoth

